nagra.

TECHNICAL REPORT 23-03

Geochemical Evolution of the L/ILW Near-Field

December 2023

Nagra | National Cooperative for the Disposal of Radioactive Waste
Hardstrasse 73 | 5430 Wettingen | Switzerland
T. +41 56 437 11 11 | info@nagra.ch | nagra.ch

nagra.

TECHNICAL REPORT 23-03

Geochemical Evolution of the L/ILW Near-Field

December 2023

G. Kosakowski[1], S. V. Churakov[1,2], M. Glaus[1], T. Guillemot[3], W. Hummel[1], D. Kulik[1], B. Ma[1], L. Martin[3], D. Miron[1] & N. L. Prasianakis[1]

[1]Laboratory for Waste Management, Paul Scherrer Institute (PSI)
[2]Institute of Geological Sciences, University of Bern
[3]Nagra

Nagra | National Cooperative for the Disposal of Radioactive Waste
Hardstrasse 73 | 5430 Wettingen | Switzerland
T. +41 56 437 11 11 | info@nagra.ch | nagra.ch

ISSN 1015-2636

Copyright © 2023 by Nagra, Wettingen (Switzerland) / All rights reserved. All parts of this work are protected by copyright. Any utilisation outwith the remit of the copyright law is unlawful and liable to prosecution. This applies in particular to translations, storage and processing in electronic systems and programs, microfilms, reproductions, etc.

Abstract

The Swiss concept for the long-term disposal of radioactive waste foresees the construction of deep geological repositories for high-level waste (HLW), comprising spent fuel and vitrified HLW, as well as for low- and intermediate-level waste (L/ILW), from the operation and dismantling of the nuclear power plants and from applications in industry, research and medicine. Nagra announced in September 2022 that they would submit a general licence application for a combined repository for HLW and L/ILW in the Opalinus Clay in the Nördlich Lägern siting region.

The L/ILW repository is specifically designed to contain large amounts of cement-based materials (concrete, mortar) used for waste conditioning, tunnel support, infrastructure elements and the backfilling of cavities. The cement-based near-field thus constitutes a safety pillar of the repository, where the cement contributes to the retention and slow release of radionuclides and maintains the high-pH environment, thereby ensuring the slow corrosion of metals and low gas generation rates. The waste inventory in the L/ILW repository section consists of a wide range of organic and inorganic materials. This report describes the spatial and temporal geochemical evolution of the cementitious near-field, and the interactions between the engineered barriers and the surrounding host rock, by reviewing the different processes which are expected to occur.

The spatial and temporal evolution of the cementitious near-field is governed by several externally and internally induced processes that are coupled with each other. The water saturation state of the repository is of central importance for the temporal evolution of the repository near-field. Under desaturated or partially saturated conditions of the emplacement caverns, the adjacent host rock or the engineered barriers, the transport of dissolved species and the chemical reactions are suppressed as they only take place in water-films on minerals. The saturation evolution of the near-field is controlled by gas production, which causes a gas pressure increase and limits the inflow of water from the host rock. Gas pressures are reduced by the transport of dissolved gases from the near-field into the host rock and gas transport through cavern seals into the tunnel system. The production of gas by anoxic corrosion of metals and by microbial degradation of organic wastes also consumes water. In addition, the reactions that give rise to concrete degradation, such as aggregate-cement interaction or carbonation may also consume or produce water, respectively. However, these reactions require a minimum humidity in the gas phase to form the necessary water films at pore surfaces. With decreasing saturation, the vapour transport in the gas phase becomes important. The vapour is in equilibrium with liquid-filled small pores and causes the formation of liquid films along mineral surfaces in which dissolved substances may be transported and react with each other.

The description of cement degradation is consistent with that reported in previous studies. It is expected that the degradation of the cementitious near-field will occur in several phases:

The first phase of cement degradation is related to the hydration of cement phases. In this phase, the porewater has a pH of 13 or even higher due to the high content of dissolved alkali hydroxides. This phase is expected to persist only for a relatively short period, especially in situations and places where strong geochemical gradients foster transport of solutes.

The second phase of the cement degradation is controlled by the equilibrium of porewater with portlandite, which is buffered at a constant pH of 12.5. The alkali concentration is reduced by mineral reactions and/or solute transport.

In the third phase of the cement degradation, the portlandite is completely dissolved due to the reaction with silicates, aluminates or carbonates present in the near-field and interaction with the groundwater of the host rock or associated with reactive waste materials or concrete aggregates.

At this stage, the porewater is in equilibrium with calcium-silicate-hydrates (C-S-H), which leads to a pH value below 12.5 to near 11 or even lower. The Ca/Si ratio of C-S-H changes from high (Ca/Si ~ 1.6) towards lower values (~ 0.7) as the composition of the C-S-H phases evolves.

In a very late phase of the cement degradation, the formation of carbonates, clays or zeolites results in a decrease of the pH to near-neutral values.

Various processes influence the geochemical evolution of the cementitious near-field. The most important are the interactions with the host rock (i.e. cement-Opalinus Clay interaction), the interactions with waste, and the degradation of cement phases by aggregate-cement interaction and by cement carbonation. Interfaces between cement and clay materials can be characterised by strong (geo-)chemical differences. The diffusion-dominated exchange of porewater between the cementitious near-field and the host rock gives rise to mineral reactions and changes in the porewater pH. Typically, dissolution of cement and clay phases are observed in combination with precipitation of secondary mineral phases at or near the material interfaces. The reduction of the free connected pore space leads to a reduction of mass and solute fluxes across the interface, slowing down the geochemical alteration processes. Such mineral reactions at the interface were investigated with the help of numerical models. The clay minerals of the host rock are dissolved and transformed into secondary minerals (e.g. zeolites) up to a distance of a few decimetres in 100,000 years. Beyond this transition zone and further into the host rock, a zone with an elevated pH of 8 – 9 is expected to develop, but without significant mineralogical changes. Under the diffusive transport regime, this zone extends a few metres into the host rock.

Conservative estimates for a fully water-saturated near-field show that concrete with an average composition is degraded up to a distance of 2 metres from the near-field-host rock interface by diffusion-dominated porewater exchange with the Opalinus Clay. This results in portlandite dissolution and cement mineral transformations, causing a decrease in the concrete porewater pH to values corresponding to the third phase of cement degradation.

Cementitious materials that contain aggregates composed of aluminosilicate minerals will be subject to cement degradation by aggregate-cement reactions. Silicon dioxide from dissolution of concrete aggregates will react with portlandite and form C-S-H phases until the aggregates are in thermodynamic equilibrium with cement phases. These transformations will convert the material into degradation Stage III in the long term. The temporal progression of this reaction is poorly constrained. From available kinetic constants of mineral dissolution reactions, it is inferred that in particular the fine-grained aggregates with a high surface area could be dissolved quickly, i.e. concrete degradation might occur within some hundreds to thousands of years if the material is water-saturated. The full or partial desaturation of concrete materials and the imperfect contact of the cement paste with the aggregates might strongly delay this reaction.

The degradation of organics in an L/ILW repository will take place by a combination of abiotic (i.e. radiolysis and hydrolysis) and biotic processes, such as methanogenesis, which produces CH_4 and CO_2. Due to the unfavourable conditions (high pH), the microbial activity-driven degradation process is expected to be slow. The released CO_2 is expected to react with the surrounding concrete and form solid carbonates. An accurate prediction of the degradation rates of organic waste is difficult since the rates depend not only on pH but also on the availability of water and potential microbial activity which depends on the presence of certain nutrients such as phosphorus and nitrogen. All of these factors limit the microbially mediated degradation of organic compounds. Based on current knowledge, it can be assumed that low-molecular-weight organic materials degrade within a few thousand years. The degradation rates of the high-molecular-weight organic substances (polymeric materials) are rather uncertain due to limited availability of experimental data. It is expected that the degradation may take at least several tens or hundreds of thousands of years, if they degrade at all.

Some inorganic waste can react with the surrounding materials, assuming that water availability is not a limiting factor. Particularly important is the anoxic corrosion of metals, specifically steel, which can produce large amounts of H_2. Corrosion products could contribute to the degradation of the surrounding cement phases. Note that this again requires percolation of a water phase in all the pores to maintain the transport of dissolved species.

The general description of concrete degradation is rather similar to the previous study (Kosakowski et al. 2014). This work puts more emphasis on the heterogeneity of near-field materials and postulates that, even after long times, geochemical conditions in the repository might be quite heterogeneous. The heterogeneity of geochemical conditions depends on the spatial material distribution and the water saturation in space, which also induces a spatially different evolution in time.

The basic mechanisms of radionuclide transport (retention) and radionuclide solubility have not changed compared to the previous study (Kosakowski et al. 2014). The refined analysis of the processes and conditions confirm that the cementitious near-field is an effective barrier for the transport of radionuclides over very long timespans. The cementitious near-field can be considered to contribute effectively to the retention of radionuclides over tens of thousands of years. The occurrence of colloid-facilitated radionuclide transport is considered as very unlikely since the host rock and near-field porewater chemistries give rise to very low colloid stabilities and thus significantly reduce colloid concentrations.

Zusammenfassung

Für die Entsorgung der radioaktiven Abfälle aus der Schweiz sind geologische Tiefenlager für hochaktive Abfälle (Brennelemente und verglaste Abfälle aus der Wiederaufbereitung) und schwach- und mittelaktive Abfälle (aus dem Betrieb und Rückbau von Kernkraftwerken, Medizin, Industrie und Forschung) vorgesehen. Im September 2022 hat die Nagra angekündigt, ein Rahmenbewilligungsgesuch für ein kombiniertes Tiefenlager für alle Abfälle in der Standortregion Nördlich Lägern auszuarbeiten.

Das geologische Tiefenlager für schwach- und mittelaktive Abfälle (SMA) ist darauf ausgelegt, grosse Mengen an zementhaltigen Materialien (Beton, Mörtel) für die Konditionierung der Abfälle, den Ausbau der Einlagerungskavernen und für die Verfüllung von Hohlräumen zu verwenden. Das zementbasierte Nahfeld repräsentiert einen Pfeiler der Sicherheit, wo der Zement zur Rückhaltung und langsamen Freisetzung von Radionukliden beiträgt und der hohe pH der Porenlösung zur Passivierung des Stahls und damit zur langsamen Korrosion und Gasfreisetzung beiträgt.

Das Abfallinventar in einem solchen SMA-Lager ist durch eine grosse Vielfallt an organischen und anorganischen Materialien charakterisiert. Im vorliegenden Bericht wird die räumliche und zeitliche geochemische Entwicklung des Zement-Nahfeldes und seine Wechselwirkungen mit den technischen Barrieren und dem angrenzenden Wirtgestein beschrieben.

Die räumliche und zeitliche chemische Entwicklung des Zement-Nahfeldes wird durch zahlreiche miteinander gekoppelte innere und äussere Einflüsse gesteuert. Von zentraler Bedeutung für viele chemische Prozesse ist die Verfügbarkeit von Wasser. Eine teilweise oder vollständige Entsättigung der Lagerkavernen, der angrenzenden Wirtgesteinsbereiche oder der Barrierensysteme verlangsamt oder verhindert den Transport gelöster Stoffe in der Wasserphase, und limitiert so chemische Reaktionen. Die Sättigungsentwicklung des Nahfeldes wird von der Gasproduktion kontrolliert, die den Gasdruck im Lager erhöht und den Wasserzufluss vom Wirtgestein limitiert. Der Transport von gelösten Gasen in der Wasserphase vom Nahfeld ins Wirtgestein reduziert den Gasdruckdruckaufbau im Lager, ebenso wie der Gastransport durch Kavernensiegel in das Tunnelsystem. Die Produktion von Gas und die anoxische Korrosion von Metall setzt nicht nur Gas frei, sondern verbraucht auch Wasser. Zudem können die zum Abbau zementhaltiger Materialien führenden Mineralreaktionen Wasser verbrauchen oder auch freisetzen. Solche Reaktionen benötigen aber (wie auch die biochemische Gasproduktion) in jedem Fall ein Mindestmass an Feuchtigkeit, so dass chemische Reaktionen ablaufen können. Bei zunehmender Entsättigung des Nahfeldes gewinnt somit die Gasphase an Bedeutung. Die Feuchtigkeit in der Gasphase ist im Gleichgewicht mit Wasserfüllungen kleiner Poren und Wasserfilmen an Mineraloberflächen, in denen gelöste Stoffe miteinander reagieren können.

Im Vergleich zu früheren Betrachtungen ändert sich die generelle Beschreibung der Zementdegradation nicht. Es wird erwartet, dass das Zement-Nahfeld verschiedene geochemische Stadien/Degradationsstufen durchläuft.

Das erste Stadium ist mit der Hydratisierung der Zementmaterialien verbunden. Das Porenwasser ist durch hohe pH-Werte (≥ 13) und erhöhte Konzentrationen gelöster Alkalihydroxide charakterisiert. Dieses erste Stadium ist zeitlich begrenzt, insbesondere in Situationen mit starken räumlichen Konzentrationsgradienten, die den Transport von gelösten Stoffen beschleunigen.

Im zweiten Degradationsstadium wird der pH des Porenwassers durch das Gleichgewicht mit Calciumhydroxid (Portlandit) bei ca. 12.5 gepuffert. Die Konzentrationen der gelösten Alkalihydroxide wurden durch Transportprozesse und/oder Mineralreaktionen abgesenkt.

In der dritten Degradationsstufe wird der Portlandit durch Reaktionen mit Silikaten, Aluminaten und Karbonaten des Wirtgesteins, oder durch Interaktion mit reaktiven Abfällen oder Aggregate verbraucht. Der pH des Porenwassers wird durch das Gleichgewicht mit Calcium-Silikat-Hydraten (C-S-H) von pH 12.5 auf ca. pH ~ 11 oder tiefer gesenkt. Durch eine Abreicherung von $Ca(OH)_2$ aus den C-S-H-Phasen verändert sich deren Zusammensetzung von solchen mit einem hohen Ca/Si-Verhältnis (~ 1.6; im Gleichgewicht mit Portlandit) in Richtung eines geringeren Ca/Si Verhältnisses (~ 0.7).

Im letzten Stadium sind sämtliche Zementphasen zersetzt, und es werden Karbonate, Tonminerale oder Zeolithe gebildet, deren chemisches Gleichgewicht mit dem Porenwasser einen etwa neutralen pH-Wert herbeiführt.

Die geochemische Entwicklung des Zementnahfeldes wird durch verschiedene Prozesse beeinflusst. Als wichtig erachtet werden die chemischen Wechselwirkungen mit dem Wirtgestein, die Wechselwirkungen mit den eingelagerten Abfällen, die Wechselwirkungen zwischen Aggregat und Zementpaste, und die Karbonatisierung der Zementpaste.

Zement-Ton Grenzflächen können durch einen starken geochemischen Gradienten charakterisiert sein. Der diffusionsdominierte Austausch von Porenwässern zwischen Zementmaterialien und dem Wirtgestein führt zu Mineralreaktionen und Änderungen des pH-Wertes im Porenwasser. Im Rahmen solcher Wechselwirkungen kommt es zur Auflösung von Mineralien im Ton- und Zementmaterial kombiniert mit der Ausfällung von Sekundärminerale in oder an der Grenzfläche. Infolgedessen kommt es zu einer Reduktion der freien verbundenen Porosität, was den Massen- und Stofftransport reduziert und die kontinuierliche chemische Wechselwirkung verlangsamt. Solche Wechselwirkungen wurden mit Hilfe von vereinfachten numerischen Modellen untersucht. Ausgehend von den Grenzflächen zwischen Zementmaterialien und Opalinuston werden im Wirtgestein die Tonminerale bis zu einigen dm in 100'000 Jahren in andere Minerale (z. B. Zeolithe) umgewandelt. Daran anschliessend wird sich eine Zone mit einem leicht erhöhten Porenwasser pH von 8 – 9 entwickeln, welche noch nicht mit signifikanten mineralogischen Änderungen verbunden ist. Diese Zone erstreckt sich in einem diffusiven Transportregime über einige Meter um das Lager. Konservative Schätzungen für ein vollständig mit Wasser gesättigtem Nahfeld zeigen, dass sich innerhalb der SMA-Kavernen der Zementstein durch ein diffusionsdominiertes Transportregime bis zu einer Entfernung von etwa 2 m von der Grenzfläche zu Zementdegradationsstufe III verändern könnte.

Falls Beton aluminosilikathaltige Zuschlagstoffe enthält, können Zementmaterialien durch die Reaktionen zwischen Zugschlagstoffen und Zementphasen degradiert werden. Hierbei reagieren kieselsäurehaltige Zuschläge mit Portlandit und C-S-H Phasen. Dieser Prozess führt zu einer pH Reduktion im Porenwasser und führt langfristig zur Degradationsstufe III im Zement. Über den längerfristigen zeitlichen Verlauf dieser Reaktion ist wenig bekannt. Die Bewertung bekannter Reaktionsgeschwindigkeiten lässt allerdings den Schluss zu, dass die Zementdegradation durch diesen Prozess relativ schnell, d. h. in einigen hundert bis tausend Jahren, in vollständig mit Wasser gesättigten Zementmaterialien erfolgen könnte. Eine vollständige oder teilweise Entsättigung, oder ein unvollständiger Kontakt zwischen Zementleim und Zuschlagstoffen, wird die Reaktionsgeschwindigkeit stark verlangsamen.

Die Degradierung organischer Abfälle in einem zementhaltigen Tiefenlager erfolgt über eine Kombination von abiotischen (z. B. Radiolyse und Hydrolyse) und biotischen Prozessen, wie z. B. Methanogenese, wobei CO_2 und CH_4 gebildet werden. Infolge der ungünstigen Lebensbedingungen (hoher Porenwasser pH-Wert, eingeschränkte Wasserverfügbarkeit) wird die für die Degradierung notwendige mikrobielle Aktivität sehr gering sein. Das gebildete CO_2 wird das die Abfälle umgebende Zementmaterial karbonatisieren. Die Degradierungsraten der organischen Abfälle sind schwer vorherzusagen, da nur wenig experimentellen Daten verfügbar sind, und da sie neben dem pH von weiteren schlecht quantifizierbaren Faktoren wie der Verfügbarkeit von Wasser und bestimmten Nährstoffen wie Phosphor und Stickstoff abhängen. Diese Faktoren

wirken limitierend auf den mikrobiellen Abbau. Basierend auf dem heutigen Kenntnisstand lässt sich vermuten, dass niedermolekulare organische Materialien innerhalb von wenigen tausend Jahren abgebaut werden. Die Abbauraten hochmolekularer organischer Substanzen sind mit grossen Unsicherheiten belastet. Es wird erwartet, dass der Abbau mindestens einige zehn- oder gar hunderttausend Jahren dauern könnte.

Einige anorganische Abfälle werden, genügend Wasser vorausgesetzt, mit den umgebenden Materialien reagieren. Herauszuheben ist hier die anoxische Korrosion von Metallen (inkl. Stahl), welche eine erhebliche Menge an H_2 produzieren kann. Die Korrosionsprodukte können wiederum zur Degradierung der umgebenden Zementmaterialien beitragen. Voraussetzung ist wiederum eine Wasserphase, in der gelöste Stoffe transportiert werden können.

Im Vergleich mit früheren Arbeiten hat sich die generelle Beschreibung der Zementdegradation nicht geändert. In dieser Arbeit wird mehr Gewicht auf die Heterogenität der Materialien im Nahfeld gelegt. Es wird angenommen, dass die geochemischen Bedingungen im Tiefenlager auch nach einer langen Zeit recht heterogen sein könnten. Die Heterogenität der Bedingungen ist abhängig von der räumlichen Materialverteilung und der Wassersättigung im Raum, was zu einer räumlich unterschiedlichen zeitlichen Entwicklung führt.

Die sich aus der Zementdegradation ergebenden Konsequenzen für den Radionuklidtransport (Retention) und die Radionuklidlöslichkeiten sind gleich wie in früheren Studien (Kosakowski et al. 2014). Die verfeinerte Analyse der Bedingungen und Prozesse im Nahfeld des SMA-Lagers bestätigen, dass langzeitig Bedingungen vorherrschen, die zur Radionuklidrückhaltung beitragen. Das Nahfeld stellt damit eine effektive Barriere für die Nuklidrückhaltung dar. Ein kolloidgetragener Radionuklidtransport wird als sehr unwahrscheinlich erachtet, da die Wirtgestein- und die Nahfeldporenwasserchemie zu sehr geringer Kolloidstabilität führen und Kolloidkonzentrationen dementsprechend sehr tief sind.

Table of Contents

List of Tables

List of Figures

List of Acronyms

AAR	Alkali-aggregate-reaction
ACR	Alkali-carbonate-reaction
AFt	Abbreviation for “alumina, ferric oxide, tri-substituted” calcium aluminium hydrates, group of cement minerals
AFm	Abbreviation for “alumina, ferric oxide, mono-substituted” calcium aluminium hydrates, group of cement minerals
ASR	Alkali-silica-reaction
C-S-H	Calcium-silicate-hydrate
C-(A-)S-H	Calcium-(aluminium-)silicate-hydrate
CCC	Critical coagulation concentration
CEC	Cation exchange capacity
CN^-	Cyanide
COx	Callovo-Oxfordian
EDTA	Ethylenediaminetetraacetic acid
EDZ	Excavation disturbed zone
ettringite	Calcium aluminium hydroxy-sulphate $Ca_6Al_2(SO_4)_3(OH)_{12}\cdot 26H_2O$, common AFt phase
GLU	Gluconic acid
HCP	Hardened cement paste
HLW	High-level waste (spent fuel assemblies and vitrified high-level waste from reprocessing)
HMW	High molecular weight (organics)
IER	Ion exchange resin
IRB	Iron-reducing bacteria
ISA	Isosaccharinic acid
L/ILW	Low- and intermediate-level waste
LMW	Low molecular weight (organics)
MB	Methanogenic bacteria
MIRAM	Model Inventory of Radioactive Materials
NAB	Nagra Arbeitsbericht
NEA	Nuclear Energy Agency
NRB	Nitrate-reducing bacteria
NTA	Nitrilotriacetate

NTB	Nagra Technical Report
OPA	Opalinus Clay
portlandite	Calcium hydroxide $Ca(OH)_2$
PC	Portland cement
PVC	Polyvinylchloride
PW	Porewater
RTM	Reactive transport model
RH	Relative humidity
SDB	Sorption database
SF	Spent fuel assemblies
SGT	Sectoral Plan for Deep Geological Repositories
SRB	Sulphate-reducing bacteria
TDB	Thermodynamic database
TST	Transition state theory
URL	Underground Research Laboratory

1 Introduction

In Switzerland, the Nuclear Energy Act requires the disposal of all types of radioactive waste in deep geological repositories (KEG 2003). The basic feasibility of the safe disposal of radioactive waste in a deep geological repository in a clay host rock was demonstrated by Nagra in Project *Entsorgungsnachweis* (the term translates into English as "demonstration of disposal feasibility") at the end of 2002. This feasibility study was based on the Opalinus Clay host rock option in the Zürcher Weinland area in Northern Switzerland and was supported by a detailed safety case (Nagra 2002a, 2002b). At the time, two repository types were foreseen in Switzerland:

- one for the disposal of low- and intermediate-level waste (L/ILW) arising from the operation and decommissioning of Swiss nuclear power plants, from medicine, industry and research and from those operations in reprocessing that produce only low-level technological waste
- one for the disposal of high-level waste (HLW), comprising spent nuclear fuel (SF) and vitrified HLW, as well as long-lived intermediate-level waste (ILW), primarily resulting from fuel reprocessing

Project *Entsorgungsnachweis* considered only the repository for SF/HLW/ILW, referred to in the following as the HLW repository.

The choice of both Opalinus Clay and the Zürcher Weinland was the result of a preliminary, safety-based evaluation of potential host rocks, in which other possible options were also evaluated but set aside by Nagra. Host rock and site selection were later carried out in a more systematic manner following the Sectoral Plan for Deep Geological Repositories.

The Sectoral Plan (Swiss Federal Office of Energy 2008) specifies how sites for deep geological repositories for radioactive waste are to be selected in Switzerland. The concept for the Sectoral Plan was developed by the Swiss Federal Office of Energy (SFOE) together with other agencies and organisations and was approved by the Federal Council in 2008. The procedure set out in the Sectoral Plan allows a transparent and fair selection of siting locations in three stages:

- Stage 1: Selection of geological siting regions
- Stage 2: Selection of at least two sites
- Stage 3: Selection of one site

In September 2022, as part of Stage 3 of the siting procedure, Nagra formally proposed the Nördlich Lägern (NL) siting region, which lies within cantons Zürich and Aargau, as the site for a combined repository for all waste types, with Opalinus Clay as the selected host rock (Nagra 2022). This argillaceous rock is characterised by very low hydraulic conductivity and high sorption capacity. Detailed descriptions and characterisations of the potential host rocks were published by Nagra following an extensive geological exploration campaign (Nagra NTB 24-17 *in prep.*). Nagra is currently in the process of preparing a general licence application for this site, supported by a safety case that it will submit at the end of 2024. The Federal Council and the Swiss Parliament will decide on the granting of the general licence and an optional national referendum can be called for on this decision.

The present report is one of several that contributes to the specific requirement for the safety demonstration that the long-term behaviour of the repository barrier system must be understood (KEG 2003).

The objective of this report is to provide information about the chemical evolution of a low- and intermediate-level waste (L/ILW) section of a combined repository in Nördlich Lägern (NL). Repository safety and performance assessment require the understanding of the long-term chemical evolution of the repository near-field at an adequate level.

Information about the repository layout and a description of the key elements of the Swiss repository concept and the corresponding safety concept are provided in Nagra (2021b). The safety concept for the post-closure phase of a deep geological repository ensures the permanent protection of humans and the environment using staged, passive barriers (Art. 3c Nuclear Energy Act, KEG 2003). In Switzerland, the safety concept for HLW and L/ILW is based on a multi-barrier system optimised with regard to long-term safety. This includes engineered barriers consisting of the waste matrix, disposal canisters, backfilling and sealing as well as the containment-providing rock zone as a natural barrier.

The multi-barrier system ensures that the repository fulfils the required safety functions over the time period of assessment. In line with Guideline ENSI-G03 (ENSI 2020), safety functions are overarching functional requirements on the multi-barrier system that, taken together, ensure long-term safety.

The L/ILW repository is designed to contain large amounts of cement-based materials (concrete, mortar) used for waste conditioning, tunnel support, infrastructure elements and the backfilling of cavities. The cement-based near-field thus constitutes a safety pillar of the repository, where the cement contributes to the retention and slow release of radionuclides and maintains the high pH environment, thereby ensuring the slow corrosion of metals and low gas generation rates. Compared to SF and HLW, the L/ILW includes a very heterogeneous mix of non-heat emitting wastes. This report updates the earlier report NTB 14-11 (Kosakowski et al. 2014) and summarises current knowledge on the geochemical evolution of an L/ILW repository. The aim of this report is to describe the expected temporal and spatial evolution of the chemistry of cementitious materials and their interactions with adjacent engineered and natural barriers and to assess the impact of possible changes to the transport and retardation of radionuclides. The geochemical evolution of a SF/HLW waste repository is described elsewhere (Curti et al. 2023). Similarly, the evolution and functionality of the sealing system is covered in Martin et al. (2023).

The performance of the natural and engineered barriers and radionuclide retention mechanisms are influenced to different degrees by chemical processes. For example:

- Chemical interactions of waste with the cementitious matrix/bitumen matrix may influence the immobilisation, retention and slow release of radionuclides in the near-field.
- Metal corrosion may have an impact on the gas pressure build-up in the L/ILW repository.
- Cement/clay interaction changes porosity at interfaces, which impacts radionuclide and gas transport across the interface.
- Cement/clay interaction might cause alteration of mineral assemblages and porewater compositions (by dissolution of clay minerals in the host rock, transformation of cement phases), which could change radionuclide retention within the altered zone around the L/ILW caverns.
- Waste/cement interactions may have an impact on the geochemical conditions within the L/ILW near-field (locally or globally) and the alkaline conditions (pH).
- A significant decrease in pH in combination with availability of water could provide niches for microbial activity where living conditions are suitable. At the same time, a lower pH would accelerate metal corrosion.

These aspects and many more are discussed within the scope of this report. The report relies on a review of literature data, mass balance calculations, thermodynamic and reactive transport calculations to develop a view of the expected geochemical repository evolution and to assess the importance of processes and process couplings.

The literature reviews and mass balance calculations give an indication of the maximum possible alteration of barrier materials, but provide only a limited insight into the spatial and temporal evolution of the overall system, the specific influence of single processes (e.g. pore space changes), and on the feedback between different processes.

Results from reactive transport calculations, including the host rock and provisional concrete materials which could be used in the Swiss disposal design, provide a much deeper insight into the system behaviour (Berner et al. 2013, Kosakowski & Berner 2013). Such reactive transport calculations not only allowed refined mass balance calculations to be made, but also introduced a new qualitative insight into system evolution since several processes, and their mutual impacts, could be considered simultaneously.

This report is split into two main parts in line with the previous report (Kosakowski et al. 2014):

- Chapter 2 provides an integral description of our current view of the geochemical evolution of the near-field of the repository. This part is an extended summary of the whole report and provides the conclusions.
- Chapter 3 goes into more depth and provides detailed information on the disposal system and descriptions of processes that influence either the geochemical evolution of the cementitious near-field or the radionuclide transport properties of the far-field.

There is no specific chapter with conclusions at the end of the report, as those are provided in Chapter 2.

The appendix summarises the calculation of the porewaters for the various cement degradation stages, used for setting up the databases for radionuclide solubility within cement porewater (Hummel et al. 2022) and the cement sorption database (Tits & Wieland 2023).

A list of processes related to the geochemical evolution of the cementitious near-field and their coverage in this report is given in Tab. 1-1. An overview of potential impacts on radionuclide transport is presented in Tab. 1-2.

Tab. 1-1: Report sections covering processes that govern or influence the geochemical evolution of the cementitious near-field and far-field covered in this report

	Cementitious near-field	**Host rock**	**Access tunnel-backfill**
Saturation/gas production	3.2	3.2	3.2
Evolution of cement/clay interfaces	3.3.2, 3.3.3	3.3.2, 3.3.4	3.3.4
(internal) concrete degradation	3.3.1, 3.3.5	-	-
Organic wastes	3.4.1	-	-
Inorganic wastes	3.4.4	-	-
Metallic wastes and iron/steel	3.4.4, 3.4.5	-	-
Heterogeneity of the near-field	3.5	-	-
Colloids	3.3.6.2	3.3.6.1	3.3.6.1

Tab. 1-2: List of report sections related to geochemical changes that potentially influence radionuclide transport

	Cementitious near-field	**Host rock**	**Access tunnel-backfill**
Change in transport parameters at material boundaries	3.3.1	3.3.1	
Influence of far-field on near-field	3.3.2, 3.3.3		
Influence of near-field on far-field		3.3.4	3.3.4
Saturation evolution of near-field	3.2	3.2	3.2
Colloids	3.3.6.2	3.3.6.1	3.3.6.1

2 Summary of the expected evolution of the L/ILW disposal system

2.1 General description of the disposal system and its evolution

L/ILW repository description

The L/ILW repository is designed to contain large amounts of cement-based materials (concrete, mortar). The cement-based near-field thus constitutes a safety pillar of the repository, where the cement phases and the high pH environment are responsible for the retention and slow release of radionuclides, the slow corrosion of metals and low gas generation rates. The L/ILW differs from that of an SF/HLW waste repository where the overall waste volumes are smaller and have better characterised properties but are more radiotoxic. Apart from the radioactive waste, the principal materials in an L/ILW repository are hydrated cementitious materials, aggregates and metallic materials such as steel. The wastes are solidified/embedded in a cement/mortar matrix, which itself is contained in steel drums or concrete containers. Some wastes will also be embedded in bitumen. The main function of the drums is related to operational requirements for the interim handling, storage and transport prior to the emplacement in a geological repository.

It is envisaged that, for the emplacement phase, the waste drums should be packed into concrete containers, with the void space between the drums being backfilled with a low viscosity mortar according to the current concept. The containers will be stacked in caverns. The void space in the cavern is planned to be filled with a specifically designed mortar (e.g. “monocorn” mortar). Fig. 2-1 shows a visualisation of an L/ILW cavern according to the current concept with tunnel support and installations, waste packages within containers and the backfilled void space. An extended description of the provisional L/ILW repository design is given in Nagra (2021d, 2021c) and is summarised in Section 3.1. As primary rock support, shotcrete and gliding arches are planned to be used for the initial convergence phase. After initial convergence has ceased, an inner-shell rock support made of transport concrete which will be emplaced by formwork. For the construction of the concrete elements, use of Ordinary Portland Cement (OPC) with siliceous aggregates is envisaged (primarily quartz). In summary, the backfilled caverns contain, in addition to the radioactive waste, hydrated cements, significant amounts of steel (drums, tunnel support and reinforcement and construction materials) and concrete aggregates.

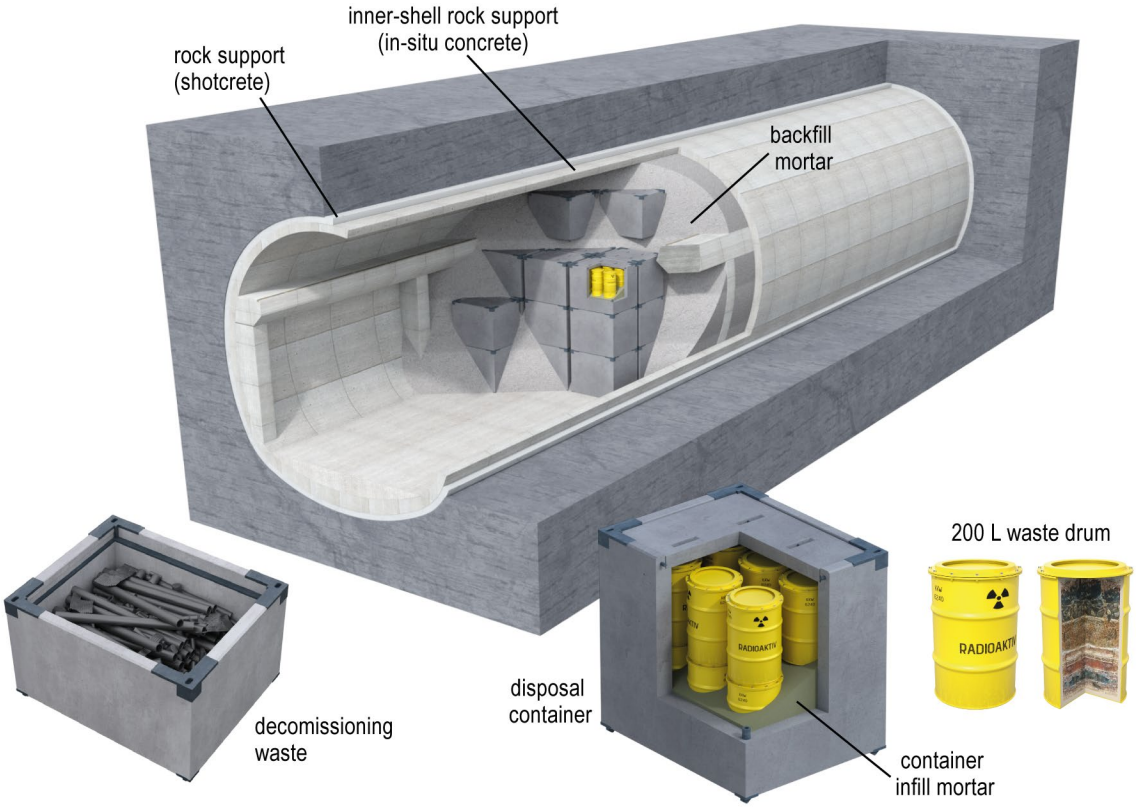

Fig. 2-1: Visualisation of the reference design of an emplacement cavern for L/ILW disposal

Chemical and physical processes in the disposal system

Chemical conditions in the repository, as well as their temporal evolution, are driven by the interactions between hydrated cement, steel, aggregates and the OPA host rock. Considering the distinct chemical nature and composition of the major materials involved, geochemical disequilibria are present once the materials are brought into place. The dominant chemical processes are the degradation of cement materials (Section 3.3.1), the corrosion of iron (Sections 3.4.4 and 3.4.5) and, to lesser degree, the degradation of organic materials (Section 3.4.1). Degradation of cement materials is related to the reactions between cement and aggregate minerals (Section 3.3.5), the influence of OPA porewater on adjacent cement materials (Sections 3.3.1 and 3.3.2) and the impact of CO_2 from organic matter degradation (Section 3.4.3).

Gas-transport-related (modelling) studies (Diomidis et al. 2016, Leupin et al. 2016a, Martin et al. 2023, Papafotiou & Senger 2016) report that large parts of the repository are only partially water-saturated during very long times, which may extend up to more than 100,000 years. Chemical reactions can only proceed if a sufficient amount of water is available, either as a (stagnant or mobile) aqueous phase or as a humid gaseous atmosphere (cf. Section 3.5.2). The inflow rate of liquid water into the caverns and the sealing system is expected to be very small, mainly constrained by the very low permeability of the OPA host rock and moderate pressure gradients. Under such conditions, the chemical reactants are transported predominantly via diffusion within the liquid phase (Section 3.3.2). This implies that, under partially saturated conditions, the overall progress of chemical reactions slows down because of a reduction in mass transport rates and limited liquid phase connectivity. Chemical gradients, in particular those associated with the strongly alkaline nature of the cementitious materials, control the direction of chemical fluxes in the aqueous phase, whereas the principles of chemical thermodynamics define the stability of the

mineral phases that are in contact with porewater solution. However, it should be noted that kinetics can also play a significant role in determining the types of products of the interactions of the barrier materials (e.g. Savage et al. 2007), for example the kinetically controlled reaction between cement and aggregate minerals (Section 3.3.5).

The system evolution is related to the chemical and physical heterogeneity of the waste and cement materials in the near-field, as well as to the coupling between the chemical transformation and mass transport phenomena (Section 3.5). Although individual processes might operate on different temporal and spatial scales, they are strongly coupled via key parameters such as porosity and water content. An example of such a coupling is the porosity reduction on the mm to cm scale at cement/clay interfaces, which might reduce the large-scale mass transport across the material interface. Spatially heterogeneous material distributions and the complex scale-dependent structure of the pore space are important aspects of the system.

Hence, in order to assess the importance of individual processes for the total system, it is necessary to evaluate several parameters and requires the modelling of coupled processes. For example, processes which are influenced by pore space changes or change the pore space itself have a significant impact on the geochemical evolution of the respective materials (Section 3.5). Such processes are related to fluid and gas transport, solute diffusion, saturation state, chemical swelling, and precipitation/dissolution controlled by reaction kinetics. Another example is related to the potential presence of microbes and, if favourable conditions prevail, their active metabolism, which can contribute to consumption of hydrogen gas produced in the L/ILW repository (Section 3.4.6) or contribute to the degradation of organic materials and produce methane and/or CO_2 (Section 3.4.1).

Evolution of the disposal system

During repository operation, and for an extended post-closure period, the geochemical processes in the repository are dominated by the de- and resaturation in the vicinity of the tunnels. Shortly after repository closure, resaturation might be hindered by gas production due to the degradation of organic materials and the anaerobic corrosion of metals. The period of gas generation might be very long, and a complete saturation of the near-field might require more than 100,000 years (Leupin et al. 2016b, Martin et al. 2023, Papafotiou & Senger 2016). Hydro-geochemical clogging processes are restricted principally to the water-saturated pore space within the micro- and mesopores (Nagra 2008a, Prasianakis et al. 2022). Gas-filled macropores should not be subject to strong porosity reduction. Similarly, mineral precipitation is expected to be hindered in small micropores (< 2 nm) (Martin et al. 2023, Prasianakis et al. 2022). During the period preceding the full saturation of the repository, the transport processes (diffusion of solutes) in the possibly unconnected fluid phase are expected to be hindered or slowed down to a considerable degree. The oxidising conditions during the operational phase are expected to quickly become reducing once the oxygen in the entrapped atmosphere is consumed (Leupin et al. 2016b). The saturation phase of the L/ILW repository is detailed in Section 3.2.1. A typical numerical simulation for the prediction of the repository saturation times taking into account realistic material properties and gas generation, using TOUGH2 software, is shown in Fig. 2-2 (Papafotiou & Senger 2016). According to the simulations, the upper part of the repository remains only partially water-saturated beyond 100,000 years.

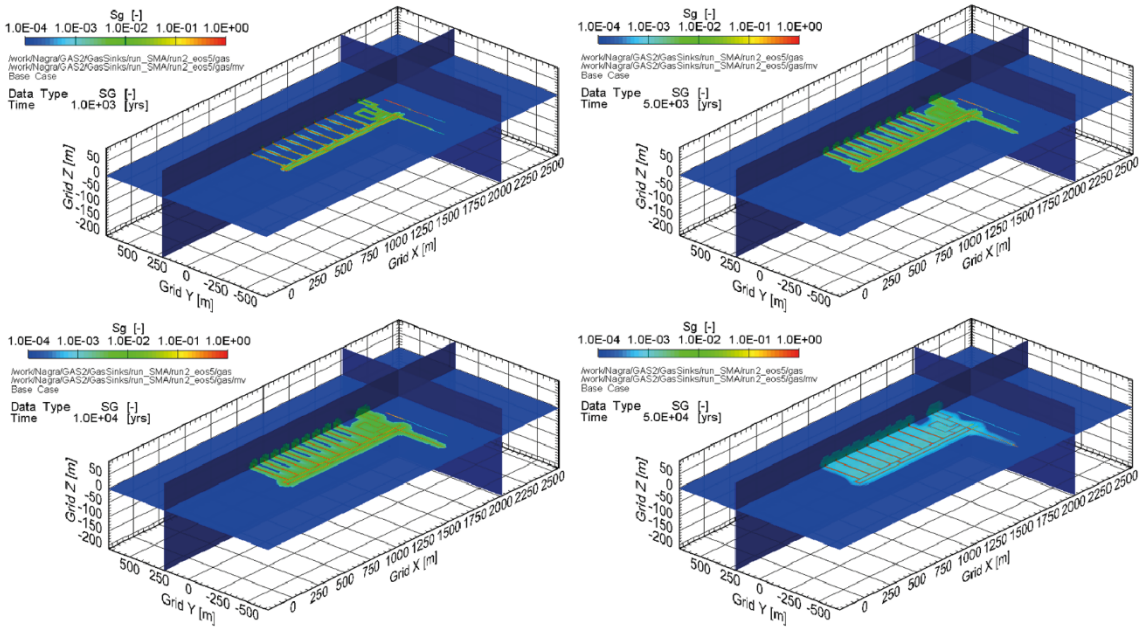

Fig. 2-2: Typical numerical simulation for the prediction of the repository saturation times taking into account realistic material properties and gas generation, using TOUGH2 software

Fig. 4-7 from Papafotiou & Senger (2016)

Shown is the gas saturation after 1,000, 5,000, 10,000 and 50,000 years.

According to the investigated scenario, the lower parts of the emplacement caverns become fully water-saturated within a few thousand years after closure if gas generation is low, whereas high gas generation rates result in a delay of the full saturation by several tens of thousands of years (Papafotiou & Senger 2016).

The major processes that are expected to control the evolution of the fully saturated domains of the repository near-field include:

- the diffusive exchange of solutes between the concrete compartment and the host rock, and
- the internal degradation of concrete due to the reaction of cement phases with the aggregates and waste materials.

A schematic sketch of the major processes driving the degradation of cementitious materials in an emplacement cavern is shown in Fig. 2-3. The left figure illustrates the effects of diffusive transport between near-field and host rock, and the effect of liquid saturation. In the higher desaturated part of the cavern, the reaction front progress is strongly delayed and the porosity reduction at the cement-host rock interface is suppressed. The right figure shows the effect of concrete degradation due to waste-cement interactions (e.g. carbonation) in waste packages and aggregate-cement interaction in the presence of reactive aggregates in cementitious materials (blue hachure). The impact of these processes will be summarised in the following sections and more detailed descriptions are given in Chapter 3.

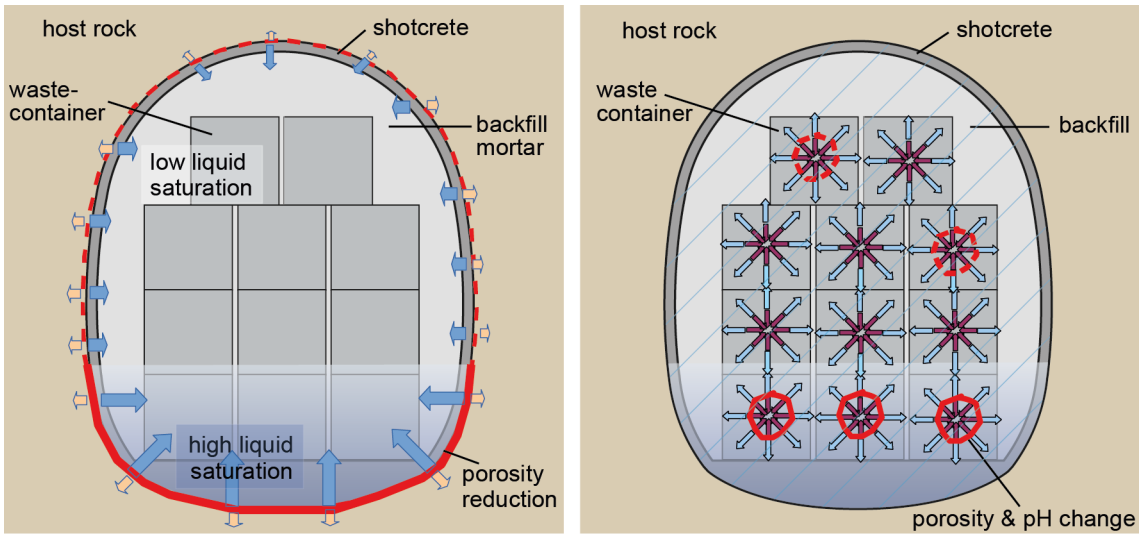

Fig. 2-3: Generic schematic sketch of cement degradation in a partially saturated emplacement cavern

Effects of diffusive transport across clay–concrete interfaces in a partially saturated cavern are shown in the left figure. Directions of diffusion, alteration and reaction fronts are indicated by differently coloured arrows to show that not all solutes and fronts move in the same direction. Lines with red colours indicate possible zones of significant porosity reduction. The right figure indicates possible internal degradation of concretes by aggregate-cement reactions (blue hachure), waste-cement reactions (purple stars) such as metal corrosion and organic matter degradation, carbonation fronts (red circles) and gas release (blue arrows) in the waste packages.

In a low-permeability porous host rock such as OPA, the diffusive transport of solutes, the long-term desaturation of the near-field and mineral reactions in the clay rock control the spatial extent of mineral and porewater alterations (see Sections 3.3.2 to 3.3.4 for details). Investigations of natural analogues, as well as reactive transport calculations, indicate porosity reduction on a cm scale for cement/clay interfaces in diffusion-controlled transport regimes (Prasianakis et al. 2022). The host rock porewater pH may increase to values between pH 8 and pH 9 in the vicinity of the interface to an extent of a few tens of centimetres via diffusive mass transport mechanisms (Kosakowski et al. 2014, Kosakowski & Berner 2013).

It is expected that the porosity reduction at the clay/concrete interfaces (left part of Fig. 2-3) significantly hinder the solute transport across the interface (Section 3.3.1). According to Prasianakis et al. (2022), the uniform and complete blocking of the pore space in compacted clays is unlikely, mainly due to the high amounts of micropores (< 2 nm) with charged surfaces in which precipitation of minerals is unfavourable. Such micropores with charged surfaces exclude the transport of anions but remain accessible for the transport of cations and solvents. The reduction in porosity leads locally to a decrease in the water flow and diffusive mass fluxes across the interface (including radionuclide fluxes).

It is expected that the gas-filled macropores and cracks in partially saturated cement/clay interfaces will not be filled with precipitates and therefore transport in the gas-filled pore space is not affected by porosity reduction (Martin et al. 2023, Prasianakis et al. 2022).

Further, a mechanism which plays a role and has not been extensively considered is the effect of mechanical processes within the near-field (e.g. fracturing), which could potentially change porosity connectivity or open transport pathways under partially saturated conditions (cf. Section 3.5.1). Cracks/fractures in the excavation disturbed zone (EDZ) and other clay materials used for sealing and backfilling are expected and assumed to self-seal upon saturation (Leupin et al. 2016b). Water-filled fractures at cement/clay interfaces, like other macropores, are expected to be preferably filled with precipitates (Prasianakis et al. 2022) and mass transport along such features should be reduced on a long timescale.

2.2 Near-field processes and materials

Concrete degradation

It is common in waste management to consider three to four stages for cement degradation to describe the lifetime of cementitious structures in repositories and their respective porewater compositions (cf. Section 3.3.1). The stages are classified by the existence of different hydrated cement phases, which buffer the porewater pH in specific ranges. The sequential dissolution or transformation of the cement phases is typically driven by external processes (solute transport, transport of gaseous CO_2) or internal processes (e.g. use of reactive aggregates not in thermodynamic equilibrium with cement phases) that remove calcium, hydroxide and other species from porewater, which causes the dissolution or transformation of hydrated cement phases. The discussion of repository evolution is based on the "classical" concept of cement/concrete degradation stages that have been formulated in earlier studies (Kosakowski et al. 2014, Nagra 1994, 2002a). These stages are:

1. The first stage is related to freshly hydrated cement/concrete. The porewater is characterised by high pH values (12.5 to 13.5) due to the significant amounts of dissolved alkali hydroxides. No exchange with the surrounding materials or host rock has yet occurred.
2. The second stage is designated as the portlandite ($Ca(OH)_2$) stability stage. This stage is characterised by a lower ionic strength and equilibrium with portlandite which fixes the porewater pH at ~ 12.5 in ambient state conditions. The dissolved alkali cations have exchanged to a large degree with the solutes of the surrounding material/host rock pore solutions (see below).
3. The third stage is termed the low-pH stage. It is characterised by the absence of portlandite due to its complete dissolution or its reaction with silicates/aluminates or even with carbonate. This stage is further characterised by congruently altered calcium silicate hydrate (C-S-H) phases depleted in Ca and by a pH range of 12.5 to 10.
4. The fourth stage is the final cement degradation state where all Ca-bearing cement phases are fully dissolved, e.g. due to reaction with CO_2. This state may be reached only when significant amounts of CO_2 have been involved in the carbonation process.

Impact of the host rock on the cementitious near-field

If solute transport in the liquid phase across the host rock/cement interface is assumed not to be affected by desaturation or strong porosity reduction, the diffusive solute exchange across the host rock/concrete interface leads to the dissolution of significant amounts of cement phases at or close to the interface. The results of reactive transport calculations, summarised in Sections 3.3.2 and 3.3.3, show that, for fully water-saturated conditions, the cement-based materials might be degraded to Stage III up to a distance of two metres from the cement/host rock interface within 100,000 years. This is a conservative estimate of the degradation extent for this process, because the desaturation of large parts of the near-field and porosity reduction at the cement/clay interface

slows down the mass transport in liquid phase and is expected to constrain the cement degradation to a smaller zone. Portlandite dissolution is accompanied by a decrease in the Ca/Si ratio of the C-S-H phases, characterised by lower Ca/Si ratio towards the interface. The degradation of concrete is not expected to generate a single uniform degradation front where all cement phases are transformed at the same time and location. Instead, it is expected that several sequential mineral transformations spatially distributed in the system will co-exist. The progress of the reaction fronts slows down with time, and each reaction front advances with a specific propagation velocity typical for diffusion-controlled reactive systems. An exact quantification of the progress of portlandite dissolution and other mineral reactions with time is currently not possible since these depend on the evolution of the repository saturation state, and on material properties and transport parameters which are not known or well constrained by the experimental data at present. Examples of such parameters are the exact composition of the concretes, the thermodynamic and kinetic data such as reaction rates and 'reactive' surface areas, the effective diffusion coefficients in different materials, and the porosity-diffusivity relationships (see Section 3.2.3). In addition, if feedback between solute transport and porosity alteration is considered, the extent of the concrete alteration is further reduced.

Interaction between cement phases and reactive aggregates

The thermodynamic instability of (alumino-)silicate aggregates (e.g. quartz, feldspars) and of carbonate aggregates (containing dolomite or siliceous limestone) which are embedded in a cementitious matrix is a well-documented phenomenon. Therefore, irrespective of kinetic constraints, this has to be assessed in connection with the long-term evolution of the cementitious near-field (Section 3.3.5). Several aggregate-cement reaction mechanisms could be identified and are explained in Section 3.3.5; these include the alkali-silica reaction (ASR) and the pozzolanic reaction that are related to silicate aggregates, while the alkali-carbonate reaction (ACR) is related to occurrence of dolomite in aggregates. These reactions, which are summarised as “aggregate-cement reactions”, are often expansive reactions, which cause an increase in local stresses and eventually accelerate the cement degradation. In contrast, thermodynamic stability is ensured in the case of calcite (limestone) aggregates, i.e. pure $CaCO_3$ aggregates, for which interaction between the cement paste and aggregates will not occur.

The sequence of phases present during the (cement) alteration processes can be predicted based on the available thermodynamic data, and corresponds to the phase sequence as described in the state-of-the-art literature on aggregate-cement reactions (cf. Section 3.3.5). Note that a general agreement on the phase sequences exists, although thermodynamic properties of individual phases are less well known.

When coupling chemical reactions with transport mechanisms, we are generally dealing with non-linear system dynamics. In such cases, the kinetics of the reactions play a significant role. If transport is much slower than the progress of a particular chemical reaction, the principles of instantaneous chemical equilibrium are applicable. Note that aggregate-cement reactions are not driven by macroscopic solute transport at the interfaces of engineered barriers. These reactions are a result of an intrinsic thermodynamic disequilibrium between cement phases and aggregate in concrete. While the kinetics of the dissolution of aluminosilicate aggregates are relatively slow, dolomite dissolution is faster. Many mineral dissolution rates are increased in high pH conditions, typical for cement-based materials.

Most aggregate-cement reactions consume water, which needs to be transported to the reaction front in either a liquid or a gaseous form (water vapour). The water transport in turn depends on the global water transport characteristics of the particular system in question. Quantitative description of such processes requires a sophisticated coupling of chemical and transport processes at microscopic and macroscopic levels.

The temporal evolution of the internal degradation currently remains an open issue because several key parameters controlling the long-term reaction rates are poorly known (cf. Section 3.3.5). However, preliminary estimates reveal that the internal degradation due to aggregate-cement reactions could be relatively fast for some materials, provided that materials are (nearly) water-saturated. This means that the cement degradation stage determined by portlandite saturation could potentially last for a much shorter period than anticipated from degradation scenarios based on diffusive interaction with host rock porewater.

Organic wastes

Decomposition of organic materials can take place via abiotic and biotic processes, fully described in Guillemot et al. (2023) and briefly summarised in Section 3.4.1.

It is assumed that the degradation of organics will take place by a combination of hydrolysis and microbial degradation. Hydrolysis reduces the molecular size of complex polymers before microorganisms can degrade them into smaller molecules. Under conditions relevant for an L/ILW repository, biotic degradation is expected to be limited due to the high pH, lack of free water and nutrient availability, and the diffusive transport environment might strongly inhibit microbial activity (Guillemot et al. 2023). Mass balance calculations suggest that the Mn-reducing and Fe-reducing microbial degradation routes for organics are negligible due to the low inventories of Mn(IV) and Fe(III) in hardened cement paste. Note that large quantities of Fe(0) exist in the near-field (waste materials, waste packages, steel reinforcements, etc.), but the conversion of Fe(0) to Fe(III)-bearing phases (magnetite) takes place at a very slow rate, making the Fe(III) an unlikely energy source for microbial activity. To some degree, the microbial decomposition of organics by sulphate-reducing microorganisms might also occur, although the SO_4^{2-} inventory in the near-field is limited by the SO_4^{2-} content of the cement paste. Note that SO_4^{2-} ingress from the host rock is expected to be limited due to the long timescale of the near-field saturation process. Thus, the microbial decomposition of organic matter is expected to occur predominately via methanogenesis, which produces CO_2 and CH_4.

Conservative rates for the degradation of organic material have been consistently used in the report by Kosakowski et al. (2014). For the calculation of gas generation, Nagra classifies organic materials into two groups, a quickly degrading group O1 (e.g. cellulose, LMW organics, complexing agents) and a slowly degrading group O_2 (e.g. ion exchange resin (IER), bitumen, PVC) (Guillemot et al. 2023, Nagra NTB 24-23 *in prep.*). Degradation kinetics for both groups are described by a first order kinetic process. Degradation rates for cellulose are < 1,000 years (O1) and > 10,000 years for polystyrene (O2) (Guillemot et al. 2023). The decomposition of the quickly degrading organic materials is expected to take place mainly during both the early oxic and anoxic stages of the repository and is typically complete within a time span of less than ~ 10,000 years or ten half-lives (i.e. for cellulose, ~ 4,000 years). The timescale for the decomposition of the slowly degrading high molecular weight (HMW) organic materials under anoxic conditions has been estimated to range from several thousand years to some tens to hundreds of thousands of years (i.e. for PVC > 100,000 years) (Wieland et al. 2018). Bulk rates for the main organic materials inventoried in the Swiss L/ILW are defined in Guillemot et al. (2023).

CH_4 and CO_2 are the major gases expected to be released via degradation of organic substances (Guillemot et al. 2023, Nagra NTB 24-23 *in prep.*). No interaction with cementitious materials is expected in the case of CH_4, while the generation of CO_2 could have an impact on the mineral composition of the cement matrix in and around waste packages and consequently on the retention properties of the cementitious near-field (cf. Sections 3.4.1 and 3.4.3). In some waste package types, the high CO_2 production could locally degrade cement materials to Stage IV and lower porewater pH towards neutral conditions. The potential porosity of the cementitious near-field thus decreases due to the formation of carbonate-containing minerals (cf. Section 3.4.3), affects the local transport properties, and strongly reduces the retention of dose-determining anions, such

as iodide, chloride and selenite due to the carbonation of AFm and C-S-H phases. The effect of carbonation on the retention of metal cations is expected to be negligibly small since the main sorbing cement phase, C-S-H, could be replaced by other sorbing phases e.g. zeolites or clay-like minerals. Moreover, the initial carbonation of C-S-H leads to decreasing Ca/Si ratios, and uptake experiments indicate that C-S-H with lower Ca/Si ratio has a larger sorption capacity for cations.

Inorganic wastes

Inorganic waste materials can be subject to transformation processes depending on their chemical stability under hyperalkaline reducing conditions (Section 3.4.1). Some materials are expected to persist over geological timescales (e.g. graphite, Hallbeck 2010, Rout et al. 2018, Wareing et al. 2013). Other materials slowly decompose over time, or consist of elements which make up the cement. Decomposition of the latter materials is expected to change the amount of existing cement phases, but does not completely alter the mineral composition of hardened cement paste, and therefore has no major influence on retention properties.

Metallic materials are subject to anoxic corrosion, which produces H_2. The production of H_2, and, to a lesser degree, the production of CH_4 and CO_2 due to the degradation of organic material, together with the initial desaturation of the host rock adjacent to the caverns from the ventilation phase, is the major driving force for the partial desaturation of the repository near-field over a long period of time (Papafotiou & Senger 2016) (see Section 3.4.1).

The release of ions during the course of the corrosion of magnesium, aluminium, and specifically the high amounts of iron (steel) could alter the mineral composition of cementitious materials (Section 3.4.4). High inventories of Mg in the waste matrix are considered to promote the formation of cement phases that stabilise the cement. Thus, any adverse effects of Mg corrosion on the cementitious materials due to changes in the porosity and sorption properties are expected to be limited. By contrast, the corrosion of Al and Fe could cause changes in the mineral phase composition of cement, with possible effects on anion retention (Section 3.4.5).

2.3 Expected near-field evolution and the impact on radionuclide transport

Spatio-temporal near-field evolution

In previous studies, e.g. Nagra (2002a), it was assumed that a fully saturated cementitious near-field would remain for very long times in degradation Stage II, thus enabling the construction of a simplified concept for radionuclide transport in the homogeneous near-field, where transport parameters, radionuclide solubilities and sorption parameters are constant in space and time.

Kosakowski et al. (2014) revised this concept and concluded that cement degradation may proceed relatively quickly to degradation Stages III or even IV in local parts of the near-field due to interaction with host rock, aggregate-cement reactions and cement carbonation with CO_2 originating from the degradation of organic matter. The temporal evolution of cement degradation is controlled by the delayed saturation of the L/ILW repository; i.e. fully water-saturated parts of the repository evolve fast, whereas cement degradation in desaturated parts is delayed. In Kosakowski et al. (2014), consumption of hydrogen and other gases in the near-field has not been considered. In this report, and more specifically in Section 3.4.6, the possible microbially mediated consumption of hydrogen and its geochemical consequences are summarised.

This report still supports the underlying conceptual picture of near-field evolution in terms of processes and process couplings proposed by Kosakowski et al. (2014). Specifically, the conceptual description of the cement degradation stages listed in Section 3.3.1, and further detailed in Section 3.3.1, does not differ from that defined in earlier studies.

However, what has been better understood and now updated in comparison to Kosakowski et al. (2014) is the importance of the spatio-temporal evolution of the near-field due to different materials and waste types. Section 3.5 summarises the role of processes and process couplings (Section 3.5.1), the influence of the desaturation of the near-field on (bio)chemical processes (Section 3.5.2), the degradation of generic cement materials (Section 3.5.4) and the evolution of typical waste types (Section 3.5.3).

The diffusion-dominated exchange of porewaters between the concrete and the surrounding host rock will also be strongly decreased in the desaturated parts of the near-field. This delays the progress of the reaction fronts, specifically into cement materials. In contrast to Kosakowski et al. (2014), it is believed that accumulation of precipitates in clay and cement materials should cause only partial clogging of the pore space. Prasianakis et al. (2022) provide evidence that small micropores (< 2 nm) with charged surfaces are not filled with precipitates, and allow transport of neutral species and dissolved gases, cations for negatively charged surfaces, or anions for positively charged surfaces.

The heterogeneous distribution of cement materials and waste types in the caverns, in combination with a complex evolution of water saturation, might result in a strong compartmentalisation of the near-field where each compartment is characterised by a different degradation stage and chemical evolution. Of major importance for temporal evolution of cement materials and wastes is the availability of water in the near-field (cf. Section 3.5.2), which not only controls local chemical conditions, but also slows down solute-transport-driven homogenisation in the near-field.

Radionuclide solubilities

The speciation and solubilities of the considered dose-relevant radionuclides in the cementitious near-field depend on the local chemical regime and the timeline of the system evolution.

In a diffusion-dominated system consisting of concrete in contact with a clay host rock, the chemical regime changes mostly near the interface adjacent to the host rock. In the host rock, the influence of high pH from the concrete becomes much less relevant, because the pH is strongly buffered in the clay.

In the case of solubility-controlled radionuclide concentrations, a pH decrease due to enhanced internal or external cement degradation could lead to lower radionuclide solubilities (no anionic hydroxo species), which may decrease radionuclide concentrations in solution. In the case of sorption-controlled concentrations, however, radionuclide sorption in cementitious materials decreases with increasing pH, which would increase radionuclide concentrations in solution. Therefore, if timescales for the high-pH Stages I and II are short, a short timescale of potentially enhanced solubilities due to the formation of anionic hydroxo species of metal cations should be expected. In addition, the quality of speciation and solubility calculations of safety-relevant nuclides strongly depends on the completeness and quality of the database.

A strong desaturation of the near-field due to consumption of water (e.g. by metal corrosion) causes a local strong increase in ionic strength of the residual porewater, which in turn may possibly cause salt precipitation. Currently, the thermodynamic databases contain the necessary thermodynamic data; however, the activity models that are typically used are not valid for such high ionic strength conditions. Therefore, radionuclide solubility is not calculated accurately under such conditions.

Radionuclide retention

Since the principal characteristics of the degradation stages do not change, it is recommended that the same K_d approach is used as in the SGT Stage 2 provisional safety assessment study (Nagra 2014b). For specific cases, such as the large inventories of organic materials, aluminium and iron, a potential impact on the retention of dose-determining anions should be considered (cf. Section 3.4.2). The impact of large inventories of iron in some waste forms on radionuclide retention is uncertain. It is currently unknown to what extent the sorption-controlling cement phases can be consumed by reactions with iron corrosion products and form different phase assemblages.

EDTA, NTA, cyanide, gluconic acid, isosaccharinic acid and ammonia are considered to be the most important complexing ligands that could have an influence on radionuclide uptake by cementitious materials. Sorption reduction factors can account for the possible impacts on radionuclide speciation. The latter are determined by the actual concentrations of the complexing ligands in the waste compartments. The relevant sorption reduction factors and ligand concentrations need to be estimated individually for the two waste categories, where waste group 1 refers to a waste type with suitable sorption and radionulide retention properties, whereas the waste types assigned to waste group 2 may have an elevated concentration of complexing ligands and/or reduced sorption properties. Therefore, for wastes being assigned to waste group 2, radionuclide retention is less effective (cf. Section 3.4.2).

Colloids, if they exist in significant concentrations and are mobile, might act as carriers for radionuclides and accelerate radionuclide transport. As outlined in Section 3.3.6, both cement (near-field) and clay (far-field) colloids are expected to be physico-chemically unstable in the engineered barrier system and in the host rock (e.g. coagulation, attachment to surfaces, dissolution, and filtration). Consequently, the colloid concentrations in the repository are expected to be very low. The impact of colloids, if present, on sorption in the cementitious near-field can be considered in the form of sorption reduction factors, the same way as the impact of complexing agents.

2.4 Uncertainties related to understanding and predicting system evolution

This section does not deal with individual parameter uncertainties such as thermodynamic constants, diffusion coefficients or K_d values. These uncertainties are described in specific sections of this report.

The description of the processes relevant for repository-evolution in safety assessment (Nagra 2014b) relies on the classical conceptual approach where individual processes are analysed separately under the assumption that they operate at different timescales and therefore feedback (coupling) among processes is ignored. The main conceptual uncertainties are thus associated with the validity of this assumption, as several of the processes are tightly coupled in repository and natural systems. Several repository-evolution-relevant processes act on similar timescales and do interact with each other (Section 3.5.1).

The decoupled treatment of the processes relies on an assumption that it is possible to identify a dominant process that controls the system evolution. Based on the analysis of different processes reported in Chapter 3 and their effect on the system parameters, it is not always possible to unambiguously identify a single process that dominates the spatial or temporal geochemical evolution of the near-field.

The following is a list of key processes and associated uncertainties that were identified in this report:

- Diffusive exchange between the fully saturated cementitious near-field and the host rock is expected to cause (minor) concrete degradation within the first tens of thousands of years (Sections 3.3.2 and 3.3.3).
- Diffusive exchange across fully saturated concrete/clay interfaces might result in decreased porosity zones surrounding the emplacement caverns and possibly reduce the solute and mass transport across the interface within relatively short times (hundred(s) to thousands of years) (Section 3.3.2).
- A strong reduction in porosity at the concrete/clay interfaces may be possible under water-saturated conditions; however, a complete blockage of the porosity down to the nanometre scale is unlikely to occur (Section 3.3.2 and Prasianakis et al. 2022).
- The water flux in Opalinus Clay is very low and, as a consequence, the concrete degradation due to inflow of Opalinus Clay water will be negligible. Nevertheless, diffusive transport over the cement/Opalinus Clay interface and Opalinus Clay water entering the lower parts of the repository over the long term will alter the cement porewater composition. This should be considered for radionuclide solubility and sorption databases (Sections 3.1 and 3.3.3).
- Internal degradation of concrete by aggregate-cement paste and waste–cement paste interaction may cause a relatively fast degradation of the concrete for the period under consideration (Sections 3.3.5, 3.4, 3.5.3 and 3.5.4). There is a high degree of uncertainty associated with the timescales of these reactions (kinetic parameters, reactive surface areas) (Section 3.3.5). These reactions consume water and are therefore strongly limited by the availability of water (Sections 3.5.2 and 3.5.3)
- The waste–cement interaction and the corrosion of metals cause a (partial) desaturation of the repository and delay the (re-)saturation. For a repository in Opalinus Clay, the gas generation rates and the design of the engineered barrier system control saturation times. Sensitivity analyses performed using two-phase flow models show that, with an appropriate design, the partially saturated phase may last more than 100,000 years even for low gas generation rates (Section 3.1).
- Some waste–cement interactions, specifically the long-term degradation and stability of most organic wastes, have not been studied in detail and therefore are not sufficiently constrained (Section 3.4.1). Some degradation pathways of organic materials are known, but there is a clear lack of experimental data for conditions relevant for a cementitious L/ILW near-field. This specifically implies high uncertainties for the degradation rates of organics. On the one hand, specifically a partially saturated cementitious near-field inhibits microbial life. On the other hand, if enough water and nutrients are available, microbiological niches can develop locally in the L/ILW near-field.
- CO_2 gas generation by microbially mediated degradation of organic material could potentially cause carbonation of large amounts of cementitious materials in waste packages and their surroundings (Sections 3.4.1 and 3.4.3). As carbonation lowers the pH towards neutral values, corrosion of embedded steel/iron would be strongly accelerated. If the biotic degradation pathway is strongly suppressed or not possible at all (see previous point), no CO_2 would be released and there would be no feedback to metal corrosion by cement carbonation.

- The desaturation of the near-field will slow down diffusive transport (of solutes and water) in the repository and delay the chemical reactions which are associated with concrete degradation (Sections 3.2.1 and 3.5.2). The exact quantification of the effective transport parameters in the system strongly depends on poorly known transport parameters under partially saturated conditions.
- Under partial saturation conditions, as long as water is present in sufficient quantities, internal concrete degradation and waste-cement interaction may continue, however with reduced reaction rates (Section 3.5.2). It may well be that under such conditions the internal concrete degradation is the dominant degradation process.

Based on this analysis, two major aspects of conceptual uncertainties affecting most transport, mechanical and chemical processes can be identified:

- the evolution of the microscopic pore space which determines material and transport parameters and
- the local availability of water

Evolution of the pore space

Precipitation and dissolution processes are always associated with volume changes (Sections 3.3 to 3.5). The extent of these volume changes is well characterised, but the impact on the geometry of the pore space is not well known. The geometry of the pore space is a key factor for various relevant material properties such as pore size distribution, connectivity, reactive surfaces, diffusion coefficients and permeabilities, and affects not only transport and mechanical properties but also chemical parameters such as kinetic rates, or even microbial activity (Prasianakis et al. 2022). Due to local chemical reactions, these material properties evolve over time and, in the case of strong geochemical gradients between different materials, this results in non-linear evolution of the local mass transport properties. There is also a strong dependence on capillary pressure – saturation properties and on the pore size distribution in partially saturated media.

The majority of currently available chemical, mechanical and transport models describe bulk macroscopic changes in porosity, but do not account for microscopic changes (Prasianakis et al. 2022). It is conceivable that a lack of microscopic knowledge may give rise to a significant uncertainty on the macroscopic scale. For example, the time dependence of mineral precipitation/ dissolution can be described by macroscopic rate laws, which require a microscopic knowledge of rate constants and reactive surface areas and their change with pore space alterations. These microscopic parameters are largely unknown for most minerals, especially for the case of mineral precipitation. Similar knowledge gaps exist for flow and transport properties, e.g. how capillary pressure – saturation curves evolve with degradation of cement materials by different processes.

Repository saturation and the availability of water

The availability of water plays a key role in the system evolution (Sections 3.1, 3.2 and 3.5.2). Internal degradation by aggregate-cement interaction (Section 3.3.5), as well as metal oxidation reactions (Section 3.4.4) and the microbial degradation of organics (Section 3.4.1) are only possible in the presence of sufficient amounts of water since these reactions consume water and/or involve dissolution/precipitation from an aqueous phase. The water has to be transported to the reaction front or has to be available from a 'reservoir', i.e. water filling the pore space (porosity). The actual availability of water, as a solvent and reactant, is the key limiting process. Moreover, once released, most radionuclides may be transported only via diffusion though a connected water phase.

Despite all the shortcomings outlined for the pore space changes, well-developed concepts for transport by diffusion, or by advection, or both, in fully saturated media are currently available. It is possible to estimate total porosities and their changes through dissolving/precipitating phases. Furthermore, concepts on how the changing porosities might affect transport are available (Poonoosamy et al. 2020, Prasianakis et al. 2022).

If water is partly replaced by a gas phase, however, the system description is more complex, since interaction of two phases (fluid and gas) which occupy variable portions of the pore space need to be considered. The actual gas/fluid ratio is itself a complex function of, for example, pore size distribution, pressure, temperature, external and internal sinks/sources for gas and water.

It is well known (Martin et al. 2023, Nagra 2008a, Prasianakis et al. 2022) that the diffusive and advective transport of solutes is significantly slowed in partially saturated media. All processes that rely on water and solute fluxes are therefore limited by the partial saturation of the system, especially the evolution (degradation) of external (cement/host rock) and internal (aggregate/ cement and waste/cement) interfaces. The diffusion of water vapour in the gas phase might be the dominant water transport process under partially saturated conditions. Vapour diffusion is relatively fast, but the total flux may be limited by the relative humidity at the given pressures and temperatures.

If water is removed from the available porosity by reactions, this internal consumption of water produces a humid system in which narrow pores contain the remaining water and the wider pores are filled with gas and water vapour. In such systems, the water transport (to reaction fronts) is enhanced due to the fast diffusion of water vapour via the gas phase, but the solute transport (towards the far-field) in a connected fluid phase will be slowed. This interplay between water consumption, gas/vapour production and nuclide transport in partially saturated systems could be an important aspect, which is at present only poorly understood (see e.g. Huang et al. 2021).

Despite some remaining uncertainties, this report is the most detailed review of processes and conditions available for the cementitious near-field of an L/ILW repository. Overall, it can be concluded that the cement-based near field accomplishes its assigned safety functions according to the assessment presented in this report. The cement phases and the associated high porewater pH, particular in the desaturated part of the repository, contribute to the retention and slow release of radionuclides. In addition, the high pH and the desaturated conditions will slow down metal corrosion rates and gas generation.

3 Chemical evolution of the disposal system: relevant processes and materials

This chapter begins with a description of the disposal system in a combined repository for SF/HLW and L/ILW. Section 3.1 describes the L/ILW near-field, Section 3.2 describes the expected evolution of the L/ILW section in terms of water and gas saturation. Section 3.3 describes the material evolution in the repository and the evolution at the interface between the cementitious near-field and Opalinus Clay far-field. The interactions of cement phases with several waste types and with aggregates are presented in Section 3.4. Section 3.5 assesses the spatial and temporal heterogeneity of material evolution in the cementitious near-field.

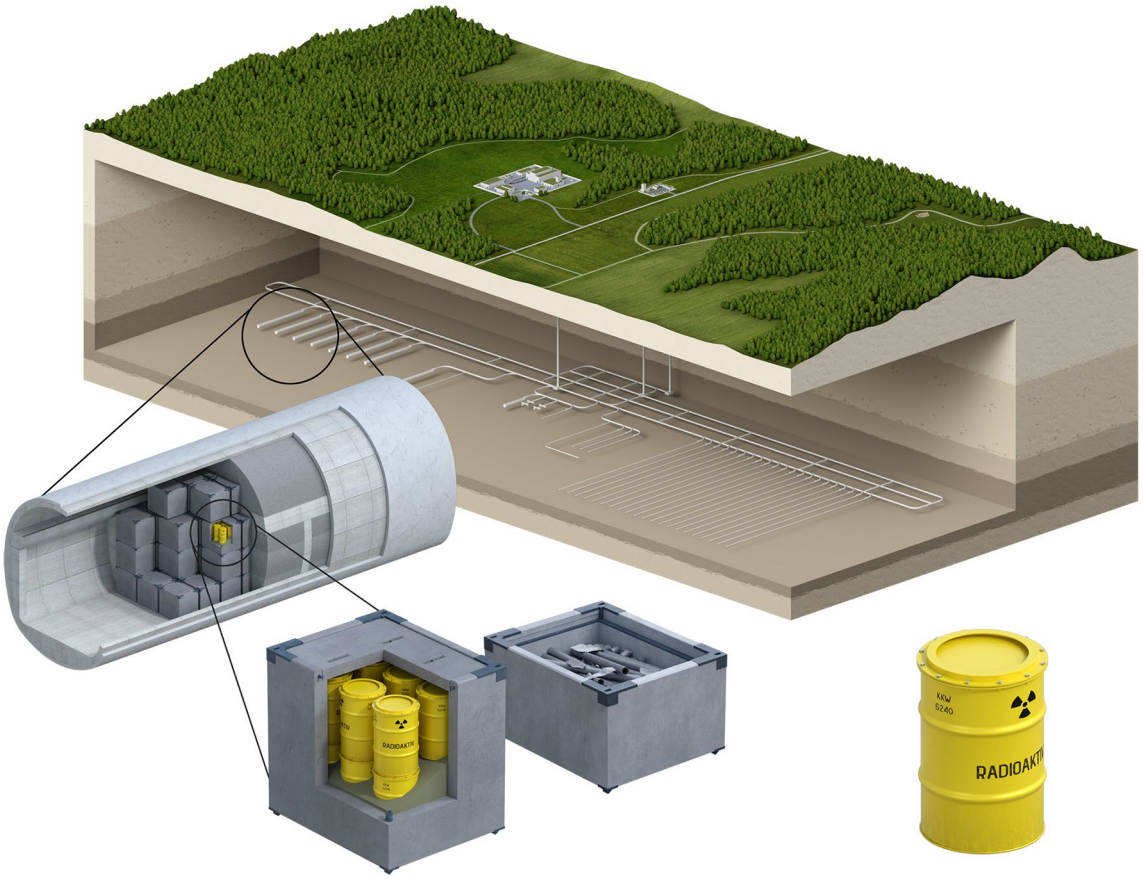

Fig. 3-1: Artistic representation of the elements of the L/ILW section for a combined L/ILW and HLW repository

The example for the L/ILW repository is based on a typical L/ILW waste package type (200 L drum) that is packaged in a disposal container and disposed of in an L/ILW emplacement cavern backfilled with cement-based reference mortar.

3.1 The L/ILW near-field safety barrier

The safety concept for the planned repository is described in Nagra (2021d) and is based on a multi-barrier system as shown in Fig. 3-1. The L/ILW near-field comprises one pillar of safety (Nagra NTB 24-22 *in prep.*), which generally includes the following elements: the waste matrix and waste packages, the disposal container, the container infill mortar, the mortar for backfilling the L/ILW emplacement caverns, the backfilling and sealing elements of the underground structures, the host rock and any confining rock units.

General concept

The generic layout of a combined repository for SF/HLW and for L/ILW is given in Nagra (2021d) and is shown in Fig. 3-2. The access to the repository is provided by

- the access shaft (labelled 8 in the figure)
- the operations shaft (labelled 1), and
- the ventilation shaft (labelled 2)

These three shafts connect the surface to the central area (labelled 3) at the disposal level, from where the HLW and L/ILW disposal areas are constructed and accessed during repository operations. Facilities for underground geoscientific investigations and demonstrations (labelled 4, 5 and 6) are also connected to this central area.

HLW disposal area

The HLW disposal area (labelled 20 in Fig. 3-2) consists of parallel emplacement drifts, connected to the central area by three tunnels:

- the operational tunnel (labelled 15)
- the ventilation tunnel (labelled 16), and
- the construction tunnel (labelled 17)

Separate construction and operations tunnels are required in the HLW disposal area for the sequence of operations foreseen during waste emplacement, which takes place in parallel with the successive excavation of individual emplacement drifts. Each drift is backfilled continuously as emplacement of canisters for SF and vitrified HLW proceeds and, once emplacement and backfilling of the drift are complete, the drift is closed as quickly as possible using a seal (for the information on the sealing system, see below)[1]. Rapid closure serves to prevent human intrusion and reduces the likelihood of damage to the repository (e.g. due to accidental flooding) and transfers the emplacement drifts to a passive state protected by the multi-barrier system.

[1] The sealing elements will be constructed with bentonite material, which is emplaced as pellets or granules. The target dry emplacement density is 1.45 kg/m^3. The current target intrinsic permeability for water of the seals is 10^{-18} to 10^{-19} m^2. The provisional length of each sealing elements is about 10 m (ca. three times the tunnel diameter; 2.8 m inner diameter and 3.5 – 3.7 m with removed tunnel support). Each sealing element is enclosed by two abutments consisting of non-reinforced, structural concrete, with transition layers of sand, gravel, masonry, etc. on either side of each of the abutments (Martin et al. 2023).

L/ILW disposal area

The L/ILW disposal area (labelled 13 in Fig. 3-2) consists of parallel dead-end emplacement caverns. The emplacement caverns are connected to the central area by two tunnels:

- the operations tunnel (labelled 9), and
- the ventilation tunnel (labelled 10)

The emplacement cavern design for L/ILW is illustrated in Fig. 2-1. According to the current design, the dead-end caverns have an internal width of about 11.5 m and a height of about 12.5 m. The length of each cavern is approximately 200 ± 50 m. The caverns are connected to the operations tunnel by branch tunnels that are enlarged at their transition sections.

The lining of the caverns is constructed based on a two-shell principle. According to the current concept, the outer shell consists of fibre-reinforced shotcrete with a thickness of about 20 to 25 cm and has a temporary function as short-term rock support. This shotcrete layer will be emplaced directly on the exposed rock surface. The tunnel is supported by gliding arches, which will take up the first convergence of the tunnel. After the initial convergence has ceased, the inner liner shell will be emplaced, consisting of in-situ concrete that is placed by formwork and is designed to withstand the final ground loads. For this reason, its thickness will vary depending on the selected site, but is expected to be about 40 cm. The base of the tunnel will contain reinforced concrete and the invert will be filled with poured concrete (not reinforced).

L/ILW disposal containers will be emplaced in the cavern. The void space between waste containers and tunnel lining, as well as transfer and unloading area are envisaged to be backfilled with a porous mortar composed of monograined aggregate material and hardened cement paste (type M1 mortar, Jacobs et al. 1994). The enlarged section of the branch tunnel at the cavern entrance will also be backfilled with this mortar. Afterwards, a V1-L/ILW seal will be installed (Martin et al. 2023, for details see Nagra 2021c). The mortar envisaged for backfilling the L/ILW emplacement cavern is very porous and permeable, aimed at providing gas storage volume until the gas is slowly released through the V1-L/ILW seal, and such that damaging gas overpressure in the L/ILW caverns is avoided.

The service and operations tunnels after the seal have a diameter of about 5 to 6 m. Rock support for the operations tunnels and for the branch tunnels that connect them to the emplacement drifts and caverns will either be formed of shotcrete or will follow the two-shell principle outlined above for the L/ILW emplacement caverns.

Pilot repository and underground research facilities

In addition to the main HLW and L/ILW disposal areas, there are pilot repositories for SF/HLW (labelled 18) and for L/ILW (labelled 12). Access to the pilot repository is provided via short tunnels that branch from the operations tunnels for the main HLW and L/ILW disposal areas. The pilot repositories will be filled with a representative mix of waste packages and their evolution will be monitored (labelled 19 and 11, respectively).

The emplacement caverns and drifts and other underground openings may remain open after excavation and installation of rock support and prior to waste emplacement. While these structures remain open or partially open, they will be ventilated and cooled to maintain the legally defined ambient working conditions for underground mining activities.

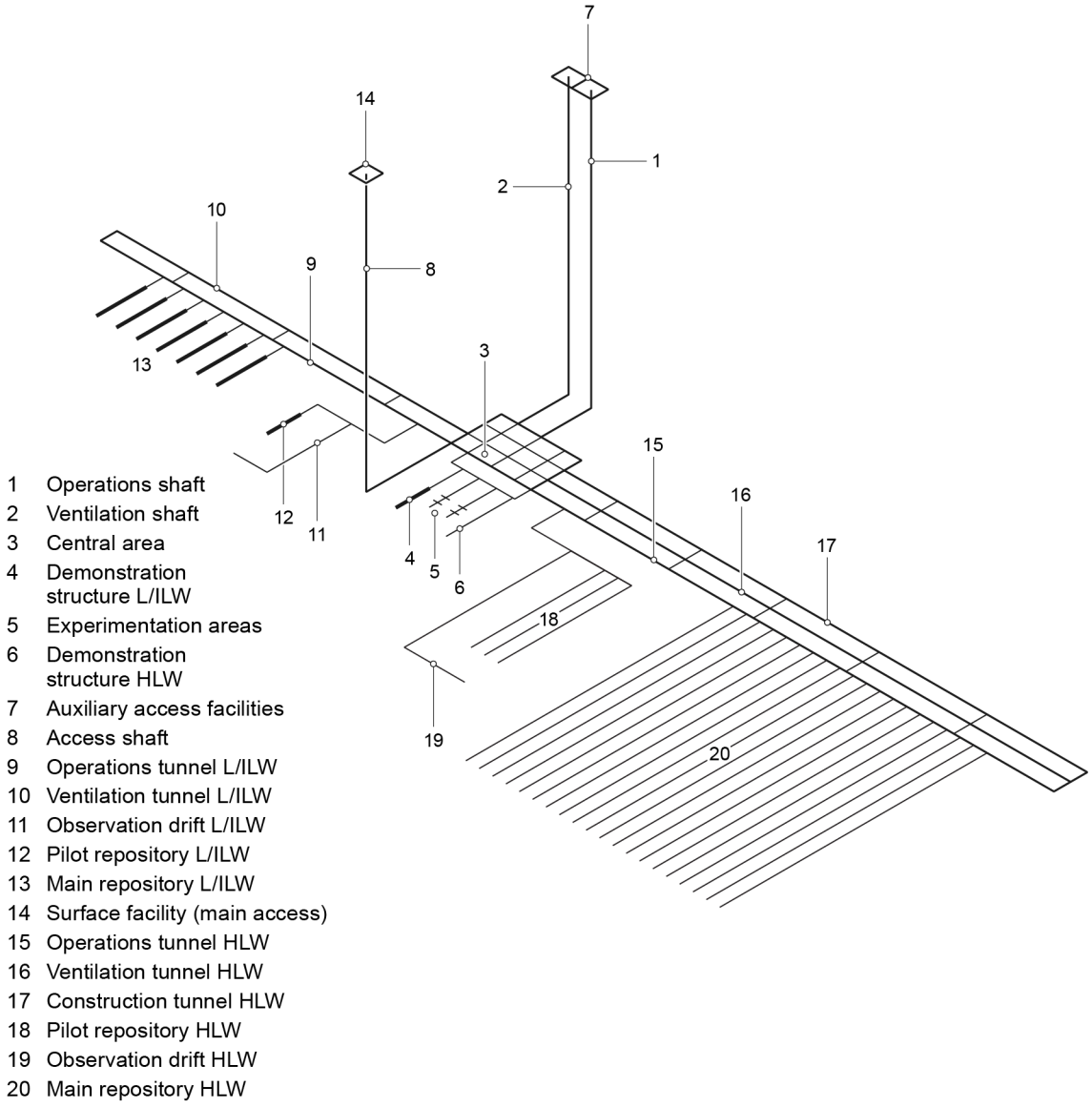

Fig. 3-2: Layout of the underground facilities of a provisional generic combined repository Nagra (2021d)

Sealing system

The sealing system is a pillar of safety of the staged multi-barrier system (Nagra NTB 24-22 *in prep.*), and serves to isolate the repository from the surface, contribute to the retention and slow release of radionuclides, prevent human intrusion and reduce the likelihood of damage to the repository (e.g. due to accidental flooding) and transfer the emplacement drifts and caverns to a passive state protected by the multi-barrier concept. The generic design of the sealing system and its successive installation and backfilling of the tunnel is described in Nagra (2021c) and the principal components of the seals are described in Section 2.2 of Martin et al. (2023). The sealing system will include multiple individual seals, together with the backfilling of the underground

openings and access structures. The current design for the combined repository foresees three different types of seals (for details see Nagra 2021c):

V1 seals, which will be placed at the entrances to SF/HLW disposal drifts and L/ILW caverns in which the wastes will be emplaced. The design of the V1 seals for the SF/HLW drifts is somewhat different to that for the L/ILW caverns because of the requirement for the latter to be more gas-permeable. Thus, the designation V1-HLW and V1-L/ILW is adopted.

V2 seals, which will close off the disposal areas for L/ILW and for HLW, as well as the pilot repository for HLW and L/ILW after the waste has been emplaced. Similar to the V1 seals, the designation V2-HLW and V2-L/ILW is adopted.

V3 seals, which will be placed in the access, operations and ventilation shafts to seal the repository from the surface environment and protect it from external impacts, including the possibility of future human intrusion.

Backfill material will be emplaced in the open tunnels and facilities between these different seals. Backfill material VF1 will be emplaced between the V1 and V2 seals and backfill material VF2 will be emplaced between V2 and V3 seals.

Backfilling and sealing of tunnel system

For the closure of the repository, the tunnel system will be backfilled with a material that should provide a storage volume for gas, in particular for the gas released via the V1-L/ILW seals from the L/ILW emplacement caverns. As such, the backfill is required to maintain a high permeability as well as a high gas-accessible porosity (cf. Martin et al. 2023). The backfill materials have the further role of ensuring mechanical stabilisation of the underground openings, preventing or limiting tunnel convergence that might potentially cause damage to the geological barrier. These requirements can be fulfilled by a swelling clay mixed with a suitable grain-supported material. Candidate materials include excavated clay which would be mixed with sand and/or gravel, or a sand-bentonite mixture (Nagra 2021c, Martin et al. 2023).

Each L/ILW disposal cavern will be closed with a V1-L/ILW seal (Fig. 3-3) that is constructed in the branch tunnel that connects the cavern to the operations tunnel.

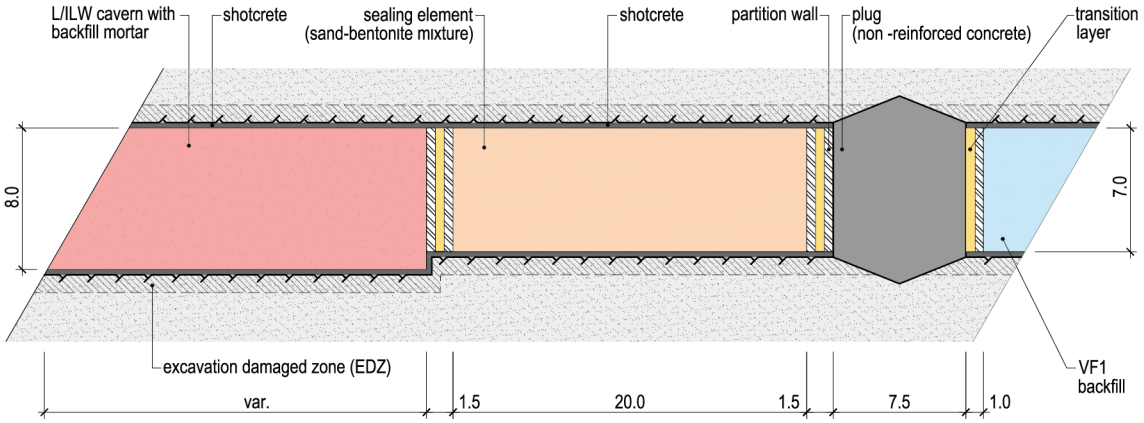

Fig. 3-3: Longitudinal section of a provisional V1-L/ILW seal

Distances are given in units of metres.

Nagra (2021c)

The sealing element separates the loose VF1 backfill from the disposal field of the L/ILW cavern. A sand-bentonite mixture in a weight-ratio of 80:20 is used. The permeability of the gas-bentonite mixture is such that it ensures gas pressure equalisation between the L/ILW emplacement cavern and the VF1 backfill, which has the role of providing additional gas storage volume.

On the cavern side of the seal, the porous backfill mortar supports the sealing element. On the other side of the sealing element, an abutment is placed as support, with a transition layer on either side. The dimensioning of the seal, based on a branch tunnel diameter of approximately 6.5 – 7 m, results in a length of ca. 30 m.

The V2 seals (Fig. 3-4) serve to close the L/ILW and HLW disposal areas and the access to the pilot repositories. The seals are constructed after all the waste has been emplaced and the tunnels are backfilled with VF1.

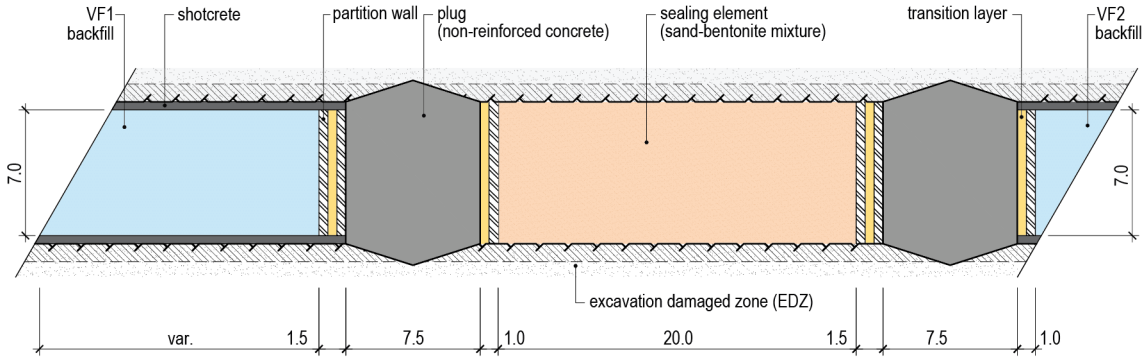

Fig. 3-4: Longitudinal section of a provisional V2-L/ILW seal, assuming that sand-bentonite is used as the sealing material (Nagra 2021c)

Distances are given in units of metres.

A sand-bentonite mixture will be used for the V2-L/ILW sealing element, with a permeability which ensures gas pressure equalisation between the VF1 backfill and the VF2 backfill over time, providing additional gas storage volume.

Each sealing element is enclosed by two abutments consisting of structural concrete, with transition layers of sand, gravel, masonry, etc. on either side of each of the abutments. The tunnel diameter in which the seals are installed is expected to be ca. 6.5 to 7 m. The pre-dimensioning of the abutment suggests they will each require a length of approx. 7.5 m. The sealing elements have a length of about 20 m, which corresponds to about three times the tunnel diameter. The entire sealing structure has a length of about 40 m, calculated conservatively, with about 1.0 m to 1.5 m for each of the four transition layers, together with their formworks.

3.2 L/ILW disposal system evolution in terms of liquid and gas saturation

This section describes the disposal system and its evolution with the focus on liquid and gas saturation. It makes use of information and repository layouts given in Martin et al. (2023) and Nagra (2021c & 2021d).

3.2.1 Water saturation of the repository and related processes

The description of pre- and post-closure saturation evolution in the following sections follows Martin et al. (2023) and is based largely on the calculations described in Papafotiou & Senger (2016).

Evolution during the pre-closure period; impact of excavation, ventilation and cooling

Even prior to the emplacement of waste, processes may occur that affect the later performance of the repository, including the rate of repository gas generation. The excavation and ventilation of the open tunnels will lead to the gradual desaturation and depressurisation of the surrounding rock (Leupin et al. 2016b), resulting in the creation of desiccation cracks in the unlined tunnel sections. Precipitation of salts may occur in these cracks due to evaporation of porewater and also increase the salinity of the pore fluid, as was observed in the ventilation (VE) experiment at Mont Terri (Bossart & Nussbaum 2007).

Due to the presence of the CO_2 in the air brought in by the ventilation, cement-based materials used, for example, as tunnel support, will be carbonated near their surfaces (Trotignon et al. 2011). This may affect the passivation of the steel reinforcement within the concrete exposed to carbonation, if the thickness of the concrete covering the rebars is too thin.

Water saturation of cement-based tunnel support will decrease, because of the ventilation and capillary suction from the desaturated rock. This process may result in a drying out of the shotcrete on the tunnel wall, potentially resulting in a concrete that is sensitive to chemical attacks due to the generated micro-cracks.

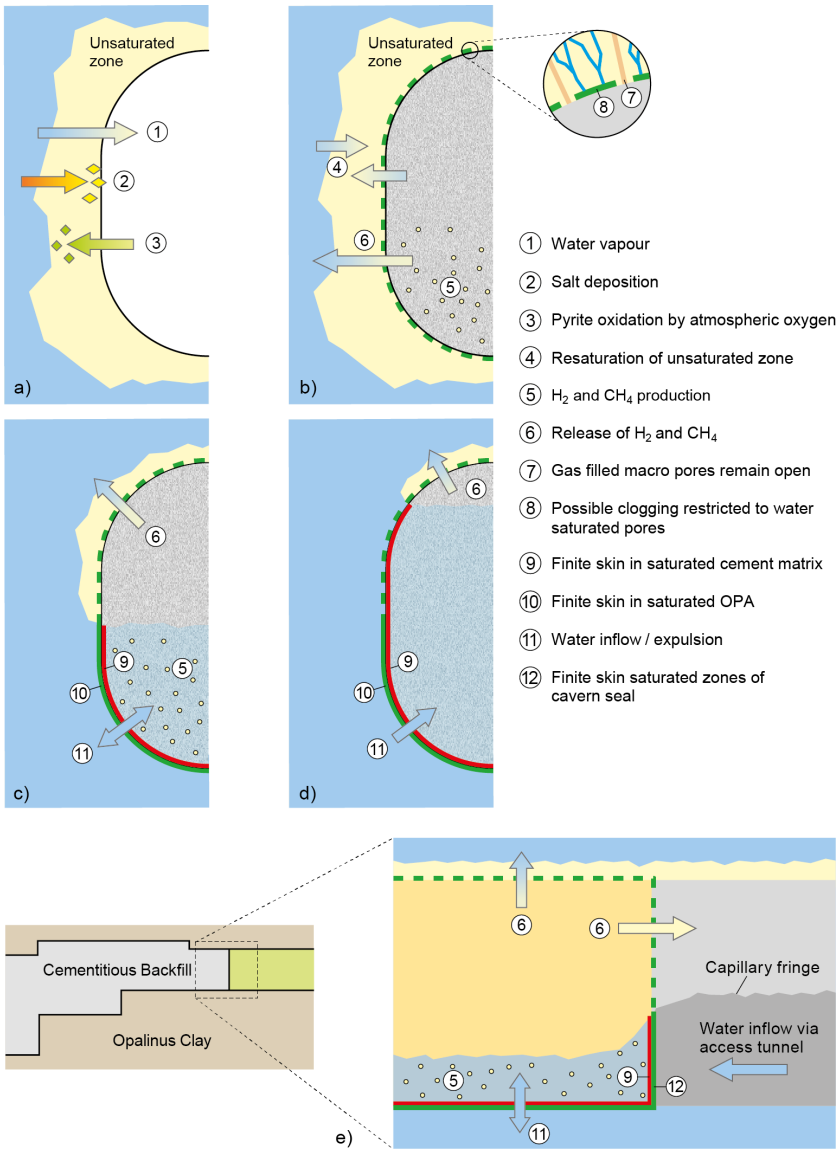

Fig. 3-5: Schematic illustration of the evolution of an L/ILW emplacement cavern and its immediate surroundings during the operational phase and after closure

a) Development of an unsaturated zone during the operational phase. b) – d) Mass transfer processes at early time, mid time and late time after closure. e) Mass transfer processes around the V1-L/ILW seal after closure (Nagra 2008a).

Post-closure evolution, saturation and the fate of gas

At the time of repository closure, the underground structures and the immediately surrounding rock will be only partly saturated with water. The post-closure evolution of the repository, including the eventual full saturation of porous materials with water and the transport of repository-generated gas, has been described in several reports (Leupin et al. 2016a, Martin et al. 2023, Nagra 2008a).

Fig. 3-5 summarises the expected evolution of the L/ILW emplacement caverns. Gas and water redistribution in the system is controlled by chemical and transport source/sink terms for gas and water as well as the capillary, buoyancy, and viscous forces acting in the different materials. As will be discussed in Section 3.4, gas is mainly produced by (bio-)chemical reactions (degradation of organic material and metal corrosion). It is then distributed in the emplacement caverns and other underground openings and will enter the Opalinus Clay, where it will be dissolved in porewater and diffuse away from the repository. A small part of the hydrogen gas will be consumed by microbial activity along the tunnel system.

As discussed in Section 3.5.2, gas and water transport as well as kinetic and equilibrium chemical reactions that change porosity in concrete and clay compartments are influenced by water saturation. As a result, gas source terms are probably influenced by water saturation-dependent degradation of cement materials used for waste conditioning (Huang et al. 2021, Kosakowski et al. 2020). Most chemical reactions consume significant amounts of water and might cause a significant change in liquid saturation locally, i.e. in an intact waste package.

Saturation of the near-field rock

Following backfilling, partially saturated domains of the near-field rock will slowly saturate due to flow from the host rock towards the caverns, driven by the pressure gradient. Saturation of the near-field rock driven by the movement of water from the undisturbed host rock is controlled by the host rock permeability and pore compressibility. Saturation of the excavation disturbed zone (EDZ) will be associated with swelling and self-sealing of EDZ features (Alcolea et al. 2014, Lanyon 2019b, 2019a). At the same time, the EDZ may further extend in spatial dimensions due to increasing pore pressure and possible ongoing compaction, caused by pore pressure recovery/ equilibration and crack growth. The (re-)saturation of the near-field rock will depend on the near-field gas pressure. High gas pressures will delay the saturation for very long times.

L/ILW caverns

After waste emplacement and sealing of the L/ILW caverns, water from the host rock will start moving towards the caverns due to the hydraulic pressure gradient. At the same time, porewaters that were present in the materials at emplacement will start to redistribute due to their different capillary suction (i.e. mortars, waste packages, concrete). The partially saturated EDZ will begin to saturate with porewater supplied from the emplacement caverns and surrounding rock. As the EDZ saturation increases, water from the rock will start moving into the caverns and some water will accumulate under gravity above the cavern floor between the shotcrete and clay (Fig. 3-5c). Accumulation of water in the lower part of the caverns may influence the evolution of underlying EDZ, which will resaturate and thus seal faster than other parts of the EDZ (Fig. 3-5c).

By the time of repository closure, it is expected that the L/ILW emplacement caverns will have a very high relative humidity but no – or little – free water will be present depending on the chosen emplacement saturation of the cavern materials. The gases present will be a mix of trapped air and repository-generated gases. Anaerobic conditions will develop during this phase due to the consumption of O_2 in the trapped air by aerobic corrosion, oxygen sorption on clay materials and other processes (Leupin et al. 2016a).

After repository closure, it is expected that a free gas phase will be present at all times in the L/ILW repository (Fig. 3-6; Papafotiou & Senger 2016). Once free oxygen is consumed, the gases will be produced by the anaerobic corrosion of metals (Section 3.4.4), which produces H_2 by microbial and chemical degradation of organic matter (Section 3.4.1). This may produce gaseous compounds such as CO_2 and CH_4 and, to a lesser degree, by radiolysis (Diomidis et al. 2016,

Guillemot et al. 2023, Leupin et al. 2016a, Nagra 2002a). There are also indications that gases will be consumed by microbial and chemical processes (Section 3.4.3 on carbonation and Section 3.4.6 on the fate of hydrogen).

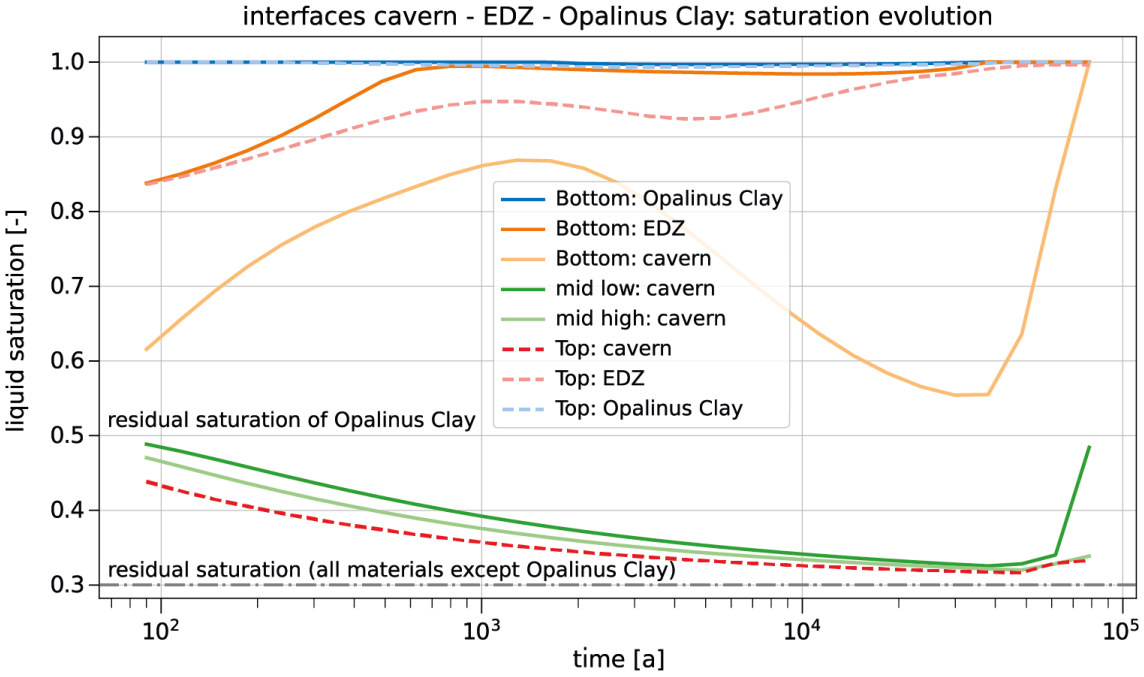

Fig. 3-6: Temporal evolution of liquid saturation of the cavern and neighbouring materials

Data extracted from base case model in Papafotiou & Senger (2016)

Overall, the amount of gas generated as a function of time depends on the inventories (steel, organic matter) and the gas generation rates, which depend on the local conditions of cement and other materials in a highly heterogeneous near-field, as well as the availability of water.

Gas generated from the corrosion and degradation of materials in the L/ILW caverns will first dissolve in porewater and then, once the solubility limit is reached, form an additional gas phase. Pressure in the cavern will begin to increase due to the simultaneous gas accumulation and porewater inflow from the surrounding rock. Model calculations indicate that the net water flow from a cavern towards the EDZ in the early post-closure phase is very low, with fluxes in the order of < 0.5 dl/m^2/a according to data extracted from Papafotiou & Senger (2016). Water flow with fluxes lower than 0.1 dl/m^2/a from the EDZ into the cavern will only start after about 40,000 years, once the EDZ is fully saturated and gas pressures decrease. During the early post-closure phase, any water that would be present is sucked out of the cavern into the V1 seal. After a few hundreds of years, the water transport direction is reversed and very low water fluxes of 0.1 dl/m^2/a across the V1 seal into the cavern are predicted by the models. Water accumulation in the caverns will occur very slowly after 40,000 years in the bottom part of the L/ILW emplacement caver (Fig. 3-6), while highly desaturated conditions with waste-generated gas will persist in the upper parts for several tens of thousands to hundreds of thousands of years. Sensitivity analyses show that gas will accumulate at pressures that are not expected to be damaging.

Saturation of the V1-L/ILW and V2 seals and the remainder of the repository

To allow for greater gas permeability and a lower gas entry pressure, the V1-L/ILW and V2 sealing elements are composed of a sand/bentonite mixture. The design goal is to enable a higher gas permeability, such that gas pressure equilibration between an emplacement cavern and specific tunnel sections is possible. This implies that, even at a high degree of saturation, these seals should allow the migration of repository-generated gas, such that the sealing system as a whole provides a gas storage volume, avoiding the possibility of high gas pressures that could damage the rock. This assumes, however, the absence of significant pore blocking, as discussed in Prasianakis et al. (2022) and Martin et al. (2023). Pore blocking is not expected in those parts of the seal and material interfaces that remain unsaturated for long times. According to Martin et al. (2023), design measures in the form of material choices for transition layers and concrete plugs are available that are expected to limit pore blocking within and around the seals.

Shortly after repository closure, porewater in the V1 seals will begin to redistribute within the seals through the interaction of capillary and buoyancy forces, while some water mass will be transported into the surrounding unsaturated EDZ (Fig. 3-7 top). The gradual increase of gas and liquid pressures in the L/ILW emplacement caverns will result in minimal water expulsion from the caverns into the V1 seals (and subsequently to the VF1 backfill). Saturation in the lower part of the less permeable sealing elements will increase slowly until pressure in the L/ILW emplacement caverns exceeds hydrostatic pressure (ca. 2,000 years in Fig. 3-7, top) and gas transport through the seals increases. At the same time, the upper part will remain unsaturated for several tens of thousands of years, forming the predominant pathway for gas release to the VF1 backfill. Accordingly, saturation in the tunnel backfill VF1 will have a similar evolution in the lower and upper part (Fig. 3-7, bottom). In the late post-closure phase (> 50,000 years), gas generation decreases significantly and the V1 seals and VF1 backfill begin to saturate with porewater from the surrounding rock.

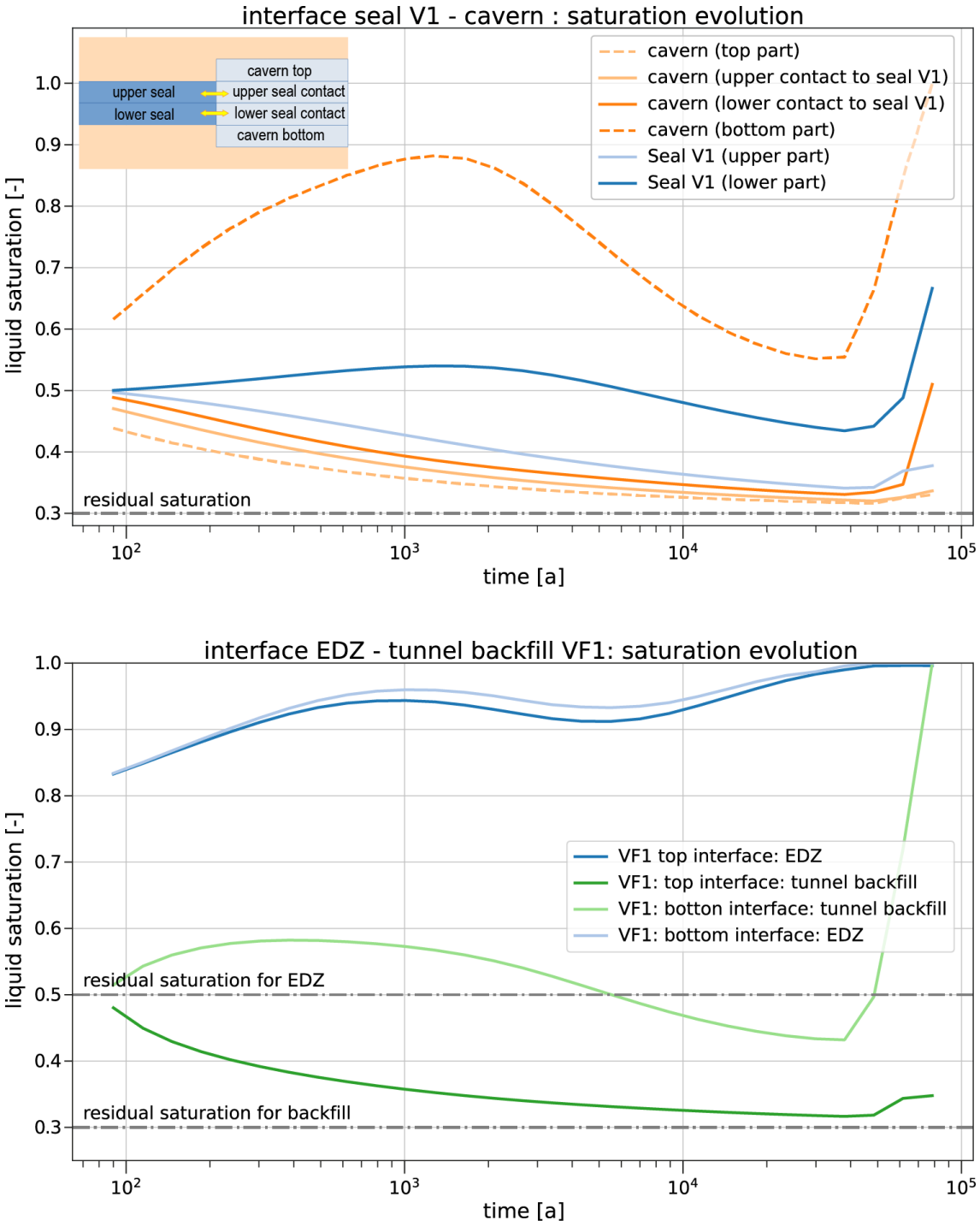

Fig. 3-7: Top: Temporal evolution of liquid saturation for seal V1 and adjacent cavern. Bottom: Temporal evolution of liquid saturation at the top and bottom interface between tunnel backfill/EDZ halfway between seals V1 and V2

Data extracted from base case model in Papafotiou & Senger (2016)

Uncertainties associated with saturation

Extensive modelling has been carried out by Nagra at different spatial scales to elucidate the saturation of the repository and the fate of repository-generated gas (Diomidis et al. 2016, Leupin et al. 2016a, Nagra NTB 24-23 *in prep.*, Papafotiou & Senger 2016, Senger & Ewing 2009).

Papafotiou & Senger (2016) systematically investigated the influence of processes and material parameters on saturation of an L/ILW repository. This includes scenarios that investigate the influence of sealing system layout, two-phase flow properties of the EDZ and Opalinus Clay, the gas generation rates and consideration of microbial consumption of hydrogen in tunnels.

They report that the parameterisation of materials is of lower impact with respect to two-phase flow parameters, i.e. the choice of residual saturation for capillary pressure – saturation relations and an enhanced gas mobility by changing the relative gas/water permeability – saturation parameterisation.

Gas generation rates have a large impact on gas pressures and the saturation of the repository. Higher gas generation rates cause a fast pressure increase above hydrostatic pressure that prevents early saturation of the repository. Peak gas pressures are reached within a few ten thousand years. The subsequent decrease in gas pressure below hydrostatic pressure causes inflow of formation water into the repository within a few ten thousand years. Due to the low water flow rates, complete saturation of the whole repository will take 100,000 years or even longer.

Very low gas generation rates cause water inflow in the first ten thousand years and result in a partial saturation of the repository. This will keep the repository at partially saturated conditions for very long times. Gas pressures will exceed hydrostatic pressure only after about 10,000 years and will remain constant for very long times.

In their models, Papafotiou & Senger (2016) considered the consumption of hydrogen by microbially mediated sulphate reduction in operations, ventilation and access tunnels. They were able to show that the consumption of hydrogen might contribute to reduction of peak gas pressures, but that it has a relatively small influence on overall saturation times. In general, the availability of sulphate in porewater is a limiting factor for sustainable hydrogen consumption.

Papafotiou & Senger (2016) found that the design and the permeability of the seals and tunnel backfill significantly influence gas pressure build-up in the repository. For low permeability seals and tunnel backfill, peak gas pressures are increased.

In general, the simulated modelling scenarios show a clear correlation between pressure build-up and the gas release via different gas pathways. Two gas release pathways are of major importance: the release via the tunnel system and repository seals into the shafts, and the release via the EDZ into the host rock. The first release pathway is generally dominant and provides the largest contribution in highly permeable sealing systems and generates lower gas peak pressures. The latter pathway becomes more important at higher gas pressures and lower permeability of the host rock. Higher gas pressures lead to an increase in the concentrations of dissolved gases and increase concentration gradients driving the diffusive transport at the gas/water interfaces.

In summary, the different scenarios calculated by Papafotiou & Senger (2016) taking into account a broad range of design variants, gas generation rates and material properties show that full saturation of the repository within the first 100,000 years is unlikely.

3.3 Evolution of cementitious near-field materials and interaction with the host rock

This section starts with a description of the classical cement degradation model considered in Kosakowski et al. (2014). The processes that cause degradation of cement materials and affect the neighbouring host rock are detailed in separate sections: cement/clay interactions in Sections 3.3.1 to 3.3.4, aggregate/cement interactions in Section 3.3.5 and carbonation in Section 3.4.3. The possibility to create and release clay and cement colloids is reviewed in Section 3.3.6.

3.3.1 Degradation of cementitious materials

Overview/general description

Cement-based materials are essential components of the engineered barrier system. From a geochemical viewpoint, their most important property is their ability to maintain a high pH of the water in the near-field. The high porewater pH and the presence of cement minerals is favourable for the sorption of many radionuclides (Tits & Wieland 2023, Wieland 2014, Wieland & Van Loon 2003), which slows down steel/iron corrosion (Diomidis 2014, Diomidis et al. 2023), and suppresses microbial activity (Small 2019). The ability of cementitious materials to maintain a high porewater pH is related to the fast reactivity of cement phases. Changes in porewater composition induced by external or internal processes therefore cause degradation of cementitious materials. Depending on the composition of the cement-based material, the solute composition and transport regime, the induced effects can be complex. Typically, calcium and OH^- leaching (by diffusive or advective transport, or other processes such as aggregate-cement reactions) causes sequential dissolution of cement phases according to the degradation model described by Berner (Berner 1992, Ochs et al. 2016, Wieland & Kosakowski 2020). In the near-field of an L/ILW repository, several processes might cause cement degradation:

- Carbonation (Section 3.4.3): CO_2 produced by degradation of organic material or present in the air during the repository operational phase can cause cement carbonation, i.e. the transformation of hydrated cement phases to carbonate and other secondary carbonation products.
- Aggregate-cement interaction (Section 3.3.5): Silica and alkali ions from dissolution of alumina-silica aggregates or accessory minerals can promote pozzolanic reactions and alkali-silica reactions (ASR).
- Cement/clay interactions (Section 3.3.1): The diffusion-driven equilibration of porewater composition at the contact of cement with the Opalinus Clay host rock might cause complex changes in cement and clay mineralogy. Typically, a thin low-porosity layer is formed at the cement/clay interface.

Cement degradation

For SGT Stage 2, chemical degradation of cement was modelled in terms of groundwater ingress from the host rock and by diffusive mixing of host rock porewaters with cement porewaters (Berner et al. 2013, Kosakowski et al. 2014, Kosakowski & Berner 2013). It was found that diffusion-controlled transport of porewater constituents from the cementitious near-field into the host rock is the main driving force for the temporal evolution of the composition of the porewater in the cementitious near-field. In accordance with the attainment of thermodynamic equilibrium, the latter process results in the sequential dissolution of cement phases from the hydrate

assemblage of hardened cement paste, thus giving rise to sequential changes in the solid phase composition with time according to the cement degradation model of Berner (Berner 1992, Kosakowski et al. 2014, Wieland & Kosakowski 2020).

The Berner model has been developed in accordance with experimental observations (Atkinson et al. 1988, Faucon et al. 1996) and was considered in earlier safety assessments performed by Nagra (Nagra 1994, 2002a). More recently, the model has been used to describe the geochemical evolution of the L/ILW near-field (Kosakowski et al. 2014) and the interface between clay rock and cementitious materials (Kosakowski & Berner 2013).

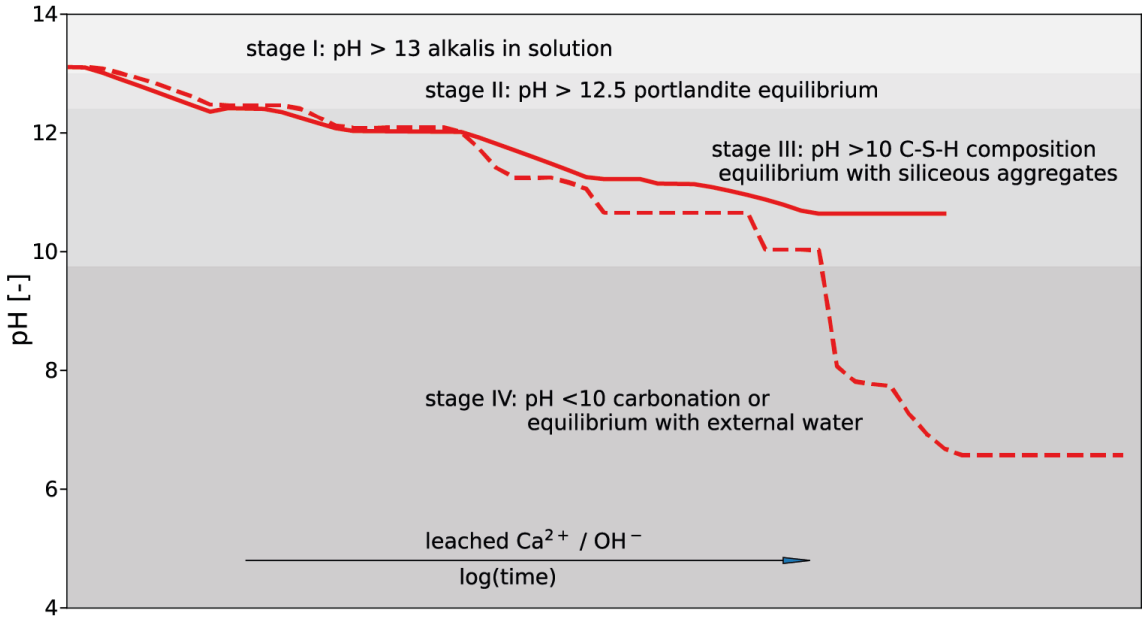

Fig. 3-8: Degradation stages for a typical cement-based material in terms of leached Ca^{2+} due to aggregate-cement reactions (solid lines) and carbonation (dashed lines) with respect to the equilibrium pH of porewater

Sequential dissolution of cement phases results in a stepwise evolution of calculated equilibrium pH.

The three stages and a final stage for completely degraded cement with progressively decreasing pH of the porewater with time are the main feature of the diffusion-controlled models of cement degradation (Berner 1992). In a simplified manner, these stages of cement degradation can be described as follows (Fig. 3-8):

Stage I: This accounts for fresh hydrated cement with pH of the porewater between 13 and 13.5 at 25 °C. The solution composition is dominated by high concentrations of free alkali metal ions, which are released from the clinker minerals during cement hydration. Equivalent OH^- concentrations are generated to fulfil charge balance.

Stage II: The pH of the porewater is controlled by portlandite solubility. The large inventory of the mobile alkalis has been significantly reduced due to uptake by alkali-binding minerals or exchange with the solutes of the porewater of the surrounding host rock. The solubility of portlandite fixes the total Ca concentration [Ca]tot at ~ $2 \cdot 10^{-2}$ M and the pH at ~ 12.5 at 25 °C. This stage is characterised by the presence of portlandite and C-S-H phases with a high Ca/Si ratio in hydrated cement.

Stage III: This stage follows once portlandite is dissolved due to uptake of Ca by secondary precipitates (e.g. $CaCO_3$ in the case of CO_2 formation), aggregate-cement reactions or exchange of Ca with the solutes of the porewater of the surrounding host rock. The pH drops continuously to lower values. The pH ranges between 10 and 12.5 at 25 °C and is controlled mainly by incongruent dissolution of C-S-H phases. The Ca/Si (C/S) ratios of C-S-H phases changes from initially ~ 1.65 at pH ~ 12.5 to ~ 0.8 at pH ~ 10.0 as a consequence of its incongruent dissolution (Atkins & Glasser 1992, Tits et al. 2014). Congruent dissolution of the C-S-H phases occurs at the end of Stage III, buffering the pH at ~ 10.0 (Ochs et al. 2016).

Stage IV: The final stage of cement degradation is reached once all Ca-bearing cement phases (portlandite, C-S-H, AFt, AFm) are dissolved. The pH is controlled by incoming water and by equilibrium with carbonates (calcite) (Ochs et al. 2016). This final stage can only be reached if the cement is carbonated with considerable amounts of CO_2, or if Ca is leached by high fluxes of incoming formation water. The latter can be excluded as a possible degradation mechanism for a repository placed in a low-permeability clay formation (Kosakowski & Smith 2014, Martin et al. 2023).

Hence, the first three stages are characterised by specific compositions of the phase assemblage of hydrated cement and the corresponding porewater in equilibrium with the solid. The latter information, that is changes in the porewater and solid phase compositions in the first three stages, has been used as input for the development of previous cement sorption databases (SDBs) (Bradbury & Van Loon 1996, Bradbury & Sarott 1994, Wieland 2014, Wieland & Van Loon 2003) as well as the current one (Tits & Wieland 2023).

In a deep geological repository, concrete degradation will not be homogeneous in space or time. Several degradation mechanisms will act concurrently on different timescales. In addition, other processes, e.g. water saturation in specific concrete materials and parts of the repository, might locally delay chemical processes in general and concrete degradation specifically.

Timescales

The time span over which most of the degradation of cement materials occurs is mainly controlled by the local saturation evolution and by processes such as aggregate-cement reactions (Section 3.3.5), cement/clay interactions (Sections 3.3.2 and 3.3.3) and carbonation (Section 3.4.3). Section 3.5.4 contains a comparison of the degradation of typical cement materials due to aggregate-cement reactions, which shows that large differences in the timescales even between neighbouring materials are possible.

Uncertainties

The degradation model for cement itself is well established, supported by experimental evidence, and can be modelled using thermodynamic models (Le Bescop et al. 2013, Glasser et al. 2008) (cf. App. A). Major uncertainties are related to the timescale of driving processes and how they affect cement materials in a heterogeneous partially water-saturated repository. Generally, chemical reactions are strongly slowed in a dry environment (Section 3.5.2), either due to lack of water or because (macroscopic and/or microscopic) fluxes of reactants are strongly reduced.

3.3.2 Cement/clay interaction: general overview

Overview/general description

This section summarises the information from the most recent reviews and studies on cement/clay interaction within the framework of radioactive waste disposal (Bildstein et al. 2019, Gaucher & Blanc 2006, Prasianakis et al. 2022, Savage et al. 1992, Savage & Cloet 2018, Seigneur et al. 2019, Wilson et al. 2021).

As detailed in Section 3.1, the cement- and clay-based materials are important components of the barrier system of an L/ILW repository. Cement suspensions, mortars and concrete are used for waste immobilisation (at waste package level), for the disposal container, container infill mortar, tunnel/cavern support, cavern backfill and for sealing tunnels. Clay-based materials are mainly present as tunnel backfill, as tunnel sealing material and in the form of the Opalinus Clay host rock.

Interfaces between cement and clay materials can be characterised by strong (geo-)chemical differences, which drive the diffusive transport of solutes into both materials and induce formation of alteration fronts. Typically, dissolution of cement and clay phases is observed in combination with precipitation of secondary mineral phases at or near the material interface. Alteration distances depend on the transport regime (diffusion vs. advection) and the magnitude of solute flux, the inventory of materials participating in reactions, as well as changes in porosity and transport properties of altered materials. In addition, the alteration fronts might be spatially smeared due to reaction kinetics. Some experimental investigations and nearly all reactive transport studies of cement/clay interactions show significant porosity changes due to precipitation/ dissolution of minerals near the interface. Most of the modelling studies investigate the geochemical evolution of interfaces in low-permeability media where diffusive transport dominates. The simulations predict a strong porosity reduction in narrow zones close to the interface. The reduction of the free connected pore space leads to a reduction of advective and diffusive mass fluxes across the interface, slowing down the geochemical alteration processes.

Savage & Cloet (2018) systematically reviewed modelling studies on evolution of cement/clay interaction with the aim of extracting the consequences for the safety requirements for the bentonite buffer and the Opalinus Clay. Wilson et al. (2021) reviewed experimental, analogue and modelling data on the impact of cement on argillaceous rocks in radioactive waste disposal. Prasianakis et al. (2022) summarised the knowledge on transport across evolving cement/clay interfaces, taking into account the latest experimental studies and state of the art multi-scale modelling approaches.

The studies largely agree in their findings, with the role of the most important processes that govern the evolution of the cement and clay materials emphasised below:

- There is a reasonably good understanding of mineralogical changes that are observed and predicted to form by the models at a contact between cement and clay materials.
- Migration of hydroxyl ions and the associated increase in porewater pH in clays are the main driving forces for mineral alterations.
- High dissolution rates of primary minerals accelerate mineralogical transformations and porosity change and limit the extent of the alteration fronts due to reduction of mass transport across zones with reduced porosity. *Kinetic data appropriate for use in compacted clay systems and under near-equilibrium conditions remain uncertain (Savage & Cloet 2018).*

- The extent of the zone of perturbed mineral and fluid chemistry is controlled mainly by mass transport across the cement/clay interface and the amount of cement material in contact with the clay. Consideration of porosity change feedback for mass transport in reactive transport models not only reduces the progress of alteration fronts, but also changes predicted mineral assemblies.
- Based on mass balance considerations and numerical modelling, it is expected that the zone of perturbed mineral and fluid chemistry in clays will be narrow. Significant changes in clay mineralogy that affect transport properties are expected, in the range of cm up to dm thick in 100,000 or more years (Savage & Cloet 2018, Wilson et al. 2021).
- The porosity is expected to reduce at the cement/clay interface due to precipitation, specifically at the clay side of the interface. It is expected that complete blocking of pore space in compacted clays containing large amounts of micropores (< 2 nm) influenced by charged mineral surfaces does not take place (Prasianakis et al. 2022).
- Recent modelling and experimental studies indicate that anion and cation transport are affected differently by porosity change (Chagneau et al. 2015, Fukatsu et al. 2017, Jenni et al. 2017, Jenni & Mäder 2021, Luraschi et al. 2020). Typically, if porosity is reduced, anion transport across reacting cement/clay interfaces is more strongly reduced than cation transport. The effect is related to an "anion exclusion effect" where anion-accessible porosity is limited due to repulsive interaction with negatively charged surfaces (Chagneau et al. 2015, Wigger et al. 2018). A diffusion pathway available for cations might be blocked for anions by overlapping of electric double layers, which occur typically in small pores or clay interlayers.

Information from experimental and modelling studies

Experimental validation of these processes in field experiments under realistic transport conditions and with real materials is difficult. Some evidence for pore blocking (Wilson et al. 2021) is seen from long-term observations on concrete/clay interfaces at the Tournemire industrial analogue (Gaboreau et al. 2011, Lalan et al. 2016, Soler 2013, Tinseau et al. 2006), from the Maqarin natural analogue (Martin et al. 2016, Pitty & Alexander 2014), the Mont Terri cement-clay interaction (CI) experiment (Jenni et al. 2014, Mäder et al. 2017, Yokoyama et al. 2021) and the Grimsel FEBEX experiment (Gaboreau et al. 2020) (see also Sections 3.3.2 and 3.3.4). Similar observations are reported for civil engineering applications, for example for concrete screw piles in clays (Lee 2001).

More recent laboratory studies conducted at the University of Madrid (González-Santamaría et al. 2020a, 2020b) and at PSI (Luraschi et al. 2020, Shafizadeh 2019, Shafizadeh et al. 2015, 2020) on small samples with cement and clay materials in contact show significant porosity changes at mm scale near the material interface over relatively short times. Diffusion measurements conducted during the course of the experiments show a reduction of diffusive flux of tracers across the interface (see also Sections 3.3.2 and 3.3.4).

Experimental studies of cement/clay interaction provide insight into mineral reactions, progress of reaction fronts and evolution of material parameters. Although long-term experiments like the Mont Terri CI experiment run for more than one decade (installed in April 2007), the timescale covered is much shorter than that of interest for assessment of materials in a deep geological repository. For prediction of the spatial-temporal effects of cement/clay interaction after hundreds of thousands of years or more, computer models calibrated with experimental data from long-term experiments and analysis of natural analogues are commonly used.

In natural analogue studies in the Philippines (Alexander et al. 2008, Reijonen & Alexander 2015) and Cyprus (e.g. Alexander et al. 2013), the stability of bentonites under the influence of alkaline natural groundwaters with the same pH range as low-pH cements has been investigated. Both studies suggested that little reaction of the bentonite has occurred over millions of years. The authors concluded with respect to these natural analogue studies that:

- The field conditions of these natural analogues are considered to realistically simulate those expected in a geological disposal facility.
- The results indicate minimal mineralogical alteration of bentonite by alkaline groundwater over periods of 105 to 106 years with only very minor alteration and replacement of smectite by palygorskite along microfractures.
- The main effect of the interaction of bentonite and alkaline groundwater is replacement of exchangeable Na in the bentonite by Ca, which can affect the swelling behaviour and plasticity of the bentonite.
- The studies suggest that it will be feasible to use bentonite clay barriers together with low-alkali cement and concrete in a deep geological repository, without deleterious effects on the bentonite barrier due to reaction with leachates derived from the cementitious materials.

Information on modelling studies for cement/clay interaction can be taken from review papers on cement/clay interactions or similar topics (Bildstein et al. 2019, Gaucher & Blanc 2006, Kosakowski et al. 2014, MacQuarrie & Mayer 2005, Metcalfe & Walker 2004, Saripalli et al. 2001, Savage & Cloet 2018, Seigneur et al. 2019, Soler 2016, Wilson et al. 2021), and from recent scientific publications (Baqer et al. 2021, González-Santamaría et al. 2020a, 2020b, Idiart et al. 2020, Jenni & Mäder 2021, Marty et al. 2015a, Pekala et al. 2021, Savage et al. 2020).

Benchmarking studies related to cement/clay interaction were conducted by Marty et al. (2015a) and Idiart et al. (2020). In general, the results obtained with different numerical codes agree well with each other. This shows that differences in predictions by numerical simulations are caused mainly by the modelling assumptions in terms of primary and secondary mineral phase selection, kinetic constraints and which type of coupling between transport and chemical processes is assumed.

As discussed in Prasianakis et al. (2022) and Martin et al. (2023), it might not be possible to completely clog pore space in clay media in order to fully suppress mass transport across zones with reduced porosity, as mineral precipitation is less probable in small pores with diameters below a few nm. For example, Martin et al. (2016) investigated a sample from the Maqarin analogue and found that the alteration rim around a seemingly totally clogged vein still had a remaining porosity of about 19%. Meldrum and O'Shaughnessy (2020) list several arguments for the inhibition of nucleation in smaller pores, which include: 1) The limited availability of reactants/ions that are needed to form nucleation clusters of critical sizes in smaller pores; 2) Interaction of reactants/ions with charged/uncharged pore walls is more probable in small pores, which might influence crystallisation; 3) Crystals with larger surface to volume ratio might have a higher solubility; nucleation probability in small pores is lower and thus favoured in larger pores; 4) The growth of crystals by accumulation of nanocrystals might be retarded in nanopores.

Jenni et al. (2017) and Jenni & Mäder (2021) modelled the evolution of cement/Opalinus Clay interfaces in the Mont Terri Cement Interaction (CI) project with a dual-porosity approach, where the porosity is split into two parts. One part is influenced by the negatively charged surfaces of clay minerals and contains excess cations compensating the surface charge. This part of the pore space is not freely accessible for negatively charged species. The other part contains the charge-neutral solution and is freely accessible for all ions and solutes. For undisturbed Opalinus Clay, the total porosity is split in approximately half between the two pore types. Donnan equilibrium can be used to calculate the composition in each part of the pore space (Jenni et al. 2017). The

model only considered precipitation of minerals in the freely accessible pore space. In addition, for a fully consistent description, the Nernst-Planck equations are used to describe diffusion of charged species in solution. In the model used by Jenni et al. (2017), a porosity decrease in Opalinus Clay led to complete clogging of the freely accessible porosity. The remaining porosity is influenced by negative surface charges (not accessible to anions), therefore only positively charged species and neutral molecules can be diffusively transported in this domain with reduced rates. Transport of negatively charged complexes and anions is blocked. Therefore, in these models, partial clogging of the interface occurs faster than in models that use only one porosity, and mineral reactions that require the flux of specific negatively charged reactants between both materials (e.g. OH^-, sulphate, carbonate complexes) will become strongly limited.

When comparing early studies and reviews with the most recent ones, it is obvious that different continuum-scale reactive transport modelling studies give a consistent picture of the evolution of cement/clay interfaces. Bildstein et al. (2019) specifically note that, in the last two decades, improvements in numerical codes and the accumulation of data acquired to feed thermodynamic and kinetic databases greatly improved the confidence in reactive transport calculations. *"Overall, these simulations provide a better understanding of physical and chemical change and how materials interact: they give more confidence in the prediction of the durability of materials by converging on the alteration extent that can be expected at the interfaces between different materials over long periods of time…this is not to say that we fully understand all the physical and chemical phenomena or that modelling is fully representative of all the processes occurring in such complex systems."*

Uncertainties and limited processes understanding

In their review, Wilson et al. (2021) list the most important areas of uncertainty in terms of understanding the spatial and temporal evolution of a cement-mudrock interface. With regard to the topics discussed in this report, these are the following:

- the effect of temperature
- the rate of precipitation/dissolution reactions in the alkali-perturbed zone of the clay (rock)
- the nature and extent of pore clogging at cement-argillite interfaces over relevant timescales
- the change in radionuclide, gas and liquid transport across the cement/clay interface and
- the detailed effects of the alkali-perturbed zone on radionuclide/contaminant sorption

In addition, the effect of liquid saturation on the evolution of cement/clay interfaces is largely unknown. Studies on the influence of water saturation on cement/clay interface processes are sparse. Bildstein et al. (2019) note that *"Another aspect of unsaturated porous media that is not yet widely treated in RTM relates to the dependence of chemical reactivity with regard to the water content, in particular looking at how the mineral and gas solubility and the aqueous speciation relate to capillary pressure at low water saturation"*.

Wilson et al. (2021) remark that in most modelling studies of cementitious barriers, the effects of temperature variation are not considered. Many models assume standard conditions, usually a temperature of 25 °C and a pressure of 1 bar (100 kPa), which are the default conditions for most common thermodynamic databases. In general, kinetic control of dissolution and precipitation show a strong temperature dependence (Marty et al. 2015b). For Portland cement-based materials when temperatures rise above about 50 °C, the stable phase assembly changes, i.e. ettringite is transformed into monocarbonate and monosulphate (Lothenbach et al. 2008). Many zeolite and clay minerals are metastable with respect to similar minerals at higher temperatures (Wilson et al. 2021). It should be noted that solubility data for most clay minerals at low temperatures are ambiguous (Jenni et al. 2019).

Savage & Cloet (2018) identified that the role of charged (clay) mineral surfaces, their effect on pore space partitioning and transport in different pore space compartments need to be included in future reactive transport modelling studies. *All modelling studies except one or two exceptions* (Berner et al. 2013, Jenni et al. 2017, Jenni & Mäder 2021) *have assumed that the total porosity in clay and bentonite is available for geochemical interactions. The nature of porosity in clays is the subject of much current debate so that alternative models should be considered in future to scope all possible outcomes of the cement/clay interaction process.*

In numerical models, the kinetically controlled dissolution and precipitation of minerals is often a key factor that controls porosity evolution at cement/clay interfaces. The publication of Marty et al. (2015b) includes an extended discussion on the sources of uncertainties for kinetic rate laws and parameters. This includes the applicability of transition state theory for continuum scale models and specifically also the role of reactive mineral surfaces. In addition, e.g. disconnected pores or partial water saturation might compartmentalise the pore space and slow down or interrupt microscopic transport of solutes. In such compartmentalised pores, the water composition might vary considerably. All these conditions make it very difficult to assign a single effective reactive surface area for reaction kinetics. In addition, the pore space geometry, the mineral grain size and surface roughness of mineral grains might change significantly during dissolution (and precipitation of other reaction products). Frequently, this effect is lumped into a "chemical reactivity" function which links liquid water saturation with a reduction of kinetic rates (Huang et al. 2021, Thouvenot et al. 2013).

3.3.3 Cement/clay interactions: influence of Opalinus Clay porewater on cement

Overview of the main processes due to the influence of Opalinus Clay porewater on cement

The interaction of the Opalinus Clay (OPA) porewater (PW) with cementitious materials (Portland cement, silica-fume-blended low-pH cement) of the L/ILW repository may lead to changes in the physicochemical properties of materials such as changes in mineralogical composition, transport (porosity, permeability) and retention properties. These changes are driven by chemical differences between the OPA PW (near neutral pH ~ 7 – 8) (Wersin et al. 2022) and the cementitious materials (highly alkaline pH ~ 10.5 – 13.5) (Vollpracht et al. 2015). Evolution depends on the type and preparation of the cementitious materials. For example, low-pH cements are used with the aim of reducing the pH differences with the clay pore solution. In low-pH cements, part of the cement clinker is substituted with pozzolanic materials such as fly ash, slag, or silica fume/microsilica (Watson et al. 2007). This leads to the decomposition of portlandite and formation of C-S-H with a reduced calcium content. The consumption of all portlandite results in a loss of the buffering capacity at pH 12.5. Furthermore, use of higher water to binder ratios for the initial cement paste leads to higher capillary porosity in the cement paste that might significantly increase the diffusive transport and produce wider alteration zones. After cement emplacement, the transport and reactions are expected to be stronger towards the cement due to higher porosity, higher water content and higher reactivity of the cement matrix compared to the Opalinus Clay minerals. Compared to Portland Cement, the reactive silica of the low-pH cement can lead to faster precipitation of secondary phases, a porosity reduction and stronger transport slowdown at the interface.

The cement phases are in disequilibrium when in contact with the OPA porewater, leading in time to a change in their composition and properties, their dissolution, and to the precipitation of secondary phases. In the presence of OPA porewater, the degradation of cement will follow the three stages described in detail in Section 3.3.1. Cement degradation starts from an initially alkali-

rich cement material with pH above 13, proceeding towards phase equilibrium with portlandite (degradation Stage II with pH ~ 12.5), and equilibrates with C-S-H (degradation Stage III with pH > 10) (Atkinson et al. 1989, Berner 1988, Kosakowski et al. 2014). After the complete dissolution of C-S-H, the cement is considered to be completely degraded. Models predict that, for fully water-saturated materials, only a very small region near the contact to the Opalinus Clay rock is fully degraded after 100,000 years of interaction, while the zone with degradation Stage III extends up to about 2 m into the cement materials (Kosakowski et al. 2014).

Tab. 3-1: Approximate porewater concentrations of interacting Opalinus Clay and cement

(Portland Cement = PC (Lothenbach & Wieland 2006), low-pH cement (Lothenbach et al. 2014)) materials and directions of chemical gradients (from Jenni et al. 2014, Mäder et al. 2017)

Concentration ranges in mM (mmol/L); left concentration values correspond to cement (hydration) age of 0.04 days and right values to 1,310 days; < below detection limit; long arrow for the low-pH cement, short arrow for PC, second arrow pair indicates the gradient at late times.

Material	**Ca^{2+}**	**Mg^{2+}**	**Na^{+}**	**K^{+}**	**SO_4^{2-}**	**Cl^{-}**	**CO_3^{2-}**	**OH^{-}**
PC	24 – 2.9	<	26 – 90	137 – 209	66 – 4.5	<	~ 0.05	> 200
Low-pH cement	9.2 – 29	0 – 0.005	100 – 22	186 – 11	2 – 1.8	<	~ 0.05	180 – 7
Gradient	↑↓–↓↑	↑↑	↑↑	↓↓	↑↓–↑↑	↑↑	↑↑	↓↓
OPA	12.7	14.3	204	2.3	11.8	237	~ 0.4	~ 10^{-7}

At equilibrium with the porewater, cement phases maintain relatively low concentrations of Si, Al, Mg in the pore solution (Vollpracht et al. 2015). This creates a chemical gradient that leads to their transport from the OPA into to the cement (Tab. 3-1). When compared to the OPA PW, the cement pore solution is relatively rich in Ca and initially also in alkalis (mainly K), especially in young cements still undergoing hydration. These elements therefore tend to diffuse from the cement into the OPA (Tab. 3-1). The concentrations of some elements are distinct for different cement types (e.g. Ca, S, Tab. 3-1) and will change as a function of hydration age. The presence of carbonate hydrates (monocarbonate) and calcite keep the dissolved CO_2 concentration in the cement pore solution at low values. Due to the higher carbonate solubility at lower pH, the OPA PW contains a much higher concentration of carbonate than the cement PW (Wersin et al. 2022). Carbonate may then diffuse into the cement and lead to carbonation (transformation of cement hydrates into solid carbonates).

The combined effect of the low OPA PW pH and the existing chemical gradient (migration of C, Mg, S, Si, Al from the OPA into the cement; migration of alkalis, OH^- and Ca from cement to OPA) may trigger different chemical disturbances in the cement materials of the L/ILW repository such as the precipitation of carbonates, secondary sulphates, and the formation of Mg, Si, Al, enriched zone(s). These processes are characterised by the following reactions: dissolution of portlandite, decalcification of C-S-H, carbonation with precipitation of calcite, precipitation of Mg hydrates, and formation of secondary C-S-H and ettringite. The occurrence, timing and spatial distribution of these reactions are influenced by the cement recipe (i.e. cement type, water/binder ratios) and local heterogeneities (presence of aggregates, shrinkage cracks). These chemical changes can be related to an increase in porosity due to the dissolution of cement hydrates but also to a decrease in porosity due to the precipitation of secondary phases. There is competition

between the dissolution and decalcification of cement phases and the precipitation of secondary phases. If enough calcite, secondary C-S-H, ettringite or other secondary phases precipitate, a low-permeability layer may develop and partially isolate the cement from future effects of the OPA PW. The sorption capacity of cement can be decreased due to the dissolution of cement hydrates that have a high surface area, but this effect may be counteracted by the formation of secondary phases such as secondary C-S-H, which has an increased sorption capacity. The lower pH of the OPA PW will destabilise portlandite and other cement hydrates and will lead to the decrease of Ca/Si in C-S-H (decalcification), since C-S-H phases with low Ca/Si are stable at lower pH. Calcium from the dissolution of portlandite can react with dissolved Si to form secondary C-S-H with lower Ca/Si that favours the uptake of aluminium and other cations from the pore solution.

Because the pH of the cement is much higher compared to the pH of the OPA PW, the presence of dissolved Mg in the high-pH environment can cause the precipitation of low-solubility Mg hydrate phases. Clay minerals and dolomite in the OPA are the source of the magnesium that is released from the exchangeable sites. Its flux is determined by the concentration gradient that is governed by the precipitation of Mg phases, which will act as a sink creating a zone enriched with Mg, surrounded by Mg-poor zones. The Mg-containing cement hydrates maintain a low Mg concentration in solution, but these phases are only stable at high pH values. Depending on the chemical composition and the availability of dissolved Al and Si, different Mg phases like hydrotalcite, Mg-phyllosilicates, M-S-H or brucite can form (e.g. Bernard et al. 2020, Dauzeres et al. 2016, Jenni et al. 2017, Lerouge et al. 2017). A source of Al and Si in the cement can be from the slow dissolution of the clay minerals in the OPA, enhanced by the increased pH of the pore solution from the cement. Another source can be from the dissolution of cement phases such as monocarbonate and ettringite because of the low pH of the OPA PW or from the dissolution of silica fume or silica-rich aggregates used in cement and concrete mixes.

The possible ingress of sulphate from the OPA PW into the cement may lead to the formation of gypsum or secondary ettringite. The sulphate in the OPA PW can originate from the dissolution of sulphate minerals (celestite, barite, gypsum) (Wersin et al. 2022) or can also be released from the oxidation of pyrite (Lerouge et al. 2017). To precipitate secondary ettringite, Ca and Al can be supplied from the cement phases (portlandite, monocarbonate and primary ettringite) or from the clay minerals. The low pH of the OPA PW and the leaching of Ca close to the interface may favour the dissolution of primary ettringite, possibly leading to the redistribution of sulphur away from the interface into the cement where conditions of equilibrium with ettringite are still maintained.

The carbonate ions from the OPA PW will react with calcium from the cement to form calcite or other polymorphs like vaterite (Bartier et al. 2013). This process lowers pH, causes the dissolution of portlandite, decalcification of C-S-H and the dissolution of other calcium cement hydrates (see also Section 3.4.3). This process is coupled to a release of calcium from cement that is consumed by calcite precipitation. Due to the difference in molar volumes (cf. Hummel & Thoenen 2023, Lothenbach et al. 2019), the replacement of portlandite with calcite will lead to a net volume increase and a decrease in the pore space. Depending on the composition of the cement (presence of portlandite in PC or absence in a low-pH cement), the initial porosity and permeability, carbonation can have opposing effects on porosity. If present, portlandite will be the first phase affected by carbonation. In the absence of portlandite or once portlandite is dissolved, carbonation will affect the composition of C-S-H. Calcium will be leached from C-S-H and change its composition towards lower Ca/Si molar ratios (Kangni-Foli et al. 2021). This compositional change is accompanied by a decrease in volume and water content of C-S-H, especially below a Ca/Si-ratio of 1.2 (Kulik et al. 2022, Miron et al. 2022), which will generate shrinkage and cracking (Kangni-Foli et al. 2021).

Under atmospheric conditions, carbonation is expected to be faster in partially saturated conditions, because the transport of CO_2 is more efficient in air than in water (von Greve-Dierfeld et al. 2020). The analysis of cement materials such as shotcrete exposed to air circulation showed stronger carbonation when compared with cement paste in saturated conditions (Gaboreau et al. 2012). As discussed in detail in Section 3.4.3, the carbonation of cement materials at clay (OPA)/cement interfaces might be suppressed because the CO_2 fluxes towards the cementitious near-field will be maintained only at very low levels. This is due to the precipitation of carbonates at the high pH front in the adjacent OPA or clay material, which lowers carbonate concentration (Kosakowski & Smith 2014). However, this might be different in the HLW repository where the heat output of waste canisters will induce strong temperature gradients in the vicinity of the disposal tunnels for a few thousand years. The increased ion diffusivity at elevated temperatures will enhance the carbonate fluxes towards the emplacement tunnels and cause the carbonation of cement-based tunnel support (Curti et al. 2023). The excess of carbonate will push the carbonation front into cement materials and prevent the progress of a high-pH front into the Opalinus Clay.

OPA porewater that contains a higher concentration of dissolved ions can cause stronger concrete degradation and can accelerate the filling of pore space due to enhanced saturation and precipitation of secondary minerals (Kosakowski & Berner 2013). The presence of Cl, C, S in the OPA PW can contribute to the formation of secondary layered double hydroxide phases (monosulphate, mono/hemicarbonate, hydrotalcite, Friedel's/Kuzel's salts) (Georget et al. 2022).

Zeolites are secondary minerals that could form due to the interactions of clay minerals with the alkaline cementitious environment surrounding the cement/clay interface (Bildstein et al. 2019, Blanc et al. 2015, Lothenbach et al. 2017, Ma & Lothenbach 2020b, 2020a). Compositionally, they sit between the cementitious materials and clays and may form during cement degradation from Si, Al, Ca and Na dissolved in the pore solution. Because of kinetic hindrance and slow dissolution of the clay minerals, they are not observed in samples of in situ cement/clay interaction experiments (Bernard et al. 2020, Dauzeres et al. 2010, Mäder et al. 2017). These phases may form at later stages of evolution beyond the timescales of existing experiments and are commonly predicted by reactive transport models in late stages of degradation.

Observations from experimental studies

Several publications provide overviews of relevant batch or in situ cement-clay interaction experiments (Bildstein & Claret 2015, Dauzeres et al. 2010, Mäder et al. 2017, Savage & Cloet 2018). The experiments regularly show a narrow alteration extent that is influenced by the cement type (Portland or low-pH cements). The low-pH cements display a higher degree of alteration with the formation of an Mg-enriched zone. Commonly observed alteration reactions are decalcification of cement, variable degrees of carbonation, dissolution and precipitation of ettringite.

Experimental data on the interaction of Opalinus Clay with cement have been collected in the Mont Terri clay-cement interaction experiment (CI), which was emplaced in 2007. The experiment consists of boreholes in the Opalinus Clay filled with different types of cement materials. Details are given in Mäder et al. (2017). The clay-cement interfaces were sampled between 2 to 10 years and have been extensively characterised using different analytical methods (Bernard et al. 2020, Dauzeres et al. 2016, Jenni et al. 2014, 2017, Jenni & Mäder 2021, Lerouge et al. 2017, Mäder et al. 2017). The interaction processes have been supported by several modelling studies (Dauzeres et al. 2016, Jenni et al. 2017, Jenni & Mäder 2021) as discussed below. The main experimental observations on the effect of OPA on cement are decalcification of cement, a variable degree of calcite precipitation, redistribution of sulphate towards the unaltered cement matrix and the precipitation of Mg phases at the interface with the low-pH cement.

The decalcification process is associated with the dissolution of portlandite in the PC and the formation of C-S-H with lower Ca/Si in the low-pH cement. Carbonation is observed to overlap

with decalcification and sulphate redistribution and can be associated with a porosity reduction zone. The Ca-aluminate-sulphate (e.g. monocarbonate) phases present in the cement materials at the interface are destabilised due to the low pH from the OPA PW, resulting in a sulphate-depleted zone. The elements from the dissolved phases and the possible additional sulphate from the OPA porewater are transported towards the inner cement matrix where the pH is still high enough to precipitate secondary ettringite (Mäder et al. 2017).

Observations show that the type of reactions, duration and alteration extent at the cement-clay interface are dependent on the cement type (PC, low pH, slag cement), which has an influence on the chemical and transport properties of the material. A decreased evolution rate with time is suggested by comparable reaction widths in the low-pH cement observed in the 2.2 and 4.9 year samples (Mäder et al. 2017). After 10 years of interaction, the extent of alteration did not exceed 10 mm in the cement. Observations suggest that most of the alteration takes place in the first two years after the emplacement. The reactions slow down in the following period (Wersin et al. 2020).

A 6-year experiment on the evolution of diffusion at the PC/Na-bentonite interface showed comparable results with the CI experiment (Luraschi et al. 2020, Shafizadeh et al. 2020, Yokoyama et al. 2021). Even though the OPA is a more complex material compared to the Na-bentonite, a considerable reduction of transport across the interface was observed, with most alterations developing during the first 5 years without reaching complete clogging within the time frame of the experiment.

Other experiments include cement materials interacting with Callovo-Oxfordian (COx) clay at the Haute Marne Underground Research Laboratory (URL) in France (Gaboreau et al. 2012, Lerouge et al. 2014), with Tournemire clay at the Tournemire URL in France (Bartier et al. 2013, Gaboreau et al. 2011, Lalan et al. 2016), and with Boom Clay at the HADES URL in Belgium (Read et al. 2001, Wang et al. 2010). Observations show very similar evolution for the different clay host rock systems. The reactions occur on comparable timescales and spatial extent. After several years (up to 15 years at Tournemire) of cement/clay interactions, the main observations are: very limited alteration extent (up to 3.5 cm); portlandite dissolution; limited carbonation of the cement (mostly shotcrete cement exposed to air circulation); heterogeneous porosity changes (e.g. increase in macropores due to portlandite dissolution and decrease in smaller pores due to secondary phase precipitation at Tournemire); overall porosity increase in cement; dissolution/ precipitation of ettringite.

The similarities between the different experiments on the interactions of cementitious materials with clay host rocks such as the OPA, COx or Boom Clay can be explained by comparable compositions and similar processes that control the clay porewater elemental concentrations (Wersin et al. 2020, 2022).

Observations from modelling studies

Reactive transport modelling commonly predicts an increase in porosity in the cement paste and a strong decrease in the clay wall rock close to the interface (Kosakowski et al. 2014, Marty et al. 2009, De Windt et al. 2008). The simulated porosity decrease leads to the isolation of the cement from the Opalinus Clay, which reduces the transport across the interface and influences the extent of the predicted transformations at the cement/clay interface. Predicted alteration pathways are comparable between different models, while the predicted temporal evolution and extent can vary as a result of different models and couplings applied for process description. Commonly predicted consequences of the clay-rock porewater interaction with cementitious materials are the dissolution of portlandite, formation of C-S-H with lower Ca/Si ratio, carbonation, and ettringite dissolution/precipitation. The extent of portlandite dissolution can be considered as a good indicator for the cement alteration and can also be compared between models and experiments.

A review on reactive transport modelling of the cement-clay interactions can be found in Savage & Cloet (2018). Most simulations are concerned with cement interaction with natural claystone. They commonly show a narrow (0.2 – 0.3 cm) alteration zone on timescales of 100,000 years. The degradation of cement paste is evidenced by the dissolution of portlandite and the precipitation of secondary ettringite. The alteration of concrete increases with time and the evolution of the system is controlled by mass transport. Due to the porosity decrease and the slowing of mass transport, only a fraction of the minerals can participate in reactions. This is a more realistic view of system evolution because mass balance calculations should be considered extreme scenarios and are not likely to represent a real repository state.

Marty et al. (2014, 2015a) performed a benchmark of reactive transport models for the cement/clay interface and an assessment of the effect of using different model complexity. The extensive modelling exercise showed that different models produced very similar results for the alteration pathways. Marty et al. compared the results of models considering different mineral assemblages, models with or without reaction kinetics, with or without porosity feedback, the effect of mesh size, etc. The calculated mineralogical transformations inside the cement are characterised by the dissolution of portlandite and monocarbonate, precipitation of secondary ettringite and C-S-H with low Ca/Si ratio. Results indicated strong porosity reduction at the interface before 100,000 years. The predicted alteration is strongly reduced when considering porosity feedback and mineral dissolution/precipitation kinetics in the model setup. In this case, limited portlandite dissolution and stable C-S-H with a high Ca/Si ratio are predicted to be stable for longer times than 100,000 years of alteration. A similar benchmark for the low-pH cement/clay interface was performed by Idiart et al. (2020), which predicted a 15 cm in alteration in concrete (characterised by the complete dissolution of C-S-H) with no clogging predicted even after 100,000 years.

The evolution of PC in contact with OPA was modelled by Traber & Mäder (2006) for different scenarios (1D model). The main processes of concrete alteration are the dissolution of portlandite and precipitation of calcite, transformation of C-S-H from high to low Ca/Si ratio and the precipitation of ettringite due to the influx of sulphate from the OPA. Traber & Mäder (2006) considered the dissolution of concrete aggregates that contribute to the pH decrease in the concrete compartment with time. The pH of the concrete is predicted to stay above 10.5 (presence of hydrotalcite) for more than 50,000 years.

The extent of alteration of PC in contact with OPA was also calculated in a 1D diffusive transport model by Kosakowski & Berner (2013) and that of a low-pH cement by Berner et al. (2013). The calculations considered a complex geochemical model including reactions with multiple minerals and solid solutions, cation exchange and surface protonation/deprotonation reactions on clay mineral amphoteric sites. For the contact with PC, the model predicts the dissolution of portlandite and a changing composition of C-S-H towards lower C/S ratios. Calculations considering low-pH cement predicted the dissolution of C-S-H, accompanied by the precipitation of hydrotalcite, zeolites, clay minerals, gypsum and calcite.

Jenni & Mäder (2017, 2021) used a dual-porosity modelling approach to simulate the short-term evolution of PC and low-pH cement in contact with OPA (2.7 and 4.8 years evolution) of the CI experiment. The splitting of porosity into a free porosity and a Donnan porosity is an important factor when clogging is predicted in simulations, since transport at the interface can continue within the Donnan porosity as the free porosity approaches zero. In addition, their simulations start with the onset of cement hydration and can account for the early effects that the unhydrated cement system can have on the cement/clay interaction. The effects on the PC in contact with OPA predicted by the model are overall porosity increase in the cement, depletion of Ca in the cement in the early stages limiting the formation of portlandite and ettringite, no pH decrease, very limited carbonation (caused by OPA PW in-diffusion), and the precipitation of M-S-H close to the interfaces that is replaced by brucite. The modelling results can reproduce the observed

trends in the analysed chemical maps of samples of the CI experiment with the exception of the predicted precipitation of the magnesium phases in the PC that were not identified in the samples. The effects on the low-pH cement in contact with OPA predicted by the model are depletion of Ca, no effect on pH, dissolution of ettringite (sulphur depletion) and C-S-H, a porosity decrease due to the precipitation of Mg phases (M-S-H, talc, and hydrotalcite), and calcite precipitation throughout the cement with limited effect on the pore volume. The model predictions are in agreement with observations from the chemical maps of samples from the CI experiment that show decalcification, depletion of sulphur, and magnesium enrichment close to the interface. The overall predicted mass transfer alteration in the case of the low-pH cement was larger than in the case of PC.

Modelling of cement/clay interaction at Tournemire, France (Soler 2013, De Windt et al. 2008, Yamaguchi et al. 2013) took into account the kinetics of mineral dissolution, exchange and sorption reactions and reproduced the main features observed in characterisation studies (Gaboreau et al. 2011). The predicted alteration of PC over 15 years is characterised by the dissolution of portlandite (3 mm from the interface), associated with a porosity increase towards the bulk cement, and the formation of secondary ettringite, aluminium-rich C-S-H and calcite, associated with a porosity decrease close to the interface. In a benchmark by several groups with different modelling codes, Marty et al. (2015a) simulated the long-term evolution of COx in contact with PC. The modelling results predict the degradation of concrete due to the dissolution of portlandite and the transformation from high Ca/Si to low Ca/Si ratio C-S-H close to the interface. According to the model, the pH in the concrete after 10,000 years of alteration remains above 10.5 and the portlandite dissolution front advances 30 cm from the interface. The evolution of a concrete overpack in contact with Boom Clay porewater modelled by Wang (2009) predicts that portlandite is present during up to 80,000 years of interaction, buffering the pH at 12.5, and even after 100,000 years of simulated evolution the pH remains close to 11, buffered by the presence of C-S-H.

Timescales

In the pre-closure period, cementitious materials in the L/ILW repository will mainly be in contact with the atmosphere as the tunnels are cooled and ventilated, which will lead to carbonation of the cement surface. Post-closure, after the emplacement of the cement materials and filling of the caverns with the backfill mortar, internal cement reactions will dominate (supplementary materials and aggregate dissolution). Reactions on the cement side initially dominate due to its higher porosity and the presence of water. Depending on the evolution of the saturation of the L/ILW repository, cement degradation will be different in different parts of the repository. Due to the diffusive transport conditions in the saturated portion, the porosity at the clay-cement interface will be reduced, causing the transport through the interface to decrease, and slowing down the cement degradation due to contact with OPA PW. The top portion of the L/ILW repository is expected to remain only partially saturated for more than 100,000 years, which will hinder the OPA PW from reacting with the cement, because solute transport and chemical reactions will be limited (cf. Section 3.5.2). In the fully saturated portions of the repository, it is expected that the effect of solute transport from OPA PW on the geochemical evolution of cement will slow down with time but not stop completely, suggesting that the complete degradation of the cementitious near-field due to the influence of OPA PW within 100,000 year is very unlikely.

Uncertainties

The high variability in the temporal evolution of saturation has a direct impact on the uncertainty in the geochemical evolution. Saturation directly affects the availability of water and solutes for chemical reactions. Diffusive and advective mass fluxes decrease strongly with decreasing saturation. Therefore, the geochemical processes driven by transport are delayed or even stopped as long as full repository saturation is not reached.

Uncertainties in the model predictions arise from the heterogeneities considered in the system, the spatial discretisation of the models and the kinetic control of mineral dissolution and precipitation (Kosakowski & Berner 2013, Marty et al. 2009). Mineral precipitation at the interface is limited by the transport of elements by diffusion and their availability due to mineral dissolution kinetics. There is strong sensitivity of the time behaviour of porosity change processes to the numerical mesh size and kinetic parameters (Hayek et al. 2012, Marty et al. 2009, Traber & Mäder 2006, Xie et al. 2015). Large uncertainties still exist related to the mineral dissolution/precipitation kinetics that influence the amount of elements available for reaction.

Uncertainties exist in the evaluation of experimental data of laboratory and in situ experiments. There are difficulties related to sampling, preparation and the measurement approach that leads to uncertainties in the evaluation of the mineralogical and porosity evolution of the samples. Another uncertainty concerns the transferability of the observations from experiments to the natural system over very long timescales.

3.3.4 Cement/clay interactions: influence of cement porewater on Opalinus Clay/tunnel backfill

Overview of main processes due to the influence of cement porewater on Opalinus Clay/tunnel backfill

At the contact with cement, the properties and mineralogical composition of the Opalinus Clay and potentially the clay-rich tunnel backfill (Nagra 2021c) will be altered due to the interaction with the alkaline cement porewater (Gaucher & Blanc 2006). This can have an impact on the safety-relevant properties of the OPA, such as cation sorption, preservation of swelling pressure in the case of bentonite and self-sealing capacity in the OPA and have an impact on the release of hydrogen into the OPA. The major and accessory minerals in the OPA are not stable under alkaline conditions and will undergo enhanced dissolution. The clay mineral surface charge and sorption properties will change, affecting the transport and retention properties of ions (cation exchange capacity and surface sorption properties). Ca^{2+} and K^{+} will diffuse into the OPA while other components such as $Si(OH)_{4(aq)}$, $Al(OH)_4^-$, SO_4^{2-} and CO_3^{2-} will diffuse towards the cement due to strong chemical gradients between the OPA porewater and the cement porewater (Tab. 3-1). Mixing of the elements diffusing from the OPA porewater and those diffusing from the cement will lead to the precipitation of secondary minerals that will affect the chemistry and transport properties in the OPA close to the interface.

The chemistry of the OPA has a significant buffering potential that can limit the rise in pH but it has a very low permeability (diffusive transport) and the clay minerals have very slow dissolution kinetics, making the OPA less reactive than the cement materials. The dissolution kinetics of non-clay minerals such as amorphous silica, carbonates and sulphates are faster than that of clays (Marty et al. 2015b). These non-clay minerals also have a pH buffering effect (e.g. silica hydrolysis, carbonate system) and are a source of elements for the precipitation of secondary phases (Gaucher & Blanc 2006).

The alkaline cement porewater alters porewater composition and cation-exchange equilibria in the OPA. The silanol and aluminol groups on the clay mineral surfaces ionise at high pH, influencing the sorption complexation reactions. The initially sodium-rich clay minerals become more potassium- and calcium-rich by exchanging Ca^{2+} and K^{+} for Mg^{2+} and Na^{+}. The cation exchange processes do not have a direct impact on the pH of the pore solution but change the cation composition of the clay exchanger and the composition of the coexisting pore fluid. This process influences the precipitation of secondary minerals. The magnesium released from the clays in the presence of a high-pH solution will induce the precipitation of Mg phases. This mechanism acts as a sink for magnesium, further enhancing the leaching of magnesium from the clay exchange sites (Gaucher & Blanc 2006).

The Opalinus Clay has a large buffering capacity against the perturbations induced by the alkaline solution from the degradation of cementitious materials. The OH^{-} from the cement porewater can be consumed by fast (reversible) protolysis reactions on the surface amphoteric hydroxyl sites (≡ SOH) of clay minerals (Bradbury & Baeyens 2005, Savage & Cloet 2018). The capacity of these sites has been determined to be about 10% of the cation exchange capacity (CEC) of the clay (CEC in Opalinus Clay: ~ 0.1 moles per kg) (Savage & Cloet 2018). The clay surface site protolysis reactions represent a small fraction (~ 1%) of the total clay buffering capacity. The dissolution of minerals in the OPA has a significantly larger potential for consuming OH^{-} than surface reactions. Even in very small amounts, the dissolution of clay minerals such as illite, kaolinite and montmorillonite (main OPA components) can neutralise the diffusing cement pore fluids, strongly limiting the advance of the alkaline alteration front. Depending on their composition, clay minerals can consume 4 to 5 moles of OH^{-} per mole of dissolved clay mineral (Savage & Cloet 2018).

The dissolution reactions of clay minerals are characterised by very slow kinetic rates and their effects are more important over long timescales. The dissolution rates increase in alkaline conditions, contributing to the OH^{-} consumption (Marty et al. 2015b). The dissolution of other non-clay minerals present in the OPA, such as quartz polymorphs, can also consume OH^{-}. Although less OH^{-} is consumed (1 – 2 moles per mole of dissolved quartz) when dissolved, quartz may be more effective at slowing down the ingress of the alkaline plume due to a faster dissolution rate compared to the clay minerals.

The precipitation of secondary minerals such as C-S-H or hydroxide phases will also contribute to the consumption of OH^{-}, while other minerals such as zeolites will generate OH^{-} upon precipitation from the pore solution (Savage & Cloet 2018). Additionally, the dissolution of organic matter can act as a weak acid buffer (Gaucher & Blanc 2006), preventing the dissolution of clays. Claret et al. (2002) attributed the lack of effect of an alkaline solution (pH 13.2) on the COx clay after one year of contact to the presence of organic matter. The dissolution of organic matter consumes OH^{-} and provides a source for carbonate that can lead to the precipitation of carbonate minerals.

The Opalinus Clay can be considered as an unlimited reservoir for buffering the pH of the cement materials. Mass balance calculations (Mäder & Adler 2004) showed that, within one million years, the pH alteration front (zone with increased pH) may extend no further than 10 metres, while the mineralogically affected zone is restricted to 4 metres, consuming about 10% of the clay buffering capacity in the affected area. Such calculations considered that everything in the system is always available for reaction, which is a very conservative assumption. In reality, the reactions will slow down over time due to porosity reduction and a decreased mass transfer between the cement materials and the Opalinus Clay.

The dissolution of clay minerals such as montmorillonite will affect the retention properties of the clay rock. This is predicted to happen only at the interface (~ 2 cm) (Savage & Cloet 2018). In such cases of advanced alteration, the dissolution of clays is accompanied by the precipitation of C-S-H, M-S-H, layered double hydroxide (e.g. hydrotalcite), and possibly zeolite phases. These new phases counteract the effect on retention by providing a sorption and cation exchange capacity increase (Hudcová et al. 2017, Ramírez et al. 2005).

Observations from experimental studies

Various batch and in situ experiments have been performed to investigate the evolution of clay rocks under the influence of alkaline solutions and have been reported in several publications (Bildstein et al. 2019, Bildstein & Claret 2015, Dauzeres et al. 2010, Gaucher & Blanc 2006, Mäder et al. 2017).

The experimental data on cement-clay interfaces for different concretes and clay rock systems point to similar processes that govern their evolution. The clay rock has a strong buffering capacity for the high-pH cement porewater, which leads to a steep pH front at the interface and to restricted mineralogical and porosity changes in the clay. Commonly observed processes are the cation exchange reactions and the redistribution of Mg, along with the advance of the pH alteration front. A reduction of the ion flux across the interface is observed after a short period of interaction time and can strongly limit the alteration extent. The dissolution of clay and non-clay minerals is modest in the experiments and the precipitation of secondary phases, often inconclusive, is limited, mainly to C-S-H, M-S-H and other magnesium phases, and varying amounts of carbonates, whereas zeolites are kinetically hindered. There is a difference between the evolution observed in batch and in situ experiments. Batch experiments show a stronger and accelerated evolution, while in situ experiments are dominated by very slow transport and reaction rates.

The effects of a synthetic cement porewater on the Opalinus Clay were investigated in the CW (Cement Water) experiment at the Mont Terri Rock Laboratory (Mäder 2009). Observations showed a strong buffering of the hyperalkaline fluid by the clay rock. Precipitates of Mg-silicate, calcite and small amounts of Fe-hydroxide were detected (Mäder et al. 2017). The monitoring data were interpreted as changes in the OPA mineralogy and porosity using a diffusive reactive transport model (Adler 2001). The model predicted dolomite, kaolinite and quartz dissolution and release of Mg from dolomite and exchange reactions, while predicted porosity changes were small. In a laboratory experiment investigating the same fluid – rock system, Adler (2001) showed that the pH of the cement porewater can be buffered by the clay rock through the precipitation of Mg-hydroxide phases (e.g. brucite).

The alteration of mudstone and OPA exposed for several months to alkaline solutions was studied in column and flow-through experiments by Bateman et al. (2021) and Taubald et al. (2000). The affected zone in the claystone was limited to < 2 cm and was characterised by the formation of C-S-H phases, carbonates, and brucite.

In situ experimental data on the interaction of different types of cement materials with the Opalinus Clay have been collected in the Mont Terri clay-cement interaction experiment (CI). These have been summarised in Sections 3.3.2 and 3.3.3.

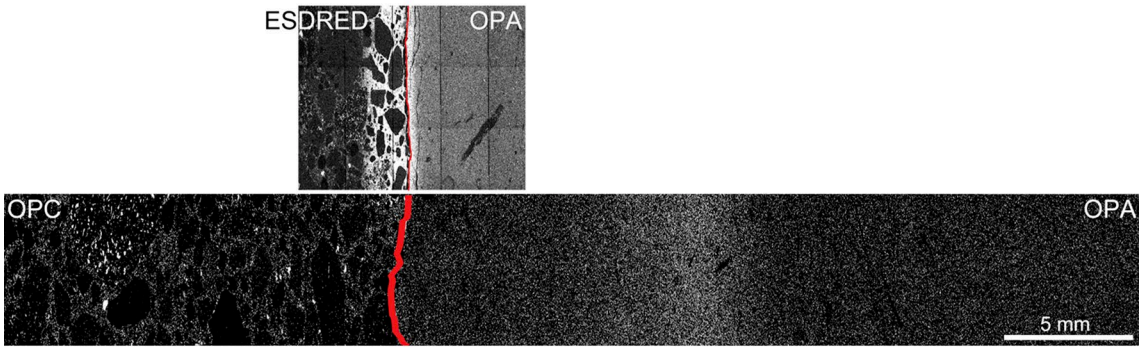

Fig. 3-9: SEM EDX maps of concrete on the left and OPA on the right from the interface (red line) showing bright areas of high Mg concentrations after 4.8 years of interaction in the CI experiment

From Jenni & Mäder (2021)

The Ca^{2+} and K^{+} from the cement porewater can be exchanged for Mg^{2+} and Na^{+} on the clay exchanger. Magnesium that results from the exchange reactions and from dolomite dissolution reacts to the advancing pH front and forms Mg-phases (brucite, silicates like M-S-H phases). These phases act as a sink for Mg and consume OH^{-}, in turn limiting the advance of the pH front. In the CI experiment, the magnesium enrichment was identified in OPA at a distance of ~ 7 mm from the interface with Portland cement (Fig. 3-9) after 4.8 years. This was explained by the migration of the pH front that pushes the magnesium front deeper into the claystone (Mäder et al. 2017). A relatively weak pH alteration front is needed to precipitate such phases because their solubility strongly decreases with increasing pH. At the contact with low-pH cement, the magnesium enrichment is observed at the actual interface or on the cement side (Fig. 3-9). This is explained by the precipitation of M-S-H (Bernard et al. 2020) that decreases the porosity and prevents further transport into the clay. Observations of Bernard et al. (2020) on aged interfaces between cement pastes and Opalinus Clay of the CI experiment suggest that the magnesium migration and enrichment in the OPA occurs with the same rate for samples of 5 and 10 years exposure time.

A reaction/diffusion cell experiment was used to monitor the evolution of a Portland cement-Na-montmorillonite interface over a time of 6 years (Luraschi et al. 2020, Shafizadeh 2019, Shafizadeh et al. 2020). Neutron imaging tomography was used by Shafizadeh et al. (2020) to study the evolution of water content and diffusion of D_2O (heavy water) at the interface between Portland cement and Na-montmorillonite as a proxy for porosity changes. A reduction of porosity in the clay at a distance of 2 mm from the interface was detected during the first 600 days of the interaction experiment. The same samples were analysed for the evolution of the diffusive flux across the reacting interface (Luraschi et al. 2020). Over the monitoring period of 6 years, no complete blocking of the pore spaces was observed, and two distinct evolution phases were identified: a first period < 2 years characterised by a strong decrease in diffusivity and a second period 2 – 6 years characterised by a slow decrease in diffusivity. No complete blockage of the transport at the interface was detected and in the diffusion experiments of Luraschi et al. (2020) pH breakthrough into the clay water reservoir behind the clay plug was observed. Mineral alterations were only observed near the interface to the cement-clay interface.

The impact of concrete materials on different clays has been analysed in field experiments in Underground Research Laboratories (URL). These investigations are summarised in Sections 3.3.2 and 3.3.3. These include concrete materials interacting with COx clay rock at the Haute Marne URL in France (Gaboreau et al. 2012, Lerouge et al. 2014, Ramírez et al. 2005), with

Tournemire clay at the Tournemire URL in France (Bartier et al. 2013, Gaboreau et al. 2011, Lalan et al. 2016), and with Boom Clay at the HADES URL in Belgium (Read et al. 2001, Wang et al. 2010). Gaboreau (2011) characterised cement/clay interface samples from Tournemire after 15 years of interaction, showing a porosity reduction in the claystone due to the precipitation of secondary minerals. Limited alteration extents (< 1 cm) have been identified at the contact of shotcrete and cement paste with COx clay after 5 years of interaction (Gaboreau et al. 2012, Lerouge et al. 2014). Changes are characterised by the precipitation of gypsum at the interface and in micro-fissures of the EDZ (COx clay porewater is close to gypsum saturation) and the alteration of the cation exchange on the clay phases (increase in K). No smectite illitisation or zeolite formation was observed, and the precipitation of C-S-H phases was suggested indirectly from the slight increase in the cation exchange capacity at the interface. Autoradiography measurements showed no significant porosity changes due to dissolution and precipitation of minerals.

Precipitation of zeolite phases due to the alteration of the clay rock from in situ experiments over a monitoring period of several years is inconclusive. These systems are characterised by high solid to liquid ratios and the dissolution of clay minerals has slower reaction kinetics than observed in lab experiments (Maher et al. 2004, Yang & Steefel 2008). Small amounts of poorly crystalline gel-like secondary C-S-H phases and zeolite precursor phases are difficult to identify (Gaboreau et al. 2011). Zeolites in the context of claystone interacting with natural or synthetic cement porewater are only observed in batch experiments with high liquid to solid ratios and at elevated temperatures (Adler 2001, Devol-Brown et al. 2007, Ramírez et al. 2005). Thermodynamically, zeolites are predicted to form in such systems (Blanc et al. 2012, Ma & Lothenbach 2020b, Zhen-Wu et al. 2021), but they may be retarded by slow precipitation kinetics and do not precipitate in the timespan of the experiments but might still form at later times.

Observations from modelling studies

Several publications present comprehensive benchmarks and reviews on reactive transport modelling of cement/clay interactions covering various chemical system setups (Bildstein et al. 2019, Bildstein & Claret 2015, Marty et al. 2014, Savage & Cloet 2018). The alterations and mineralogical transformations predicted by different reactive transport models are comparable. The calculated effect of an alkaline cement porewater on the clay host rock is spatially limited over a long period of time due the porosity reduction. The predicted alteration of the clay rock is defined by the extent of cation exchange reactions affecting clay minerals, by the extent of the magnesium redistribution front, and by the extent of dissolution of non-clay minerals such as quartz and dolomite and of clay minerals such as montmorillonite.

In their review on reactive transport modelling of cement/clay interactions, Savage & Cloet (2018) conclude that “there is a broad degree of similarity in terms of the predicted thickness of the altered zone of clay, the types of secondary solid products and changes in porosity”. The mineralogical perturbation predicted by different models in the clay due to the ingress of the alkaline fluid did not exceed 0.6 m after 100,000 years (Fig. 3-10) and the extent of the total loss of montmorillonite in clay rock was below 0.02 m. The models predict the dissolution of clay and non-clay minerals from the clay rock and the precipitation of C-S-H phases, secondary clay minerals, zeolites and feldspars. Porosity is predicted to decrease with time, which leads to a decrease in mass transport, reducing the degradation extent of the clay rock. Including dissolution/precipitation kinetics and porosity feedback in the models has the effect of slowing the degradation and of reducing the alteration extent. Using faster dissolution rates leads to accelerated filling of the pore space.

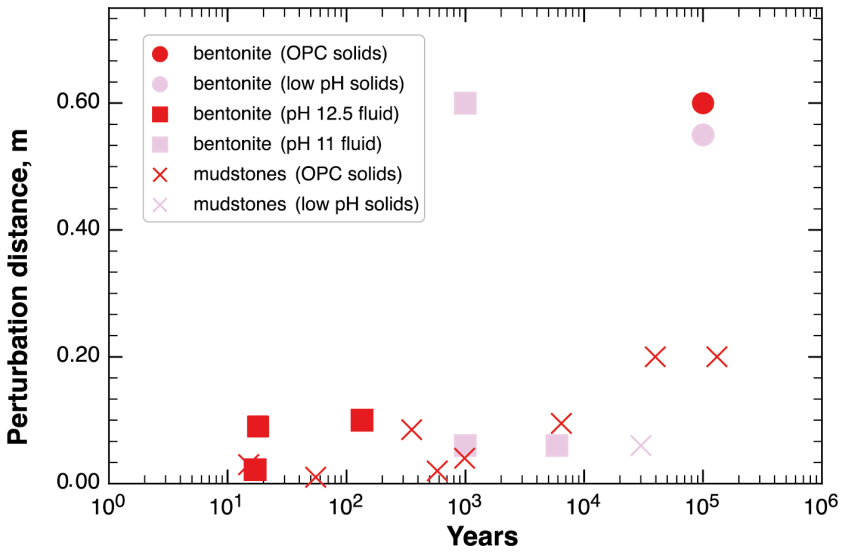

Fig. 3-10: Extent of mineralogical changes in clay rocks due to interaction with cement (any change in mineralogical composition, including modifications to the cation exchange)

From Savage & Cloet (2018)

Marty et al. (2014) performed a comprehensive study assessing the impact of increasing model complexity on the results of cement/clay reactive transport simulations. Irrespective of the model details, results indicate transformations very close to the concrete/clay interface and a strong porosity decrease before 100,000 years. Major reaction pathways are not strongly affected by different modelling assumptions and are mainly controlled by the underlying chemistry and transport properties of the system.

Kosakowski & Berner (Kosakowski et al. 2014, Kosakowski & Berner 2013) estimated the extent of alterations in the OPA after 100,000 years caused by a constant diffusive exchange across a concrete-OPA interface assuming thermodynamic equilibrium. Calculated major mineralogical changes, in areas with pH > 10, are characterised by a complete conversion of montmorillonite into zeolites, C-S-H, illite and additional minor phases. These mineralogical transformations are limited to 30 cm in the OPA. The alkaline alteration front extends further than the zone of mineralogical alteration, to 50 cm, and is buffered to around pH 8.4 by the presence of montmorillonite. The predicted extent of affected OPA compares well with the modelling results of Traber & Mäder (2006) that predicted a maximum extent of 30 cm for the mineralogical alteration and a 23 cm wide zone with a pH > 9 after 50,000 years within the Opalinus Clay. These studies (Kosakowski et al. 2014, Kosakowski & Berner 2013, Traber & Mäder 2006) rely on conservative assumptions regarding mineral reactivity and possibly overestimate the possible mineralogical alterations.

Jenni et al. (2017) & Jenni & Mäder (2021) used a dual-porosity approach to model different cement/clay interfaces from the Mont Terri CI experiment. The model produces comparable results for the effect of the alkaline pore solution with observations from the CI experiment. Only small fractions of the free porosity are predicted to be filled in the OPA in contact with Portland cement due to the precipitation of Mg phases. The precipitation of Mg phases follows the evolution of the pH alteration front. The calculations show a complete filling of the free porosity in the OPA in contact with the low pH cement during the first 2.7 years of evolution. This is caused by the precipitation of Mg phases (hydrotalcite, talc and brucite). The transport and

exchange of cations is still possible in the Donnan porosity. In the model, anions such as OH^- can only be transported through the free porosity. This has an impact on the predicted extent of the pH increase in adjacent clay materials.

Results of models of cement/clay interactions studied at the Tournemire Underground Rock Laboratory (Soler 2013, De Windt et al. 2008) are comparable with experimental observations. The calculations of Soler (2013) predict minor dissolution of clay minerals (mainly kaolinite and illite) and filling of the porosity in the clay rock due to the precipitation of C-A-S-H, calcite and ettringite close to the interface. The precipitation of the Mg phase hydrotalcite is also predicted to occur in the clay rock. Zeolites were excluded from the model since they were not confirmed by observations at Tournemire. The modelling results for COx clay interacting with cement show a maximum alteration front of 0.5 m in the clay rock, indicated by montmorillonite dissolution after 100,000 years of evolution and an extent of the pH front up to 0.8 m in the clay rock (Marty et al. 2014).

Observations from natural and industrial analogues

A review of natural and industrial analogues related to alkaline alteration of host rocks has been performed by Savage (2011). These are also discussed in other publications (Bildstein & Claret 2015, Gaucher & Blanc 2006). Analogues show that alkaline fluids reacting with clay rocks (rich in aluminosilicate minerals) will lead in time to a porosity reduction and sealing of fractures and host rock matrix due to the precipitation of secondary minerals.

Cement is commonly used as stabilising agent for clays and clay soils (Diana et al. 2019, Herzog & Mitchell 1963, Prusinski & Bhattacharja 1999). The process is employed for increasing the strength and durability of clay materials used in construction or in soil stabilisation. Although these systems are not directly comparable with the repository ones, they show the same defining processes. The alkaline cement pore solution reacts with the clay minerals; they become more calcic and dissolve, releasing Si and Al that leads to the formation of secondary gels like C-A-S-H phases. The secondary phases fill the porosity and fractures, leading to lower permeability and increased strength for the clay rich matrix (Diana et al. 2019).

Tinseau et al. (2006) describe the clay rock alteration after contact for 125 years with the Tournemire railroad tunnel masonry (siliceous lime). Interactions occurred under oxidising conditions in both water-saturated and unsaturated zones. The unsaturated zones showed no significant alteration of the clay after 125 years (minor pyrite dissolution and gypsum precipitation). The saturated system was more reactive and was affected by the water flow rate (advective transport). Analysed samples showed the dissolution of quartz and kaolinite, changes in illite/smectite proportions, oxidation of Fe-chlorites, precipitation of carbonates (calcite and dolomite), gypsum, and recrystallisation of feldspars. In the affected wall rock zone, an overall decrease in Si and Al and an increase in Ca and Mg concentration was observed. The maximum extent of the alteration in the clay rock was 17 cm.

Maqarin, in northern Jordan, is a natural cement analogue interacting with surrounding clay rock. The system has been described in detail by several studies (Martin et al. 2016, Smellie 1998) (see above) and its evolution has been extensively modelled (Shao et al. 2013, Soler 2016, Steefel & Lichtner 1998, Watson et al. 2016). Hyperalkaline waters, similar to cement waters with a high pH, circulated through fractures in a clayey biomicrite (limestone). The main alteration products observed in the wall rock matrix are C-S-H aluminium-rich phases (C-A-S-H). These mainly fill pores of the host rock adjacent to the fractures, that are later filled by ettringite and occasionally thaumasite, with zeolites being identified only in the distal regions (Martin et al. 2016). A narrow zone close to the fracture wall indicated the dissolution of calcite, dolomite and silicates (Smellie 1998). The disturbed area was estimated to extend no more than 40 mm from the fracture after roughly 100,000 years of interaction (Gaucher & Blanc 2006). The system is characterised by

different opening/closing episodes of fractures dominated by advective flow. Open fractures with sealed interfaces may have developed, protecting the rock matrix from further alteration. In distal parts, the fluid diffused slowly in the host rock, allowing sufficient equilibration time for silicate dissolution and the precipitation of zeolites (or zeolite precursors). The Maqarin site is highly fractured and promotes a more extensive alteration of the highly alkaline plume by advective flow. This is in contrast to what is expected in a diffusion-dominated repository situation such as in Opalinus Clay.

Timescales

After the emplacement of the cement materials, a sharp pH front forms at the clay-cement interface and advances into the Opalinus Clay. The zones with reduced porosity are formed in the early phase of the cement-clay interaction, which slows down the progress of the alteration front due to the reduced porosity, as observed in the study by Yokoyama et al. (2021). The extent of the interaction with the cement porewater is strongly dependent on the evolution of the saturation conditions in the repository. In dry unsaturated conditions, chemical reactions are hindered due to the lack of water and no changes are expected to take place in unsaturated domains. The saturation starts earlier in the repository bottom part and only later proceeds to the top part of the repository. According to the models of Papafotiou & Senger (2014), the lower sections of the repository should remain unsaturated over several 10,000s of years. The ingress of cement porewater into the OPA will initially lead to changes in the clay exchanger composition. The initially high pH of cement porewater is quickly buffered by protolysis reactions on the clay surface and dissolution of minerals in the OPA. Most major minerals in OPA react slowly, e.g. clay minerals, and their dissolution is kinetically controlled. In general, the rate is higher at elevated pH. The dissolved elements and the effect of the cement pore solution will lead to the precipitation of secondary minerals that results in a porosity reduction and a slowdown of transport through the interface. By dissolving a small amount of clays, the system will rapidly approach equilibrium conditions where the dissolution kinetics are slowed (Gong et al. 2019), as is observed in in situ experiments on the dissolution of clay minerals. The advance of the pH alteration front through diffusion may outpace the geochemical reaction front which is characterised by slow chemical reaction kinetics. Based on the available modelling information and the slowdown with time, the pH front is not expected to advance more than 1 m into the OPA over 100,000 years. Within this period, the increased pH can be buffered by the OPA since it has sufficient buffering capacity from not only clay mineral hydrolysis, but also by mineral precipitation.

Uncertainties

The uncertainties related to our understanding of the effect of the cement pore solution on the OPA and tunnel backfill come from difficulties in experimental analytical investigation of these phenomena, limited timescales of the experiments and from variable parameters and heterogeneities considered in the models. Lab and in situ experiments for these systems under realistic transport conditions and with real materials are difficult because of the very slow kinetics of the processes that control their evolution, making it difficult to extrapolate the results over long timescales.

There are large uncertainties in the model parameters for mineral dissolution-precipitation kinetics, potential formation of metastable phases and challenges related to the conceptual upscaling of data from laboratory to natural systems (Marty et al. 2009). The publication of Marty et al. (2015b) includes an extended discussion on the sources of uncertainties for kinetic rate laws and the corresponding parameters. In addition, in Section 3.2 of Jenni et al. (2019), uncertainties

related to thermodynamic and kinetic modelling of bentonite and clay minerals (also under high-pH conditions) are discussed. Marty et al. (2015b) state the following: *"Moreover, laboratory experimental rates and those measured in situ vary by up to several orders of magnitude*s (Luttge et al. 2013, Marty et al. 2009, Velbel 1990, White & Brantley 2003, Zhu 2005).

Uncertainties in the model predictions arise from the heterogeneities considered in the system, the spatial discretisation of the models and the kinetic control of mineral dissolution and precipitation (Kosakowski & Berner 2013, Marty et al. 2009). Mineral precipitation at the interface is limited by the transport of elements through diffusion and their availability due to mineral dissolution kinetics. Simulations looking at the influence of model spatial discretisation found that clogging time and alteration extent are strongly affected by the grid size (Marty et al. 2009). A decrease in the grid size by a factor of 10 leads to a factor of 100 faster clogging time. The extent of the predicted pH ingress into the OPA, geochemical alteration, and porosity change are influenced by the kinetic control of mineral precipitation/dissolution, the grid resolution of the model used and choice of secondary minerals that are allowed to precipitate (Savage & Cloet 2018). Considering the modelling uncertainties, the existing models still converge to very similar reaction pathways and evolution trends and differ mainly in the time and spatial extent of the geochemical alteration. The reason for the apparent consistency of the model predictions is the fact that the models use the same underlying thermodynamic databases.

In addition, the effect of liquid saturation on evolution of cement/clay interfaces is largely unknown. Studies on the influence of water saturation on cement/clay interface processes are sparse. Bildstein et al. (2019) note that *"Another aspect of unsaturated porous media that is not yet widely treated in RTM relates to the dependence of chemical reactivity with regard to the water content, in particular looking at how the mineral and gas solubility and the aqueous speciation relate to capillary pressure at low water saturation"*.

3.3.5 Interaction between cement paste and aggregates (internal cement degradation)

Overview/general description

Large amounts of cementitious materials are considered for use in the L/ILW repository, such as those for waste conditioning, encapsulation, tunnel support and as a backfill of void space (Leupin et al. 2016b, Nagra 2021b, 2021d).

The materials used include a wide variety of mortars, concretes and other cement-based materials. Some materials which could potentially be used were described in Kosakowski et al. (2020). A common feature of concrete materials is the use of aggregates that comprise up to 70 vol% of the material. Due to the high amounts of aggregates needed for most materials, it is advantageous to use locally available sedimentary or crushed hard rocks as aggregates to reduce transport costs and minimise ecological impact.

Concrete made of cement and aggregates provides the necessary mechanical and hydraulic properties according to the demands of construction norms and other requirements. As part of the tunnel support system and sealing elements, cement-based elements may have an influence on water and gas transport. Within the L/ILW emplacement caverns, the cement-based materials should provide a favourable alkaline chemical environment with pH > 10.5 of the cement pore solution that slows down corrosion of reinforcement, metallic waste, and microbially mediated degradation of organic materials (Diomidis et al. 2023).

The projected long-term performance of concrete or mortar is based on the assumption that aggregates can be treated as inert fillers. However, from a thermodynamic point of view this assumption is not always justified. It is known that many common aggregates are not chemically

stable in a high-pH alkaline environment. The so-called alkali-aggregate reaction (AAR) can be (mechanically) deleterious to structural concrete. The AAR reaction can be subdivided into two reaction types (Leemann et al. 2016, Sims & Brown 1998, Winter 2009):

- Alkali-silica reaction (ASR), which is an expansive reaction, originating from the interaction of alkalis (and hydroxyl) in alkaline pore fluid with reactive forms of silica in the aggregate. Detailed studies of the reaction products were performed by Shi et al. (2020) and Leeman et al. (2020). The reaction of the aggregates with the alkali-rich pore solution can subsequently cause expansion and cracking of concrete and significantly shorten the service life of concrete infrastructure (Lindgård et al. 2012).
- Alkali-carbonate reaction (ACR), which is a reaction originating from the interaction of the alkaline pore fluid and some aggregates in which calcium-magnesium carbonate is present (Winter 2009). The alkalis in the cement porewater might react with the dolomite crystals present in the aggregates, inducing the production of brucite, $Mg(OH)_2$, and calcite ($CaCO_3$). ACR is an expansive reaction and is similar to ASR in terms of deterioration of concrete properties.

In addition, the pozzolanic reaction that occurs in the setting of the mixture of lime (or release Ca^{2+} by the decomposition of portlandite) and pozzolanic materials also has features similar to ASR but is not considered a (mechanically) deteriorating reaction in the sense of AAR. By the pozzolanic reaction, portlandite is consumed and C-S-H phases are formed with a decreased Ca/Si ratio. Due to the degradation of the portlandite, the buffering capacity is lost, and pH will decrease consecutively as silica becomes consumed by the high-pH pore solution.

As indicated, with regard to construction and civil engineering in general, ASR and the ACR mainly have implications for the mechanical stability of the concrete elements.

In the context of deep geological disposal, the mechanical damage caused by AAR is of often of minor importance. Most relevant are the chemical changes associated with the various forms of AAR that generally cause a reduction of pH.

Commonly, the potential of aggregates regarding AAR is investigated with the help of tests which investigate the mechanical deformation/expansion of prisms or cylinders stored at elevated temperatures for times typically not more than one month (Grattan-Bellew & Katayama 2019). Such tests can provide information on the potential degree of AAR within the lifetime of engineered structures of typically 50 years.

The focus of these tests (Lindgård et al. 2012, Thomas et al. 2013) and associated model development (Esposito & Hendriks 2019) is on the deterioration of mechanical properties, and not so much on the induced changes in the chemical environment (mineralogy and porewater).

Other test methods are based on petrographic examination of aggregates. Such information will give an insight into whether rock-forming minerals can be identified which could be potentially reactive.

In geochemistry, the temporal progression of mineral dissolution is a commonly investigated process that controls the long-term evolution of many geological or other systems, for example aquifers, oil reservoirs, soils, or ore deposits (Brantley et al. 2008). For several decades, rates of mineral dissolution have been measured and are available in specialised databases (Marty et al. 2015b, Palandri & Kharaka 2004). Several kinetic models exist, often tailored for certain applications. For reactive transport, the so-called “Lasaga”-type kinetic models are popular. They are based on transition state theory (TST) as detailed in Lasaga (1981b, 1981a). Dissolution rates of common rock-forming minerals show a strong dependence on water pH and temperature (cf. Fig. 3-11). Typically, rates increase strongly under alkaline (and/or) acidic conditions and elevated temperatures. For example, at pH ~ 12.0 the dissolution rate of quartz is in the order of

10^{-10} and 10^{-9} mol $m^{-2} \cdot s^{-1}$, when temperature ranges from 25 °C to 60 °C (Bickmore et al. 2006, Brady & Walther 1990, Dove & Elston 1992). More recently, Bagheri et al. (2022) measured dissolution of silica (quartz, amorphous silica) and feldspars at pH 13.0 at 40 and 60 °C. It should be noted that measured rates for amorphous silica are significantly higher than those for crystalline silica (e.g. quartz) (cf. Fig. 3-11). The rates for quartz and feldspars are well within the range predicted by common parameterisations in kinetic databases (Marty et al. 2015b, Palandri & Kharaka 2004). However, the rates are normalised per area of reactive surface of mineral grains. This implies that, for a given amount (volume), very small aggregate grains have a much higher surface area than larger sized aggregates. For spherical grains, there is a linear relationship between grain surface and grain volume, i.e. 1 kg of sand grains with 1 mm diameter will have a 1,000 times smaller surface area than 1 kg of silica fume with grain diameters of 1 µm. This explains why, for a given dissolution rate, small aggregate fractions dissolve faster. If particles are fine enough, they will react while the cement is setting. It is known from many studies that dissolution rates derived from field data are orders of magnitude lower than rates measured in the laboratory (Jung & Navarre-Sitchler 2018b, Marty et al. 2015b). This is related to difficulties in obtaining effective reactive surface areas for minerals in heterogeneous porous media, but also other processes, e.g. secondary mineral precipitation (Poonoosamy et al. 2020), spatial heterogeneities of geochemical or transport parameters (Jung & Navarre-Sitchler 2018a, 2018b), or the water saturation.

Glasser (2013) states in his review on use of cements in radioactive waste disposal: *"Most Portland cement is combined with mineral aggregate into concretes, grouts and mortars. There is potential in the longer term (> 100 – 1 000 years) for siliceous aggregates to react with cement. This factor, the impact of aggregate on long term performance, has probably received insufficient attention in assessing performance lifetimes especially when cement-based products are used in warm, wet conditions."*

Information from experimental and modelling studies

Siliceous aggregates

The early-stage reaction between siliceous aggregates and cement paste is beneficial for the formation of a dense matrix where aggregates are fully attached to the cement paste. However, the late-stage reaction of silica in aggregates often results in a detachment of the cement paste from the aggregate and thus degrades the mechanical properties of the concrete. This reaction takes place between silica and the Na/K content in concrete pore solution, thus denoted as the "alkali-silica-reaction (ASR)" (Leemann et al. 2016, 2020). The resulting ASR product consists mainly of silica and alkali hydroxide plus some calcium (Leemann et al. 2016, 2020, Shi et al. 2020). In the presence of moisture, this product may expand and exert internal pressure, which generates cracks first in aggregates and later into hardened cement pastes. ASR damage is among the most commonly diagnosed durability problems for aged infrastructures (Fernandes et al. 2004). During formation of ASR products, alkalis will be removed from the cement porewater, which lowers the pH.

It is expected that silica will continue to dissolve as long as the pH of the concrete pore solution is buffered at ~ 12.5 by $Ca(OH)_2$ (Glasser 2001). Studies of historical concrete infrastructure have revealed that the outstanding longevity of these materials is a result of the pozzolanic reaction between the lime and the (alumino)siliceous constituent (Malinowski 1979, Moropoulou et al. 2005, Silva et al. 2005). Abundant calcium silicate hydrates were found both in crystalline and amorphous forms (Jackson et al. 2017). On the one hand, this silica-lime reaction is clearly beneficial to the structural integrity of the aged concrete, but, on the other hand, it will cause a long-term reduction in pH that might promote metal corrosion and degradation of organic matter.

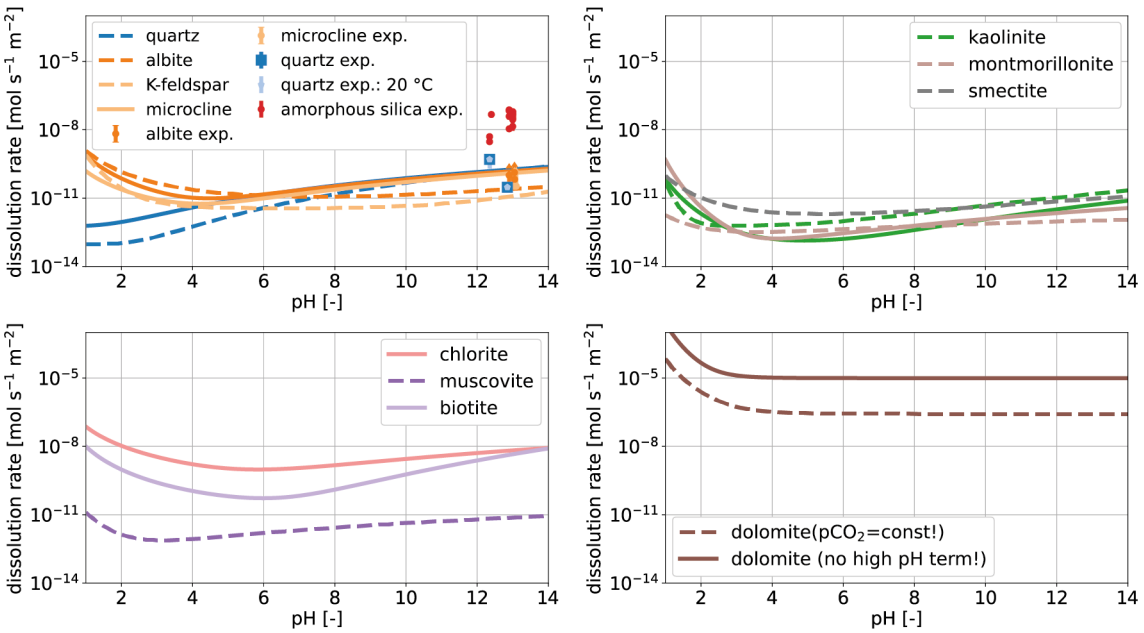

Fig. 3-11: Plot of pH dependence of normalised dissolution rates for some common rock-forming minerals at 25 °C, mineral saturation index[2] **Ω** ≈ 0 (maximum under-saturation) and normalised to a reactive surface of 1.0 m^2

Kinetic data from the Thermoddem DB (Marty et al. 2015b) are plotted as solid lines, while data from Palandri & Kharaka (2004) are plotted as dashed lines. Experimental data for dissolution of quartz, albite, microcline and amorphous silica at 40 ºC and pH > 12 from Bagheri et al. (2022) are added for comparison.

The pozzolanic reaction is the chemical reaction that occurs in Portland cement upon the addition of pozzolans. In chemical terms, the pozzolanic reaction occurs between portlandite ($Ca(OH)_2$), and silicic acid (H_4SiO_4) and produces calcium-silicate-hydrate C-S-H:

$$Ca(OH)_2 + H_4SiO_4 \rightarrow CaH_2SiO_4{\cdot}2\,H_2O \qquad (3\text{-}1)$$

According to Thomas (2013) *"typically, the C/S ratio ... of the C-S-H that forms from this reaction will be lower than the C/S ratio measured for C-S-H in hydrated Portland cement without pozzolan, and the difference will vary depending on the age, type, and amount of pozzolan"*. In the context of cement degradation stages (see Section 3.3.1), the cement is gradually moved from cement degradation Stage II to Stage III. Porewater pH is lowered towards ~ 10 where C-S-H with low C/S ratio is in thermodynamic equilibrium with dissolved siliceous aggregate (in terms of equilibrium silica concentrations in porewater).

[2] **Ω** = IAP/K with the ion activity product IAP and the equilibrium constant K (ion activity product for equilibrium conditions) for a mineral in contact with a solution. For **Ω** = 1 the mineral is in equilibrium with solution, for **Ω** > 1 the solution is oversaturated and the mineral tends to precipitate while for 0 <= **Ω** < 1 the solution is undersaturated and the mineral has the tendency to dissolve.

Thomas (2013) writes that *"The alumina present in pozzolans will also react with the $Ca(OH)_2$ from Portland cement and may produce a variety of phases, the principal ones including strätlingite or gehlenite hydrate (C_2ASH_8) and hydrogarnet (C_3AH_6), and others being calcium aluminate hydrate (C_4AH_{13}), ettringite ($C_3A{\cdot}3Cs{\cdot}H_{32}$), calcium monosulphoaluminate ($C_3A{\cdot}Cs{\cdot}H_{12}$), and calcium carboaluminate ($C_3A{\cdot}Cc{\cdot}H_{12}$)"*[3].

An example for the mineralogical changes in a concrete material upon the release of silica from dissolution of quartz aggregates was calculated by Kosakowski et al. (2020) and is shown Fig. 3-12. The first three stages of cement degradation (Section 3.3.1) can be identified. The initial system (zero Si released) corresponds to a fully hydrated concrete (Stage I). With increasing amount of Si released, portlandite is consumed and C-S-H is formed (Stage II). If more than ~ 1 mol dm^{-1} Si is released, the concrete will be in Stage III. The C-S-H amount will increase until quartz is in equilibrium with the pore solution (at ~ 3.95 mol dm^{-1} Si released).

In their overview of AAR, Leemann et al. (2016) list silica (SiO_2 independent of speciation) as a major source for reacting minerals. Specifically, opal, chalcedony, certain forms of quartz, such as cristobalite, tridymite and rhyolitic, dacitic, latitic, or andesite glass or cryptocrystalline devitrification products and synthetic siliceous glass are listed as reactive substances by Thomas et al. (2013).

The reactivity of quartz is related to the degree of crystallinity. Leemann et al. (2016) write that *"overall, quartz is responsible for slowly developing ASR and leads to damage in concrete structures after one to a few decades"*. Furthermore, they write *"common rock-forming minerals such as feldspars, micas, nepheline, clays and zeolites may release alkalis especially when weathered, thus contributing to deleterious ASR"*.

As most important deleterious alkali-reactive rocks (containing excessive amounts of one or more reactive minerals), Thomas (2013) lists: "opaline cherts, chalcedonic chert, quartzose cherts, siliceous limestones, siliceous dolomites, rhyolites and rhyolitic tuffs, dacites and dacitic tuffs, andesites and andesitic tuffs, siliceous shales, phyllites, opaline concretions, fractured, strained, and limestone-filled quartz and quartzites." All these materials have in common that the SiO_2 occurs in microcrystalline or partially amorphous forms or has been exposed to mechanical strain or thermal impact.

Siliceous aggregate dissolution rates

Common databases (Marty et al. 2015b, Palandri & Kharaka 2004) contain dissolution rates of various rock-forming minerals under alkaline conditions. Dissolution rates for tectosilicates, quartz and feldspars at high pH (pH > 10) are between 10^{-10} and 10^{-11} mol/s/m^2, while dissolution rates for aluminosilicates, such as phyllosilicates, clays, and muscovite are slightly lower between 10^{-11} and 10^{-12} mol/s/m^2. Chlorite and biotite are higher at 10^{-9} mol/s/m^2. From kinetic databases and literature, it is known that the dissolution of amorphous silica or common polymorphs of silica (e.g. cristobalite) is much faster than quartz.

Dissolution of minerals that release significant amounts of alkalis (e.g. feldspars and micas) might cause an increase in the pH of the pore solution, which might further accelerate dissolution and cause precipitation of ASR products.

[3] Cement nomenclature: A = Al_2O_3, C = CaO, c = CO_2, S = SiO_2, s = SO_3, H = H_2O

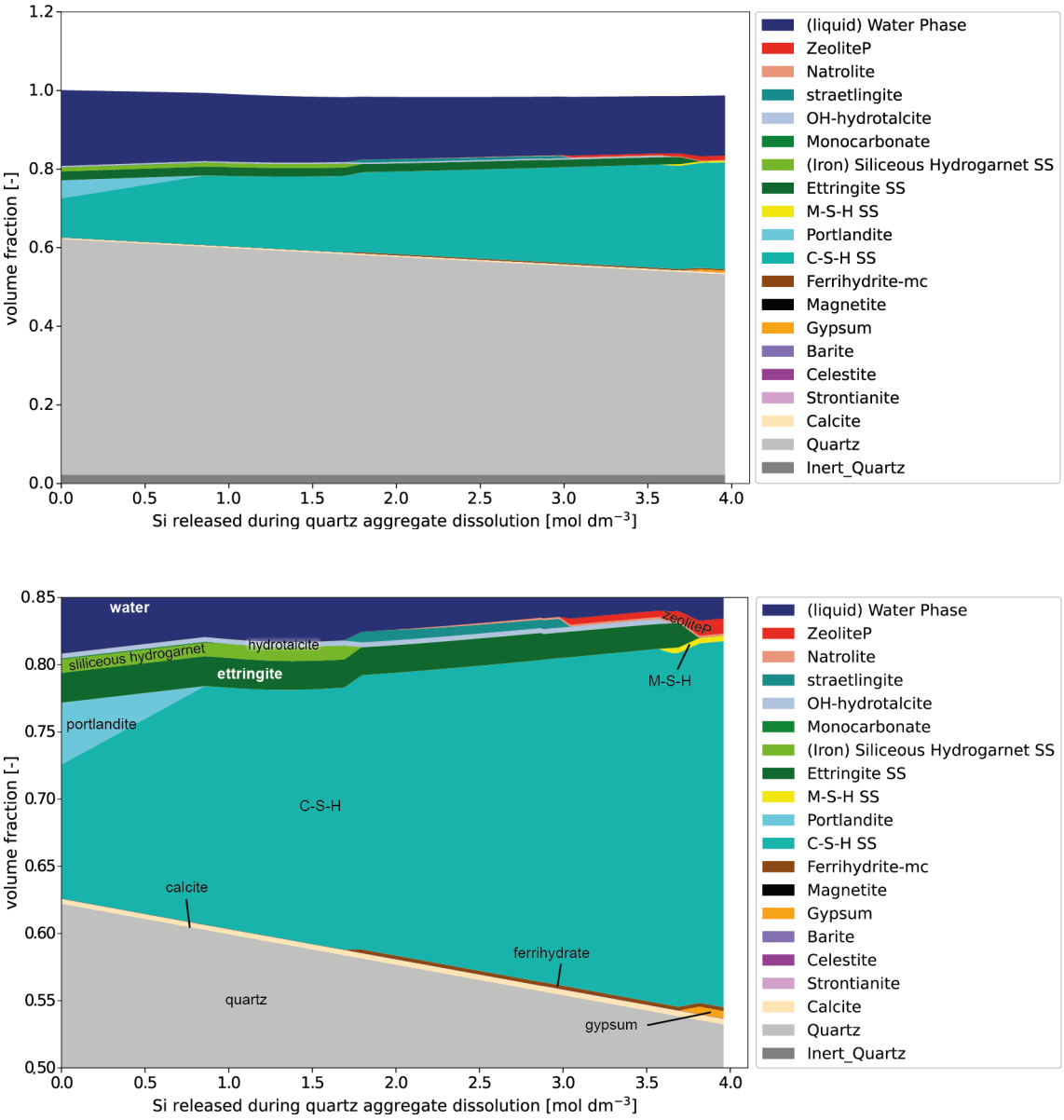

Fig. 3-12: Example of calculated mineralogical evolution of a fully hydrated concrete used in SGT Stage 2 (Kosakowski et al. 2014) upon dissolution of quartz

Full-scale view top and detailed view bottom. Mineral phase names are given as in thermodynamic setup: Inert_Quartz: inert mineral phase with density of quartz; SS: solid solution.

Calcareous aggregate – cement paste reaction

Calcareous aggregates consist mostly of carbonate rocks, e.g. limestone, dolomite or even marble. The main constituent of limestone is the mineral calcite ($CaCO_3$). Calcite is the most stable calcium carbonate form under standard conditions (1 bar, 25 °C). During carbonation of cementitious materials, CO_2 together with calcium leached from cement hydrates forms calcium carbonate as the main reaction product. Calcite is formed during carbonation only at very high relative humidity, whereas, at lower relative humidity, other metastable crystalline polymorphs (vaterite and aragonite) are formed (Steiner et al. 2020).

Calcium carbonate itself is an important addition as filler material to Portland cement (Matschei et al. 2007). Addition of limestone will cause formation of monocarboaluminate and hemicarboaluminate phases instead of monosulphoaluminate. If limestone addition is high enough, calcite – or more generally calcium carbonate - is in thermodynamic equilibrium with the cement phases and is not subject to long-term reactions with cement phases.

The term "alkali-carbonate reaction" (ACR) is mainly used for the reaction between alkaline pore fluids and calcium-magnesium carbonates, i.e. dolomite (Grattan-Bellew & Katayama 2019, Winter 2009). The alkalis in the cement porewater might react with the dolomite crystals present in the aggregates, inducing the production of brucite, $Mg(OH)_2$, and calcite ($CaCO_3$).

The mechanism was tentatively proposed by Swenson and Gillott (1964) and may be written as follows for sodium:

$$CaMg(CO_3)_2 + 2\ NaOH \longrightarrow CaCO_3 + Na_2CO_3 + Mg(OH)_2 \qquad (3\text{-}2)$$

For potassium, a similar reaction can be written. According to Leemann et al. (2016), the precipitation of brucite ($Mg(OH)_2$) occurs in pores within the dolomite and is not connected to expansion. Alkalis (Na, K) and CO_3 will react with portlandite to form calcite in the cement paste adjacent to aggregates. This reaction is a kind of dedolomitisation and can be regarded as ACR in a narrower sense (Leemann et al. 2016). As Ca from cement phases is consumed during these reactions, cement is promoted towards degradation Stage III (cf. Section 3.3.1).

Dolomite dissolution rates

ACR in the presence of dolomite (Ca-Mg carbonate) is orders of magnitude faster than the pozzolanic reaction in the presence of aluminosilicate aggregates. The dissolution rates of dolomite are by far the highest, ranging in value up to 10^{-6} mol/s/m^2 at high pH (Fig. 3-11). This might be related to the missing kinetic data for alkaline conditions. There are indications in the literature that dissolution rates for dolomite are lower at high pH. The calculated rates are a possible upper limit. Likewise, the rates calculated for biotite (phlogopite) dissolution, an Mg-containing mica, are two orders of magnitude lower (at most 10^{-8} mol/s/m^2). It can be calculated that, for ACR with unlimited availability of dolomite aggregate, all Ca from cement phases will be leached (Fig. 3-13) and the equilibrium pH of the porewater drops below 10.

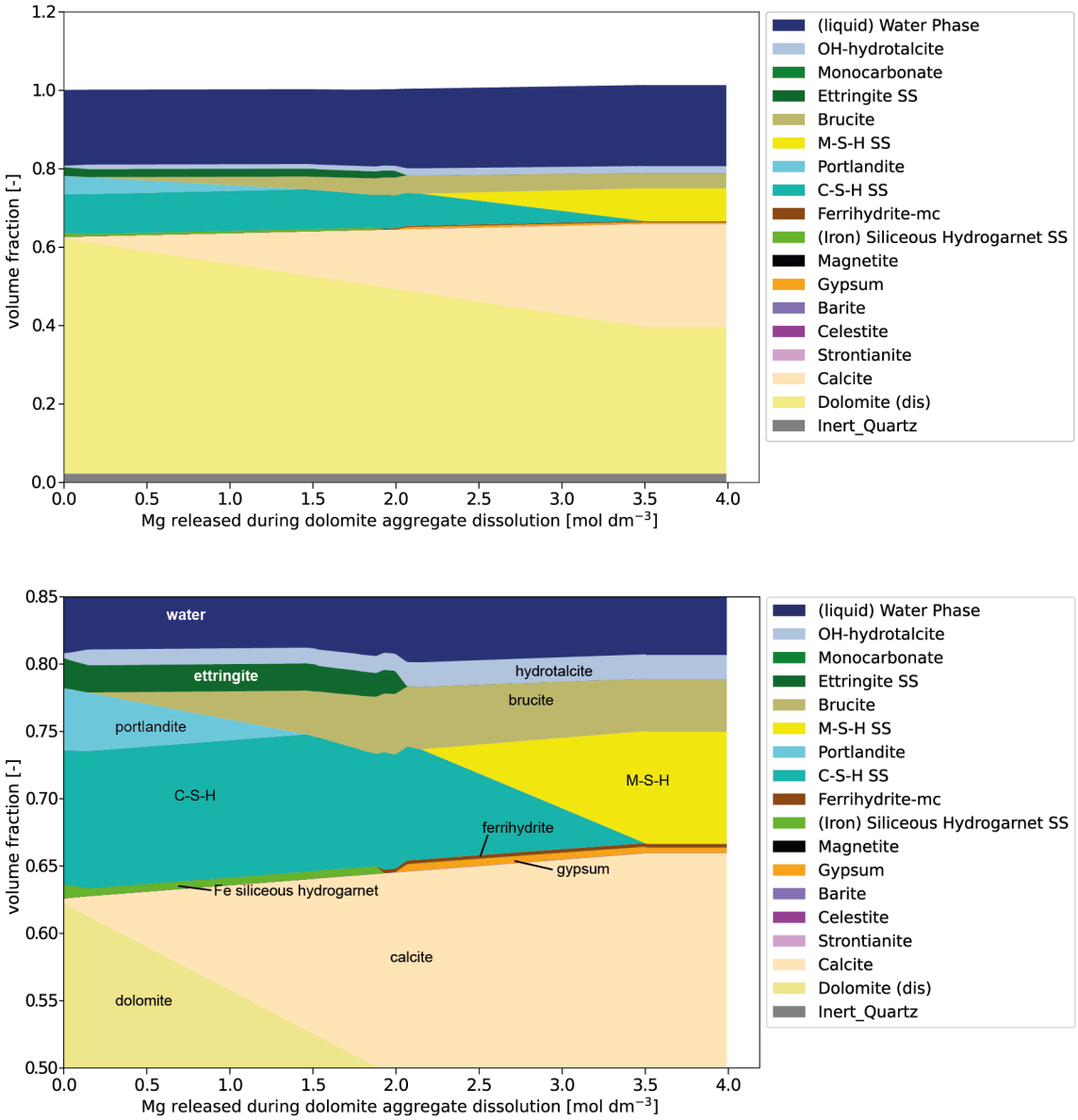

Fig. 3-13: Example for calculated mineralogical evolution of a concrete used in SGT Stage 2 (Kosakowski et al. 2014) upon dissolution of dolomite

Full-scale view top and a more detailed view bottom. Mineral phase names are given as in thermodynamic setup: Inert_Quartz: inert mineral phase with density of quartz; SS: solid solution.

Aggregates used in concrete in Switzerland

In Chapter 5 of "Die mineralischen Rohstoffe der Schweiz" (Kündig et al. 1997), sand and gravel deposits are presented in detail. Natural sand and gravel used for concrete are mostly found in (fluvio)glacial deposits and, to lesser degree, in weakly cemented "Molassennagelfluhen" in the Swiss "Mittelland (plateau)". The composition of deposits is related to the petrography of the place of origin (Claude et al. 2017, Kündig et al. 1997, Weltje & von Eynatten 2004). Due to the diverse petrography of the most important source area, the Swiss Alps, the petrography of the rock is correspondingly diverse. With increasing transport distance, hard rock types and minerals, e.g. limestone, siliceous limestone, quartz and other silica-rich rocks, are enriched (Kündig et al. 1997).

In addition, crushed rock can generally be used as aggregate. In Tab. 4.1 of Bärtschi (2012), twelve active sites for production of gravel and split (stone chippings) in Switzerland are given. Most of them mine siliceous limestone and otherwise flysch, subalpine molasse or glauconitic sandstone. Siliceous limestones and the sandstones are potentially reactive due to their relatively high quartz content. Specifically, the reactivity of Swiss siliceous limestone was investigated by Bourdot et al. (2018). They found that the presence of finely dispersed micro to cryptocrystalline quartz causes the high reactivity of siliceous limestone in terms of ASR (and pozzolanic reaction).

Timescales

As mentioned before, temporal progression of out-of-equilibrium geochemical processes is often described with the help of reaction rates. This makes it possible to include a timeline in the process description. In Kosakowski et al. (2020), the degradation of selected representative concrete materials (concrete for SGT Stage 2, a backfill mortar M1 and a container concrete) due to reaction with siliceous "quartz" aggregates was calculated (Fig. 3-14). For calculation of the quartz aggregate dissolution rates, the parameterisation from Palandri & Kharaka (2004) was used. The reactive surface area of aggregates linearly influences the dissolution rates. The results presented in this section are conservative, as it is assumed that the complete surface of aggregate grains is in contact with the alkaline pore solution and the aggregate grains are homogeneously dissolved. As discussed further below, the limited availability of water and uncertainties related to the reactive surface area of partially saturated dense cement materials will lead to an inhomogeneous and therefore slower aggregate dissolution.

For mortar M1 and the concrete labelled SGT Stage 2, we can assume that the reactive surface area does not change strongly until equilibrium between the cement phases and the quartz aggregate is reached. Only a small fraction of the aggregate needs to be dissolved to reach equilibrium due to the high amount of aggregates compared to the amount of cement paste. As aggregate grains in these materials all have the same size of 2.8 mm diameter, the changes in diameter and consequently surface area are small. The assumption of a constant surface area during the course of degradation is not accurate for the container concrete as the aggregate has a wide grain size distribution (Kosakowski et al. 2020). The fine aggregate size classes (clay – silt – sand) dissolve quickly with decreasing aggregate size, due to their high surface to mass ratio. Coarse aggregates (gravel) have a low surface to weight ratio and dissolve slowly. For a structural concrete such as the container concrete as a general example, the change in total reactive surface area upon degradation in terms of changing grain diameter for the (measured) aggregate size classes has been included in the calculation of the kinetic rates. The calculated aggregate dissolution of the three materials at three temperatures in terms of silica released due to dissolution of quartz aggregates is shown in Fig. 3-14 (upper figure). The released silica will react with (cement) minerals, which will change the mineral assemblage (cf. Fig. 3-12) and alter the mineral saturation index for quartz. In addition, the pH of the solution is reduced as indicated in Fig. 3-14. The drop in pH and mineral saturation index cause a reduction of dissolution rates with time.

The influence of temperature increases from 30 °C to 42 °C on the dissolution reaction is not negligible and accelerates the system by about a factor of 3 (cf. Fig. 3-14).

For the container concrete, the initial silica release is high, as the aggregates contain a considerable fraction of very small aggregates. Once these aggregate particles are dissolved, the reactive surface area decreases and silica release drops. Aggregate dissolution stops after several tens of thousands to hundreds of thousands of years, when thermodynamic equilibrium between quartz and cement phases (C-S-H) is reached. At that stage, the concrete is in degradation Stage III, characterised by a very low calcium/silica ratio and a solution pH close to 10.

Mortar M1 and the concrete SGT Stage 2 use the same monocorn aggregate. They have a higher reactive surface area per volume compared to the container concrete (after fine aggregates are dissolved) and their cement content per volume is lower. Therefore, they reach the equilibrium state much faster, typically after several hundreds of years up to a (few) thousand years.

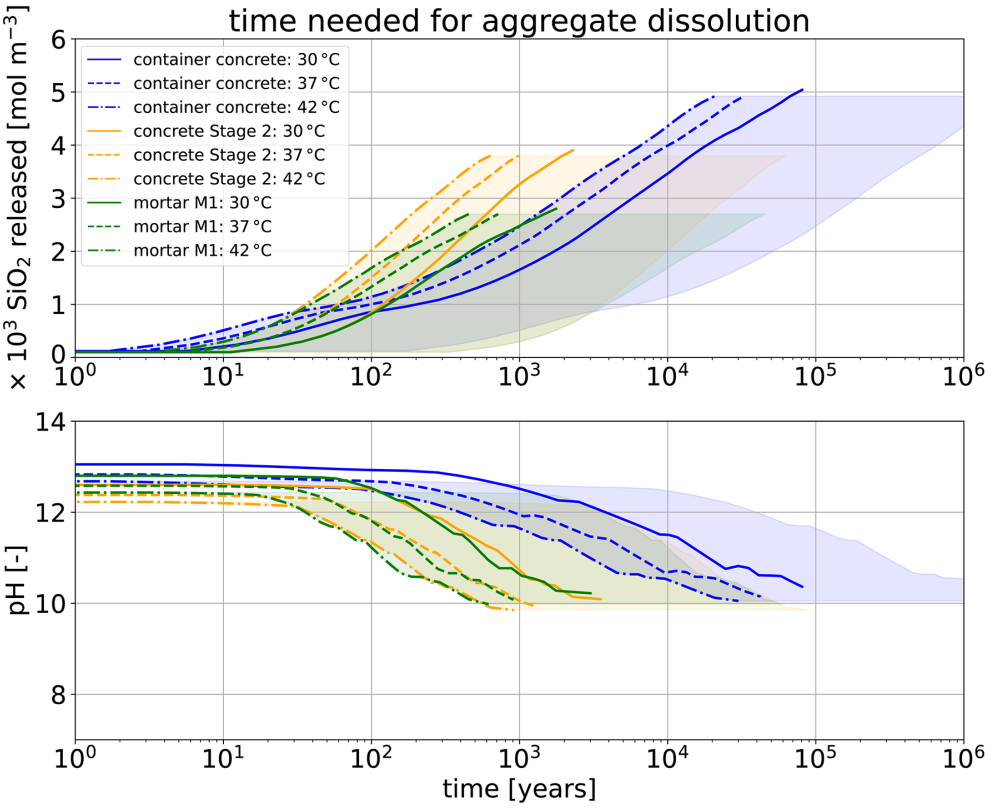

Fig. 3-14: Estimates of aggregate dissolution with time (upper figure) and pH evolution with time due to aggregate dissolution only (lower figure)

The vertical lines indicate the completion of aggregate dissolution, i.e. quartz is in thermodynamic equilibrium with the other mineral phases. The shaded areas show slowdown of aggregate dissolution rates of up to two orders of magnitude for the materials at 42 ºC due to lower reactive aggregate surface area and desaturation. In principle, for a certain slowdown, curves are shifted to the right, i.e. for 100 times slower dissolution rates the curves are shifted from the left boundary of the shaded area to the right boundary. In reality, in highly desaturated (“dry”) materials aggregate dissolution rates are probably close to zero.

The reaction times given above for aggregates of 2.8 mm diameter are surprisingly short, and this leads to the question whether the applied rate equation and its parameters really make physical sense. A simple consistency check can be made by applying the rate equation to low-pH ESDRED concrete where SiO_2 reaction rates have been measured (Lothenbach et al. 2014). ESDRED concrete includes reactive silica fume with a grain size of only 11 µm, leading to a very high reactive surface area. For such a high reactive surface area, the kinetic parameterisation of the model used predicts that only 14 years are required to completely neutralise the concrete system. This is in agreement with the results of Lothenbach et al. (2014) who report that about 3 years is required for the depletion of most of the reactive silica for samples completely immersed in water.

Hence, the predictions for dissolution of siliceous aggregates seem to be not too far from reality in fully saturated media, and we conclude that the internal degradation of concrete by reacting SiO_2 may be a reasonably fast process at high pH.

Uncertainties

There is a vast amount of information on aggregate-cement reaction in the literature (Sims & Poole 2017) that demonstrates that rock-forming minerals, if they are included as aggregates in cementitious materials, react with cement phases and alter material properties. These reactions are kinetically controlled and effective kinetic rates are not well constrained (see discussion in Marty et al. 2015b).

One important, if not the most important, source of uncertainty in kinetic rates is the value of the effective reactive surface area, which is important for the description of the dissolution process. Kinetic rates are frequently measured with dissolution experiments of small mineral particles suspended in a relatively high amount of solution (which is constantly stirred/mixed). Firstly, it is straightforward to measure the BET surface area for mineral powder and, secondly, during the experiment the whole grain surface is in equal contact with the solution, although possibly not all surfaces dissolve at the same rate (Fischer et al. 2014). Furthermore, the mineral powder used in experiments is often a freshly crushed material, which might not be representative for cement-aggregate reactions.

In petrology, the reaction rates commonly estimated from field observations are often significantly lower than those measured in lab experiments (Brantley 2008, White & Brantley 2003). In rocks and artificial media like concrete, the liquid to solid ratio is much lower and the surface of mineral grains is not evenly in contact with the pore fluid. Recent experimental studies demonstrate that the pore-scale reactivity of minerals in combination with microscopic and macroscopic transport controls the evolution of the corresponding material at macroscopic scale (Kurganskaya & Rohlfs 2020, Noiriel & Daval 2017, Poonoosamy et al. 2020, Prasianakis et al. 2017).

In addition, disconnected pores or partial water saturation might compartmentalise the pore space and slow down or interrupt microscopic transport of solutes. For such a compartmentalised pore space, the porewater composition might vary considerably. All these conditions make it very difficult to assign a single effective surface area. In addition, the pore space geometry, the mineral grain size and surface roughness of mineral grains might change significantly during dissolution (and precipitation of other reaction products). Frequently, this effect is lumped into a “chemical reactivity” function, which links liquid water saturation with a reduction of kinetic rates (Huang et al. 2021, Thouvenot et al. 2013). It should be noted that the reactive surface area is normally used as a lumping factor in reactive transport calculations (Beckingham et al. 2017).

It might be possible that part of the aggregate surfaces is passivated as they become coated with secondary precipitates (e.g. C-S-H). Such behaviour is reported for example by Offeddu et al. (2015) for the passivation of limestone surfaces by gypsum in the treatment of Acid Mine Drainage. Similarly, Poonoosamy et al. (2020) observed passivation of grain surfaces in flow-

through experiments where celestite was dissolved and replaced by barite. For the case of cement materials, and if the precipitation product is C-S-H, complete passivation of aggregates surfaces seems unlikely. C-S-H precipitates are themselves porous and solute transport in the so-called gel porosity is relatively fast. In addition, C-S-H can be easily dissolved again if conditions change. In fact, the Alkali-Aggregate Reactivity (AAR) Facts book (Thomas et al. 2013) states that from many tested substances, only a pre-treatment of aggregates with lithium compounds (e.g. lithium nitrate) effectively suppresses ASR. They state that the exact process is not known, but the *"simplest and most commonly used explanation is that lithium salts will react with reactive silica in a similar way to sodium and potassium salts, but for the reaction product is an insoluble lithium-silicate with little propensity to imbibe water and swell. The lithium silicate forms around reactive aggregate particles and protects the underlying reactive silica from "attack" by alkali hydroxides".*

With the help of thermodynamic models and a kinetic description of dissolution of aggregate minerals, it is possible to predict the long-term evolution of mineralogy and porewaters in concrete. Nevertheless, conservative estimates of reaction rates for fully saturated concretes shown in Fig. 3-14 indicate that rates might be fast enough to degrade cement materials completely within a few thousand years or even faster (Kosakowski et al. 2014, 2020, Wieland et al. 2018). The effective kinetic rates for dissolution of aggregate minerals are uncertain, specifically under partially saturated conditions and if combined with highly uncertain "reactive surface areas". The effect of slower rates is exemplified via the shaded areas connected to the concrete labelled SGT Stage 2 in Fig. 3-14. The upper limits of these reaction rates are relatively well defined, because quartz dissolution rates for fully saturated conditions are known and the upper limit for the reactive area is close to the geometric area for smooth surfaces. The lower limit of reaction rates is highly dependent on local conditions, i.e. pore space geometry and how much surface is accessible for the solution. De-saturation of the concrete might further delay dissolution reactions. In extreme cases (very dry conditions), the aggregate dissolution might be delayed even further than indicated by the right boundary of the shaded area in Fig. 3-14.

For cases where such aggregate-cement reactions need to be avoided or reduced, the use of inert aggregates should be evaluated, i.e. aggregate minerals that are in thermodynamic equilibrium with cement phases. For OPC-based materials, the obvious choice would be pure limestone (calcium carbonate, calcite). Real limestone often contains impurities (e.g. micro-silica or magnesium-bearing minerals like dolomite). In order to assess the amount of impurities that can be tolerated in terms of chemical changes, the type of calculations conducted in this work can be used to assess the cement degradation for completely reacting those aggregate components. For these reasons, it could be evaluated to use relatively pure $CaCO_3$ for the backfill mortar M1, which is possibly the material which is the most susceptible to cement-aggregate interaction from a silica dissolution kinetic point of view (Fig. 3-14) in the L/ILW repository (Martin et al. NAB 22-44 *in prep.,* Nagra 2021b).

3.3.6 Cement and clay colloids

Overview

Colloids are semi-crystalline and amorphous particles with dimensions varying from a few nanometres to sub-micrometres in diameter. Such particles are omnipresent in subsurface environmental systems. Under rather specific chemical and hydrodynamic conditions, colloidal particles can provide a significant contribution to the mass transport and mechanical degradation of the repository barrier materials or eventually facilitate transport of radionuclides (Kretzschmar & Schafer 2005). If, however, the necessary conditions for colloid mobility and stability are not met (see below), the importance of colloidal transport is limited. In the context of radionuclide transport, the colloidal particles are classified as "intrinsic colloids" and "pseudocolloids" (Kim

1994). The intrinsic colloids are formed by polymerisation of hydrolysed metal cations and anionic ligands. Specifically, for radioactive waste disposal systems, poorly soluble tetravalent actinides can form highly stable intrinsic colloids (Geckeis 2004). Pseudocolloids, on the other hand, are formed by radionuclide adsorption onto pre-existing colloidal particles such as clay minerals, iron oxyhydroxides, alumina or humic colloids. Due to the very high specific surface area (10 – 800 m^2 g-1), pseudo-colloids have a significant retention capacity and thus mobilisation potential of strongly sorbing radionuclides.

The key factors controlling colloid-facilitated transport are the presence, stability, and mobility of colloids themselves and their interaction with the radionuclides (McCarthy & Zachara 1989). To contribute significantly to radionuclide transport, several conditions must be fulfilled simultaneously (Zänker & Hennig 2014):

- Colloidal particles must be present in a non-negligible concentration.
- The colloids must be mobile and form a stable suspension in the repository in situ conditions.
- Radionuclides should be irreversibly bonded to colloids and/or have slow desorption kinetics.

If any of these conditions are not fulfilled, the contribution of colloids to the transport of radionuclides would likely be negligible.

Colloids relevant for disposal systems in argillaceous rocks can be formed by clay minerals, cement phases (e.g. C-S-H, AFm/AFt), mineral precipitates (e.g. Fe, Al, Mn, or Si oxides and hydroxides, carbonates, phosphates) and organic matter. The mobility of colloids is strongly dependent on fluctuations in water saturation, flow velocity, and temporal variations in aqueous solution composition, ionic strength, pH and redox potential of porewater (Bradford & Torkzaban 2008). The interaction between these factors is complex and is not yet fully understood in terms of model-based mechanistic description. Whereas frequent periodic fluctuation of chemical conditions in the repository near-field is unlikely, strong chemical gradients are imposed by the use of different barrier materials (e.g. cement-clay interface). Furthermore, heterogeneities are present at different scales. Large-scale variations in porewater salinity are reported in host rocks and small-scale heterogeneities are present in waste packages.

Either stable or unstable populations of colloids in porewater solution depend on particle properties and porewater chemistry. In unstable systems, colloidal particles agglomerate and undergo deposition under gravitational forces. Coagulation-sedimentation processes depend not only on the physical properties of the colloidal material, such as size, density and compactness, but also on the chemical properties of the surfaces and ambient solution, which determine the strength of binding between the colloidal particles. Electrical potential, chemical reactions as well as microbial activities are key processes for the production and degradation of colloids and macromolecules (Buffle & Leppard 1995).

The forces that affect dispersion or coagulation of particles are electrochemical in nature and are related to the surface charge of colloidal particles, which essentially depends on the pH and the ionic strength of the solution. The surface charge density can be either positive or negative. Consequently, the surface potential can be positive or negative, favouring the uptake of anionic and cationic species respectively. Electrostatic repulsion forces between equally charged surfaces are counterbalanced by the van-der-Waals-type dispersive interaction. These attractive forces make particles stick together when they come within a few nm of each other. The van der Waals attraction arises from the fact that each ion in a particle induces an interaction in the neighbouring atoms of an adjacent particle leading to the net attractive force. The underlying physical mechanism of these forces is described by the so-called DLVO theory (Derjaguin & Landau 1993, Verwey 1947).

The following sections summarise the status of knowledge regarding the generation, stability and migration of colloids in cementitious systems and clay-rich materials relevant for the deep geological disposal of radioactive waste.

3.3.6.1 Clay colloids

Overview/general description

Colloids are present in all types of water, even in quasi-stagnant water where they are found at rather low concentrations (Degueldre et al. 2009). Their concentrations, however, may be enhanced by chemical and/or physical gradients (Degueldre 1996, McCarthy & Degueldre 1993, Ryan & Elimelech 1996). This section summarises the information in the literature and applies the concept of colloid generation near cement-clay interfaces in the sealing system and at the cement–host rock formation interface.

Information from experiments

A literature overview of relevant experiments on clay colloid stability is presented in Kosakowski et al. (2014) and will not be repeated here.

The colloid occurrence, stability and mobility in Opalinus Clay porewater have been evaluated in Degueldre et al. (2003). The colloid concentration is expected to be very low (< 105 m/L for 100 nm sized particles or [col] < 1 µg /L) because of the very large attachment factor for the colloids in the Opalinus Clay porewaters (see Tab. 3-2). Even if colloids (clays, silicates, hydroxide polymers) are generated at elevated pH in OPA, it is expected that they would coagulate or attach themselves to the clay minerals in the host rock, thus limiting their migration. Accordingly, colloids are considered to be of minor relevance for a cementitious repository located in Opalinus Clay.

Tab. 3-2: Main colloid parameters and concentrations in Opalinus Clay porewater

Kosakowski et al. (2014)

Water	**Opalinus Clay**
Type	Na-Cl
Na [mol/L]	1.6×10^{-1}
Cl [mol/L]	1.6×10^{-1}
pH [-]	7.2
α [-]	10^{-1}
$N_{(100nm)}$ [m/Lnm^{-1}]	$10^4 – 10^5$
$N_{(>100nm)}$ [ml^{-1}]	5×10^5
[col]* [ppb]	0.5

Conditions: aquifer in quasi-stagnant conditions, I ionic strength, α attachment factor, N colloid number concentration, [col] colloid concentration

* for colloid size of 10 – 100 nm.

3.3.6.2 Cement colloids

Overview/general description

Cementitious materials are expected to be the main source of colloids in the repository near-field due to the large amount of cement employed in the L/ILW repository. The gel-type semi-crystalline hydrates of the mineral assemblage of hardened cement paste (HCP), in particular C-S-H and calcium aluminates (AFm-type phases), could disperse if the concentration of alkaline and alkaline-earth metal cations at the HCP/water interface is below the critical coagulation concentration (CCC) threshold, or in the case of high water flow. For oxide-type colloids, the CCC is typically around ~ 1 mmol/L in Ca^{2+} solutions and about a factor of 100 larger in Na^{+}- and K^{+}-containing solutions. The alkali and Ca concentrations in the near-field are determined by the interaction of infiltrating groundwater with the cementitious materials. Release of alkali elements in the early stage of the cement degradation, and portlandite and C-S-H solubilities in the later stages of cement degradation, control the pore-water conditions. The high ionic strength (range ~ 0.01 – ~ 0.3 mol/L), determined by the presence of NaOH and KOH, along with the high Ca concentrations (range ~ 2×10^{-3} – ~ 20×10^{-3} mol/L) of cement-type porewater in all of the stages of cement degradation, are favourable for keeping a low colloid inventory in solution since colloid-colloid interaction and colloid attachment to surfaces is favoured. Hence, favourable conditions limiting colloid dispersion in the cementitious near-field are expected to prevail throughout the various stages of the cement degradation. In general, colloid mass concentrations were determined to be typically below 100 µg/L in leachates from cementitious materials under conditions of quasi-stagnant water flow. Furthermore, these colloids were found to be C-S-H-type solid materials. The experimental conditions for the quasi-stagnant water flow do not reflect the in-situ conditions in OPA, for which the advective water flow is negligibly low.

Cement-type colloids are subjected to chemical alteration in the pH range 10.5 – 12.5, which transforms C-S-H phases with high C/S ratios into C-S-H phases with lower C/S ratios. Chemical instability of C-S-H phases is anticipated to occur below pH 10. Therefore, it is conceivable that complete dissolution of C-S-H-type near-field colloids occurs at the interface between the cementitious near-field and the host rock, where hyperalkaline cement-type porewater and pore-water with pH < 10 intermix. Consequently, it is anticipated that the transport of cement-type colloids in the fractures of the host rock can only occur if cement-type porewater conditions are maintained, i.e. pH above ~ 10.

Cement-type colloidal matter is expected to play a minor role in radionuclide migration from the near-field into the far-field, because

- the concentration of dispersed colloids is very low in the near-field, which limits colloid-facilitated radionuclide transport
- cement-type colloidal matter is expected to be unstable, i.e. to dissolve, at the interface between the near- and far-field, thus releasing radionuclides associated with the colloidal material
- advective water flow necessary for colloid transport is negligibly low in OPA

Information from experimental/modelling studies

Laboratory-scale experiments indicate that colloids will be present in the saturated cementitious near-field of an L/ILW repository. The colloids have a composition similar to that of C-S-H phases, which are the main component of hardened cement paste (Fujita et al. 2003, Ramsay et al. 1988). Calcium silicate hydrate phases are poorly crystalline gel-like materials with a high surface area and colloidal properties (cf. Section 3.6.1 in Kosakowski et al. 2014 and references therein).

The concentration of cement-type colloids in the porewater of a porous backfill mortar has been reported to be very low, i.e. far below 1 mg/L, with measured values of 0.01 – 0.2 mg/L (Wieland & Spieler 2001). Fujita et al. (2003) determined the colloid concentration in leachates collected from different cement formulations and found that their concentrations ranged between 1,011 and 1,012 particles per L. This corresponds to a colloid mass concentration ranging between ~ 0.1 and ~ 1.1 mg/L on the assumption that a large portion of the colloidal matter was C-S-H phases with a mean particle diameter of 100 nm. The influence of high ionic strength and high Ca concentrations on colloid stability has been demonstrated in numerous studies (Filella 2007, Wieland 2001). The surface charge of cement particles is low (either slightly negative or positive) or zero over the entire pH range of cementitious systems ($10.5 < pH < 13.5$) (see e.g. Churakov et al. 2014). This promotes aggregation and surface sorption of cement-type colloidal matter.

C-S-H-type materials undergo incongruent dissolution in the pH range 10.5 – 12.5 due to the transformation of C-S-H phases with high C/S ratios into C-S-H phases with lower C/S ratios (Berner 1988, Harris et al. 2002). Furthermore, C-S-H phases were found to dissolve rapidly below pH ~ 10 (Schweizer 1999).

The impact of C-S-H-type colloids on radionuclide mobilisation in the cementitious near-field of an L/ILW repository was predicted to be negligibly small due to the low concentration of colloids in the cementitious near-field (Wieland et al. 2004). Uptake of radionuclides by C-S-H-type materials is a reversible or partly reversible process, depending on the radionuclide involved (Tits & Wieland 2018).

The effect of colloids on radionuclide uptake in sorption databases is accounted for using the sorption reduction factor F_{red}, by analogy with the impact of complexing ligands on radionuclide uptake (Wieland & Van Loon 2003). Sorption reduction factors for uptake by HCP in the presence of cement-derived near-field colloids has been estimated assuming a typical colloid concentration of 10^{-4} kg m^{-3} (Tits & Wieland 2023).

Timescales

The hydraulic properties of the host rock control the time-dependent evolution of the cementitious near-field. The temporal composition of the cement-type porewater in the near-field, in particular with respect to pH, ionic strength and Ca concentration, is controlled by mineral reactions occurring in the course of the different stages of cement degradation and in particular the saturation evolution within the L/ILW emplacement caverns. The latter process eventually controls the inventory of dispersed colloids in a cementitious near-field with a quasi-stagnant flow regime.

Boundary conditions/uncertainties

High ionic strength and Ca concentrations in the millimolar range limit colloidal dispersion. Furthermore, a low inventory of dispersed colloids requires a low flow or stagnant water in the near-field in order to minimise colloid generation. Under (quasi-) stagnant flow conditions, the shear forces generated are expected to be too small to allow colloid generation by colloidal disaggregation or the detachment of surface-bound colloids.

While cement-type colloidal material is chemically unstable in contact with groundwater from the host rock, calcium-carbonate-type colloidal matter may be chemically stable in both the near- and far-field. However, the impact on radionuclide migration is expected to be very limited due to the significantly lower sorption capacity of calcium carbonate compared with cement-type colloidal matter.

As a conservative estimate, the effect of colloids on retention and transport is described using sorption reduction factors (Tits & Wieland 2023).

The influence of cement leachate chemistry on the mobilisation of colloids in sediments was investigated by Li et al. (2012). A sharp front of mobile colloids was found to form after introduction of a cement leachate simulant. Observed mobile colloids consisted of goethite and, to a lesser extent, kaolinite. The released colloids had negative surface charges and the mean particle sizes ranged primarily from 200 to 470 nm. Inherent mineralogical electrostatic forces appeared to be the controlling colloid removal mechanism in this system. With a background pH of ~ 6.0, goethite had a positive surface charge, whereas quartz (the dominant mineral in the immobile sediment) and kaolinite had negative surface charges. Goethite acted as a cementing agent, holding kaolinite and itself onto the quartz surfaces due to the electrostatic attraction. Once the pH of the system was elevated, as behind the cementitious high-pH front, the goethite reversed to a negative charge, along with quartz and kaolinite, then goethite and kaolinite colloids were mobilised and a sharp spike in turbidity was observed. Simulating conditions away from the cementitious source, essentially no colloids were mobilised at 1:1,000 dilution of the cement leachate or when the leachate pH was ≤ 8. Extreme alkaline pH environments of cementitious leachate may change mineral surface charges, temporarily promoting the formation of mobile colloids.

3.4 Interactions between cement and waste

3.4.1 Degradation of organic materials

Polyvinylchloride (PVC), ion exchange resins (IER), bitumen, plastics, polycarboxylates, cellulose and Plexiglas® (polymethyl-methacrylate) are the main abundant organic materials in term of mass which will be disposed of in the L/ILW repository (cf. Fig. 3-15) (Nagra 2023b).

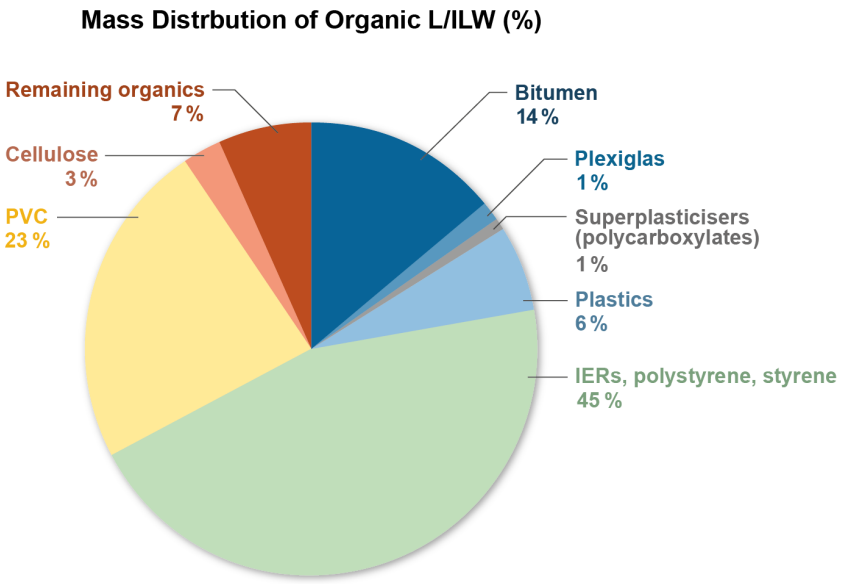

Fig. 3-15: Mass distribution of total organic materials (waste matrix and filling) based on the waste package type inventory

Nagra (2023b)

The degradation of organics in an L/ILW repository will take place by a combination of abiotic (i.e. radiolysis and hydrolysis) and biotic processes, the abiotic ones reducing the molecular size of complex polymers before microorganisms can degrade them into even smaller molecules. An extensive literature review of abiotic and biotic degradation of the main organic materials present in the Swiss L/ILW repository in conditions relevant for a cementitious near-field was made in Guillemot et al. (2023). The main important aspects are summarised in this section.

As detailed in Section 3.5.2, both abiotic and biotic degradation processes need the presence of free water (Guillemot et al. 2023, Warthmann et al. 2013). As outlined in Section 3.2.1, water saturation is low in the L/ILW repository for very long times, specifically in the waste packages positioned in the upper part of the disposal caverns. The rates and the degree of degradation of organics in the near-field of an L/ILW repository are influenced by the chemical structure of the polymers, the environmental conditions (pH, water content, redox, temperature) and the microbial activity.

Radiation-induced degradation

Shortly after closure of the L/ILW repository, the degradation of the organic materials is expected to be mainly radiolytic due to the initial dose rate, the presence of remaining O_2 and water in the waste matrix. The influence of radio-oxidative degradation might however be strongly limited by O_2 supply (through diffusion), rapidly consumed at the initial dose rate. In the near-field of an L/ILW repository, the total absorbed dose and associated radiation-induced degradation are mainly controlled by the presence of ^{60}Co, present in activated metals. It is the main γ-emitter in the L/ILW inventory and has a short half-life ($t_{1/2}$) of 1,925 days. The dose rate in the near-field of an L/ILW repository will thus rapidly decrease over time. In the long term, β-irradiation is expected to have only a negligible impact on the degradation process due to its lower energy (typically < 1 MeV). Hence, radiation-induced degradation of organics is mainly caused by α-decay of radionuclides with longer half-lives but being scarce in the L/ILW inventory (Nagra 2023b) and affecting only the organics directly in contact with these radionuclides (i.e. IERs and bitumen). In the literature review of Guillemot et al. (2023), the total absorbed dose seems to determine the amount of degradation products formed, and therefore the degree of degradation, irrespective of whether this dose has been accumulated in a short time at a higher dose rate or over a longer time at a lower dose rate.

When exposed to radiation, polymers undergo various chemical changes at a microscopic level, comprising:

1. the formation of chemical bonds between different molecules (crosslinking), leading to an increase in molecular weight and resistance to further degradation processes
2. the irreversible cleavage of bonds resulting in fragmentation (scission), leading to a decrease in molecular weight
3. the formation or disappearance of unsaturated compounds (C=C)

The resistance of the different types of polymers to radiation is largely determined by their chemical structure. In general, polymers with aromatic groups have a significantly higher radiation resistance than aliphatic polymers, regardless of the position of the aromatic groups in the chain. For example, polystyrene is stabilised by the aromatic ring and changes less quickly under radiation than PVC, polyethylene and polypropylene, which have a basic aliphatic structure. Plexiglas® is a polymer with quaternary (tetra-substituted) carbon atoms in the main chain that is more susceptible to radiation-induced degradation. Similarly, polyester and cellulose with a high content of strongly electronegative elements in the backbone structure are susceptible to radiation-induced degradation. It should be noted that commercially available products made from most polymeric materials contain various additives such as stabilisers, antioxidants, fillers,

pigments and flame retardants that are added to produce or improve certain material properties. The additives are selected so that they remain in the polymer structure and are therefore also subject to radiation-induced degradation.

It is generally observed that irradiation of organics leads to the production of small radicals such as •H, •CH_3, •CO, •CO_2. These radicals can recombine with the polymer itself or with each other, the latter resulting in the formation of H_2, CO, CO_2, CH_4, and C_2H_4. The irradiation of polymers therefore generates small gaseous products. Some of the products generated by the radio-oxidation of the material are low-molar-mass oxidised species which can also be dissolved in water and released when polymer waste comes into contact with water. Low molecular weight (LMW) molecules can also be produced by scission and available as substrates for microbial activity. On the other hand, crosslinking improves the stability of the polymers, by forming a three-dimensional network of polymer chains, against alkaline hydrolysis and microbial degradation. Hence, the chemical stability of the carbon backbone of PVC, IERs, bitumen, polyethylene and polypropylene may have improved over time, resulting in a non-negligible proportion of the L/ILW organics not being further susceptible to degradation.

Chemical degradation

Anaerobic conditions are expected to develop rapidly after closure of the deep geological repository (i.e. maximum up to several hundreds of years) (Wersin et al. 2003), implying that oxidative chemical degradation of organic matter is likely to occur only over a very short period of time and at high pH conditions:

$$C_6H_{12}O_6 + 6\ O_2 \rightarrow 6\ CO_3^{2-} + 12\ H^+ \qquad (3\text{-}3)$$

Hydrolysis and hydrogenation are the two chemical processes responsible for the degradation of organic polymers in the near-field of an L/ILW repository in the long term. To make these two processes occur, the presence of water, either as free water or as moisture, is crucial (Wieland et al. 2018, Wieland & Kosakowski 2020). In general, it has been observed that a minimum humidity of 60% is necessary to create a continuous water film on the reactive materials and to allow these chemical reactions to occur (Wieland & Kosakowski 2020).

The interaction of water with the cementitious near-field of an L/ILW repository generates alkaline conditions. Under the alkaline conditions of a cementitious near-field, the hydroxyl concentration of the porewater is high, i.e. $[OH^-] > 10^{-4}$ M in all stages of cement degradation (cf. Section 3.3.1). Alkaline hydrolysis refers to a nucleophilic substitution reaction involving OH^- on reactive carbon atoms, such as carbonyl carbon (C=O). Alkaline degradation is thus indicated by nucleophilic attack of the OH^- ion on the polymer chain or by deprotonation (Van Loon & Hummel 1995):

$$RX + OH \rightarrow ROH + HX \qquad (3\text{-}4)$$

Hydrolysis is the first and often limiting step to transforming long-chain polymeric matter into soluble and smaller molecules accessible to biotic degradation. Reaction *3-5* accounts for the hydrolytic degradation of cellulose where the polymeric molecule $[C_6H_{10}O_5]_x$ is hydrolysed to form monomeric glucose units:

$$[C_6H_{10}O_5]_x + x\ H_2O \rightarrow x\ C_6H_{12}O_6 \qquad (3\text{-}5)$$

Hydrolysis is either purely abiotic or mediated by microorganisms, the amount of water available being considered as the crucial parameter for estimating the kinetics of degradation. On the other hand, hydrolysis has no influence on pH.

The presence of reactive carbon atoms susceptible to nucleophilic attack is the most important factor determining whether hydrolysis occurs. The reactivity of a carbon atom is largely determined by the functional groups attached to the atom. Electronegative functional groups (e.g. carbonyl) or heteroatoms (N, O, S) attached to the carbon atom can withdraw electron density, resulting in an electron-deficient (partly positively charged) carbon atom susceptible to nucleophilic attack and therefore easily accepting hydrolysis. In contrast, alkenes do not react with water because the O-H bond in the water molecule is too strong to allow the hydrogen to act as an electrophile. Water cannot protonate a double bond and therefore C=C double bonds cannot be subject to hydrolysis reactions unless a strongly acidic catalyst is present.

In general, two categories of polymers can be distinguished with respect to their chemical reactivity under alkaline conditions: i) addition polymers insensitive to alkali attack such as PVC, polystyrene, plastics such as polyethylene and polypropylene and Plexiglas®; and ii) condensation polymers sensitive to alkaline attack, regrouping cellulose and plastics such as polyester and polycarbonates (Lodge & Hiemenz 2020, Van Loon & Hummel 1995).

Hydrogenation is a process in which an organic compound is reduced by the addition of H_2. In the near-field of a deep geological repository, H_2 is likely to be present in significant quantities due to the anoxic corrosion of metals. However, the reaction is usually very slow and negligible at room temperature. At elevated temperatures and in the presence of a catalyst, however, the reaction proceeds much faster. In the near-field of an L/ILW repository, hydrogenation could in principle cause the reduction of some organic compounds such as alkenes, aldehydes, fatty acids and esters to the corresponding alcohols. A typical example of hydrogenation is the reaction of alkenes with H_2 in the presence of a catalyst:

$$R_2C{=}CR_2 + H_2 \rightarrow R_2C(H)\text{-}C(H)R_2 \qquad (3\text{-}6)$$

Thermal degradation

In the context of an L/ILW repository in the proposed Nördlich Lägern siting region, the temperature at 900 m below ground level is expected to be ~ 47 °C after closure (cf. Section 3.5.1). Therefore, "pure" thermal degradation processes such as pyrolysis, only occurring at strongly enhanced temperatures (in the range from ~ 200 ºC to ~ 600 ºC, depending on the polymer), are of no importance. There is a slight temperature dependence of the radiation-induced and chemical degradation of organics in the temperature range relevant for an L/ILW repository. Between 25 and 65 ºC, the degradation rates actually increase by less than a factor of ~ 2 (Guillemot et al. 2023).

Microbial degradation

In the near-field of an L/ILW repository, microbial degradation is expected to be limited due to (i) the highly alkaline conditions present in the cemented waste forms and surrounding cementitious backfill (pH ~ 12.5); (ii) low water availability; (iii) limited nutrient accessibility; and (iv) gamma radiation field dominated by the decay of ^{60}Co contained in activated metals (Guillemot et al. 2023). In general, it might be assumed that the more extreme conditions co-exist, the less likely that microbial activity will occur. It should however be noted that methanogenesis is possible from a thermodynamic point of view up to pH 12.5 and a low water availability does not in itself fully inhibit microbial life (Guillemot et al. 2023) (cf. Section 3.5.2). Due to the

heterogeneity of the waste and conditioning processes, there may be small-scale niches in the L/ILW repository where relatively good living conditions for microbial activity exist, especially at the bottom of the caverns, saturating more quickly, or in waste packages solidified by bitumen or styrene with near-neutral to slightly alkaline conditions. A slow spread of microbes from these niches is, however, expected due to the limited water availability and pore space. Hence, how important microbial activity is cannot be accurately estimated over the whole period for assessment (Guillemot et al. 2023).

Over time, microbial activity may increase due to: (i) the presence of LMW molecules from scission and hydrolysis which could be used as substrates; (ii) the weakened radiation field; (iii) the slow saturation of the caverns from the bottom and (iv) the presence of small-scale environments of lower pH due to the ongoing internal degradation and carbonation of the solidifying cementitious matrix.

Under anoxic conditions, the biotic degradation of organic matter occurs in the presence of nitrate-, manganese-, iron- and sulphate-reducing microorganisms, which can mediate the degradation process tentatively described for high pH conditions as follows (reactions *3-7* to *3-10*):

$$C_6H_{12}O_6 + 4.8\ NO_3^- \rightarrow 6\ CO_3^{2-} + 2.4\ N_2 + 2.4\ H_2O + 7.2\ H^+ \quad (3\text{-}7)$$

$$C_6H_{12}O_6 + 12\ MnO_2 \rightarrow 6\ MnCO_3 + 6\ Mn(OH)_2 \quad (3\text{-}8)$$

$$C_6H_{12}O_6 + 24\ FeO(OH) \rightarrow 6\ FeCO_3 + 18\ Fe(OH)_2 + 24\ H_2O \quad (3\text{-}9)$$

$$C_6H_{12}O_6 + 3\ SO_4^{2-} \rightarrow 6\ CO_3^{2-} + 3\ HS^- + 6\ H^+ \quad (3\text{-}10)$$

Hence, the classic redox progression of terminal electron-accepting processes might occur in the order: NO_3, Mn(IV), Fe(III) and SO_4^{2-} with decreasing redox potential [V]. The decomposition reactions imply the formation of CO_3^{2-} by microbial degradation of organic matter, whereas the formation of CH_4 does not occur. The NO_3^- inventory in the waste is small, while hardened cement paste (HCP) contains large inventories of Fe(III) and SO_4^{2-}. In contrast, manganese is a trace element in cement (< 200 ppm MnO_2). Estimates of the material inventories show that the total amounts of NO_3^-, Fe(III), SO_4^{2-} and Mn(IV) required for the microbially mediated oxidation of the organic materials is in all cases larger than the known inventories of the above electron acceptors accessible in waste materials and HCP. Consequently, the decomposition of organic matter is expected to occur predominantly via methanogenesis in the long term, leading to the formation of CH_4. Methanogenesis is therefore the final stage of the degradation in anoxic conditions and can be illustrated by the following reactions using the glucose molecule as substrate:

$$C_6H_{12}O_6 + 3\ H_2O \rightarrow 3\ HCO_3^- + 3\ CH_4 + 3\ H^+ \quad (6 < pH < 10) \quad (3\text{-}11)$$

$$C_6H_{12}O_6 + 3\ H_2O \rightarrow 3\ CO_3^{2-} + 3\ CH_4 + 6\ H^+ \quad (pH > 10) \quad (3\text{-}12)$$

Hence, microbially mediated degradation of organic compounds (i.e. methanogenesis) may contribute over the period for assessment of 100 ka to both gas production (i.e. CH_4, CO_2) and carbonation of the cementitious materials. It should however be noted that the nature and amount of the degradation products strongly depends on the type of polymer (structure, chemical composition) and the local environment and it is currently impossible to provide a list of all the

compounds that are formed over time from the abiotic and biotic degradation processes. This approach is further consistent with the notion that, at complete thermodynamic equilibrium, CO_2 (or its aqueous species HCO_3- and CO_3^{2-}) and CH_4 are the thermodynamically stable carbon species in anoxic alkaline conditions (Wieland & Hummel 2015). In contrast to the other microbially mediated degradation processes mentioned above, methanogenesis requires water.

Timescales

Despite the extensive literature survey made by Guillemot et al. (2023) of the abiotic and biotic processes of degradation, no kinetic model was found to quantitatively predict with certainty the progress of degradation over the period for assessment for the L/ILW repository. The most advanced models have been developed for cellulose degradation but the lack of understanding of the relevant long-term degradation reactions (i.e. mid-chain scission) introduces large uncertainties into the predictions. A simplified kinetic model has been developed by Wieland et al. (2018) and used the gas production rates (CO_2 and CH_4) as source terms in the thermodynamic modelling GEM-Selektor code for chemical equilibrium calculations.

In SGT Stage 2, the gas generation rates used were 0.07 mol gas/kg a^{-1} for the group of easily degradable organics (O1), including cellulose and LMW organics, and 0.005 mol gas/kg a^{-1} for the group of less degradable substances (O2), containing PVC, IERs, polystyrene, bitumen, plastics, and Plexiglas® (Diomidis et al. 2016). This classification, however, represents a simplification of the complexity of the degradation processes to which the organic materials are exposed in an L/ILW repository. In the Swiss L/ILW waste inventory, group O_2 corresponds to ~ 93% of the total mass of organics present (Nagra 2023b).

In Wieland et al. (2018), degradation kinetics for both groups is described by a first order kinetic process, corresponding to a typical exponential decay law. The rate constants, derived from the gas production rates, were equal to 1.89×10^{-3} a^{-1} for the decomposition of cellulose, while those for polystyrene reached only 6.51×10^{-5} a^{-1}. The first-order kinetic model predicts that cellulose will be almost completely degraded (10 half-lives: ~ 0.1% residual inventory) within ~ 3.7 ka (Fig. 3-16), while the degradation of polystyrene is much slower, with a 0.1% residual reached after ~ 106 ka.

This simplified kinetic model was also used to predict the evolution of cemented waste packages based on thermodynamic calculations (Wieland et al. 2018, 2020) and the spatial-temporal evolution of chemical conditions in cemented waste packages, based on reactive transport calculations (Huang et al. 2021, Kosakowski et al. 2020). For the general licence application (German: “Rahmenbewilligungsgesuch”; RBG), the kinetic model was further updated with the new gas generation rate defined in Guillemot et al. (2023) for cellulose, polyester and polycarbonate-based plastics at 0.02 mol gas/kg a^{-1}. The degradation of O1 is expected to be complete at an early stage after L/ILW repository closure (maximum after ca. 10,000 years), whereas the decomposition of O_2 is expected to be much slower and potentially incomplete for PVC, polyethylene and polypropylene over a period of 100 ka (Guillemot et al. 2023). However, the kinetic model involves simplifications for some organic compounds by considering the stoichiometry of the carbon source term (including H_2 and O_2), while other heteroatoms (e.g. N, S, P) are not considered. For example, the splitting off of sulphonated and tertiary amine groups in IER degradation is currently not taken into account, meaning that IER degradation is simplified as the degradation of the polystyrene backbone. Further improvement of the model is thus needed for all organic materials that have specific C, N, S stoichiometry (e.g. IERs, bitumen, superplasticisers). A thermodynamic and kinetic approach for this has recently been published (Bagaria et al. 2021).

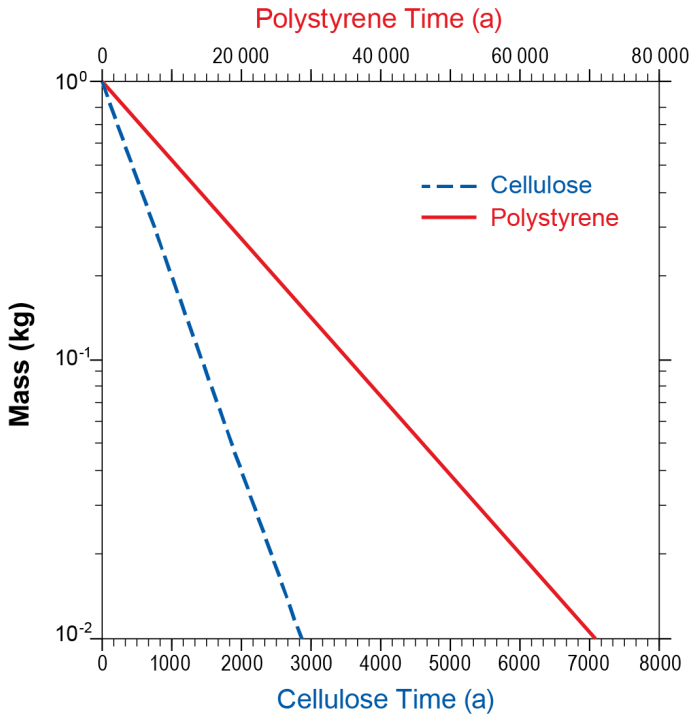

Fig. 3-16: Kinetics of the degradation of cellulose and polystyrene
Wieland et al. (2018)

Uncertainties

As the degradation rates of organics and associated gas generation rates are based on limited experimental data, most of the time not in conditions relevant for a cementitious near-field of the L/ILW repository, many uncertainties exist regarding the degree to which organic materials can be degraded over the period of assessment. They involve: (i) the kinetics of abiotic cleavage or hydrolysis, which transform long-chain polymeric matter into soluble and smaller molecules accessible to biodegradation; (ii) the kinetics of biotic degradation under hyperalkaline conditions; and (iii) the presence of water, crucial for all the degradation steps and also consumed by the anaerobic corrosion of metals and the pozzolanic reaction within the cement matrix.

3.4.2 Organic ligands: impact on sorption and aqueous speciation

Overview/general description of radioactive waste may contain compounds that could influence radionuclide sorption and mobility in the near-field. Ethylenediaminetetraacetate (EDTA), cyanide (CN^-), gluconic acid (GLU), and isosaccharinic acid (ISA) are considered to be the most important complexing ligands for radionuclides (Cloet et al. 2014, Nagra 2008b, 2023a).

Maximum concentrations of the ligands can be estimated based on their inventories in the waste, their amounts formed during degradation reactions and the assumption of solubilisation in the available pore volume. Consequently, these maximum concentrations critically depend on a broad variety of model assumptions and the physico-chemical conditions assumed in the safety case.

The maximum concentrations in the near-field were estimated on the basis of the MIRAM[4] RBG database (Nagra 2023a). Concentration limits are applied to classify waste package types into waste groups 1 and 2 (Tab. 3-3). Waste group 1 either does not contain the previously mentioned complexing ligands, or contains them but at concentrations below the limits defined in Tab. 3-3. In contrast, waste group 2 has larger inventories of the complexing ligands, which increase the radionuclide concentrations in the porewater and reduce the radionuclide sorption and retention (Nagra 2023a).

An established method for taking into account the influence of organic ligands on radionuclide sorption and solubility is the use of sorption reduction factors. They may be used to modify sorption and solubility data (Van Loon & Glaus 1998, Ochs et al. 2022), according to the composition of the solids and porewater solutions applied for the abstraction of the near-field calculation for the safety analysis (Nagra 2023a). Recent research has, however, demonstrated that radionuclide speciation may also be governed by the formation of mixed-metal organic ligand complexes, in which one metal is the radionuclide of interest and the second metal typically a representative of the dominant porewater constituents of cement porewater, such as Ca^{2+}. Such complexes may also be formed in some cases of the ligands listed in Tab. 3-3 (Adam et al. 2021, DiBlasi et al. 2021, 2022, Pallagi et al. 2014, Tasi et al. 2018, 2021). The actual effect of such species on the mobility of radionuclides and their distribution between solid phase and solution is still largely unexplored.

Tab. 3-3: Complexing ligands in the L/ILW repository

Tab. 3-1 in Nagra (2023a)

Material	**Maximum concentration** [mol/L]	**Concentration limit**[1] [mol/L]
EDTA	$2.5 \cdot 10^{-2}$	10^{-5}
Gluconic acid	$5.1 \cdot 10^{-6}$	10^{-5}
Cyanide	0.18	10^{-5}
Isosaccharinic acid	$8.6 \cdot 10^{-4}$	10^{-4}
NTA	$6.5 \cdot 10^{-2}$	$2 \cdot 10^{-2}$
NO_3	0.48	$5 \cdot 10^{-2}$

[1] Limits for separation between type 1 and 2 waste types

[4] MIRAM stands for “Model Inventory of Radioactive Materials” and is a database developed specifically for Nagra’s purposes for the management, radiological calculation and automated analysis of all of Switzerland’s radioactive waste that exists today and will be produced in the future, including spent fuel assemblies (Nagra, 2023b).

EDTA

EDTA is used in nuclear decontamination chemistry because of its ability to bind radionuclides and remove them from contaminated surfaces (Keith-Roach 2008). Instantaneous release of this organic ligand into the porewater yields a maximum concentration of ~ 0.025 mol/L in the near-field (Tab. 3-3) (Nagra 2023a). Speciation calculations predicted that EDTA influences the speciation of only a few cations under alkaline conditions (Hummel et al. 2022) and is therefore considered only in terms of sorption reduction factors for Ca, Fe(III), Pb(II), Fe(II), Ni(II), U(IV), Np(IV), Pu(IV), Th(IV), Ho, Ac, Am, Cm, and Cf (Tits & Wieland 2023).

Nitrilotriacetate (NTA)

As in the case of EDTA, NTA is used in nuclear facilities as a decontaminant (Keith-Roach 2008). It is also added to cement for solidification of sludge. It was not listed in the MIRAM database prior to SGT Stage 2 (MIRAM 14: Nagra 2014a). Values for NTA are given by Nagra (2023a). It is assumed that the effect of NTA on radionuclide sorption is negligible (cf. Cloet et al. 2014) and thus no sorption reduction factor is attributed to this complexing agent (Tits & Wieland 2023).

Gluconic acid (GLU)

A significant proportion of cemented waste types will contain GLU which is used as a concrete admixture during waste solidification. Maximum GLU aqueous concentrations are given in Tab. 3-3 (Tab. 3-1 in Nagra 2023a). These were estimated without consideration of sorption on HCP. In reality, GLU will sorb on HCP, which was modelled by a Langmuir isotherm by Glaus et al. (2004). The complexation of safety-relevant radionuclides or representative chemical analogues at high GLU concentrations in some waste types is accounted for in terms of sorption reduction factors (Tits & Wieland 2023, Wieland 2014). However, the calculated concentration levels for GLU are so low that no waste containing GLU is assigned to waste group 2. Therefore, only a low sorption reduction factor for waste group 1 according to Tab. 7-4 in Tits & Wieland (2023) is applied.

Cyanide

Prussian Blue ($Fe^{III}_4[Fe^{II}(CN)_6]_3$) is present in only one waste type (Nagra 2023b). Prussian Blue readily dissolves under alkaline conditions (Hummel 2004). Free cyanide would be released if hexacyanoferrate ($Fe(CN)_6^{4-}$) is further decomposed in the cementitious near-field. However, the latter compound is expected to be stable in the dark even under alkaline conditions (pH > 8), while complete photodecomposition occurs in the light within days. The effect of gamma irradiation on its biodegradation is not known under L/ILW near-field conditions. A total dissolution and decomposition of $Fe(CN)_6^{4-}$ is therefore assumed (Wieland 2014) as the worst case scenario for the assessment of a potential detrimental effect. On the assumption that biotic or abiotic decomposition of free cyanide cannot be excluded, high CN- concentrations might be present in only one waste sort (Nagra 2023a). Hummel (2004) showed that cyanide influences the speciation of only a very limited number of metals, in particular Ni and Co.

Cellulose degradation products

Cellulose corresponds to only ~ 2% of the total organic mass and is sensitive to hydrolysis (Guillemot et al. 2023). The maximum loading in some waste types is about 14% of the HCP mass. The main degradation products of cellulose are α- and β-ISA, which are powerful complexing agents, in particular for 3- and 4-valent actinides (Glaus & Van Loon 2008). The kinetics of cellulose degradation are still disputed due to significant differences between the rate constants determined in short- and long-term experiments and those deduced from degradation studies at

enhanced temperatures (cf. Kosakowski et al. 2014). Furthermore, it was observed that α-ISA can be converted to short-chain aliphatic carboxylic acids with only moderate complexing properties in the presence of stoichiometric amounts of oxygen. The concentration of ISA in the near-field porewater was estimated by considering ISA sorption on HCP, which was modelled using a simplified one-site Langmuir isotherm. Sorption reduction of radionuclides caused by high ISA concentrations (ISA > 10^{-4} mol/L) is accounted for in the sorption database for some waste types (Tab. 3-3) (Nagra 2023a).

Nitrate and nitrites

Various waste package types contain nitrate and nitrites, e.g. ammonium nitrate ($NH4NO_3$), calcium nitrate ($Ca(NO_3)_2$), chromium-III-nitrate ($Cr(NO_3)_3$, iron-II-nitrate ($Fe(NO_3)_2$), potassium nitrate (KNO_3), potassium nitrite (KNO2), sodium nitrate ($NaNO_3$) and silver nitrate ($AgNO_3$) (Nagra 2023b). It is to be assumed that all these salts are highly soluble and will be released once the waste comes into contact with water. NO_3^- will therefore be available as an oxidant to oxidise other substances (e.g. chemical complexes, metals). Consequently, this may lead to a higher mobility of some redox-sensitive radionuclides. A concentration limit of 0.05 mol/L is recommended as the limit to be used to classify waste groups 1 and 2 in Nagra (2023a) (Tab. 3-3).

Polymeric organic materials and detergents

The effect of polymeric organic materials and their degradation products on radionuclide solubility and sorption was found to be negligibly small compared to that of cellulose degradation products (Kosakowski et al. 2014). Therefore, it is expected that polymeric organic materials and detergents will have only a negligibly small influence on radionuclide solubility and sorption.

Concrete admixtures

Concrete admixtures are unavoidable components of cement and concrete used as backfill, for the waste matrix, containers, the construction of the L/ILW caverns and the deep geological repository in general. In most cases, concrete admixtures are polymeric organic compounds, with compositions which are often only partly known for proprietary reasons. The most important components are polynaphthalene-sulphonic acids (PNS), polymelamine-sulphonates, ligno-sulphonates, GLU and polycarboxylate-ether-based molecules (PCEs). It was observed that all concrete admixtures, with the exception of the formerly used GLU and lignosulphonates, form only weak complexes with radionuclides. This view is also supported by recent research work (Adam et al. 2021, Frohlich et al. 2019). For example, the use of modern PCE-based concrete admixtures at typical levels leads to concentrations in the porewater of the cementitious near-field (solid-to-liquid ratio of ~ 2 kg/L), which are expected to have no adverse effect on radionuclide uptake by HCP. Currently there are no indications that possible degradation products of concrete admixtures have stronger complexing properties than their parent compounds (Chernyshev et al. 2018, Garcia et al. 2018). Hence, sorption reduction effects caused by concrete admixtures will not be taken into account. GLU is a special case, which was treated in the previous section.

Boundary conditions/additional information

The degradation of cellulose, polymeric materials, and spent IERs, the sorption properties and chemical stability of the degradation products under hyperalkaline conditions, and the inventory of concrete admixtures (e.g. GLU) determine the porewater concentrations of radionuclide complexing ligands. For a discussion of studies related to biodegradation of these materials in alkaline water, see Guillemot et al. (2023) and the short summary in Section 3.4.1.

Information from modelling/experimental studies

A recent experimental study (DiBlasi et al. 2021) investigated the impact of Ca^{2+} on the aqueous speciation, redox behaviour and environmental mobility of Pu(IV) in the presence of EDTA using a combination of undersaturated solubility studies and advanced spectroscopic techniques.

For this purpose, DiBlasi et al. (2022) performed undersaturated solubility experiments using a well-characterised PuO_2(ncr,hyd) solid phase and chemically controlled, well-defined redox conditions in solution, in combination with advanced spectroscopic techniques. They found previously unreported quaternary Ca-Pu(IV)-OH-EDTA complex(es). As a result of this finding, they could show that the thermodynamic models available in the literature for the Pu(IV)-OH-EDTA ternary system result in a systematic overestimation of the plutonium solubility data determined in the absence of calcium. Based on this work and available formation constants, they revised the overall formation constants for the ternary complexes $Pu(OH)(EDTA)^-$, $Pu(OH)_2(EDTA)_2^-$, and $Pu(OH)_3(EDTA)_3$. The formation of quaternary Ca-Pu(IV)-OH-EDTA complex(es) is strongly supported by solubility experiments conducted over a wide range of total calcium concentrations (1 mM < $[Ca(II)]_{tot}$ < 3.5 M).

However, additional experimental efforts are required to conclusively determine the stoichiometry of the quaternary complex and its impact on the Pu(III)/Pu(IV) aqueous redox boundary (DiBlasi et al. 2021). In order to properly assess this effect, similar work will also be conducted with Pu(III) to evaluate the possible formation of stable Ca-Pu (III)-OH-EDTA quaternary complexes.

Beyond the effect of calcium on the Pu(IV)-OH-EDTA system, such stabilisation effects may be anticipated for other di- and trivalent metal ions. The possible formation of quaternary M(II)/M(III)-Pu(IV)-OH-EDTA complex(es) emphasises the importance of reinterpreting the role of major cations. In the context of the revision of the TDB, data for EDTA have been reviewed and revised solubility calculations have been performed for the dose-relevant nuclides by Hummel et al. (2022). As a result of the reduced solubility, sorption reduction factors had to be defined for the cement sorption data base for 3- and 4-valent actinides, which can form complexes with EDTA. Further, the waste group classification criteria have been reduced from 10^{-3} mol/L (Cloet et al. 2014) to 10^{-5} mol/L (Nagra 2023a). It should be noted that the results from Di Blasi et al. (2021) are conservative and the experiment does not contain cement paste in contact with fluid. Therefore, Hummel et al. (2022) concluded that although the mentioned Ca – Pu(IV) – OH – EDTA complex completely dominates the aqueous cementitious Pu system, there are no experimental data yet as to whether and to what extent this and chemically analogous complexes may sorb to cement solid phases.

Metal cyanide complexes, such as $Fe(CN)_6^{4-}$, decompose to free cyanide in UV-vis light, while the complexes are stable in the dark even under alkaline conditions (Hummel 2004 and references therein). It is expected that the effect of gamma irradiation on the decomposition of metal cyanide will depend on the dose rate in the near-field (Hummel 2004). Biodegradation of free cyanide under anaerobic conditions was reported in laboratory systems, but the extrapolation of these findings to field conditions, particularly the hyperalkaline conditions of a cementitious near-field, is uncertain (PSI internal report). The thermodynamic calculations by Hummel (2004) showed that free cyanide only has an effect on the speciation of Ni and Co under alkaline conditions.

The sorption of GLU onto HCP can be modelled in terms of a two-site Langmuir-type isotherm (Glaus et al. 2004), while the approximation by a one-site Langmuir isotherm is possible at lower concentrations (GLU < 10^{-4} mol/L) (Bradbury & Van Loon 1996). Several authors have investigated the influence of GLU on the uptake of safety-relevant radionuclides by HCP (Kosakowski et al. 2014 and references therein). These studies show that GLU only forms strong complexes with tetravalent actinides (An(IV)). Gaona et al. (2008) reviewed the speciation

scheme and the stability constants of An(IV)-GLU complexation. The complexation constants reported by these authors indicate the formation of strong An(IV)-GLU complexes in solution, which explains sorption reduction at GLU concentrations ≥ 10^{-5} mol/L.

The study of Glaus & Van Loon (2008) indicated that the assumption of a complete cessation of the alkaline hydrolysis of cellulose after a short peeling-off reaction phase is not justified. Complete degradation of cellulose and formation of α- and β-ISA is therefore indicated as a conservative assumption. The experimental studies on the complexation behaviour of α-ISA with safety-relevant radionuclides unequivocally showed a significant effect on the speciation of metal cations (Kosakowski et al. 2014 and references therein). The results show significant sorption reduction caused by α-ISA at ligand concentrations > 10^{-4} mol/L.

A review by Glaus, which is summarised in Kosakowski et al. (2014), recapitulates our current understanding of the degradation of IERs, which produces ammonia and amines, and the effect of these ligands on radionuclide complexation. The main conclusions presented earlier by Van Loon & Hummel (1995) are still valid. First, the radiolytic and chemical (alkaline) degradation of products of organic IERs have no or only a negligible influence on the speciation of radionuclides in a cementitious near-field and therefore their specific consideration in safety analysis is not required. Secondly, the nature of the ligands formed allows significant complexation with "soft" metals such as Ag and Pd, which are not dose-determining elements in performance assessment.

Greenfield et al. (1992, 1994) studied the influence of polymeric materials and their degradation products on radionuclide solubility. Note that the above studies are currently the only source of information on the complexation of radionuclides by the degradation products of these materials. The authors investigated radionuclide solubilities in solutions prepared from aged, crushed cements and up to 20 wt.-% of polymeric materials. They observed no detrimental effects on radionuclide solubilities. Therefore, sorption reduction effects caused by polymeric materials and their degradation products are not taken into consideration when assessing radionuclide uptake by HCP.

The complexation of radionuclides by concrete admixtures has been investigated with the aim of developing a generic approach for assessing their impact on radionuclide mobility (Glaus et al. 2004). The degradation products of concrete admixtures, which mainly consist of organic monomers, are expected to be very weak complex formers (PSI internal report).

Timescales

The time span over which radionuclide-complexing ligands persist depends on the scenarios invoked for the possible degradation or transformation of organic matter. Chemical and radiolytic processes facilitate the generation of the ligands, while biodegradation will significantly reduce their impact over time.

Uncertainties

The main uncertainties are associated with the kinetics involved in the different possibilities for biotic, abiotic and radiolytic degradation or transformation reactions and the availability of water. These reactions control the porewater concentrations of most of the radionuclide-complexing ligands. In particular, the kinetics of abiotic cleavage (or hydrolysis), which transforms long chain polymers into smaller more soluble molecules, is not well known.

The formation as well as the role complexing ligands can play depends on whether a free water phase is present in the L/ILW repository. According to the data extracted from Papafotiou & Senger (2016) and summarised in Section 3.2.1, the availability of water will be strongly limited in an L/ILW repository and full saturation will not be reached within 100,000 years.

The concept of complexing ligands in safety assessment calculations relates to a so-called mixing tank approach, where it is assumed that the dose release from a homogeneously dissolved waste in a fully saturated L/ILW cavern is calculated. This assumption is therefore highly conservative, in particular with respect to the fact that the availability of free water is highly limited in the L/ILW repository.

As outlined before for GLU, the sorption of organic ligands on HCP is often expressed in terms of measured sorption isotherms. Such a description cannot take into account the effects of competition with other organics or changes in major element chemistry. The equilibrium concentration of organic ligands in solution might be highly variable due to the heterogeneity of the waste sorts, strong changes in water saturation, and variable contents of competing complexing ligands in waste packages.

With regard to EDTA, there are no experimental data available yet as to whether and to what extent this and chemically analogous complexes may sorb on cement solid phases.

3.4.3 Impact of CO_2 from organic matter degradation on cement-based materials

Overview/general description

Carbonation of cementitious materials is a chemical process in which dissolved CO_2 reacts with calcium from hydrated cement phases to form calcium carbonates and other minerals. It should be noted that these reactions release the water structurally bound in cement hydrates. After complete carbonation, i.e. after hydrated cement phases are completely consumed, the originally high pH of the cement porewater drops to neutral values and the cement is in degradation Stage IV (cf. Section 3.3.1).

Carbonation of hydrated cements involves the transformation of portlandite ($Ca(OH)_2$), calcium silicate hydrates (C-S-H) ($xCaO{\cdot}SiO_2{\cdot}nH_2O$), ettringite and AFm to calcium carbonate, gypsum and other secondary aluminium and silica oxyhydroxides (Venhuis & Reardon 2001). Portlandite and C-S-H are the most abundant cement phases in HCP and they are therefore considered to preferentially undergo transformation. For example, in cement paste produced from Portland cement CEM I 52.5 N HTS (Lafarge, France), which is used for the solidification of L/ILW in Switzerland, the proportions of $Ca(OH)_2$ and C-S-H are ~ 20 wt.-% and ~ 50 wt.-% (Lothenbach & Wieland 2006), indicating that the CO_2 neutralisation capacity of hydrated cement is substantial.

Gaseous CO_2 will react in hyperalkaline water to form predominately carbonate:

$$CO_2(g) + 2\ OH^- \rightarrow CO_3^{2-} + H_2O \qquad (3\text{-}13)$$

In the cementitious near-field porewater, dissolved carbonate will react primarily with portlandite:

$$Ca(OH)_2 + CO_3^{2-} \rightarrow CaCO_3 + 2\ OH^- \qquad (3\text{-}14)$$

The overall reaction is:

$$Ca(OH)_2 + CO_2(g) \rightarrow CaCO_3 + H_2O \qquad (3\text{-}15)$$

The corresponding reactions for complete or partial carbonation of a C-S-H phase can be expressed as follows:

$$xCaO{\cdot}SiO_2{\cdot}n\ H_2O + x\ CO_2(g) \rightarrow xCaCO_3 + SiO_2 + n\ H_2O \quad (3\text{-}16)$$

$$1.6CaO{\cdot}SiO_2{\cdot}x\ H_2O + 0.8\ CO_2(g) \rightarrow 0.8CaCO_3 + 0.8CaO{\cdot}SiO_2{\cdot}y\ H_2O + (x\text{-}y)\ H_2O \quad (3\text{-}17)$$

In a deep geological repository, carbonation of cementitious materials might be related to:

- Atmospheric carbonation of cement-based materials during operation of the repository (cf. Section 3.2.1). Modelling studies predict limited carbonation of cement-based materials in the operational phase of a typical deep geological repository (Trotignon et al. 2011). Carbonation is commonly observed in cement materials that are in contact with atmosphere under humid conditions. A thorough description of carbonation mechanisms and possible consequences is given in von Greve-Dierfeld et al. (2020).
- Carbonation at the contact of cement- and clay-based materials (e.g. host rock). Clay materials, specifically clay rocks like Opalinus Clay, have a lower pH and lower stability of carbonate minerals, which results in a higher carbonate concentration in clay porewater (cf. Section 3.3.2). This will cause transport of carbonate towards the cement materials. The position of carbonation fronts depends on the (temporally variable) pH values and pH gradients at the clay/cement contacts. If a high-pH front moves into the clay materials (cf. Section 3.3.2), carbonate precipitation will be at the high-pH front (in the clay) and the carbonation of cements will be suppressed.
- Degradation of organic waste materials into equimolar amounts of CH_4 and CO_2 by abiotic and biotic processes is assumed for gas generation in an L/ILW repository (cf. Section 3.4.1). Large amounts of CO_2 might be released by the degradation of organic waste materials and will be by far the dominant source for CO_2 in the repository.

The carbonation process could have an influence on the immobilisation of metal cations and anions. Cationic waste constituents have a lower leachability from carbonated HCP than from non-carbonated HCP, probably due to the reduced porosity, permeability and diffusion coefficients of the cementitious materials (Kosakowski et al. 2014 and references therein). Note that the reduction of the Ca/Si ratio of C-S-H due to carbonation is not expected to have a significant impact on cation retention. In contrast, anionic waste constituents could show greater leachability upon carbonation due to the transformation of AFm-SO_4 to AFm-CO_3 and a lower anion sorption by C-S-H with a Ca/Si ratio < 1.1 (Tits & Wieland 2023).

The degradation of cement materials in single waste packages was investigated (Wieland et al. 2018, 2020) with the help of so-called mixing tank models. This modelling included the effect of CO_2 produced by decomposition of organic compounds in the waste package (cf. Section 3.5.3). In these model assumptions, the complete degradation of all organic matter in the waste package would produce CO_2 that can freely react in the model and degrade the cement materials in the waste package. Once all cement materials in the waste package are carbonated, CO_2 will be released from the waste package and can carbonate the cement surrounding the waste containers. Tab. 3-6 in Section 3.5.3 shows the amount of gaseous CO_2 released per waste package for two variants of the model waste sort BA-PH-PF and the potential volumes of other cement materials that can be degraded with this amount of CO_2.

The operational waste sort BA-PH-PF, which is described in detail in Wieland et al. (2018), contains different types and amounts of organic materials, metals, and other inorganic materials in the form of organic-rich mixed solid waste. The waste type is conditioned in cementitious

materials and the waste package volume is about 0.217 m^3. Wieland et al. (2018) made the (conservative) assumption that all organic matter in the package can be degraded, and produces about the same amount of CO_2 and CH_4. The CO_2 will be partly consumed during carbonation of the cement infill of the waste packages. The excess CO_2 will be released from one waste package and might result in the carbonation of between 0.5 and 1.5 times the waste package volume of other cementitious materials near the waste package (cf. Section 3.5.3).

Information from experiments and modelling

Carbonation is commonly observed in cement materials that are in contact with the atmosphere under humid conditions. The progress of carbonation fronts is known to depend on gas diffusion and relative humidity (Ashraf 2016, Leemann & Moro 2017, Russell et al. 2001, Steiner et al. 2020, Winter 2009) and is fastest for relative humidity between 60 – 80%. Under such conditions, the concrete is desaturated to such a degree that relatively fast diffusion of atmospheric CO_2 is possible and that enough water exists in contact with the cement phases to allow dissolution of reactants. The OH^- and Ca^{2+} ions consumed during the course of cement carbonation arise mainly from the dissolution of portlandite and C-S-H (see Section 3.3.1). Atmospheric carbonation of Ordinary Portland cement (paste) decreases porosity and transport parameters, while carbonated blended cements show an increase in transport parameters. Dutzer et al. (2019) could show that these observations are related to the competition between porosity reduction and (micro-) cracking induced by carbonation.

Experimental investigations show that carbonation fronts are not sharp (Parrott & Killoh 1989, Thiery et al. 2007), which is attributed in part to the influence of chemical reaction kinetics (Morandeau et al. 2014, Thiery et al. 2007). The role of the ratio between the characteristic time of carbonation reaction and a characteristic diffusion time was discussed for example by Muntean et al. (2011). In general, if the characteristic time for reaction is much smaller than the time for diffusion of CO_2, then the zone of reaction is small compared to the progress of the reaction front. The carbonation reactions are assumed to be quite fast, at least compared to the lifetime of a deep geological repository, and carbonation progress depends mainly on the production and transport of carbon species towards unreacted cement phases.

In the context of radioactive waste disposal, atmospheric carbonation of cement-based materials during operation of a repository was investigated by Trotignon et al. (2011). They predicted a minimal carbonation of materials. Savage & Cloet (2018) state that, in systems involving natural clay formations, the high partial pressure of carbon dioxide (P_{CO2}) plays a key role in the alteration process, and leads to an abbreviated zone of alteration of aluminosilicate minerals due to the rapid reduction of porosity at the cement/clay interface, as a result of Ca^{2+} and OH^- ions leached from the cement/concrete reacting with CO_2(aq) diffusing from the clay formation to form solid calcium carbonate (calcite/aragonite).

Gaboreau (2011) characterised cement/clay interface samples from Tournemire after 15 years of interaction, showing a porosity reduction in the claystone due to the precipitation of secondary minerals. They could show that the perturbations (in terms of mineralogical and porosity changes) were limited to 3.5 cm and 1.5 – 2 cm from the interface in cement and clay rock respectively. The concrete and clay rock were not homogeneous and contained a fissure network. Alterations were observable near the material interface and near the fissure. The porosity in the concrete increased due to portlandite dissolution. The porosity in the clay rock was strongly reduced, which the authors attributed to carbonate, C-S-H and C-A-S-H precipitation in the fissure network (Techer et al. 2012) and mainly to precipitation of C-(A)-S-H phases in the clay matrix. Limited alteration extents (< 1 cm) have been identified at the contact of shotcrete and cement paste with COx clay after 5 years of interaction (Gaboreau et al. 2012, Lerouge et al. 2014).

Within the framework of the Mont Terri CI project, the precipitation of carbonate at the cement side of the interface between different cements and Opalinus Clay was observed at early experimental times, but not to a degree that porosity was significantly affected (Jenni et al. 2014, Mäder et al. 2017, Yokoyama et al. 2021). In their modelling study for the CI experiment, Jenni et al. (2017) and Jenni & Mäder (2021) could reproduce the absence of a strong carbonation layer on the cement side. The absence of carbonation in cement and at the cement/clay interface is related to the progress of a high-pH front in clay which causes minimal amounts of carbonate to dissolve and to reprecipitate at the high-pH front. In their model for the low-pH concrete/Opalinus Clay interface (Jenni & Mäder 2021), clogging of free porosity in the Opalinus Clay near the interface was observed due to precipitation of Mg-containing minerals (hydrotalcite, brucite), while for the OPC/Opalinus Clay interface precipitation of Mg was much more distributed and affected porosity only slightly (Jenni et al. 2017).

Furthermore, Nakarai et al. (2021b, 2021a) used a dedicated experimental setup to try to enforce porosity clogging at cement/bentonite interfaces by adding sodium carbonate to the bentonite. They were only able to enforce near-instantaneous porosity clogging by adding sodium carbonate in very high amounts (porewater concentration close to solubility limit), which quickly created a few-micrometre-thick carbonate layer between cement and bentonite due to mixing of cement and clay porewater. If sodium carbonate addition was below a certain threshold, formation of a carbonate layer at early times resulted in an incomplete carbonate layer directly at the interface and solute fluxes across the interface were reduced. On the long term, driven by the high concentrations of dissolved CO_2 in bentonite, a carbonation front moved into the cement, accompanied by dissolution of cement phases, precipitation of calcite, a drop in pH, a slight decrease in porosity and an increase in pore sizes.

One consequence of carbonation is a possible change in porosity and associated transport parameters (see e.g. Dutzer et al. 2019, von Greve-Dierfeld et al. 2020 and references therein). Commonly a decrease in porosity and transport properties (diffusivity and permeability) for OPC-based materials is reported, while for blended cements transport properties increased although total porosity decreased. Dutzer et al. (2019) and others explain this by a competition between pore clogging (dominant for OPC) and micro-cracking induced by carbonation (dominant in blended cements). Porosity decrease and pore blocking are associated with (mainly) transformation of $Ca(OH)_2$ to carbonate which is precipitated in capillary pores. Upon complete carbonation, the pore size distribution is shifted towards larger pore diameters, as C-S-H is transformed which reduces gel porosity. The reduction of transport parameters for OPC seems moderate, e.g. effective gas diffusion coefficients for a given liquid saturation are reduced by less than a factor of 10 (Boumaaza et al. 2020, Dutzer et al. 2019).

The leachability of cations and anions was studied in standardised static and dynamic tests using carbonated samples (Venhuis & Reardon 2001). Carbonation resulted in lowering the leachability of cations (strontium, caesium), which was explained by a significant reduction in porosity and permeability of the carbonated cementitious materials. The leachability of anions (chloride, nitrate, arsenate) was found to increase with increasing degree of carbonation (Venhuis & Reardon 2001). This is explained by the release of anions from ettringite and calcium monosulphoaluminate, which are converted into CO_3^{2-}-bearing cement phases during the course of carbonation.

Timescales

The time span over which most of the degradation of cement paste occurs is mainly controlled by the temporal evolution of CO_2 generation. This process is determined by the decomposition rates of LMW and HMW organic materials in the near-field (see Section 3.4.1). Rates for the degradation of the organic compounds are given in Section 3.4.1.

Uncertainties

Uncertainties exist regarding the time span over which LMW and HMW organic materials degrade in a repository environment (see Section 3.4.1) and regarding the influence of very low liquid saturation on the possibility of carbonation and chemical reactions in general (Huang et al. 2021).

3.4.4 Inorganic material – cement interactions

Overview/general description

Inorganic waste materials are expected to be subject to transformation processes in the repository. The degree of transformation depends on the chemical stability of the waste materials under the alkaline, reducing conditions of the cementitious near-field. In NTB 14-11 (Kosakowski et al. 2014), the potential processes for the inorganic waste materials have been evaluated and discussed. As shown in Tab. 3-4, the waste materials have been classified as "reactive" or "inert" with respect to possible impacts on the evolution of HCP. "Reactive" materials are expected to convert into products that may have an adverse effect on the mineral composition of HCP over the timescale of a repository. Inert materials, such as Be, B_4C, Cu, and zircaloy, are expected to persist over geological timescales, or they decompose with time and generate reaction products that have no significant influence on the mineral composition of HCP. Other materials mainly consist of components in the cement matrix. For example, asbestos, ash, slag, ceramics and glass are such types of materials that decompose over time and generate products with compositions similar to those of cement-type minerals. Hence, decomposition of these waste materials is expected to have only a minor effect on the mineral composition of HCP.

As demonstrated in Kosakowski et al. (2014), most metallic materials, e.g. Al, Fe (e.g., steel), Mg, and Zn, will be subject to anoxic corrosion taking place at different rates according to the equations below, assuming that hydroxide is in most cases the stable end-product.

$$Al(s) + 3\,H_2O \rightarrow Al(OH)_3(s) + 1.5\,H_2(g) \qquad (3\text{-}18)$$

$$3Fe + 4\,H_2O \rightarrow Fe_3O_4 + 4\,H_2 \qquad (3\text{-}19)$$

$$Mg(s) + 2\,H_2O \rightarrow Mg(OH)_2(s) + H_2(g) \qquad (3\text{-}20)$$

$$Zn(s) + 2\,H_2O \rightarrow Zn(OH)_2(s) + H_2(g) \qquad (3\text{-}21)$$

These reactions typically produce H_2 gas. In some waste types, the inventories of Mg, Al and Fe per mass of HCP in the tunnel are large enough that corrosion products may have a considerable influence on the volume and composition of HCP. Otherwise, the corrosion process itself would not modify the HCP significantly. The dissolution of the corrosion products and the re-precipitation with the cement hydrates can have a long-term influence on the HCP. The generated metal hydroxides/oxides possess significantly different solubility in cement pore solution. For instance, the amphoteric compounds, e.g. $Al(OH)_3$ and $Zn(OH)_2$, are highly soluble under hyperalkaline conditions (pH ~ 13). In the presence of OH^-, most metal ions favour formation of relatively soluble hydroxide complexes. The predominant species of Al, Fe, Mg, Pb and Zn ions under high pH and reducing conditions are predicted by thermodynamic calculations to be $Al(OH)_4^-$, $Fe^{III}(OH)_4^-$ and FeS(aq), $MgOH^+$ and Mg^{2+}, $PbS(HS)^-$ and $Zn(OH)_4^{2-}$, respectively (Hummel et al. 2022).

Tab. 3-4: Overview of inorganic materials in cementitious waste disposal and their reactivity in HCP

Inorganic waste	**Comment**	**Reactivity/impact**
Aluminium (Al)	Oxidation to Al(III); gas generation; question of grain sizes (kinetics); new cement phases, e.g. C-A-S-H phases	Reactive – formation of new cement-like minerals, e.g. C-A-S-H phases – impact possible
Asbestos	$Mg_3Si_2O_5(OH)_4$; long-term thermo-dynamic stability not clear in cementitious environment; known to be used as an aggregate in concretes in the alpine region	Probably hardly reactive – chemical impact not relevant
Fly ash	Generally oxidised materials; usually show alkaline reaction; common to cementitious materials; may show pozzolanic reaction; formation of new, cement-like minerals if portlandite is available	Reactive – formation of new cement-like minerals – impact not relevant
Beryllium (Be)	No further information available; relevant compounds probably just $BeO/(OH)_2$ and $BeSO_4$; $BeSO_4$ is soluble in water; sulphate forms double salts; Be could be taken up by AFm/AFt phases replacing $CaSO_4$; highly toxic from a chemical point of view; release to the environment has to be controlled	Inert – important in conjunction with toxicological issues
Lead (Pb)	Pb(0), Pb(II); reactions with S^{2-}, CO_3^{2-}, SO_4^{2-}, Cl^-	Probably hardly reactive – impact not relevant
Boron carbide (B_4C)	Chemically nearly inert and very hard material; no chemical reaction below 1,000 ºC; resistant against nitric acid and HF	Inert
Metals	Production of H_2 gas by anoxic corrosion; may produce oxides with different sorption properties; corrosion probably kinetically controlled (or by surface); formation of new minerals may induce volume/porosity changes	See Fe, Mg, Al

Tab. 3-4: Cont.

Inorganic waste	Comment	Reactivity/impact
Magnesium (Mg)	Formation of cement-like minerals possible, e.g. M-S-H phases; possibly enhanced formation of hydrotalcite-like phases; volume changes	Reactive – formation of new cement-like minerals, e.g. M-S-H phases – impact possible
Iron (Fe)	Phases: pyrite & magnetite; formation of cement-like minerals possible, e.g. Fe-hydrogarnets, Fe-AFm, Fe-AFt, and Fe-containing C-S-H phases, volume changes	Reactive – impact possible
Copper (Cu), silver (Ag)	Formation of sulphide phases	Inert
Steel	Release of carbon species; Fe source; release of e.g. Ni, Cr, Mn from alloys	Reactive (see Fe)
Slag	From Zwilag plasma facility (Heep 2010, Nagra 2014a); no specific information available. Might be similar to volcanic glass or slag. Thermodynamically unstable under alkaline conditions	Reactive – formation of new cement-like minerals – impact not relevant
Inorganic residuals	No specific information available	Unknown
Metallic residuals	No specific information available	See Metals
Zinc (Zn)	Production of H_2 gas, forms soluble products; incorporation into C-S-H	Reactive – impact not relevant
Zircaloy (Zr)	Contact between porewater and compacted hulls will cause anaerobic corrosion of Zircaloy once water accesses the Zircaloy in the Mosaik containers. The corrosion rates are however very small, i.e. 3 nm per year (Diomidis et al. 2023). Resulting in ZrO_2, which is inert; release of alloyed metals	Inert
Glass	Acid/base reactions; question of kinetics and reactivity; chemical composition resembles that of cementitious materials; source of SiO_2	Reactive – impact not relevant

Often, these metal ions can replace the lattice atoms of the common cement hydrates via isomorphic substitution and thus affect the mechanical properties of HCP. The main factors limiting the extent of the isomorphic substitution of ions in solids include the relative ratios of ion radii, coordination number, electronegativity ratio, ionisation potentials, long-range electrostatic interactions, charges, chemical reactions and the structure of the solids (Ione & Vostrikova 1987). Based primarily on crystal chemistry and geometric considerations, Pauling (1931) formulated the main criteria for the occurrence of isomorphous substitution in the entity package of metal (Me) and oxygen anion (O^{2-}), which is widely applicable in the cement hydration system.

According to Pauling, cations prefer tetrahedral coordination if the ionic radius ranges from $r_{Me}/r_{O}^{2-} = 0.214 – 0.4$ and octahedral sites for $r_{Me}/r_{O}^{2-} = 0.4 – 0.6$. Considering the ionic radius of O^{2-} to be 1.36 Å, ions larger than 0.55 Å prefer octahedral coordination in oxygen lattices. A list of representative atoms and corresponding radii and radius ratios is given in Tab. 3-5. It is worth mentioning that all rules described above are based on empirical observation. Although the exact boundary between tetrahedral and octahedral coordination might not be at $r_{Me}/r_{O}^{2-} = 0.4$, the ions definitely favour coordination numbers larger than 4 with increasing radius ratio.

Tab. 3-5: Radii and radius ratios of substituted ions after Shannon (1976)

The ionic radius of O^{2-} (rO^{2-}) is taken as 1.36 Å.

Ion	**Coordination number**	**Radius/Å r_{Me}^{z+}**	**Distance/Å r_{Me-O}**	**Radius ratio r_{Me}/r_{O}^{2-}**
Si^{4+}	IV	0.26	1.62	0.19
Al^{3+}	IV	0.39	1.75	0.29
	VI	0.535	1.895	0.39
Fe^{3+}	IV	0.49 (high spin)	1.85	0.36
	VI	0.645 (high spin)	2.005	0.47
Mg^{2+}	IV	0.57	1.93	0.42
	VI	0.72	2.08	0.53
Zn^{2+}	IV	0.60	1.96	0.44
	VI	0.74	2.1	0.54
Fe^{2+}	IV	0.63 (high spin)	1.99	0.46
	VI	0.78 (high spin)	2.14	0.57
Ca^{2+}	VI	1.00	2.36	0.74
Pb^{2+}	VI	1.19	2.55	0.88

The common cement hydrates such as C-S-H phases, AFm phases, ettringite, hydrogarnet, hydrotalcite, etc., offer a variety of lattice sites for accommodating the waste metal ions by isomorphous substitution, forming solid solutions or even complete conversion into the end members. Whether the corrosion products of the waste and the dissolved species can lead to significant changes in HCP composition or not strongly depends on their total amount and reactivity. Their chemical interactions are complicated and have been extensively investigated in recent years. The relevant updates with respect to Kosakowski et al. (2014) are given in the following section.

Updates from recent studies

Aluminium (Al)

The precipitation of α- and γ-$Al(OH)_3$ (gibbsite and bayerite) and the formation of strätlingite ($Ca_2Al_2SiO_7 \cdot 8H_2O$) could occur, which would cause changes in the mineral phase composition. Thermodynamic calculations revealed that high inventories of Al lead to the dissolution of portlandite while Al-containing phases, e.g. hydrogarnet, strätlingite, ettringite or other AFm phases, form favourably. The structural incorporation of Al^{IV} in C-S-H, forming C-(A-)S-H, has been

investigated extensively at a molecular scale in the past few years. Tetra-coordination of aluminium (noted as AlIV) is the predominant environment in C-(A-)S-H. At a Ca/Si ratio of 1.0 and higher, penta- and hexa-coordination (noted as Al^{V} and Al^{VI}, respectively) become more important, with all of them favouring bridging sites at ambient temperature (Kunhi Mohamed et al. 2020, L'Hôpital et al. 2015, Lothenbach & Nonat 2015, Yang et al. 2021).

Iron (Fe)

Some progress was made recently in understanding the interaction of Fe^{2+}/Fe^{3+} with the cement matrix (Mancini et al. 2020, 2021a, 2021b), but some knowledge gaps still remain. Al-Fe siliceous hydrogarnet solid solutions have been shown to be stable hydrates for accommodating considerable amounts of Fe^{3+} (Lothenbach et al. 2019); however, they are the long-term hydration products in thermodynamics and hardly observed in cement hydration studies due to kinetic hindrance. According to Tab. 3.1, isomorphous substitution of Mg^{2+} (0.72 Å) by Fe^{2+} (0.78 Å) might occur e.g. in hydrotalcite phases, due to similar ionic radii, while replacement of Ca^{2+} (1.00 Å) by Fe^{2+} in relevant hydrates may be unlikely. A recent in-situ high-energy X-ray scattering study found that $(Fe_{1-x},Ca_x)(OH)_2$-like solid solution could transiently form on the surface of corroded zero-valent iron but quickly turn to the more stable $Fe(OH)_2$ (Ma et al. 2018). Only a few studies on interactions between FeII/III and C-S-H were recently carried out. It was reported that both Fe^{II} and Fe^{III} can be strongly sorbed by C-S-H in octahedral coordination on the surface and in the interlayer (Mancini et al. 2020, 2021b). Over the long term, the degradation of hydrated cement would promote the formation of zeolite at the interface of cement and clay, where Fe^{III} could be structurally incorporated into the framework of zeolite (Ma et al. 2021). The redox behaviours of the $Fe^{II/III}$ sites in various cement hydrates are scarcely known.

Magnesium (Mg)

In HCP, the nearly insoluble brucite ($Mg(OH)_2$) is expected to prevail in the magnesium corrosion products. Thus, the process of exchanging with other ions by Mg^{2+} should be quite slow. In Mg-rich cement, magnesium silicate hydrates (M-S-Hs), characterised by nano-crystallite hydrated phyllosilicates with relatively short coherence length (1.2 nm) and small particle size (> 200 m^2/g), could form by destabilising C-S-H (Bernard et al. 2017a, 2017b). Low Ca/Si C-S-H is stable in the pH range 9.6 to 11.5 and adding $MgCl_2$ can decrease the pH below 9.6 at 20 °C in lab experiments. Experimentally, the persistence of some brucite is observed as the dissolution of brucite is very slow and minor in the presence of silicate, while modelling predicts only the presence of M-S-H that is thermodynamically more stable.

Zinc (Zn)

Experimental studies showed that Zn^{2+} could be taken up into the C-S-H structure by binding to the pairing silicate tetrahedral site, the bridging silicate site, and cation exchange in the interlayer site of C-S-H (Stumm et al. 2005, Tommaseo & Kersten 2002, Ziegler et al. 2001a, 2001b). Conversely, the structural incorporation may bring changes to the nucleation/crystallisation kinetics and thermodynamic stability of the C-S-H phases.

Lead (Pb)

Lead is not expected to corrode under anoxic conditions (Pourbaix 1974). However, there is a new study available that measures corrosion rates for lead in synthetic cement porewaters (Senior et al. 2023). It was unclear in this study if a steady state representative for long-term corrosion was reached or not. Thus, the reported corrosion rates of 0.3-0.5 nm/a should be considered as upper bounds leading to a very slow corrosion of lead under repository conditions, if at all.

Nevertheless, any reaction products would have no adverse effect on HCP because no change in the mineral composition of HCP is expected. The interaction of Pb^{2+} with the cement matrix is dominated by surface sorption onto cement phases. Experimental studies showed that Pb^{2+} interaction with cementitious materials predominantly occurs via the formation of surface complexes on C-S-H phases at low Pb concentrations.

Boundary conditions/additional information

The availability of water and the reactive surface area control metal corrosion. The corrosion process may be inhibited by the formation of a corrosion layer on the metallic waste over time.

Timescales

Corrosion rates for different metals can be found in Tab. 4-1 of Diomidis et al. (2023). The corrosion of magnesium and aluminium is expected to be fast. The formation of protective layers, e.g. the formation of brucite or bayerite, may inhibit the dissolution in the long term. In contrast, the corrosion of iron in alkaline media was found to be very slow under anoxic hyperalkaline conditions (three to four orders of magnitude lower; Diomidis et al. 2023).

Uncertainties

The corrosion kinetics and the degree of interaction of Mg^{2+}, Al^{3+} and Fe^{2+} with components of the cement matrix are only partly understood. Similarly, Fe^{2+} could react with HCP, e.g. by substituting for Mg^{2+} in hydrotalcite-type phases. Nevertheless, the degree to which this substitution occurs is uncertain since Mg^{2+} forms predominantly $Mg(OH)_2$ in cementitious environments.

3.4.5 Iron-cement interactions: effect of iron on cementitious materials

Overview

Hardened cement paste (HCP) originally contains iron from the clay material used together with limestone as raw material in the kiln. The main Fe-bearing phase in the clinker is C_4AF – calcium aluminate ferrite (as $Fe^{(III)}$). Fe may also be present in supplementary materials (e.g. blast furnace slag as $Fe^{(0)}$) as well as in concrete aggregates. Upon hydration, the clinker is fastest to react. The components of the supplementary material tend to react slower or remain unreacted for a longer period, while the aggregates are generally the slowest to react. The release of iron upon hydration will lead to the formation of primary Fe-bearing cement hydrates. Furthermore, secondary phases may form in aged cementitious materials from the iron released by the slowly reacting components of the supplementary material and finally by the cement-aggregate interaction. Additionally, iron is released due to corrosion of metals, and it will diffuse into the surrounding cementitious material, giving rise to interaction with cement phases or, depending on solubility, to the formation of specific Fe-containing minerals (corrosion products). Steel corrosion and the precipitation of secondary corrosion products is characterised by a net volume increase (Fig. 3-17) which may affect the integrity at the cement/steel interface, leading to mechanical stress and cracking.

Part of the iron will diffuse through the aqueous pore solution and may react with the cement phases or may be sorbed or incorporated, affecting their stability and their retention properties. The corrosion products may also retard different radionuclides via sorption and/or incorporation into the structure of the secondary phases. Local sorption competition between corrosion products and radionuclide uptake by the hardened cement paste may develop. The iron species may affect the radionuclide uptake by cement phases. The effect of iron disturbance in cementitious materials

can be characterised by the precipitation of secondary iron phases (e.g. iron steel corrosion products, iron-containing cement hydrates) and the extent of iron diffusion into the cement paste (mainly retention by cement phases).

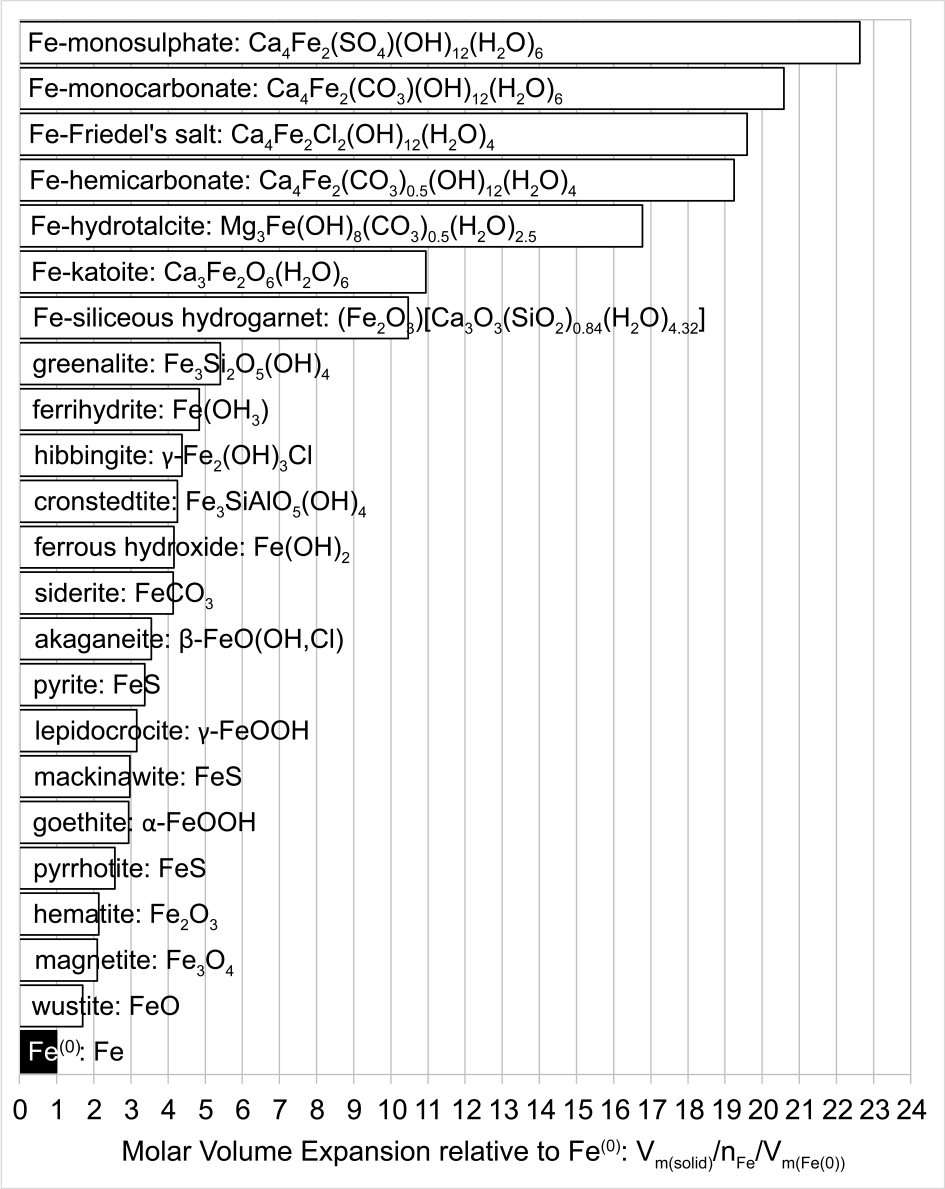

Fig. 3-17: Relative volumes of possible corrosion products and Fe cement hydrates as compared to pristine Fe(0), calculated as the molar volume of the secondary iron phase ($V_{m(solid)}$) per moles of iron (nFe) in the solid divided by the molar volume of Fe(0)

The solids shown here have idealised formulas and in real cement they can have different degrees of hydration with an effect on the phase volume. Molar volumes collected from several sources (Blanc et al. 2012, Lothenbach et al. 2019, Robie & Hemingway 1995, Rozov et al. 2011, Taylor 1997).

Steel corrosion

The alkaline conditions determined by the cement pore solution lead to very low corrosion rates due to the formation of a passivation layer (Diomidis 2014, Elsener & Rossi 2018, Senior et al. 2021). The corrosion rates tend to decrease with time until a steady state dissolution/precipitation and diffusion conditions in the passivation film are established (Diomidis 2014). The evolution of the cementitious near-field will probably be heterogeneous in space and time; highly alkaline cement pore solutions in equilibrium with portlandite (pH > 12.5) might exist in certain areas of the near-field for very long times (cf. Section 3.3). Conditions with lower alkalinity (pH < 10) can be expected in carbonated materials, materials affected by cement-aggregate reactions and materials close to the contact with the Opalinus Clay where the pH may decrease due to the effect of the Opalinus Clay pore solution. In such cases, corrosion rates will be higher but they are also expected to decrease with time due to the growth of a protective corrosion-product layer (Necib et al. 2018).

Different types of corrosion products and of iron-containing cement phases are expected to form under the influence of changing physico-chemical conditions in the near-field of an L/ILW repository (solution composition, pH, redox conditions, temperature, saturation conditions, availability of moisture, etc.) (De Windt et al. 2020). Conditions in the near-field of an L/ILW repository are oxidising at first, due to the ventilation period during the construction phase. Studies on aerobic corrosion products of steel identified poorly crystalline phases of iron such as oxyhydroxide hydrates, ferrihydrite ($5Fe_2O_3 \cdot 9\ H_2O$), lepidocrocite (g-FeOOH) and goethite (a-FeOOH), maghemite (g-Fe_2O_3) and hematite (a-Fe_2O_3) and magnetite (Fe_3O_4) as corrosion products (e.g. Broomfield 2003, Criado et al. 2013, Poursaee 2016, Zhao & Jin 2016).

Under anaerobic conditions relevant to the post-closure phase of the L/ILW repository, the main iron corrosion products identified are magnetite (Diomidis 2014, López & González 1993, Pally et al. 2020) and "black rust", a mixture mainly composed of magnetite and other iron oxides (Broomfield 2003, O'Donovan et al. 2013). The presence of different ligands in the solution will influence which corrosion products will form. For example, the presence of carbonate, sulphate or chloride can contribute to the formation of various carbonates, "green rust" (GR), layered double hydroxides containing both $Fe^{(II)}$, $Fe^{(III)}$, and sulphides.

Archaeological metal artefacts are used as analogue materials to study such corrosion products. Samples of these materials have undergone corrosion in a natural environment over a very long period of time and goethite (a-FeOOH) and magnetite/maghemite (Fe_3O_4/Fe_2O_3) were identified to be the main corrosion products (Chitty et al. 2005, L'Hostis et al. 2009, Monnier et al. 2011, Neff et al. 2005).

Fe-containing cement hydrates

In cement hydrates, Fe(III) can replace Al in Al-containing cement phases, such as AFm (aluminate ferrite monosulphate), AFt (aluminate ferrite trisulphate) and siliceous hydrogarnet phases, often forming solid solutions. Fe-ettringite, Fe-monosulphate, Fe-hemicarbonate, and Fe-monocarbonate (Dilnesa et al. 2011, 2012, Möschner et al. 2009), Al/Fe hydrotalcite and Al/Fe hydrogarnet (hydroandradite) (Dilnesa et al. 2014a, 2014b, Vespa et al. 2015) have been reported in different cements and under varying conditions. Solubility experiments show that the Fe-containing hydrates (AFm, AFt) have very similar stabilities compared to their Al-containing analogues, being only slightly more stable (Dilnesa et al. 2011, 2012, Lothenbach et al. 2019, Möschner et al. 2009). In contrast, the data on the stability of iron-containing hydrogarnet show that it is ~ 7 log units more stable than its Al counterpart and its stability increases with temperature. For a Portland cement system, in the presence of Fe hydroandradite is always preferred (Dilnesa et al. 2014b), while in the case of the AFm and AFt phases, their Al-bearing analogues are more stable. Fe/Al siliceous hydrogarnet was identified in cement paste hydrated for 10 and

50 years (Dilnesa et al. 2014a, Vespa et al. 2015), ferrite-rich cement (Elakneswaran et al. 2019), and sulphate-resistant cement (HTS) (Dilnesa et al. 2014a). Experiments and modelling show that Fe/Al silicious hydrogarnet is the most stable iron-containing hydrate from ambient to elevated temperatures in Portland cement systems. The hydrogarnet phase may not form in the early stages due to kinetic hinderance but is identified in aged cement samples. Its formation will be at the expense of Ca and Si from portlandite and C-A-S-H and lead to a decrease in Al bound to C-A-S-H.

In low-pH cement systems (pH < 12), Fe-ettringite and mainly ferrihydrite/lepidocrocite phases are favoured (De Windt et al. 2020). In the presence of Cl^-, iron-containing layered double hydroxides can form (e.g. $Fe^{(III)}$-Friedel's salt, $Fe^{(II)}$-hydrotalcite). Hallet et al. (2022) identified the formation of (Mg/$Fe^{(II)}$/$Fe^{(III)}$, Al)-layered double hydroxide upon hydration of slag blended cements. These phases are known to have a high sorption capacity for anionic and cationic species (Kayali et al. 2012, Triantafyllidis et al. 2010, Yang et al. 2020).

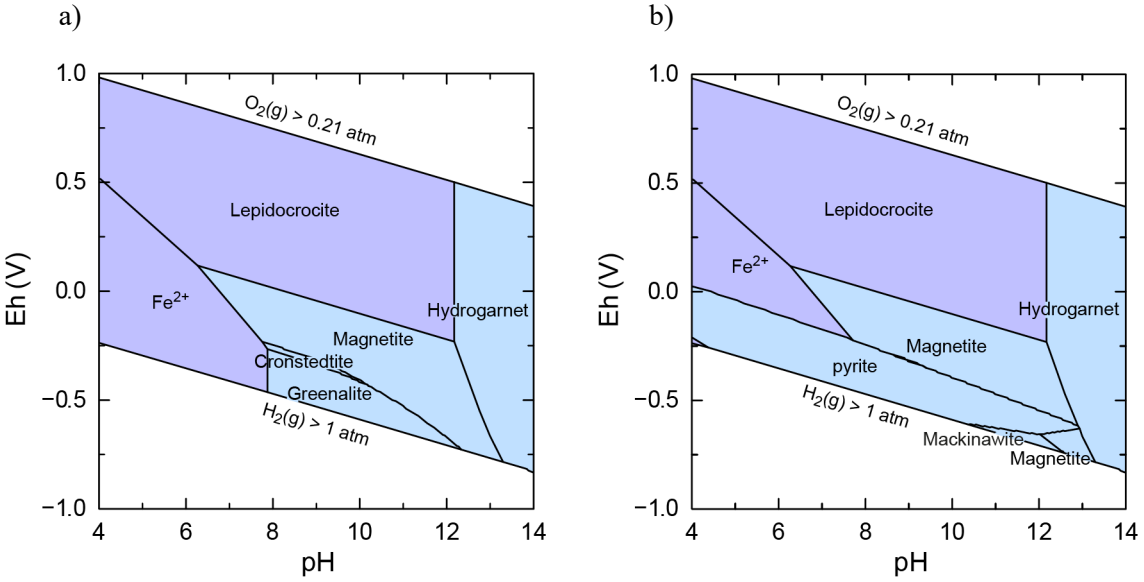

Fig. 3-18: Eh-pH diagram for the Fe-cement pore solution (Ca-Al-Si-C-S-Na-K-Cl-OH) at 1 bar 25 °C

With (a) and without (b) suppressing the reduction of sulphur. Calculated using the PSI Chemical Thermodynamic Database 2020.

For cementitious materials under portlandite-saturated conditions, the stabilisation of magnetite is strongly favoured (De Windt et al. 2020). In the presence of Ca, Si and Al, siliceous hydrogarnet (hydroandradite) will be stable. In experiments with carbon steel in contact with a cement slurry for 90 days at 80 °C, layers of siliceous hydrogarnet and magnetite were observed at the steel-cement interface (Pally et al. 2020). At pH conditions < 12, ferrihydrite/lepidocrocite (under oxidising conditions) or magnetite (under reducing conditions) are thermodynamically stable (De Windt et al. 2020).

Calculations for the major iron species distribution as a function of pH and Eh in a system with the composition of an SGT Stage 2 cement pore solution (Fig. 3-18) show that Fe/Al silicious hydrogarnet is the most stable phase at high pH in oxidising and reducing conditions, followed by magnetite. In anoxic conditions at pH < 12, iron-containing phyllosilicate or iron sulphides are predicted to be stable depending on whether reduced sulphur is present. In mildly reducing and oxic conditions, magnetite and lepidocrocite are the major stable Fe species.

It is expected that iron generated from corrosion will diffuse into the cement paste and interact with the cement phases. As described previously, Fe(III) can replace Al(III) in Al-containing cement phases, and Fe(II) can replace Mg in hydrotalcite phases. In addition, C-S-H phases (most abundant cement phases) were found to accommodate Fe(III), as previously observed with Al(III). The uptake of iron by C-S-H was mentioned in early studies (Faucon et al. 1996, Labhasetwar et al. 1991) and was quantified experimentally by Mancini et al. (2020). The experimental data show that the uptake of iron in C-S-H is ~ 1 order of magnitude stronger compared to the uptake of aluminium, but in measurements carried out at lower concentrations, uptake is limited by the low solubility of iron hydroxides. On the other hand, the interaction of Fe(II) with C-S-H phases is much weaker, showing ~ 3 orders of magnitude lower uptake than Fe(III), with uptake values close to those observed for other divalent cations (e.g. Sr^{2+}) (Mancini et al. 2021a). Fe(II) is expected to favour other phases such as layered double hydroxides like hydrotalcite or oxidise to Fe(III) because the hydrolysed species of ferric iron are significantly more stable than the ferrous ones.

Aqueous speciation of Fe

Depending on the system composition and phase assemblage, measured $Fe^{(III)}$ concentrations in pore solutions are generally < 0.01 mM (Furcas et al. 2022). At high pH, the dissolved iron in solution will exist in its hydrolysed form of $Fe^{(II)}(OH)_3^-$ and $Fe^{(III)}(OH)_4^-$. The presence of Cl^- can increase the concentration of dissolved iron due to the formation of aqueous complexes with iron (Sagoe-Crentsil & Glasser 1993). Complexes are also possible between iron and other elements (e.g. silicon) present in the pore solution but currently there is a lack of data on their existence and stability (Furcas et al. 2022). Additionally, there is strong competition for these ligands between iron and other cations in solution (De Windt et al. 2020), thus favouring the iron hydrolysed species.

In situ experiments and modelling of iron-cement interaction

Modelling of iron behaviour in cementitious materials has improved due to the experimental analysis of iron-containing phases and the consequent re-evaluation of thermodynamic data for them. Cemdata18 (Lothenbach et al. 2019) contains properties of several Fe(III)-bearing AFm and AFt phases, Al/Fe siliceous hydrogarnet, and hydrotalcite phases in addition to common cement hydrates. Furcas et al. (2022) provide a review of data on iron speciation in cementitious systems. Critically assessed data for cement phases and iron speciation can be found in the Thermoddem TDB (Blanc et al. 2012). In the new version of the PSI Chemical Thermodynamic Database, TDB 2020 (Hummel & Thoenen 2023), the data for iron were updated and are based mainly on the recent OECD NEA's volume on the thermodynamics of iron by NEA (2013).

Existing experimental data and modelling are mainly concerned with the corrosion of iron and steel of waste containers under conditions relevant for L/ILW and HLW disposal and less on the iron-cement interactions (Crusset et al. 2017, Diomidis 2014, Landolt et al. 2009, Mon et al. 2017, Necib et al. 2018, Pally et al. 2020, Robineau et al. 2021, Senior et al. 2021, Smart 2009, Smart et al. 2017, Taniguchi et al. 2010).

Recent improvements of data for the stability of iron phases and speciation make it possible to better account for the effect of iron from corrosion on the cement paste and model the evolution of the cement/steel interface. Ongoing work on this topic exists within the framework of the EURAD project (work package "Assessment of chemical evolution of ILW and HLW disposal cells (ACED)) (De Windt et al. 2020). In the project sub-task on cement/steel interaction, results from the BACUCE experiments are analysed and compared with modelling results from de Windt et al. (2020). Related work is underway for assessing the evolution of clay host rock and bentonite barriers in contact with corroding metallic materials in the ACED and CONCORD work packages of the EURAD project.

Mancini et al. (2021b) analysed the iron speciation in slag-containing cements exposed to river water (carbonate-rich fresh water) or sea water (chloride-rich) for a period of 6 to 34 years. Observations show the passivation of the slag particles of the samples exposed to river water. In addition to $Fe^{(0)}$, iron sulphide, goethite, and siliceous hydrogarnet were detected. No $Fe^{(0)}$ was detected in the cement exposed to sea water, but iron sulphide, hematite, magnetite, siliceous hydrogarnet and goethite were identified as corrosion products. Modelling results are comparable with observations and predict that most iron is stable as magnetite, iron sulphide, and Fe/Al silicious hydrogarnet in the cement exposed to sea water (Mancini et al. 2021b). The predicted uptake of iron in C-S-H was negligible, with other mentioned phases predicted to be the major sinks for iron.

Timescales

The evolution at the cement/steel interface and the possible effect of iron from corrosion on the cement materials will depend on water saturation state of the system.

While in operation, i.e. during waste emplacement, the repository will be under oxidising conditions. The corrosion of steel and other iron-based materials in contact with cement will be slow due to high-pH conditions. The main corrosion products will be iron oxides, oxyhydroxides and Fe/Al silicious hydrogarnet. Soon after closure, the system is expected to quickly evolve towards anoxic conditions and magnetite is predicted to be the most stable corrosion product. Magnetite precursor corrosion products will be transformed to magnetite. In the presence of the cement pore solution, Al/Fe silicious hydrogarnet is a stable corrosion product. The precipitation of magnetite and Al/Fe silicious hydrogarnet may create a protective layer on the steel that will decrease the corrosion rate and will limit the interaction of iron with the surrounding cementitious materials. In cement systems with pH < 12, magnetite may form but also the formation of Fe(II) silicates and layered double hydroxide phases is feasible. These phases have a high sorption capacity and might also contribute to the passivation effect by isolating the steel from the adjacent system (Triantafyllidis et al. 2010, Zhang et al. 2021).

Over short timescales, in the order of months to years, that characterise laboratory experiments and in situ measurements, the formation of metastable intermediate phases such as micro-crystalline ferrihydrite, layered double hydroxides, and iron silicates might be relevant for the evolution of the system. The formation of these phases is influenced by dissolution-precipitation and redox kinetics, temperature and local heterogeneities. The evolution of the cement-steel interface is controlled by an interplay of local composition, metastable phases, kinetics of oxidation/reduction and precipitation and the change in transport properties of the affected area (Stefanoni et al. 2020).

For longer periods of the order of thousands of years, the phase assemblage is expected to evolve towards the more stable crystalline phases like magnetite and, depending on the silicon concentration, towards Al/Fe siliceous hydrogarnet, or iron silicates in lower-pH systems.

Over long periods of time, as a limiting case the iron and steel in the repository can be assumed to be completely corroded and transformed into magnetite (Diomidis et al. 2016). Precipitation of poorly soluble iron phases and the uptake of iron in C-S-H supports the idea that iron species originating from corrosion can be strongly retarded by the cement paste and will thus be retained close to the iron/steel-cement interface (De Windt et al. 2020).

Uncertainties

Uncertainties related to the interaction of iron with the cementitious materials from the near-field of an L/ILW repository are mainly related to the lack of information on the kinetics of dissolution/ precipitation of iron-bearing corrosion products (metastable phases) and limited knowledge on the fate of Fe(II) interacting with the cement (Havlova et al. 2020, De Windt et al. 2020). Observations on the ingress of iron from steel corrosion show that iron penetrates into cement paste at a larger distance from the steel interface than predicted by thermodynamic models (Angst et al. 2020). Additional uncertainties come from the lack of accurate values for the corrosion rates of steel under anoxic and moderately alkaline conditions (pH 10.5 – 11.5). With the advance of the analytical techniques, additional data have been collected (Necib et al. 2018, Senior et al. 2021). Results from in situ and lab experiments will be compared with newly developed reactive transport models for iron/steel corrosion to assess the effect of iron on the cement paste at the iron/steel interface as part of the ongoing work within the framework of the EURAD project "ACED".

3.4.6 Impact of H_2 on cement/clay backfill materials

Overview

Hydrogen produced by the anaerobic corrosion of metals present in the repository (Diomidis 2014) is calculated as being the major gas component with between 80 and 100% of the volume of total gases produced (Poller et al. 2016) in the L/ILW and SF/HLW repositories, respectively. The main hydrogen-producing reaction is the oxidation of iron to form magnetite (reaction 3-18).

For each mole of corroded iron, 4/3 moles of hydrogen are formed. The high pH sustained by the cementitious materials in the L/ILW emplacement caverns maintains a low corrosion rate due to the formation of a passivating layer of iron oxide phases (cf. Section 3.4.4). Highly alkaline cement pore solutions in equilibrium with portlandite (pH > 12.5) are expected to exist in some cementitious materials of the near-field for long time periods (cf. Section 3.5.4).

The presence of hydrogen can have different effects such as pressure build-up, porewater displacement, impact on saturation time, effect on the chemistry of the porewater and solid phases, and an influence on microbial activity.

In natural inorganic systems, hydrogen tends to form strong covalent bonds with oxygen or form molecular hydrogen (H_2) either as gas or dissolved in the aqueous phase. The chemical reactivity of molecular hydrogen (as a reducing agent) is strongly limited at ambient temperatures (Truche et al. 2009, Zivar et al. 2020). It can be enhanced by catalysts (metals, mineral phases and their surfaces) (Truche et al. 2013b), aqueous speciation (presence of intermediate redox species), and microbial activity (hydrogenotrophic bacteria).

Compared to other gases, hydrogen has a very low solubility in water (44 times lower solubility in water than CO_2, and 1.6 times lower than methane) (Wiesenburg & Guinasso 1979) and water-saturated rocks can act as barriers (seals) for hydrogen in the time frame of years. Due to its low molecular weight, H_2 will slowly diffuse through the confining rock layers (Zivar et al. 2020). The fully saturated conditions in the Opalinus Clay host rock will act as a barrier for the generated hydrogen, which will accumulate in the available pore space leading to a possible delay in the

saturation of the system (Papafotiou & Senger 2016). The effective transport of hydrogen in the near-field of an L/ILW repository will occur in unsaturated or partially saturated conditions as a gas phase through fractures of the EDZ, or through a high porosity/permeability backfill material or by diffusion through the pores of the Opalinus Clay.

Hydrogen can be absorbed by different materials in a DGR (e.g. clay minerals, zeolites, metals, etc.) through weak interactions with the material surface (physisorption, e.g. adsorption on clay mineral surfaces) (Broom 2011). Clay minerals are known to be able to sorb gases through weak van der Waals interactions with the pore surfaces, known as physisorption (Broom 2011, Truche et al. 2018). Part of the generated hydrogen may be adsorbed on clay surfaces (Owusu et al. 2022). Because of the weak forces involved, adsorbed hydrogen may be easily desorbed. The sorption capacity of hydrogen is dependent on the water saturation and on the competition with other gases for sorption sites (Didier et al. 2012b, Edge et al. 2014).

Hydrogen may be consumed through different redox reactions. Oxidised substances (carbonates, sulphates, ferric iron-containing phases) present in the cement/clay backfill materials may react with hydrogen, leading to the formation of reduced phases (e.g. methane, magnetite, pyrite/ pyrrhotite). Such reactions are often very slow at ambient conditions, but may be mediated by bacteria, which use hydrogen as an energy source. Therefore, in most cases, hydrogen can be treated as an inert species.

Details on the gas production mechanism, consumption and repository-induced effects can be found in several Nagra reports (Diomidis et al. 2016, Leupin et al. 2016a, 2016b, 2017).

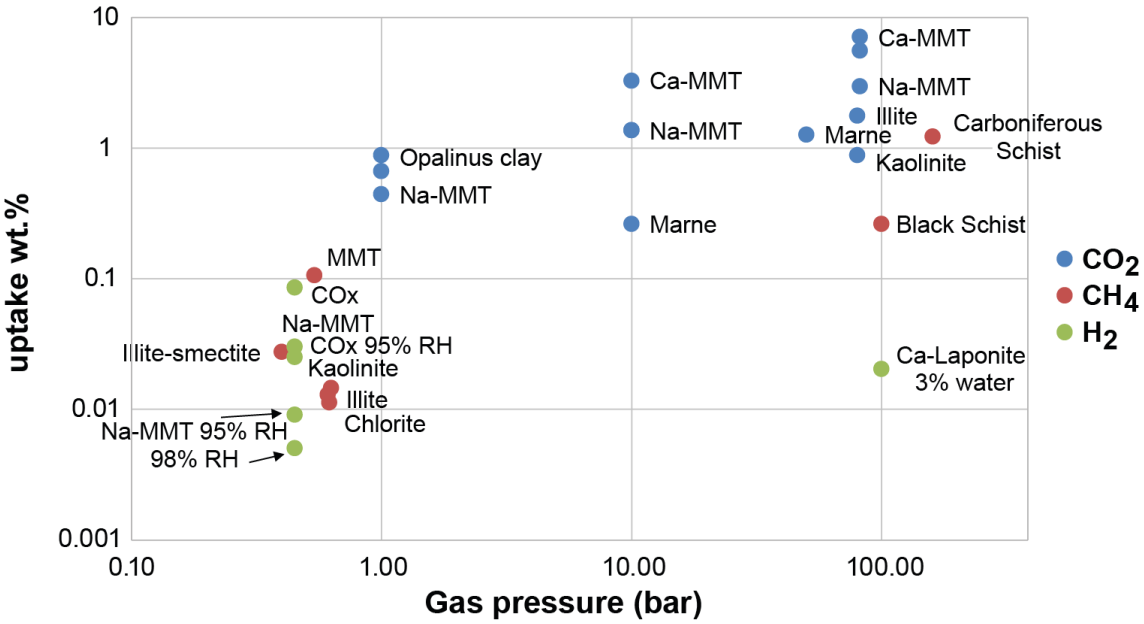

Fig. 3-19: Measured gas adsorption on different clays and clay-rich rocks at temperatures of 10 – 45 °C and different gas pressures, adapted from Didier (2012a)

Montmorillonite (MMT)

H_2 retention by clays and clay rocks

Experimental data show that dry clays and clay minerals may retain significant amounts of hydrogen (around 0.05 wt.-%) even at low pressures and close to ambient temperatures (Fig. 3-19) (Bardelli et al. 2014, Didier 2012a, Didier et al. 2012b, Edge et al. 2014, Mondelli et al. 2015, Pini et al. 2018). This value would translate into a sorption capacity of around 14.8 m^3 of H_2 per one m^3 of dry Opalinus Clay (density of 2.4 g/cm^3, at 25 °C, 1 bar). In the presence of water and other gases, the sorption of hydrogen competes for the sites on the clay surfaces. Simulations of methane and carbon dioxide sorption in clay minerals have shown that water may significantly reduce the sorption of gases (Jin & Firoozabadi 2014).

Adsorption of gases is strongly correlated with the pore size distribution and the specific surface area, with smectites having the largest dry sorption capacity, while clay minerals with low or no interlayer charge adsorb gases on their external surfaces (Edge 2014, Ji et al. 2012, Liu et al. 2013, Xiong et al. 2017).

Existing simulations and measured data tend to show that hydrogen and methane may have comparable qualitative sorption behaviour in clays, with hydrogen sorbing in lower amounts compared to methane, while carbon dioxide is sorbed about one order of magnitude higher (Fig. 3-19).

Hydrogen abiotic reactions

Inorganic reactions involving molecular hydrogen are kinetically constrained and are too slow to consume significant amounts of hydrogen below 150 – 100 °C, (relevant for the L/ILW system) even on timescales of hundreds of thousands of years (McCollom & Seewald 2001, Thom & Anderson 2008, Truche et al. 2009). The rate of such reactions may increase in the presence of mineral surface catalysts or in the presence of intermediate reduced aqueous species.

Methanogenesis occurs only under hydrothermal conditions (> 150 °C) enhanced by the presence of a mineral surface catalyst (e.g. olivine/magnetite) (Berndt et al. 1996, McCollom & Seewald 2001). For abiotic sulphate reduction, Truche et al. (2009) extrapolated a half-life of 2.7 billion years at 25 °C. The presence of intermediate reduced sulphur species like sulphite (SO_3^{2-}), thiosulphate ($S_2O_3^{2-}$) and bisulphide (HS-), for example in blended slag cements (Lothenbach et al. 2012), can act as a bridge between sulphate and sulphide, thus facilitating the electron transfer (Thom & Anderson 2008). Truche et al. (2013b, 2013a) observed the reduction of nitrate within days in the presence of a carbon steel surface at 90 °C. The rate is decreased at pH > 9. Truche and Betelu et al. (Betelu et al. 2012, Truche et al. 2010, 2013c) describe the reduction of pyrite to iron monosulphide in the presence of H_2, producing H_2S. This reaction is enhanced in alkaline conditions and may have a significant rate at pH > 10 and ambient temperatures. This reaction may be relevant for cementitious materials with a high content of sulphides, which is not the case for the L/ILW near-field. No significant hydrogen redox reactions are expected to occur in the cement/clay backfill materials of the L/ILW near-field.

Hydrogen reactions mediated by bacteria

Redox reactions involving hydrogen can be mediated by bacteria. Hydrogenotrophic bacteria use the energy from the redox reaction that they mediate between hydrogen as electron donor and other species (electron acceptor, e.g. carbonate, sulphate, nitrate, $Fe^{(III)}$, etc.) (Libert et al. 2011). Microbial metabolism enhances the rate of certain redox reactions (kinetically constrained at ambient temperatures) to harvest the necessary energy. Bacterial activity is dependent on different factors such as availability of water, physical space, the abundance of nutrients, the temperature, pressure, the pH and salinity of the aqueous solution (Taborowski et al. 2019). Bacterial activity leads to the dissolution of oxidised primary phases (carbonates, sulphates, iron oxides/hydroxides,

etc.) and to the precipitation of reduced secondary phases, as well as material fluxes to (nutrients) and from the bacteria (excretions). This can affect the porosity, permeability, and other properties of the medium (e.g. swelling properties, reduced structural iron in clays). All hydrogenotrophic bacteria that use hydrogen as a primary electron donor will cause a pH increase involving proton-consuming reactions (e.g. sulphuric acid is a stronger acid than hydrogen sulphide).

Bacteria need sufficient space to grow (pore space > 2 µm) and a continuous supply of nutrients. Bacterial development is strongly limited in diffusion-dominated water-saturated systems. Bacteria tend to thrive close to ambient temperatures (20 – 40 °C), although some thermophilic bacteria (e.g. thermophilic sulphate-reducing bacteria) can survive temperatures up to ~ 110 °C (Cross et al. 2004). Elevated pH (> 9) and increased salinity inhibit the activity of bacteria. Bacterial activity was found to slow down with increasing pH and cease above pH 11 or in solutions at salt concentrations above 35 g/l (Albina et al. 2019, Alquier et al. 2014, Berta et al. 2018).

Anaerobic bacteria that use hydrogen as an energy source and that may be relevant for the near-field of an L/ILW are nitrate-reducing bacteria (NRB), iron-reducing bacteria (IRB), sulphate-reducing bacteria (SRB), and methanogenic bacteria (MB) (Leupin et al. 2017). Alquier et al. (2014) showed that NRB could survive in elevated-pH pore solutions (pH 9 – 11) in cementitious systems at the contact with bituminous materials. IRB are often present together with SRB and may promote the reactivation of corrosion processes as they can alter the protective layer of the metal surface (Esnault et al. 2011, Herrera & Videla 2009). SRB may also enhance steel corrosion either by using hydrogen resulting from corrosion or the iron directly from the steel (Enning & Garrelfs 2014), but they do not thrive in highly alkaline solutions maintained by cement materials. MB live in similar conditions to SRB and can use the carbon from carbonate dissolution or the degradation of organic matter and hydrogen from corrosion to produce methane.

The presence of bacteria in the near-field materials of the L/ILW repository will be limited by the availability of space, water, and nutrients. The least favourable conditions would be dried materials (desaturated areas) and compacted clays. Fully saturated low-permeability materials, such as undisturbed Opalinus Clay and compacted bentonite, when advective transport is limited, will strongly inhibit bacterial activity. The most favourable places for bacterial development would be partially saturated porous materials and areas with a relatively high flux of nutrients, such as interfaces between materials, at the contact between clay and steel, clay and cement. In addition, the pH must be favourable for bacterial metabolism, and strong gradients are needed for fast transport of necessary species (iron and hydrogen from steel, sulphate (± carbonate) from cement, organic carbon from the clay). Although cementitious materials are relatively porous and contain residual porewater, their pH is highly alkaline (> 11) and is not favourable for bacterial activity. Therefore, cementitious materials (dry, partially, or fully saturated) are expected to offer protection from bacteria to the internally stored materials (steel, organics), unless advection channels to the external parts of the repository emerge. Bacteria may develop on the external surfaces of concrete materials in contact with clay, surrounding e.g. any low-pH shotcrete.

Experiments and models

Due to the inert behaviour of hydrogen, there are few experimental studies on the abiotic reactivity of hydrogen close to ambient conditions. No effect or changes due to the presence of hydrogen were observed in the experiments of Yekta et al. (2018) on the reactivity of hydrogen in a dry sandstone buffered system at 100 – 200 °C and up to 100 bar after 6 months.

Hassannayebi et al. (2019) modelled the effect of injecting hydrogen into a clay-rock-buffered system (related to hydrogen storage in the Molasse Basin, Austria). When sulphate reduction was allowed in the calculations, results predicted an increase in pH, which promoted the dissolution of carbonates and of muscovite. A pH increase when allowing sulphate reduction was also

predicted in the model of Lassin et al. (2011) who evaluated the effect of hydrogen on the COx porewater. Pichler (2013) modelled fluid-gas-rock interaction in a lithic sandstone. With the addition of hydrogen, pH increased, dolomite was replaced by calcite, and no reduction of pyrite to pyrrhotite was predicted by the calculations.

The presence of bacteria has been identified in the repository environment and considered in modelling of processes in the repository near-field (Arter et al. 1991, Bachofen 1991, King et al. 1999, Leupin et al. 2017, McKinley et al. 1997, McKinley & Grogan 1991). A detailed review of relevant studies can be found in Leupin et al. (2017). Experimental studies found the presence of sulphate-reducing (main type), iron-reducing, methanogenic, and acetogenic bacteria (Bagnoud et al. 2016, Berta et al. 2018, Boylan et al. 2019). The experiments carried out in contact with Opalinus Clay (Bagnoud et al. 2016, Boylan et al. 2019) found that bacterial activity is connected with the presence of clay and natural clay porewater, with bacterial activity being absent in experiments with clay and synthetic porewater. The initial aerobic bacteria were replaced by anaerobic sulphate-reducing bacteria (production of H_2S) as the conditions quickly changed from oxidising to reducing (Bagnoud et al. 2016). A detailed overview of the bacterial activity in bentonite is given by Taborowski et al. (2019); their experiments showed that SRB may form local colonies in compacted clays mainly in locations where there are impurities, higher porosity, and cracks. Details on the bacterial activity relevant to the waste repository system can be found in Leupin et al. (2016a, 2017).

The Nagra sealing system employs sand-bentonite mixtures and microbial activity in such materials has therefore been specifically investigated. In particular, the formation of a microbial biofilm in a sand-bentonite mixture has been investigated in the Microbial Activity (MA) experiment at the Mont Terri Rock Laboratory; for details on the experimental setup, see Burzan (2021). In this experiment, the injection of hydrogen gas, an efficient electron donor for microbial metabolism, stimulated microbial growth in bioreactors filled with a sand-bentonite mixture, which were fed with Opalinus Clay porewater. Mineralogical alterations were also observed in some of the bioreactors. It has been shown that hydrogen was consumed by sulphate reduction and methanogenesis. Biofilm formation did not prevent gas transport across the sand-bentonite mixture.

Shrestha et al. (2022) studied the effect of low-pH concrete and bentonite on indigenous bacteria. The two-month study showed that the abundance of bacteria was significantly lower in bentonite and concrete samples as compared to bentonite only samples.

Bacterial activity drives kinetically constrained reactions towards equilibrium. Therefore, thermodynamic equilibrium, or partial equilibrium (metastability constraints) can be used as a first approximation for considering bacterial activity when looking at timescales much larger than their typical life cycles. Jakobsen and Cold (2007) proposed a metastability modelling approach, in which the bacteria-mediated redox reactions only proceed after a concentration threshold is reached. Bacterial activity can be connected to the rates of chemical reactions and microbial growth models (Monod kinetic models) are used to couple biochemical processes and chemical reactions with flow and transport (Hagemann et al. 2016, Schäfer et al. 2005). For large-scale models, chemical equilibria can produce good approximations for “fast” reactions and on “long” timescales (Schäfer et al. 2005).

King et al. (1999) included microbial reactions (using Monod kinetics) in a reactive transport model for container corrosion in a waste disposal system. They simulated the sulphate reduction, growth and death of SRB, supply and consumption of hydrogen and sulphate (nutrients), and the precipitation of iron sulphide. Results show that the microbial activity is strongly limited to ~ 2 years by the availability of nutrients, mainly sulphate.

Kiczka et al. (2021) applied a reactive transport model that takes into account bacterial activity to better understand processes taking place in diffusion cell experiments of sandy porous rock in contact with different bentonites (Maanoja et al. 2020). The natural samples showed the existence of indigenous microorganisms that can be activated in favourable conditions. The experiments and calculations showed that the development of bacteria is limited by the availability of nutrients (organic carbon and sulphate).

The Hydrogen Transfer (HT) experiment is an in situ experiment at the Mont Terri URL to study the transport and reactivity of hydrogen injected into a borehole in Opalinus Clay (Damiani et al. 2022, Vinsot et al. 2017). Monitoring data show a very fast decrease in hydrogen concentration after each gas injection. The decrease of hydrogen is significantly larger than the expected decrease by diffusion and is attributed to hydrogen consumption by bacteria such as SRB or IRB. Bagnoud et al. (2016) analysed the chemistry and biology of the borehole porewater. Results show the development of a bacterial population, specifically SRB, that may have used hydrogen to reduce sulphate to sulphide, indicated by its increase in the pore solution. The evolution of gases in the HT experiment was reproduced by modelling using the assumption that the hydrogen is consumed by kinetically constrained sulphate reduction by SRB (Damiani et al. 2022).

Natural and industrial analogues

The Cigar Lake uranium ore deposit (northern Saskatchewan, Canada) (Pagel et al. 1993) can be considered a natural analogue for the uptake and effect of hydrogen in clay rocks. The deposit is hosted in clay-rich rocks, mainly composed of illite, chlorite, and kaolinite (no swelling clays) where hydrogen generated from water radiolysis was accumulated (Truche et al. 2018). Truche et al. (2018) measured the content of hydrogen in rock samples around the deposit and reported hydrogen concentrations of up to 0.05 wt.-%. This value is comparable with the measurements on clays and clay minerals (discussed before) and is especially surprising, considering that no swelling clay minerals are present, the rocks are fully saturated, low in organic matter, and with other adsorbed gases present. One important factor leading to the observations may be the exceptionally long evolution period of more than 1 Ga, which is not comparable to the time frame of any laboratory experiments and also exceeds the expected repository lifetime.

For shorter timescales, underground gas storage facilities (UGS) can be used as analogues for gas-related processes comparable to those in the L/ILW repository (Leupin et al. 2016a). Examples of town gas storage and underground hydrogen storage show bacterial activity, especially related to hydrogen consumption (Muhammed et al. 2022, Reitenbach et al. 2015, Zivar et al. 2020). The main reactions observed are the degradation of organic carbon, accumulation of organic acids, generation of methane, and generation of hydrogen sulphide. In places where the underground porewater had high salt concentrations, no effects on the town gas were observed (Leupin et al. 2016a). In hydrogen storage, one proposed method is the injection of H_2 and CO_2 that is then converted to CH_4 by methanogenic bacteria (Panfilov & Panfilov 2010). These systems show that microbes will use hydrogen produced in the L/ILW repository as an energy source, if acceptable conditions for bacteria exist.

Besides the change in the gas composition, the activity of bacteria promotes the precipitation of secondary phases such as carbonates (Phillips et al. 2013) or sulphides (iron reacting with the generated hydrogen sulphide). The precipitation of these phases and the growth of the bacterial population may result in a porosity decrease (Eddaoui et al. 2021). The secondary precipitation (mainly calcium carbonate) due to the effect of bacterial activity is suggested as a remediation method to improve properties and crack sealing in cement materials (Alshalif et al. 2016, Anbu et al. 2016, Kalhori & Bagherpour 2017).

Bacteria have been shown to form subsurface lithoautotrophic microbial ecosystems (SLiMEs) (Gregory et al. 2019, Lau et al. 2016). These are mainly hydrogenotrophic bacteria active in deep-sea hydrothermal fields, the sea floor and in continental aquifers. A common characteristic of these systems is that they are related to tectonically active areas, with high permeability (Parnell et al. 2013). Lin et al. (2006) suggested a long-term (millions of years) sustainability of sulphate reducers that use radiolytically produced hydrogen and sulphate (from barite in the rock) transported through fractures. Bacterial activity has also been suggested in nutrient-limited and low-permeability subsurface systems such as in deep continental crystalline rock (2,500 m drill hole in Outokumpu, Finland and 500 m drilled into Cretaceous Toki granite, Japan) (Nyyssönen et al. 2013, Suzuki et al. 2014). In these low-energy and nutrient-transport conditions, bacteria may develop various metabolic strategies offering them resilience over geological timescales (Nyyssönen et al. 2013).

Timescales

The timing for the evolution of gases in the repository is controlled by the rate of gas production and consumption. The rate of hydrogen generated from the anaerobic corrosion of metals will decrease over time due to the formation of a protective layer.

The presence of cementitious materials in the L/ILW system will maintain very low corrosion rates (Diomidis et al. 2016). Highly alkaline cement pore solutions in equilibrium with portlandite (pH > 12.5) are expected to exist in the cementitious materials of the near-field for a long period, but they are strongly affected by aggregate cement reactions and carbonation (cf. Section 3.5). Timescales of hydrogen generation and consumption are interconnected with the saturation evolution of the repository because metal corrosion and other chemical reactions are controlled by the presence of water.

Development of bacteria that can consume hydrogen is strongly supressed due to the highly alkaline conditions maintained by the cementitious materials and their desaturated state. Their development is expected to be limited to the domains near the host rock and the access tunnel system, in partially saturated areas with porous backfill and materials having close-to-neutral-pH porewater. In their review on the effect of environmental conditions on bacterial activity, Tecon & Or (2017) show that bacterial development takes place between 90 and 100% relative humidity. Bacterial activity decreases with decreasing water potential and transport of nutrients is one of the main factors regulating their development (Schimel 2018).

Bacterial activity may exist shortly after repository closure but may cease thereafter due to inhospitable conditions that develop with lack of liquid water in a desaturated system, or lack of nutrients in a diffusion-dominated environment. Calculations that account for bacterial effects on the gas evolution in an L/ILW repository have been considered in Papafotiou & Senger (2016).

Uncertainties

The uncertainties in assessing the impact of hydrogen on cement, clay and other backfill materials are associated with the processes of hydrogen generation, transport and consumption. Hydrogen generation through metal corrosion is influenced by the stability of the cement materials and the evolution of the saturation time in the L/ILW system. Prolonged desaturated conditions limit the extent of corrosion. The presence of high-pH cement porewater keeps the corrosion rates low while strong cement degradation through carbonation and cement aggregate reaction may promote increased corrosion rates. Hydrogen may be consumed through chemical reactions mediated by bacteria. There is a large uncertainty regarding the abundance, diversity, and sustainability of bacterial communities over geological timescales. The development of bacteria over the time span of thousands of years is a poorly constrained process and is dependent on the availability of space, water and nutrient fluxes. It is difficult to estimate the bacterial activity in a

diffusion-dominated system where the transport of hydrogen and other nutrients is limited. In conditions of very slow hydrogen generation, the amount of hydrogen produced may not be large enough to sustain bacterial activity. Bacteria may exist in a dormant state in the OPA but their viability is inconclusive unless they are brought in a laboratory setting or studied in an in situ experiment where a significant amount of hydrogen is introduced. Bacteria may develop in some parts of the repository but not in others and their activity will be strongly connected with the saturation evolution of the system that is linked to the availability of water and hydrogen generation rate.

3.5 Evolution of the near-field considering heterogeneity on different spatial and temporal scales

3.5.1 System evolution as complex interactions between processes with feedback loops

The development of a holistic understanding of repository evolution requires process understanding, a complete thermodynamic and material dataset, and corresponding software tools. In the last two decades, the development of more sophisticated software tools has allowed the assessment of complex systems, taking into account several processes and their mutual interactions. Although it is not yet possible to model a repository with all the relevant process couplings in a predictive way, the available models are well-suited to investigating selected process couplings and their possible effects on the geochemical evolution of in situ conditions (Ahusborde et al. 2021). In addition, from an experimental point of view, information from more specifically designed experiments has become available. This leads to a more realistic view of the role of various processes and couplings and provides more complex models for the chemical evolution of deep geological disposal cells, as for example in the HORIZON 2020 European Joint Programme on Radioactive Waste Management (EURAD) (Govaerts et al. 2022, Neeft et al. 2022, Samper et al. 2022).

Fig. 3-20 shows the main relevant processes that are believed to influence the geochemical evolution of the L/ILW near-field (Kosakowski et al. 2014). For a specific repository layout, the timescales may vary. The colour intensity indicates in a non-quantitative way their expected importance over time. Most of these processes are described in more detail in this report. This section focuses on the coupling between processes. Some process couplings, specifically those related to material interfaces, are included in the analysis; for example, the influence of cement/clay interaction on diffusive transport and porosity change. Other important couplings need to be investigated further in the future. This particularly concerns the interaction between the saturation state of the near-field on various (bio-)chemical processes that influence the saturation state, either in terms of water and gas transport properties (diffusivity, porosity), or in the form of sources or sinks for gas and water. First attempts to implement such couplings on a waste package scale were implemented by Huang et al. (2021). What is missing so far is the implementation of such process couplings at the repository scale. Fig. 3-21 gives an example for such process couplings between two-phase multi-component transport and bio-(chemical) processes, which do not only change transport properties, i.e. there is specifically a strong coupling between the local saturation state of materials and those chemical processes that consume/release water and/or gases, as those processes strongly depend on the availability of water and will be suppressed under dry conditions.

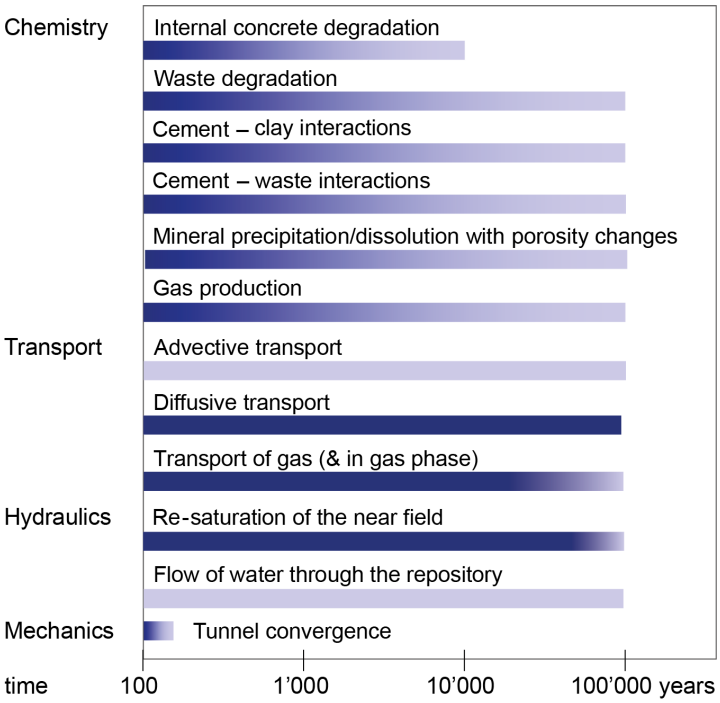

Fig. 3-20: Chemical and physical processes influencing the evolution of a cementitious repository

Couplings between processes are not considered. The colour intensity and the length of the bars indicate, in a qualitative way, the impact of the individual process (modified after Kosakowski et al. 2014).

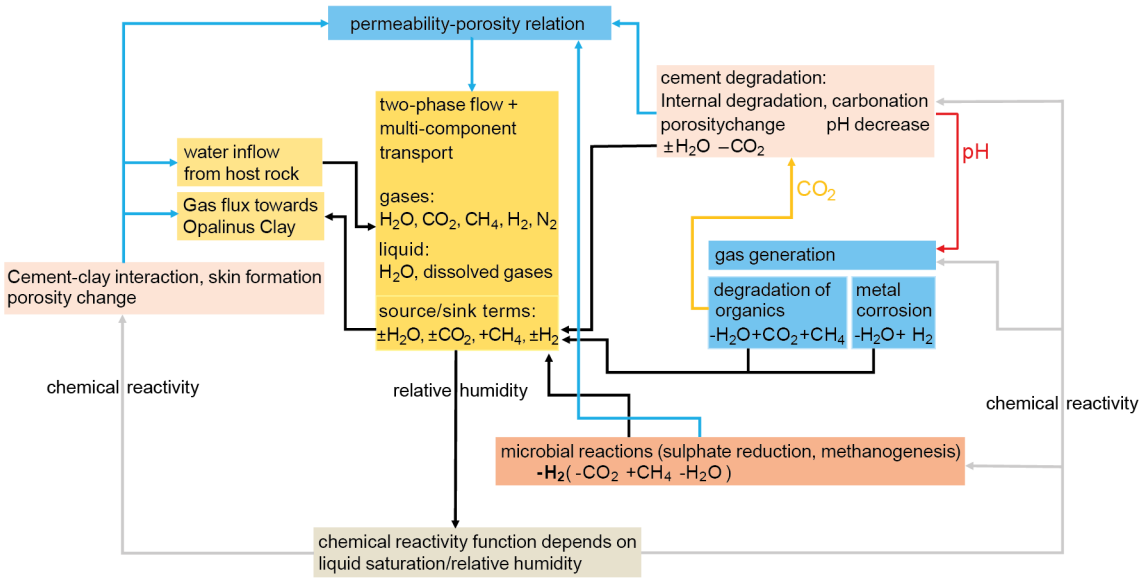

Fig. 3-21: Coupled processes that control the fate of gas in an L/ILW repository

Note that only gas generation in the L/ILW emplacement caverns is shown in the figure, since this is the primary source of repository-generated gas (modified based on Huang et al. 2021).

In addition to the different processes and the process couplings, the heterogeneous distribution of cement and waste materials that evolve within the L/ILW near-field influences system evolution. There has been some progress in the qualitative understanding of the evolution pathways and timescales for selected cement-based materials and waste types (Kosakowski et al. 2020, Wieland et al. 2018). There has been no attempt so far to model a heterogeneous L/ILW near-field taking into account different materials, waste types and two-phase flow and transport processes coupled to bio-(geochemical) processes (Neeft et al. 2022).

Many process couplings include feedback between processes by changing material or transport parameters; this includes permeability, diffusivity, porosity or two-phase flow parameters. All the transport parameters and some chemical parameters, such as reactive surface areas of minerals, are connected to a knowledge of the pore structure. As processes might act at different scales, understanding how pore space is affected and how to upscale those changes to an appropriate representative scale is key to the adequate modelling of transport in evolving materials (Ladd & Szymczak 2021, Molins & Knabner 2019, Prasianakis et al. 2017, Seigneur et al. 2019, Tournassat & Steefel 2019).

Chemistry

Concrete, clays and wastes are chemically very different materials. As discussed in Sections 3.3.2 to 3.3.4 in this report, their interactions are likely to be influenced by various chemical and transport processes and their coupling. At cement/clay material interfaces, mineral precipitation and dissolution might alter the pore space with accompanying changes in material properties (transport and mechanical characteristics). Similar effects can be expected locally for the interactions of waste and cement materials inside waste drums and emplacement containers (cf. Section 3.5.3).

The evolution of the safety barrier system depends on chemical processes or is influenced by chemical processes to various degrees. For example:

- The chemical interactions of waste with the concrete/bitumen matrix may influence the radionuclide fixation and retention capacity in the waste drums.
- Metal corrosion leads eventually to the breach of the steel drum containment.
- Cement and grout degradation may weaken the waste isolation with time.
- Cement/clay interactions may weaken the mechanical stability of the tunnel support. This may result in producing features of higher permeability and effective diffusivity.
- Waste-cement interactions may increase or decrease the release rates of radionuclides.
- Waste-cement or cement/clay interactions may lower (locally) the pH in the concrete compartment and influence metal corrosion rates.
- Alteration of mineral assemblages (dissolution of clay minerals in the host rocks, transformation of cement phases) may alter radionuclide sorption/retention.
- Dissolution of minerals in materials may increase porosity, alter mechanical properties and increase the gas and water transport properties.
- Precipitation of minerals near material interfaces may lower porosity and decrease transport across interfaces.
- Changes in the chemical environment (e.g. pH, ionic strength) may cause the production of colloids or increase their stability (cf. Section 3.3.6).

Gas production

Gases (H_2, CO_2, CH_4) will be produced by the anaerobic corrosion of metals and by microbial degradation of organic matter (Diomidis et al. 2016, Guillemot et al. 2023, Leupin et al. 2016a). CO_2 will react with the cement material causing carbonation and porosity changes near the source. In contrast, H_2 and CH_4 are not expected to interact with cementitious materials but the formation of these gases determines the pressures in the near-field, and, depending on the overpressure, delay the saturation of the emplacement caverns (Martin et al. 2023, Papafotiou & Senger 2016). The amount of gas (H_2, CH_4) generated as a function of time depends on the inventories (steel, organic matter) and rates, i.e. the corrosion rate in the case of H_2 and the degradation rate of organic matter in the case of CH_4 (Diomidis et al. 2016, Wieland et al. 2018).

Redox conditions

Several waste types consist of, or contain, metallic materials, in particular different types of steel. The latter materials include waste packages (e.g. steel drums, etc.), reinforcement within the containers and the tunnel support system, which are susceptible to corrosion (oxic, anoxic) over time (Duro et al. 2014a, 2014b, Wersin et al. 2003). Consumption of the residual oxygen in the near-field is expected to occur relatively quickly after repository closure due to the aerobic corrosion of metals, which generates no H_2 gas, and the degradation of easily degradable organic matter (Nagra 2002a). Thus, redox conditions are expected to be oxidising in the very early stage of an L/ILW repository.

After O_2 depletion, the near-field will remain anoxic. Redox conditions will be determined by various reactions between dissolved and solid redox-active species in the alkaline environment of the near-field. It has been stated that the redox potential is largely determined by the anaerobic corrosion of steel (Kosakowski et al. 2014, Wersin et al. 2003). The latter process produces a thin magnetite film on the steel surface and the redox-active species are considered to be magnetite and dissolved Fe(II). Note, however, that other waste materials could have an effect on redox conditions. For example, the degradation of large amounts of organic matter could decrease the redox potential.

Temperature

For the ambient temperatures in the proposed Nördlich Lägern siting region for a repository at ca. 850 m depth below surface using a geothermal temperature gradient of 0.043 °C/m and assuming an average surface temperature of 10 °C, the calculated temperature is expected to be in the order of 47 °C. A temperature rise in the range of 5 to 10 °C is not expected to have a strong impact on the complex interplay between chemical and physical processes. Some processes will be accelerated, for example kinetically controlled mineral dissolution important for aggregate-cement reactions (cf. Fig. 3-14 in Section 3.3.5) or the degradation of organic compounds (Leupin et al. 2016b).

According to Nagra (2002a), Section 5.4.2, an ILW (only) repository will contain heat-emitting wastes, most prominently ILW containers with compacted hulls and ends. They state that, for the ILW tunnels, a temperature rise of ~ 5 – 10 °C above the ambient value was predicted over a period of several decades. The hydration heat from the backfill mortar will cause a temperature increase due to the hydration process of about 12 – 15 °C above the ambient, which will cause a short temperature pulse which ceases within few days to weeks (Martin et al. NAB 22-44 *in prep.*).

In Nagra (2021a), a preliminary assessment of the influence of a temperature pulse originating from the HLW/SF part of a combined repository on the L/ILW caverns is calculated. In general, a temperature rise of up to 5 – 8 ºC above ambient host rock temperature is observed within 1,000 years after repository closure.

For cement stability, temperatures for a longer time above 50 °C might cause some changes in cement phases, which might influence the porosity and mechanical properties of cement materials. At ~ 50 °C, destabilisation of monosulphate in favour of hydrogarnet was observed (Cloet et al. 2018). Malik et al. (2021) report in their review the reversible evaporation of physically bound water and contraction of the crystal lattice of the C-S-H gel for 60 – 90 °C. This causes porosity coarsening for cementitious materials, i.e. a change in pore size distribution towards larger pores, which results in increased permeability. Malik et al. (2021) note indications of complete reversibility of dehydration reactions in terms of phase composition and stoichiometry, but *"however, a major drawback or rehydration is the development of progressive cracks, which is an irreversible phenomenon".* Similarly, the gradual destabilisation of ettringite due to water loss is reported for temperatures > ~ 50 °C. Baquerizo et al. (2016) studied the stability of ettringite with respect to water activity (relative humidity) and temperature. In ambient conditions, ettringite at low RH between 3 – 62% will transform to metaettringite, which can be thermodynamically modelled as monosulphoaluminate and anhydrite (Baquerizo et al. 2016). In "dry conditions" below 3% RH, ettringite will decompose to katoite and anhydrite. The transformation from ettringite to metaettringite is assumed to be reversible, while the latter reaction is irreversible. With increasing temperature, the zones of decomposition will shift towards higher relative humidity, e.g. at 80 °C monosulphoaluminate and anhydrite will be formed at RH 20 – 80% and katoite and anhydrite at RH < 20%.

Radiolysis

Possible effects of radiation-related processes are summarised in Nagra (2002a), Section 5.4.1, and mentioned in Leupin et al. (2016b). The effects of radiation-related processes are assumed to be negligible. Locally oxidising conditions might occur for ILW waste types with a very high α-activity (compacted fuel hulls and ends) once water enters the waste packages, since H_2O_2 will be produced by α-radiolysis (Nagra 2002a, Papafotiou & Senger 2014). Furthermore, radiolysis of water might contribute to hydrogen production, or contribute to degradation of organic materials via a radiolytic pathway (Section 3.4.1).

Rock mechanics

Cementitious materials are subject to mechanical damage caused by chemical reactions, temperature changes or moisture transport. *The induced chemical and physical alterations to the microstructure translate into internal stresses and can lead to the formation of cracks* (Langton & Kosson 2009). Specifically, aggregate-cement reactions (Section 3.3.5) might cause (local) damage to cement materials that contain reactive aggregates. The diffusion of sulphate and other solutes from Opalinus Clay (Section 3.3.2) could trigger potentially expansive reactions, e.g. delayed ettringite formation, at the cement/Opalinus Clay interface (Kosakowski & Berner 2013).

Mechanical processes such as tunnel convergence may also lead to cracking of the concrete elements of the tunnel support and might also change the pore space and the associated transport parameters (see Section 5.4.3 in Nagra 2002a and Leupin et al. 2016b). It was found that deformation of cement materials under pressure (creep) is related to a dissolution-precipitation mechanism, active at nanoscale grain contacts of C-S-H (see e.g. Pignatelli et al. 2016). This so-called "pressure solution" is well known in geology (see e.g. Renard et al. 2000) and has been observed specifically in sedimentary basins for sandstones and limestones.

Tunnel convergence is expected to induce (micro-) cracks at surfaces and interfaces and would override any effects of pore clogging due to mineral precipitation. This would enhance the transport of solutes, if the interface is fully liquid-saturated, or gases, if the interface is partially liquid-saturated. Mineral precipitation might re-close the (micro-) cracks (pathways) again, only if cracks are fully water-saturated (Prasianakis et al. 2022).

Transport and hydraulics

In terms of transport, the water saturation state, the flux of water and the transport of solutes across material interfaces will strongly influence the extent and timescale on which chemical processes occur. Water fluxes are low (Martin et al. 2023, Papafotiou & Senger 2016). Therefore, it can be expected that advective transport in the liquid phase will be small and transport of solutes will be dominated by diffusion.

Initially, the residual water in emplacement caverns and the host rock pore-waters will not be in equilibrium. In terms of solute concentrations, the compartments will proceed towards equilibrium predominantly by diffusive transport across the concrete – host rock interfaces. The water saturation state of the repository, and possible porosity reduction at material interfaces, will slow down the equilibration process and may even prevent the complete equilibration between the emplacement cavern and host rock porewaters within 100,000 years (cf. Section 3.2.1).

Due to the very low permeability of argillaceous host rocks, solvent and solute transport are dominated by diffusion. The long timescale of the diffusive processes, which limit the rate of chemical changes, implies that such systems cannot be readily studied in laboratory experiments. Consequently, the information from relevant natural and industrial analogues and results from reactive transport calculations, in combination with simple mass balance calculations, are normally used to assess possible changes in the engineered and natural barriers on performance assessment-relevant timescales (Savage & Cloet 2018).

3.5.2 Influence of water saturation on mass transport and (bio)chemical reactions

The evolution the L/ILW repository in terms of water saturation according to latest knowledge (Diomidis et al. 2016, Leupin et al. 2016a, Martin et al. 2023, Papafotiou & Senger 2016) is summarised in Section 3.2.1. In summary, the partial saturation conditions are expected to hold for an extended time in most parts of the repository. This section will therefore give an overview of the possible influence of partially saturated conditions on other processes.

Overview/general description

During the operational and monitoring phase, all open sections of the repository cause a spreading zone of partial desaturation in the host rock. Once the open parts of the repository are backfilled, the adjacent host rock and the backfilled sections can start to saturate. Due to the very low permeability of the host rock and the gas production in the repository, saturation is expected to start after about 40,000 years (see Papafotiou & Senger 2016). Even after 100,000 years, large parts of the repository could still be partially saturated (Section 3.2.1).

As outlined in Section 3.5.2, the saturation state of materials and material interfaces has a strong influence on other processes. In the L/ILW near-field this includes transport in liquid and gas phases, and the availability and activity of water to drive (bio)chemical reactions that cause degradation of cement materials, porosity changes at cement/clay interfaces and gas generation (corrosion, microbially mediated degradation of organic matter). The competition between repository saturation and gas production in the repository was investigated by Papafotiou et al.

(2014, 2016). They concluded that, for bounding (high and low) gas generation rates, full water saturation everywhere in the repository was not reached within 100,000 years. These calculations did not include any coupling between gas generation and saturation state of the repository.

Information from modelling studies/experimental studies/natural analogues/observations in nature

The presence or absence of solvents influence the chemical reactivity, i.e. solvents can have an effect on solubility, stability and reaction rates. In chemical engineering, choosing the appropriate solvent allows for thermodynamic and kinetic control over chemical reactions (Yan & Dyson 2013). Most chemical reactions in a geological repository require the presence of liquid water as a solvent to break or create bonds between atoms. These reactions cannot proceed without presence of water.

The availability and thermodynamic properties of water in a porous medium depend on the pore size distribution and the saturation degree of the medium. Under partially saturated conditions, the smaller pores are more likely to be water-filled, due to the operation of capillary forces

- upon desaturation, the largest pores desaturate first, and
- upon (re-)saturation, smaller pores become water-filled first

Saturation occurs either by the migration of liquid water or by the condensation of water from the vapour phase. Capillary condensation is the *"process by which multilayer adsorption from the vapour into a porous medium proceeds to the point at which pore spaces become filled with condensed liquid from the vapor"* (Schramm 1994). The Kelvin equation relates the equilibrium vapour pressure of a fluid to the curvature of the fluid-vapour interface and predicts that vapour condensation will occur in pores or irregularities that are sufficiently small (Deinert & Parlange 2009). The ratio of equilibrium vapour pressure to saturation vapour pressure can be thought of as the relative humidity of a gas phase. The relative humidity of a gas phase is often used as a proxy to describe the change in chemical reactivity with the availability of water as a solvent. In such a concept, the chemical reactivity is a function of pore size distribution, of the fraction of pores that are completely or partially water filled and of the minimum water film thickness or pore size at which transport of reactants is still possible.

Generally, for reactions in porous media, the threshold relative humidity below which specific reactions are suppressed depends on the pore size distribution, which connects the (partial) water saturation of the medium with the relative humidity of the gas phase (Ahlström 2015). For example, it is well known that iron corrosion rates depend on relative humidity (Stefanoni et al. 2018). Corrosion stops almost completely as soon as the relative humidity is lower than a threshold value (Roberge 2019). In fact, threshold values might be different for different corrosion reactions (Roberge 2019). For example, corrosion of an iron surface exposed to the atmosphere was found to slow down strongly below a first threshold relative humidity of 55% and was reduced even more below a second threshold value of 20% (Watkinson & Lewis 2004). Stefanoni et al. (2018) link the portion of the steel area that is in contact with liquid-water-filled pores to the relative humidity and the saturation degree of the porous medium. At low relative humidity, large pores are gas-filled and only a few monolayers of adsorbed water are present on steel and pore surfaces (Gimmi & Churakov 2019). The electrochemical reactions are strongly limited in such thin films, because the transport of charged species involved in the anodic and cathodic processes responsible for steel corrosion is barely possible (Stefanoni et al. 2018). Conversely, in water-filled (capillary) pores, transport of charged species and electrochemical reactions are possible. Harrison et al. (2017) used microfluidics experiments in partially water-filled capillary pore networks to examine mineral dissolution-precipitations reactions. They found that the pore-scale distribution of gas-water mineral interfaces controls the rate and extent of reactions. The

effect of reduced "chemical reactivity" at low water saturation was included in the form of material-dependent empirical relations that couple relative humidity to chemical reactivity in reactive transport models and experimental studies (Bažant & Najjar 1972, Huang et al. 2021, Mercury & Tardy 2001, Seigneur et al. 2019, Suckling et al. 2011, Trotignon et al. 2011).

Warthmann et al. (2013) state that the availability of water in the cementitious near-field and specifically in waste packages are limiting factors for microbial activity. They further comment that water films at pore surfaces, which are formed if relative humidity is high, are difficult to exploit by microbes. In their review paper on biophysical processes that support diversity of microbial life in soil, Tecon & Or (2017) give more details on the impact of pore size and water-saturation-related parameters (water potential, relative humidity and water film thickness) on microbial activity. They state that, for slightly desaturated soil media, *"the thickness of aqueous films on most smooth mineral surfaces is in the range of 10 to 20 nm, too thin to support immersion of typical microbial cells (~ 0.5 to 2 μm) or flagellated motion"*. Furthermore, they state that, for rough surfaces, film thickness is about an order of magnitude thicker. Such film thicknesses will still not allow cell motion but will allow microbial activity as nutrient transport in such films is possible.

The importance of water films in partially saturated porous media, including the film thickness and the effect of pore size, pore solution chemistry and mineral type, was investigated by Nishiyama & Yokoyama (2013, 2021). They developed a model that allows the effects of water saturation on the dissolution of mineral grains to be predicted where water flows in films, which is typical for water infiltration processes (Nishiyama & Yokoyama 2013). They found that the reactive surface area for mineral dissolution is largely independent of the saturation state of the porous medium, since, in air-filled pores, the mineral grain surfaces are still covered by thin water films. They showed that the film thickness for silica increases with decreasing ionic strength and with increasing pore radius and pH (Nishiyama & Yokoyama 2021). Furthermore, they state that the water film is thick when the sign of surface charge of the mineral is the same as that at the air/water interface, which is the case, e.g., for quartz and montmorillonite at neutral pH.

The progress of chemical reactions is largely controlled by the availability and transport of reactants in the liquid phase. Solute transport is heavily influenced by the liquid saturation of materials. It is known that the advective and diffusive transport of solutes in a porous medium strongly decreases with decreasing water content (van Genuchten 1980, Martys 1999, Zhang et al. 2018), while gas transport is enhanced (Abbas et al. 1999).

Tyagi et al. (2013) and Gimmi & Churakov (2019) used numerical simulations on simulated clay(stone) structure maps to estimate the effective diffusion coefficient of solutes in samples as a function of porosity and liquid saturation degree, with and without consideration of surface water films. According to their results, the presence of gas in 10 – 20% of the pore space is sufficient to lead to a significant decrease in diffusivity, especially for anions. These results are supported by several experimental studies which found a strong decrease in ion diffusion coefficients in clay-cement media upon desaturation (Martys 1999, Olsson et al. 2018, Revil & Jougnot 2008, Savoye et al. 2017, 2018a).

In the case of gaseous reactants, the existence of a connected gas phase in partially saturated porous media might accelerate reaction rates, particularly if reactants can be transported in the gas phase. A prominent example is the atmospheric carbonation of cement materials. Carbonation fronts move faster at about 50 – 70% relative humidity than at higher relative humidity in most concrete materials (Russell et al. 2001, Šavija & Luković 2016, Winter 2009). At higher humidity, the CO_2 fluxes decrease as increasingly more pore space becomes water-filled and fast diffusion in gas-filled pores is replaced by slow diffusion in water-filled pores. In a recent study, Savoye et al. (2018b) compared diffusion of hydrogen and tritiated water in partially saturated cement. They found that HTO diffuses 4 orders of magnitude slower than hydrogen gas. Nevertheless,

desaturation has a stronger influence on diffusion of ions than on HTO diffusion, from which they conclude that HTO is partly transported in the gas phase (humidity transport) and partly in the liquid phase.

Timescales

At very low gas generation rates, the saturation of most parts of the repository is likely to occur within a period of a few thousand years (Papafotiou & Senger 2016). Taking into account gas production, complete saturation may occur over an even longer time frame, i.e. over a hundred thousand years (Papafotiou & Senger 2016).

Uncertainties

This high variability in the temporal evolution of saturation has a direct impact on the uncertainty in the geochemical evolution. Saturation directly affects the availability of water and solutes for chemical reactions. Diffusive and advective mass fluxes decrease strongly with decreasing saturation, therefore the geochemical processes driven by transport are delayed or even stopped as long as full repository saturation is not reached.

At material interfaces, where water saturations remain high (e.g. host rock – shotcrete), the geochemical evolution of the interfaces may be slowed significantly (Prasianakis et al. 2022), but will not stop completely.

3.5.3 Waste package evolution

General description

In Kosakowski et al. (2014), the chemical evolution of the L/ILW repository was assessed based on a generic concrete labelled as “concrete SGT Stage 2” that served to represent all cement-based materials in the repository in a simplified manner. Processes that were considered are cement degradation by the interaction with the host rock, carbonation of cement paste by the degradation of organics and the dissolution of aggregate materials used to make the generic concrete SGT Stage 2. Furthermore, for safety assessment calculations, assumptions are that all materials (waste, backfill, container, etc.) inside the cavern are evenly distributed (i.e. homogenised in accordance with a “mixing tank” approach).

More recently, work has been undertaken to quantify the temporal evolution of the geochemical conditions in waste packages based on mass balance calculations and geochemical modelling of the dominant chemical reactions of the waste materials (Kosakowski et al. 2020, Kosakowski & Wieland 2022, Wieland et al. 2018, 2020). The relevant chemical processes are quantified with the aim of predicting the temporal evolution of the chemical conditions of selected waste types.

The modelling obtains geochemical information (volume and chemical composition of gas phase, solution and mineral assemblage) for homogenised waste packages over the entire period of concern for the L/ILW repository (105 years). It should be noted that this type of mass balance calculation approach is still rather conservative. However, the results allow trends in the long-term behaviour of the various waste types to be identified and potential impacts on the engineered near-field barriers to be assessed, thus providing a tool for the evaluation of design options for the repository.

Information from modelling

The waste sorts included in the waste package modelling are operational (in German "Betriebsabfälle (BA)") and decommissioning ("Stilllegungsabfälle (SA)") waste mainly from the Paul Scherrer Institute and from the five nuclear power plants (NPP) in Switzerland. The inventories of all waste sorts were taken from the MIRAM 14 databases[5] (Nagra 2014a), which was the actual basis at the time the calculations were performed. Five operational and two decommissioning waste sorts were selected, for which the temporal evolution of the chemical conditions and composition of the matrix were modelled (detailed infos in Kosakowski et al. 2020 and Wieland et al. 2018).

Operational wastes in 200 L drums:

- The BA-G-HB waste sort (ion exchange resin bituminised in 200 L drum) mainly consists of polystyrene, which is the backbone of spent ion exchange resins, the bitumen confinement and steel. Polystyrene, bitumen and the very small amount of rubber present in this waste sort are expected to slowly degrade and the waste type is therefore expected to react slowly.
- The BA-G-KB waste sort (salt concentrate bituminised in 200 L drum) mainly consists of inorganic material (concentrated salts), the bitumen confinement and steel. Bitumen and the very small amount of rubber that are present in this waste sort are expected to degrade slowly. The concentrated salts present in the waste sort are considered to be chemically stable.
- The BA-B-HP waste sort (ion exchange resin cement-stabilised in 200 L drum) mainly contains spent ion exchange resins solidified in concrete. Each waste package contains a large amount of slowly degradable polystyrene, which is the backbone of ion exchange resins, and sand (i.e. quartz) as a concrete aggregate, a considerable amount of iron and steel, and very small amounts of readily degradable LMW organics and zinc.
- The composition of the BA-M-H waste sort (ion exchange resin cement-stabilised in 200 L drum) resembles that of the cement-stabilised waste sort BA-B-HP. It also contains mainly spent ion exchange resins solidified in concrete. Both waste sorts contain a large amount of slowly degradable polystyrene (backbone of ion exchange resins) which is, however, a factor of about two lower in this waste sort than in the BA-B-HP waste sort. The amount of sand (quartz) is much lower in this waste sort than in the BA-B-HP waste sort, while the amount of steel is about a factor of two lower than in the BA-B-HP waste sort. The amount of readily degradable LMW organics is a factor of six higher than in the BA-B-HP waste sort. The initial water content is much higher in this waste sort than in the BA-B-HP waste sort, which prolongs the time period of water availability.
- The waste sort BA-PH-PF (mixed solid waste cemented in 200 L drum) contains several metals, such as steel and zinc, as well as small amounts of aluminium and copper. The inventory of organics includes large amounts of cellulose, PVC, rubber, and small amounts of LMW organics, synthetic resins and ion exchange resins (polystyrene). Ceramics and glass are considered as non-reactive materials in this waste sort. A total of 63.73 kg cement and 20.84 kg Supplementary Cementitious Materials (SCM), i.e. silica fume, amorphous silica and clinoptilolite, were used to fabricate the solidifying concrete. The water content is relatively high. The large inventory of sand is a major silica source in the solidifying concrete. For this waste sort, several alternative recipes for the solidifying concrete were investigated.

[5] MIRAM 14 is based on waste sorts, where similar waste types have been grouped together to a waste sort. In the updated MIRAM-RBG database, the detail of the information is higher, as the database is based on waste types.

Decommissioning wastes in concrete containers:

- The SA-L-MX waste sort (decommissioning waste in concrete containers) contains several metallic materials, such as large amounts of steel and iron, moderate amounts of copper and brass, while the inventories of aluminium and zinc are much smaller. Furthermore, the inventories of the organic materials are small compared to the cemented operational waste sort, i.e. containing only readily degradable LMW organic compounds and PVC. Ceramics and glass are considered as non-reactive materials in these conditions. Large amounts of HTS cement, supplementary cementitious materials (SCM), i.e. silica fume and clinoptilolite, quartz sand and water, are part of this model waste sort to be used for fabricating the solidifying concrete. For this waste sort, several alternative recipes for the solidifying concrete were investigated.
- The SA-PW-MX waste sort (decommissioning waste in concrete containers) consists only of large amounts of steel and some iron conditioned in a cementitious material. The amount of LMW organic materials is small. Large amounts of OPC and HTS cement along with SCM, i.e. silica fume and clinoptilolite, aggregate and water, are part of the solidifying concrete according to MIRAM 14.

These waste sorts were selected as they contribute significantly to the total mass (SA-PW-MX), to the total activity (SA-PW-MX), or to the total volume (SA-L-MX) of the L/ILW, or because they contain large quantities of organics (BA-M-H; BA-G-HB) or metals (SA-L-MX). Other waste sorts contain mixed inventories of steel, organics, salts and other materials (BA-PH-PF, BA-G-KB).

Detailed inventories, thermodynamic model setup, kinetic control of metal corrosion, organic matter degradation and dissolution of concrete aggregates, as well as investigated scenarios (limited or unlimited water availability, reactivity of aggregates, recipes for cement infill) are described elsewhere (Kosakowski et al. 2020, Kosakowski & Wieland 2022, Wieland et al. 2018, 2020).

The following processes were considered to affect the long-term degradation of the waste types:

1. (bio)chemical degradation of organic waste materials into CH_4 and CO_2
2. interaction of CO_2 (and it bases) with hydrated cement
3. (pH-dependent) corrosion of the metallic waste materials, and
4. internal degradation of cementitious materials due to interaction of highly alkaline cement porewater with siliceous aggregates

Wieland et al. (2018) and Kosakowski et al. (2020) conclude that:

- The geochemical modelling shows that the reactivity of all waste sorts, except waste sort BA-M-H containing spent ion exchange resins, comes to a halt after a few hundred up to a few thousand years at the latest once the amount of free water in the waste type is consumed. The reactions considered all consume water, except the carbonation of cement that frees up water. Thus, the availability of water is an important parameter controlling the temporal evolution of the waste sorts. The reactions in waste sort BA-M-H are not limited by availability of water due to its initially very high water content and the additional release of water by carbonation of cement.
- The water-consuming reactions further progress if continuous water supply into the waste packages is assumed, for example due to the flux of water via a gas phase through openings in the waste packages. Overall, the availability of water is expected to determine the reactivity of the waste with time.

- Iron/steel corrosion is slow at pH ≥ 10.5, while corrosion strongly increases when the pH drops below 10.5, with a factor of 100 higher corrosion rate considered in near-neutral conditions according to the applied model assumptions. The consequences of the significantly enhanced rate below pH 10.5 are remarkable: once pH drops below 10.5 the inventory of iron/steel in the waste sorts completely corrodes within a short time period, i.e. a few thousand years, compared to 100,000 years. It should be noted that Nagra has revised the corrosion rates (Diomidis et al. 2023).
- The degradation of organic materials produces CO_2, which converts cement phases (e.g. portlandite, C-S-H phases) into calcite (Section 3.4.3). This reaction continuously degrades the cementitious materials used to condition the wastes and accounts for the pH drop below 10.5 in the cemented operational waste sorts.
- For operational waste sorts, the amount of CO_2 produced by degradation of organic matter can exceed the amount of CO_2 consumed by full carbonation of cement phases in the waste drum.
- Tab. 3-6 shows the amount of surrounding cement materials that can be carbonated by CO_2 released from one 200 L waste drum of BA-PH-PF (cement-mixed solid waste in 200 L drum). Depending on the volumetric amount of cement phases in the cement-based materials, between 0.5 up to 1.5 times the waste package volume can be carbonated under the assumption that complete degradation of the organic materials occurs.
- The degradation of the cementitious materials by carbonation is negligible in the cemented decommissioning waste sorts where the inventory of organic compounds is very low. Instead, the type of aggregates used for fabrication of the solidifying mortar is decisive. Models that consider reactive siliceous aggregate (quartz sand) calculate a drop in pH below 10.5 and predict accelerated iron/steel corrosion. This coincides with the production of a large H_2 volume within a short time period compared to the period of concern for the L/ILW repository.
- The type of aggregates has only a minor effect on the temporal evolution of the chemical conditions of the operational waste sorts. In these waste types, the calculated temporal evolution of the chemical conditions is mainly determined by the degradation of the organic materials and subsequent carbonation of the Ca- and Mg-containing cement phases and by conversion of magnetite (the main corrosion product) into siderite if the P_{CO2} is very high. Replacing siliceous aggregates by calcareous aggregates for fabrication of the solidifying mortar only extends the time period in these waste types before pH drops below 10.5 and accelerated iron/steel corrosion starts.
- The partitioning of the alkali ions (Na^+, K^+) between the aqueous phase and alkali-bearing mineral phases (i.e. C-S-H phases) has a distinct effect on the temporal evolution of pH. For example, allowing zeolite formation in the thermodynamic models, which are important host phases for the alkali uptake, results in a significant shift of the point in time where pH decreases below 10.5. The latter pH value is the critical threshold value concerning iron/steel corrosion. The decrease in pH occurs significantly earlier in the presence of zeolites. Therefore, the model implemented for alkali equilibria with potential host phases plays a crucial role in the geochemical modelling of the waste types. It should be noted that kinetic hindrance often prevents or delays the formation of zeolites in experiments (Chen et al. 2021).

- The degradation of PVC produces Cl^-, which is a non-reactive species in the current setup of the geochemical system. Chloride is not taken up by any phase and therefore accumulates in the aqueous phase with time. Degradation of PVC leads to increasing Cl concentrations and, according to electro-neutrality of the solution, reduces the OH^- concentration in solution. This promotes the pH drop below the critical threshold of 10.5 to be shifted to an earlier point in time.
- The temporal evolution of the H_2 production in the geochemical models of Wieland et al. (2018) is strongly linked to the temporal evolution of the chemical conditions in the individual waste sorts as the corrosion of iron and steel is pH-dependent. The total amounts of H_2 produced over the period of concern for the L/ILW repository that are mimicked with the geochemical model and the gas formation tool ("Gasbildungstool", GBT) (Diomidis et al. 2016), however, agree very well because, in both modelling approaches, H_2 is a non-reactive chemical species.
- The differences in the production of CO_2(g) between the geochemical model and the GBT are related to the reactivity of CO_2 in the geochemical model. In the geochemical models, the CO_2 reacts immediately with cement and, only after carbonation of cement is complete, the existence of CO_2(g) is calculated.
- In most waste sorts, the porosity within the waste packages increases, except in the case of the decommissioning waste, where the total volume of all solid phases increases due to formation of iron corrosion products. Volume changes of solid phases with time are different for each waste sort and depend on the iron/steel inventory, as well as on the ratio between the inventories of organic materials and iron/steel. For all waste sorts, except for decommissioning waste with high iron/steel inventory, porosity changes do not have a strong impact on gas storage capacity.
- For decommissioning waste, the total volume of all solid phases considered in this study increases with time by ~ 35 vol%. The increase in the total volume is caused by the corrosion of large amounts of iron/steel in the decommissioning waste and the subsequent formation of corrosion products with lower density (magnetite, siderite). The total volume of all solid phases after complete corrosion of iron/steel inventory is larger than the waste package volume itself. This would drastically increase internal stresses in the container and the surroundings of the waste package. Due to limitations in available space, it seems doubtful that the reaction will proceed in the modelled way until all steel is reacted.

Tab. 3-6: Amount of gaseous CO_2 released for waste sort BA-PH-PF per 200 L waste drum (after all cement in the drum is carbonated) and potential volumes of other cement materials that can be degraded with this amount

The mole amounts of CO_2 needed to completely degrade 1 m^3 of a specific cement material were extracted from the degradation calculations for cement materials described in Kosakowski et al. (2020).

	CEM II/B-T based container infill material	**Container wall concrete**	**Mortar M1**	**Model concrete SGT-E2**
Amount (mol) of CO_2 needed to completely degrade 1 m^3 cement material	8,000	4,500	2,600	3,500
Volume (m^3) of cement material degraded from CO_2 released by one waste drum in 100k years (780.1 mol)	0.10	0.17	0.30	0.22

Temporal behaviour

The temporal evolution of waste packages depends on several interlinked processes that are connected via the availability and consumption/release of water and the porewater pH. In terms of design options, the type of backfill/infill material (bitumen vs. cement), the recipe for cement-based infill, and specifically the use of (slowly) reacting siliceous aggregates in cement infill materials influence the rate of porewater pH evolution. At pH values below 10.5 it is assumed that steel/iron corrosion will be strongly accelerated (Sections 3.4.3 and 3.4.4). Fig. 3-22 shows pore-water pH with time for cemented operational and decommissioning waste packages as calculated by Wieland et al. (2018) for a scenario with unlimited availability of water (pore space is fully saturated). In this case, porewater pH acts as an indicator for the degradation of cement materials. The degradation kinetics differs significantly between the waste types. The evolution of waste packages starts once enough water is available to run the reactions. This model implies that external water can freely enter the waste package, i.e. the steel walls of 200 L waste drums are corroded and container walls are not an impermeable barrier.

One way to increase the stability of waste packages is to suppress the internal degradation of cement materials, i.e. the reaction between cement phases and aggregates (cf. Section 3.3.5).

Fig. 3-23 visualises the link between the temporal change in pH of the pore solution (left figure) and the mole amount of hydrogen gas produced by metal corrosion (right figure) for a decommissioning waste type (SA-L-MX). The models assume that the waste packages are saturated with water all the time. More realistic de- or partially saturated conditions are expected to delay the reactions. The reference composition corresponds to the recipe from MIRAM 14 described in Wieland et al. (2018); it uses a CEM I cement blended with silica fume, which is a pozzolanic material, clinoptilolite as a sorbing agent to prevent possible release of radionuclides during interim storage, and quartz sand as an aggregate which is assumed to react with time in the models. The addition of highly reactive silica fume causes portlandite to dissolve during hydration of cement or shortly thereafter. Furthermore, the degradation of the relatively small inventory of rapidly degrading organic substances lowers the pH further within a few hundred years

(carbonation due to CO_2 produced by degradation of organic matter). The slow dissolution of clinoptilolite only affects the pH on the long term. The dominant process that controls the pH for the cement recipe is the dissolution of quartz sand grains that is expected to cause the pH to drop below 12 within a few hundred years and below 10.5 within a few thousand years for the assumed aggregate degradation rates (left Fig. 3-23). We compare the reference model (CEM I + quartz aggregates) with a CEM I cement with carbonate aggregates and one realisation where, in addition to carbonate aggregates, also the clinoptilolite is removed from the recipe. For the carbonate aggregates, the pH drops below 12 within 10,000 years due to the carbonation by organic matter and a bit faster if clinoptilolite dissolution is considered. Finally, a CEM II/B-T based cement without addition of silica fume, clinoptilolite or aggregates is shown. This material shows no internal degradation and provides a long-term stable pH.

The iron corrosion model follows Diomidis et al. (2016) and is parameterised such that corrosion rates above pH 10.5 are low and increase a hundredfold as soon as the pH drops below 10.5. All modelled scenarios that use this corrosion parameterisation therefore show the same gas release until pH drops below 10.5. The exact drop in corrosion rates between pH 12 and 10.5 is not yet well constrained due to a lack of experimental data. We show scenarios with alternative pH dependence of steel corrosion, where the corrosion rates change linearly (V1) or non-linearly (V2) from the low rate (above pH 12) to the high rate below pH 10.5. Note that as soon as hydrogen is no longer produced, the metal inventory is completely corroded. The fast hydrogen production in the first three years is related to the corrosion of minor amounts of aluminium and zinc, which are modelled with a fast constant corrosion rate following Wieland et al. (2018).

Independent of the corrosion model, the CEM II/B-T based backfill without addition of silica fume or reactive aggregates provides a high-pH environment and keeps steel corrosion constantly low (right Fig. 3-23). For all other material variants, the pH evolution and the choice of steel corrosion model is reflected in the temporal evolution of the hydrogen production. The results in Fig. 3-23 demonstrate that gas generation in the waste packages is sensitive to the composition and degradation of backfill materials and to (the parameterisation of) steel corrosion rates at alkaline pH values.

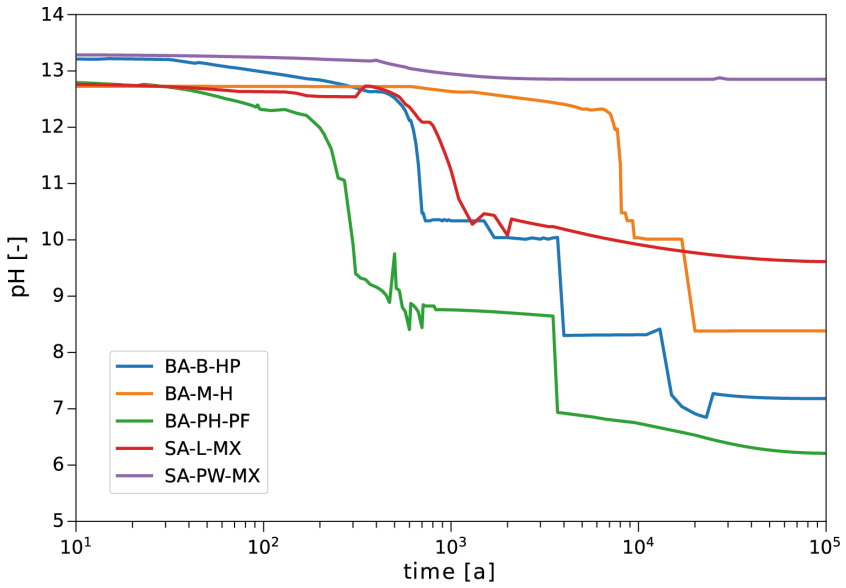

Fig. 3-22: Comparison of pH evolution with time for different waste types, considering unlimited availability of water and zeolite formation

Modelling results from Wieland et al. (2018)

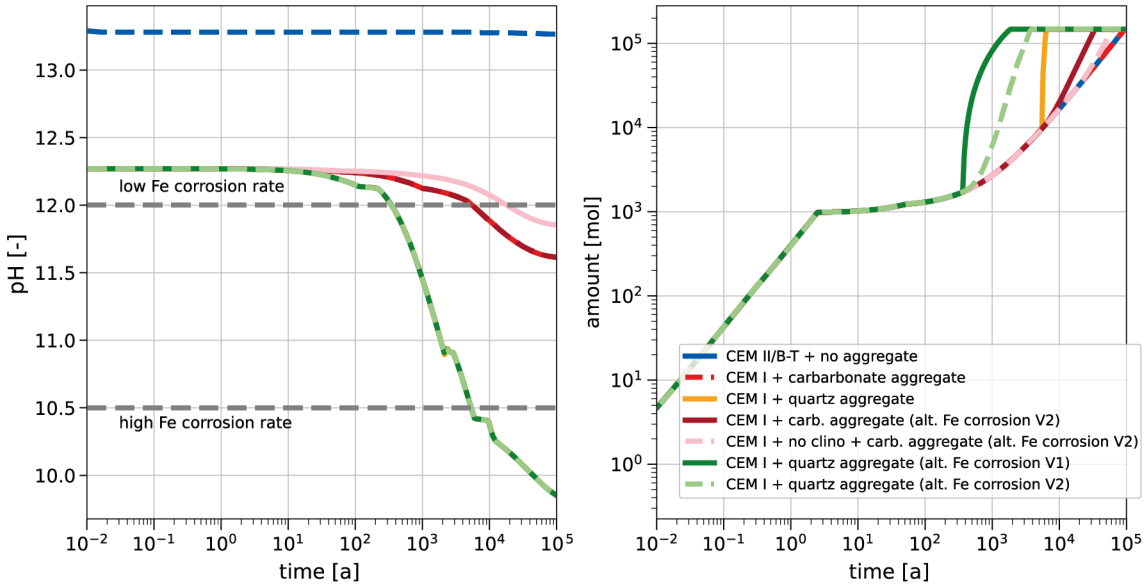

Fig. 3-23: pH evolution of the pore solution in an SA-L-MX container with time for different modelled scenarios (left) and cumulative hydrogen gas released by metal corrosion (right)

Scenarios differ in terms of cementitious infill and the rate laws used for iron corrosion. sf: silica fume, clino: clinoptilolite (Kosakowski & Wieland 2022).

Uncertainties

The prediction of evolution of waste packages with mixing tank models is associated with several sources of uncertainties. They can be grouped into two categories; uncertainties related to the waste package itself and uncertainties related to waste package interaction with the near-field.

Uncertainties related to the waste package itself are:

- The intrinsic heterogeneity of the waste package may not be properly represented in a mixing tank approach.
- For example, waste type BA-P-HB contains smaller 100 L drums with waste cemented in a 200 L drum. In this case, the inner drum needs to be corroded before any water can reach the waste and organic waste degradation can start.
- Even more complicated is the structure of BA-PH-PF which is composed of compacted smaller steel waste cans (pucks) with mixed waste pressed into (open) steel or concrete pipes that are cemented into a 200 L drum. For this waste type, it is not clear how the integrity of the steel walls of the waste cans is affected by compaction. In addition, liquid water, gas and humidity transport in the waste package are hindered by the pipe. For such a waste package, Huang et al. (2021) investigated the influence of internal geometry on gas production (steel pipe filled with waste and only in contact with high-pH cement backfill at top and bottom). They assumed that the pucks can be treated as a homogeneous medium, i.e. the integrity of the steel cans is completely destroyed during compaction. They found that the combined effect of high corrosion rates in the pipe, where pH is low, and the limitation of water and humidity transport in the drum causes partial drying in the drum. Gas production rates are then controlled by the water/humidity fluxes from cement backfill (or open top of the drum) to the waste compartment (inside the steel pipe). Gas production rates for the modelled scenario were much smaller than those calculated with a mixing tank approach (Fig. 3-24).
- The initial water content of waste packages after up to decades of interim storage under conditions with controlled conditions with “low” humidity of maybe 60% is not known. It can be assumed that waste packages dry out under these conditions, but how quickly this can be achieved for 200 L drums is unknown.
- The mixing tank modelling approach, used for example in Wieland et al. (2018), assumes that all water in the aqueous phase of the thermodynamic model is available to drive the reactions. In real cements, a large part of the water is bound in the nanopores (gel porosity) or C-S-H interlayers. This water is only partly available for some reactions and may be not available at all for others. It is difficult to “remove” this water fraction from the nanopores, therefore Huang et al. (2021) assigned a residual water saturation for different types of materials in relation to relative humidity and liquid saturation to obtain a more realistic description of water available for chemical reactions. This allows cessation of a reaction when relative humidity of the gas phase falls below reaction-specific thresholds.
- Chemical reactions that control the evolution of waste packages, specifically reactions that control gas generation rates for metal corrosion and for degradation of organic matter, need to take into account local conditions in the waste package. This includes the availability of water, porewater composition, pH, and availability of other nutrients for microbiologically mediated reactions. Averaged gas generation rates might significantly over- or underestimate reaction rates.

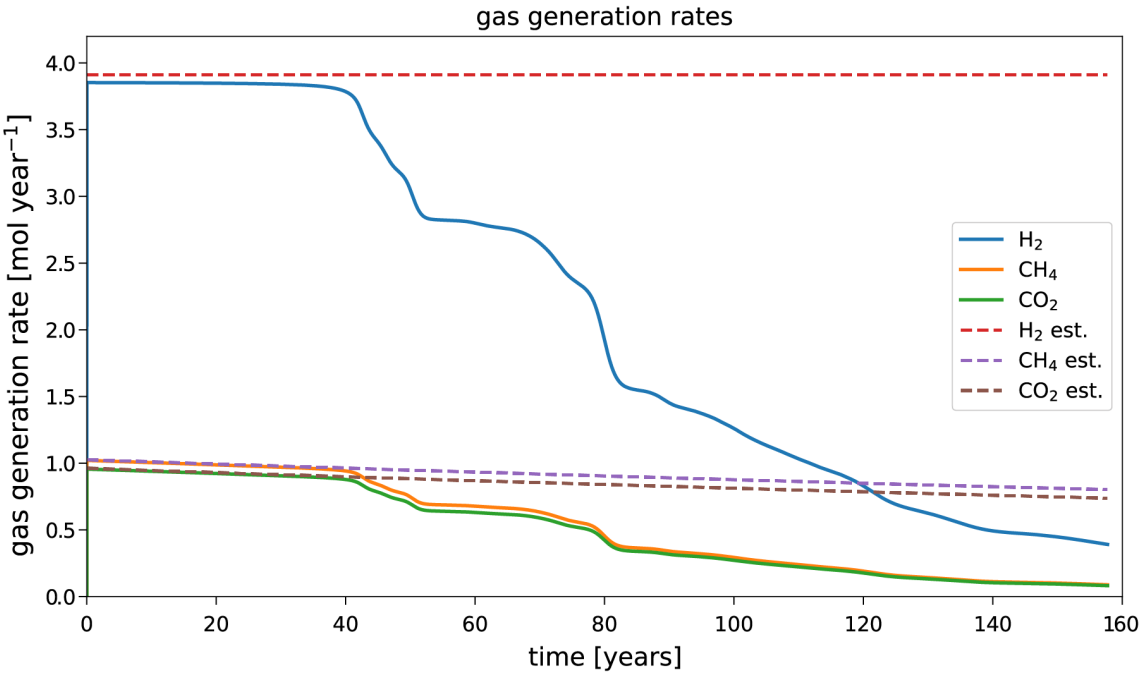

Fig. 3-24: Comparison between gas generation (corrosion of steel and degradation of organic matter) in a simplified waste package similar to waste type BA-PH-PF calculated with a mixing tank model (dashed lines) and a multi-component two-phase reactive transport model (solid lines)

Huang et al. (2021)

The boundary conditions have a strong influence on the state of the system:

- Conditions of infill materials in terms of humidity and external water composition are critical for the corrosion rate at external steel surfaces of waste packages (such as 200 L drums). Without knowledge of external conditions, predictions of integrity of steel walls are highly uncertain.
- Similarly, the influx of external water into waste packages depends largely on the overall evolution of water and gas saturation in the near-field of the repository, while gas generated in waste packages largely controls the gas pressure in the repository. Repository- and waste-package scale models that contain a feedback loop between local availability and consumption of water in waste packages and water transport on the repository scale are needed to reduce uncertainties related to gas generation rates in waste packages.

In summary, the gas generation rates calculated with the mixing tank approach are conservative, i.e. the models exclude processes that suppress or delay onset of gas generation, most significantly the effect of partial saturation of materials and lack of water to drive reactions. The homogenisation of the internal structure of waste packages might be conservative if internal barriers that prevent water and gas transport are ignored, but then separation of waste and cement might also favour the existence of locally favourable conditions for microbial life or cause enhanced corrosion of metals.

3.5.4 Evolution of cement materials in the near-field

This section essentially contains the conclusions of Chapter 5 of Kosakowski et al. (2020) and Wieland & Kosakowski (2020) on the degradation of different cement materials in the repository near-field.

Overview/general description

A specific characteristic of an L/ILW repository is the use of different cement-based barrier materials for tunnel support, as backfill material, as waste disposal container material, for filling the containers and for waste conditioning. Depending on their functions, these materials might be based on very different recipes, with different cement contents and aggregates. Also, their mechanical and transport properties may vary considerably. It should be noted that, at this stage of the project, cement formulations presented here are generic for most cases. Previous calculations of gas and water transport in single emplacement caverns have already taken into account the complex spatial distribution of materials with different transport properties (Senger & Ewing 2009).

In the previous study (Kosakowski et al. 2014), the chemical evolution of the L/ILW near-field was described. One element of the description was the definition of a model concrete for SGT Stage 2 ("Stage 2 concrete") that represents, in a generic and simplified way, all cement-based materials in the near-field. This concrete was based on a cement currently used for waste conditioning. As a simplified assumption, porosity was equal to the average porosity of the disposal tunnel and it contained siliceous aggregates similar to a backfill mortar. Using this generic concrete, it was possible to describe degradation of cement materials by various external (cement/clay interaction, ingress of water, carbonation) and internal processes (aggregate-cement reaction).

Kosakowski et al. (2020) and Wieland & Kosakowski (2020) investigated how well this generic "SGT Stage 2 concrete" represents different possible cement materials present in an emplacement cavern. The properties and degradation of this concrete by carbonation and aggregate-cement reactions was compared with three typical cement-based materials:

- a mortar M1 that is a provisional material for backfilling large void volumes in emplacement caverns
- a provisional container infill mortar, which is a hydraulic binder based on CEM II/B-T cement that could be used for backfilling small void spaces in waste containers and for conditioning of decommissioning waste
- a container concrete which could be used for disposal container construction and might act as a "generic functional concrete" for all types of infrastructural elements and concrete for the inner-shell tunnel support

A possible distribution of the three materials in an L/ILW emplacement cavern is visualised in Fig. 3-25.

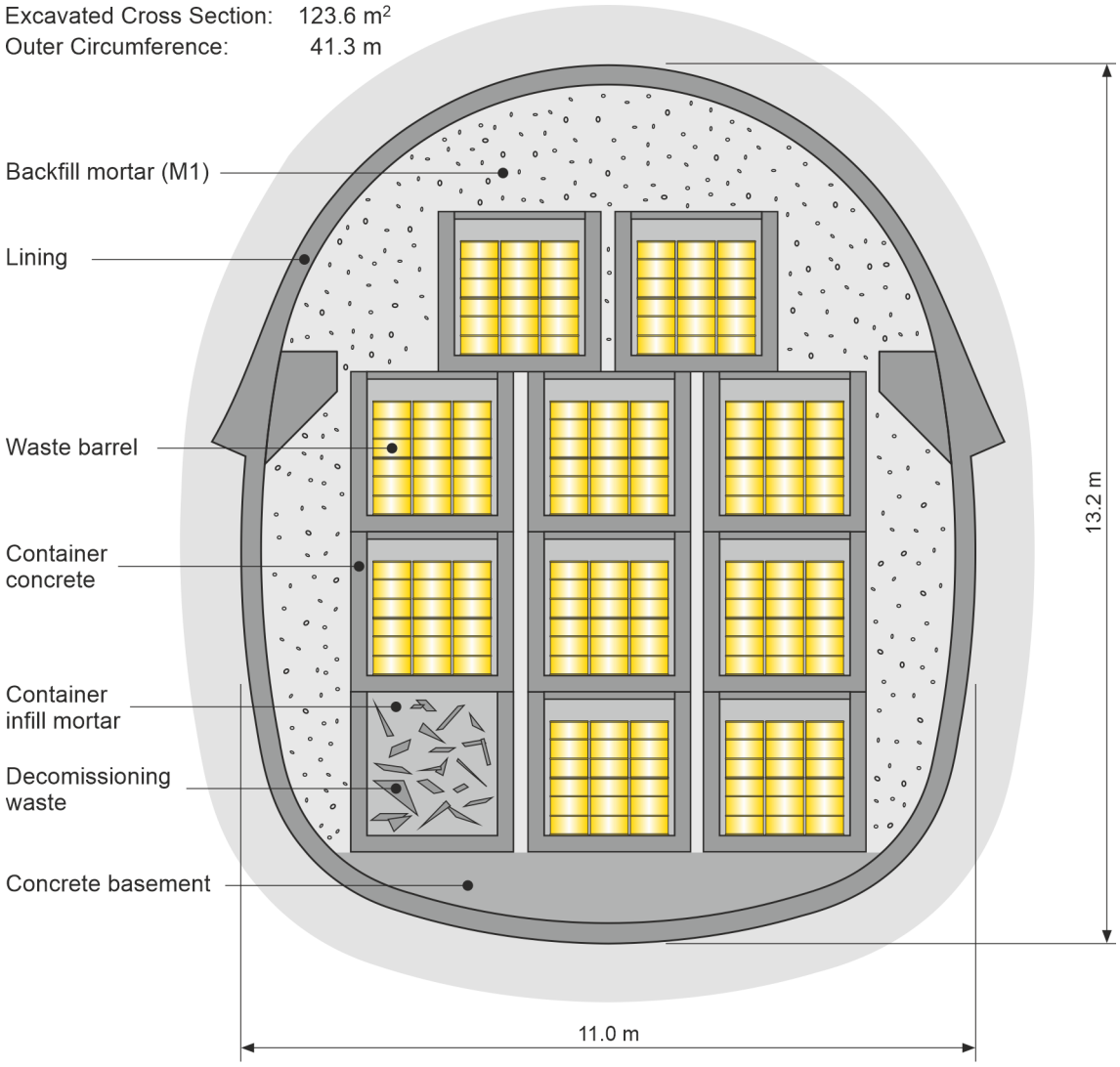

Fig. 3-25: Cross-section of a possible L/ILW emplacement cavern
Kosakowski et al. (2020)

Information from model/experimental studies/natural analogues/observations in nature

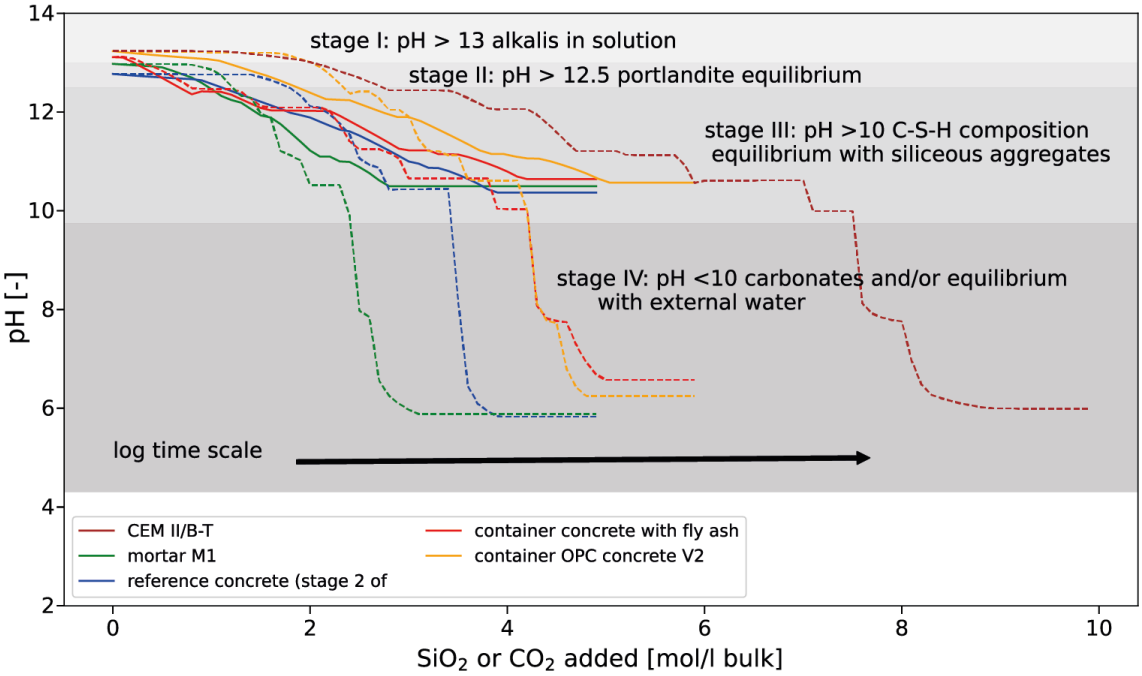

Fig. 3-26: Degradation of cement-based materials due to aggregate-cement reaction (solid lines, SiO_2 addition) and carbonation (dashed lines, CO_2 addition) at 41 °C based on data from Kosakowski et al. (2020)

Note that the time for degradation is highly variable for each material and depends on internal and external factors, including the type of aggregate minerals, aggregate size distribution, temperature and CO_2 production and transport in the near-field.

Fig. 3-26 summarises the degradation of the cement materials in terms of aggregate-cement reactions by adding SiO_2 (Section 3.3.5) and the effect of carbonation by adding CO_2 (Section 3.4.3). For these calculations, it is assumed that water and CO_2 are sufficiently available and that the whole surface of the aggregate is in full contact with alkaline pore solution and is dissolved homogeneously.

Based on thermodynamic batch calculations, Kosakowski et al. (2020) state that the degradation of all cement components follows the general evolution as described in detail in Section 3.3.1. The main difference between the cementitious materials in Fig. 3-26 is the amount of CO_2 and SiO_2 needed to reach a specific degradation state. In general, the resistance to degradation is directly related to the amount of cement per unit volume in each material.

For carbonation, the container-filling mortar contains the highest amount of cement per unit volume and, therefore, the carbonation resistance is the highest. The mortar M1 has the lowest volumetric content of cement and its carbonation resistance is therefore the lowest.

In connection with aggregate-cement reactions, not only the amount of aggregates and their reactivity is important, but also the aggregate grain size distribution and the surface area available for reaction (see Fig. 3-14). The container-filling mortar, which does not contain siliceous aggregate, is not subject to aggregate-cement interaction. The backfill mortar M1 contains “monocorn” aggregate that gives rise to complete degradation of concrete in about 1,000 years. It should be noted that, for the mortar M1, calcareous aggregates are considered as a possible

alternative to siliceous aggregates, which would suppress the internal degradation due to aggregate dissolution (Martin et al. NAB 22-44 *in prep.*). The container concrete contains more cement per volume and a mix of silica and carbonate aggregate with a broad distribution of grain sizes. Although the very small siliceous aggregate grains react fast and quickly cause partial degradation of the cementitious material, the final degradation stage is reached only after about 30,000 years as the larger grains react very slowly. Fig. 3-14 in Section 3.3.5 demonstrates this by comparing the calculated amount of silica released due to dissolution of siliceous aggregate with time (upper part) and the associated drop in pH (lower figure) which slows down aggregate dissolution rates. The vertical lines in the upper part of Fig. 3-14 indicate that, if aggregates are in thermodynamic equilibrium with pore solution (dissolved silica), aggregate dissolution stops.

Note that carbonated cementitious materials are not subject to additional aggregate-cement reactions, as cement phases have already been converted into carbonates. For materials degraded by aggregate-cement reactions, carbonation "resistance" is the same, i.e. the same amount of CO_2 will be consumed for complete carbonation, as the total amount of Ca bound in the cement phases does not change if portlandite is transformed into C-S-H during reaction with dissolved silica.

Spatial and temporal heterogeneity

Thermodynamic calculations do not provide transport or mechanical properties, or even changes in such properties, upon material degradation. The container-filling mortar and the provisional mortar M1 are formulated such that they are highly porous and have a very high permeability, while the container concrete, which is a functional concrete as used also for concrete structures, has a comparatively low permeability. When considering the spatial distribution of materials as shown in Fig. 3-25, the near-field can be characterised by strong porosity, permeability and diffusivity contrasts that should give rise to preferred transport pathways for water and gases. One could speculate that carbonation of materials might occur locally in specific transport pathways of low-permeability materials and more widespread in high-permeability materials. The spatial heterogeneity in material parameters, however, is superimposed by differences in the temporal evolution of the materials affected by aggregate-cement reactions (Fig. 3-14). The strong spatial heterogeneity might cause very different geochemical conditions to exist in close proximity in the near-field.

Influence of temperature and pressure

Temperature has a large effect on the kinetics of mineral dissolution and precipitation reactions, as well as on the stability of mineral phases. Compared to the HLW/SF repository, the temperature increase above the geological formation temperature is small for the L/ILW repository. As stated in Section 3.4.1, the temperature increase in an L/ILW repository due to hydration heat from cement materials and heat-emitting waste forms with short-lived radionuclides might cause a small temperature increase for a few hundreds of years in some parts of the repository (Leupin et al. 2016b). As soon as the temperature exceeds 50 °C, some small shifts in cement composition are predicted compared to a system at 25 °C. Nevertheless, no major changes occur in terms of portlandite or C-S-H composition.

The elevated temperature in a repository accelerates the temporal evolution of concrete degradation affected by aggregate-cement reactions (Fig. 3-14). In general, the mineral dissolution rates strongly increase with temperature (Palandri & Kharaka 2004). Notably, the kinetic rate for quartz dissolution (aggregates) is increased by a factor ~ 5 at 42 °C as compared to 30 °C.

The dependence of kinetic and thermodynamic properties on absolute (gas/fluid) pressure is weak compared to their temperature dependence. Therefore, the impact of absolute pressures expected in a repository on, e.g., mineral solubility or reaction rates is minor and can be disregarded for cement degradation processes. The influence of external or internal stress on the chemical evolution of materials might be not negligible; therefore, chemo-mechanical processes are briefly summarised in Section 3.5.1.

Uncertainties

The calculations described in Kosakowski et al. (2020) and summarised in this section do not consider several processes that might influence the evolution of cement materials in time (and space).

- All calculations assume fully water-saturated materials and do not consider the influence of a desaturated near-field (cf. Section 3.5.2). Strong desaturation of the pores will for example delay or prevent aggregate-cement reactions.
- The progress of aggregate-cement reactions will depend not only on a kinetic rate, but also on "reactive surface area". The "reactive surface area" often acts as a kind of "fudge factor" and may include for example pore scale transport processes that limit reaction rates. The calculations assume that the reactive surface area is identical to the surface of spherical grains of a given diameter. Comparison of kinetic rates measured in laboratory and field experiments show that rates measured in dense materials in the field are orders of magnitude lower than rates measured in the lab at a high liquid to solid ratio. This indicates that, in dense materials, not the complete surface area of minerals is affected, or that other processes affect the dissolution of aggregates.
- The calculations summarised in this section do not consider degradation by ingress of formation water or diffusion from the host rock. These scenarios are described in Section 3.3.2. Such processes have consequences for cement porewaters, specifically in terms of alkali and chloride concentrations. The influence of adjusted alkali and chloride concentrations on cement/concrete degradation is small but might be important for radionuclide sorption (Wieland & Kosakowski 2020). Therefore, it is not possible to simply take porewaters without considering such processes as a base case for radionuclide sorption or solubility calculations. The derivation of such cement porewaters for use with safety assessment-derived sorption databases and solubility calculations is described in App. A.

4 References

Abbas, A., Carcasses, M. & Ollivier, J.-P. (1999): Gas permeability of concrete in relation to its degree of saturation. Materials and Structures, 32/1, 3-8. https://doi.org/10.1007/BF02480405

Adam, N., Hinz, K., Gaona, X., Panak, P. J. & Altmaier, M. (2021): Impact of selected cement additives and model compounds on the solubility of Nd(III), Th(IV) and U(VI): screening experiments in alkaline NaCl, $MgCl_2$ and $CaCl_2$ solutions at elevated ionic strength. Radiochimica Acta, 109/6, 431-443. https://doi.org/10.1515/ract-2021-1010

Adler, M. (2001): Interaction of clay stone and hyperalkaline solutions at 30 °C: a combined experimental and modeling study. Doctoral Thesis. University of Bern, Bern, Switzerland.

Ahlström, J. (2015): Corrosion of steel in concrete at various moisture and chloride levels. Energiforsk AB. Report 2015:133.

Ahusborde, E., Amaziane, B., Baksay, A., Bátor, G., Becker, D., Bednár, A., Béreš, M., Blaheta, R., Böhti, Z., Bracke, G., Brazda, L., Brendler, V., Brenner, k., Březina, J., Cancès, C., Chainais-Hillairet, C., Chave, F., Claret, F., Domesová, S., Havlova, V., Hokr, M., Horák, D., Jacques, D., Jankovsky, F., Kazymyrenko, C., Kolditz, O., Koudelka, T., Kovács, T., Krejci, T., Kruis, J., Laloy, E., Landa, J., Lipping, T., Lukin, D., Mašín, D., Masson, R., Meeussen, J.C.L., Mollaali, M., Mon, A., Montenegro, L., Montoya, V., Pepin, G., Poonoosamy, Prasianakis, N., Saâdi, Z., Samper, J., Scaringi, G., Sochala, P., Tournassat, C., Yoshohika, K. & Yang, Y. (2021): State Of The Art in the fields of numerical analysis and scientific computing. Deliverable D4.1 of the HORIZON 2020 project EURAD. EC Grant agreement no: 847593.

Albina, P., Durban, N., Bertron, A., Albrecht, A., Robinet, J.C. & Erable, B. (2019): Influence of hydrogen electron donor, alkaline ph, and high nitrate concentrations on microbial denitrification: A review. International Journal of Molecular Sciences, 20/20, 5163. https://doi.org/10.3390/ijms20205163

Alcolea, A., Kuhlmann, U., Lanyon, G.W. & Marschall, P. (2014): Hydraulic conductance of the EDZ around underground structures of a geological repository for radioactive waste – A sensitivity study for the candidate host rocks in the proposed siting regions in Northern Switzerland. Nagra Arbeitsbericht NAB 13-94.

Alexander, W.R., Arcilla, C.A., McKinley, I.G., Kawamura, H., Takahashi, Y., Aoki, K. & Miyoshi, S. (2008): A New Natural Analogue Study of the Interaction of Low-Alkali Cement Leachates and the Bentonite Buffer of a Radioactive Waste Repository. MRS Online Proceedings Library (OPL), 1107, 493-500. https://doi.org/10.1557/PROC-1107-493

Alexander, W.R., Milodowski, A.E., Pitty, A.F., Hardie, S.M.L., Kemp, S.J., Rushton, J.C., Siathas, A., Siathas, A., Mackenzie, A.B., Korkeakoski, P., Norris, S., Sellin, P. & Rigas, M. (2013): Bentonite reactivity in alkaline solutions: interim results of the Cyprus Natural Analogue Project (CNAP). Clay Minerals, 48/2, 235-249. https://doi.org/10.1180/CLAYMIN.2013.048.2.06

Alquier, M., Kassim, C., Bertron, A., Sablayrolles, C., Rafrafi, Y., Albrecht, A. & Erable, B. (2014): Halomonas desiderata as a bacterial model to predict the possible biological nitrate reduction in concrete cells of nuclear waste disposals. Journal of Environmental Management, 132, 32-41. https://doi.org/10.1016/j.jenvman.2013.10.013

Alshalif, A.F., Irwan, J. M., Othman, N. & Anneza, L.H. (2016): Isolation of sulphate reduction bacteria (SRB) to improve compress strength and water penetration of bio-concrete. In MATEC Web of Conferences (Vol. 47, p. 1016). EDP Sciences. https://doi.org/10.1051/matecconf/20164701016

Anbu, P., Kang, C.-H., Shin, Y.-J. & So, J.-S. (2016): Formations of calcium carbonate minerals by bacteria and its multiple applications. SpringerPlus, 5/1, 250. https://doi.org/10.1186/s40064-016-1869-2

Angst, U., Moro, F., Geiker, M., Kessler, S., Beushausen, H., Andrade, C., Lahdensivu, J., Köliö, A., Imamoto, K., von Greve-Dierfeld, S. & Serdar, M. (2020): Corrosion of steel in carbonated concrete: mechanisms, practical experience, and research priorities – a critical review by RILEM TC 281-CCC. RILEM Technical Letters, 5, 85-100. https://doi.org/10.21809/RILEMTECHLETT.2020.127

Arter, H.E., Hanselmann, K.W. & Bachofen, R. (1991): Modelling of microbial degradation processes: The behaviour ofmicroorganisms in a waste repository. Experientia 1991 47:6, 47/6, 578-583. https://doi.org/10.1007/BF01949880

Ashraf, W. (2016): Carbonation of cement-based materials: Challenges and opportunities. Construction and Building Materials, 120, 558-570. https://doi.org/10.1016/j.conbuildmat.2016.05.080

Atkins, M. & Glasser, F.P. (1992): Application of portland cement-based materials to radioactive waste immobilization. Waste Management, 12/2-3, 105-131. https://doi.org/10.1016/0956-053X(92)90044-J

Atkinson, A., Everitt, N.M. & Guppy, R. (1988): Evolution of pH in a rad-waste repository: Internal reactions between concrete constituents. Report DOE-RW-89.025(PT.2).

Atkinson, A., Everitt, N.M. & Guppy, R.M. (1989): Time dependence of pH in a cementitious repository. In W. Lutz & R. C. Ewing (Eds.), 12. international symposium on the scientific basis for nuclear waste management, Berlin (Germany, F.R.) (pp. 439-446). Materials Research Society, Pittsburgh, PA (USA).

Bachofen, R. (1991): Microorganisms in nuclear waste disposal. Conclusions. Experientia 1991 47:6, 47/6, 583-584. https://doi.org/10.1007/BF01949881

Bagaria, F., Riba, O., Albrecht, A., Robinet, J.C., Made, B. & Roman-Ross, G. (2021): Predicting degradation of organic molecules in cementitious media. Progress in Nuclear Energy, 140. https://doi.org/10.1016/j.pnucene.2021.103888

Bagheri, M., Lothenbach, B., Shakoorioskooie, M. & Scrivener, K. (2022): Effect of different ions on dissolution rates of silica and feldspars at high pH. Cement and Concrete Research, 152, 106644. https://doi.org/10.1016/J.CEMCONRES.2021.106644

Bagnoud, A., Chourey, K., Hettich, R.L., de Bruijn, I., Andersson, A.F., Leupin, O.X., Schwyn, B. & Bernier-Latmani, R. (2016): Reconstructing a hydrogen-driven microbial metabolic network in Opalinus Clay rock. Nature Communications, 7/1, 12770. https://doi.org/10.1038/ncomms12770

Baqer, Y., Bateman, K., Tan, V.M.S., Stewart, D.I., Chen, X. & Thornton, S. F. (2021): The Influence of Hyper-Alkaline Leachate on a Generic Host Rock Composition for a Nuclear Waste Repository: Experimental Assessment and Modelling of Novel Variable Porosity and Surface Area. Transport in Porous Media, 140/2, 559-580. https://doi.org/10.1007/s11242-021-01702-2

Baquerizo, L.G., Matschei, T. & Scrivener, K.L. (2016): Impact of water activity on the stability of ettringite. Cement and Concrete Research, 79, 31-44. https://doi.org/10.1016/j.cemconres.2015.07.008

Bardelli, F., Mondelli, C., Didier, M., Vitillo, J.G., Cavicchia, D.R., Robinet, J.C., Leone, L. & Charlet, L. (2014): Hydrogen uptake and diffusion in Callovo-Oxfordian clay rock for nuclear waste disposal technology. Applied Geochemistry, 49, 168-177. https://doi.org/10.1016/j.apgeochem.2014.06.019

Bartier, D., Techer, I., Dauzères, A., Boulvais, P., Blanc-Valleron, M.-M. & Cabrera, J. (2013): In situ investigations and reactive transport modelling of cement paste/argillite interactions in a saturated context and outside an excavated disturbed zone. Applied Geochemistry, 31, 94-108. https://doi.org/10.1016/j.apgeochem.2012.12.009

Bärtschi, C. (2012): Kieselkalke der Schweiz: Charakterisierung eines Rohstoffs aus geologischer, petrographischer, wirtschaftlicher und umweltrelevanter Sicht. Beiträge zur Geologie der Schweiz, Geotechnik Serie (SGTK) (Vol. 97). Schweizerische Geotechnische Kommission, Zürich, Switzerland.

Bateman, K., Murayama, S., Hanamachi, Y., Wilson, J., Seta, T., Amano, Y., Kubota, M., Ohuchi, Y. & Tachi, Y. (2021): Evolution of the Reaction and Alteration of Mudstone with Ordinary Portland Cement Leachates: Sequential Flow Experiments and Reactive-Transport Modelling. Minerals 2021, Vol. 11, Page 1026, 11/9, 1026. https://doi.org/10.3390/MIN11091026

Bažant, Z.P. & Najjar, L.J. (1972): Nonlinear water diffusion in nonsaturated concrete. Matériaux et Constructions, 5/1, 3-20. https://doi.org/10.1007/BF02479073

Beckingham, L.E., Steefel, C.I., Swift, A.M., Voltolini, M., Yang, L., Anovitz, L.M., Sheets, J.M., Cole, D.R., Kneafsey, T.J., Mitnick, E.H., Zhang, S., Landrot, G., Ajo-Franklin, J.B., DePaola, D.J., Mito, S. & Xue, Z. (2017): Evaluation of accessible mineral surface areas for improved prediction of mineral reaction rates in porous media. Geochimica et Cosmochimica Acta, 205, 31-49. https://doi.org/10.1016/j.gca.2017.02.006

Bernard, E., Jenni, A., Fisch, M., Grolimund, D. & Mäder, U.K. (2020): Micro-X-ray diffraction and chemical mapping of aged interfaces between cement pastes and Opalinus Clay. Applied Geochemistry, 115/February. https://doi.org/10.1016/j.apgeochem.2020.104538

Bernard, E., Lothenbach, B., Le Goff, F., Pochard, I. & Dauzères, A. (2017a): Effect of magnesium on calcium silicate hydrate (C-S-H). Cement and Concrete Research, 97, 61-72. https://doi.org/10.1016/j.cemconres.2017.03.012

Bernard, E., Lothenbach, B., Rentsch, D., Pochard, I. & Dauzères, A. (2017b): Formation of magnesium silicate hydrates (M-S-H). Physics and Chemistry of the Earth, Parts A/B/C, 99, 142-157. https://doi.org/10.1016/j.pce.2017.02.005

Berndt, M.E., Allen, D.E. & Seyfried, W.E. (1996): Reduction of CO_2 during serpentinization of olivine at 300 °C and 500 bar. Geology, 24/4, 351. https://doi.org/10.1130/0091-7613(1996)024<0351:ROCDSO>2.3.CO;2

Berner, U. (1988): Modelling the Incongruent Dissolution of Hydrated Cement Minerals. Radiochimica Acta, 44-45/2, 387-394. https://doi.org/10.1524/ract.1988.4445.2.387

Berner, U. (1992): Evolution of pore water chemistry during degradation of cement in a radioactive waste repository environment. Waste Management, 12/2-3, 201-219. https://doi.org/10.1016/0956-053X(92)90049-O

Berner, U., Kulik, D.A. & Kosakowski, G. (2013): Geochemical impact of a low-pH cement liner on the near field of a repository for spent fuel and high-level radioactive waste. Physics and Chemistry of the Earth, Parts A/B/C, 64, 46-56. https://doi.org/10.1016/j.pce.2013.03.007

Berta, M., Dethlefsen, F., Ebert, M., Schäfer, D. & Dahmke, A. (2018): Geochemical Effects of Millimolar Hydrogen Concentrations in Groundwater: An Experimental Study in the Context of Subsurface Hydrogen Storage. Environmental Science & Technology, 52/8, 4937-4949. https://doi.org/10.1021/acs.est.7b05467

Betelu, S., Lerouge, C., Ignatiadis, I., Berger, G. & Giffaut, E. (2012): Mechanistic study of pyrite reduction by Hydrogen in NaCl 0.1 m at 90 deg. C using Electrochemical techniques. In: Andra (Ed.): Clays in natural and engineered barriers for radioactive waste confinement, 5th international meeting.Book of abstract, 265-266.

Bhatty, J.I. (2006): Effect of Minor Elements on Clinker and Cement Performance: A Laboratory Analysis. Portland Cement Associtation Research Development Bulletin RD130.

Bickmore, B. R., Nagy, K. L., Gray, A. K. & Brinkerhoff, A. R. (2006): The effect of $Al(OH)_4^-$ on the dissolution rate of quartz. Geochimica et Cosmochimica Acta, 70/2, 290-305. https://doi.org/10.1016/j.gca.2005.09.017

Bildstein, O. & Claret, F. (2015): Stability of Clay Barriers Under Chemical Perturbations. Developments in Clay Science, 6, 155-188. https://doi.org/10.1016/B978-0-08-100027-4.00005-X

Bildstein, O., Claret, F. & Frugier, P. (2019): RTM for Waste Repositories. Reviews in Mineralogy and Geochemistry, 85/1, 419-457. https://doi.org/10.2138/rmg.2019.85.14

Blanc, P., Lassin, A., Piantone, P., Azaroual, M., Jacquemet, N., Fabbri, A. & Gaucher, E.C. (2012): Thermoddem: A geochemical database focused on low temperature water/rock interactions and waste materials. Applied Geochemistry, 27/10, 2107-2116. https://doi.org/10.1016/j.apgeochem.2012.06.002

Blanc, P., Vieillard, P., Gailhanou, H., Gaboreau, S., Marty, N.C.M., Claret, F., Madé, B. & Giffaut, E. (2015): ThermoChimie database developments in the framework of cement/clay interactions. Applied Geochemistry, 55, 95-107. https://doi.org/10.1016/j.apgeochem.2014.12.006

Bossart, P. & Nussbaum, C. (2007): Mont Terri Project – Heater experiment, engineered barrier emplacement and ventilation experiment. Reports of the Swiss Geological Survey / Berichte der Landesgeologie 1.

Boumaaza, M., Turcry, P., Huet, B. & Aït-Mokhtar, A. (2020): Influence of carbonation on the microstructure and the gas diffusivity of hardened cement pastes. Construction and Building Materials, 253, 119227. https://doi.org/10.1016/j.conbuildmat.2020.119227

Bourdot, A., Thiéry, V., Bulteel, D., Cuchet, S. & Hammerschlag, J.-G. (2018): Alkali-reactivity of a Swiss siliceous limestone caused by finely dispersed quartz. Cement and Concrete Composites, 91, 97-107. https://doi.org/10.1016/j.cemconcomp.2018.04.016

Boylan, A. A., Perez-mon, C., Guillard, L., Burzan, N., Loreggian, L., Maisch, M., Kappler, A., Byrne, J. M. & Bernier-latmani, R. (2019): H_2-fuelled microbial metabolism in Opalinus Clay. Applied Clay Science, 174/March, 69-76. https://doi.org/10.1016/j.clay.2019.03.020

Bradbury, M.H. & Baeyens, B. (2005): Experimental And Modelling Investigations on Na-Illite: Acid-Base Behaviour And the Sorption Of Strontium, Nickel, Europium And Uranyl. PSI Report No. 05-02.

Bradbury, M.H. & Sarott, F.-A. (1994): Sorption databases for the cementititous near-field of an L/ILW repository for performance assessement. Nagra Technical Report NTB 93-08.

Bradbury, M.H. & Van Loon, L.R. (1996): Cementitious near-field sorption data bases for performance assessment of an L/ILW repository in a Palfris marl host rock. Nagra Technical Report NTB 96-04.

Bradbury, M.H., Berner, U., Curti, E., Hummel, W., Kosakowski, G. & Thoenen, T. (2014): Geochemical near-field evolution of a deep geological repository for spent fuel and high-level radioactive waste. Nagra Technical Report NTB 12-01.

Bradford, S.A. & Torkzaban, S. (2008): Colloid Transport and Retention in Unsaturated Porous Media: A Review of Interface-, Collector-, and Pore-Scale Processes and Models. Vadose Zone Journal, 7/2, 667-681. https://doi.org/10.2136/vzj2007.0092

Brady, P.V. & Walther, J.V. (1990): Kinetics of quartz dissolution at low temperatures. Chemical Geology, 82, 253-264. https://doi.org/10.1016/0009-2541(90)90084-K

Bran Anleu, P.C. (2018): Quantitative Micro XRF Mapping of Chlorides: Possibilities, Limitations, and Applications, from Cement to Digital Concrete. Doctoral thesis. ETH Zürich. https://doi.org/10.3929/ethz-b-000328911

Brantley, S.L. (2008): Kinetics of Mineral Dissolution. In Kinetics of Water-Rock Interaction (pp. 151-210). Springer New York, New York, NY. https://doi.org/10.1007/978-0-387-73563-4_5

Brantley, S.L., Kubicki, J.D. & White, A.F. (Eds.) (2008): Kinetics of Water-Rock Interaction. Springer Science+ Business Media, New York. USA.

Broom, D.P. (2011): Hydrogen sorption properties of materials. Green Energy and Technology, 27, 61-115. https://doi.org/10.1007/978-0-85729-221-6_3

Broomfield, J.P. (2003): Corrosion of steel in concrete: Understanding, investigation and repair. (2nd ed.). Taylor & Francis, London.

Buffle, J. & Leppard, G.G. (1995): Characterization of Aquatic Colloids and Macromolecules. 1. Structure and Behavior of Colloidal Material. Environmental Science & Technology, 29/9, 2169-2175. https://doi.org/10.1021/es00009a004

Burzan, N. (2021): Growth and viability of microorganisms in bentonite and their potential activity in deep geological repository environments. Doctoral Thesis. EPF Lausanne.

Caruso, F., Mantellato, S., Palacios, M. & Flatt, R.J. (2017): ICP-OES method for the characterization of cement pore solutions and their modification by polycarboxylate-based superplasticizers. Cement and Concrete Research, 91, 52-60. https://doi.org/10.1016/j.cemconres.2016.10.007

Chagneau, A., Claret, F., Enzmann, F., Kersten, M., Heck, S., Madé, B. & Schäfer, T. (2015): Mineral precipitation-induced porosity reduction and its effect on transport parameters in diffusion-controlled porous media. Geochemical Transactions, 16/1, 13. https://doi.org/10.1186/s12932-015-0027-z

Chen, C.-T., Iyoki, K., Hu, P., Yamada, H., Ohara, K., Sukenaga, S., Ando, M., Shibata, H., Okubo, T. & Wakihara, T. (2021): Reaction Kinetics Regulated Formation of Short-Range Order in an Amorphous Matrix during Zeolite Crystallization. Journal of the American Chemical Society, 143/29, 10986-10997. https://doi.org/10.1021/JACS.1C03351

Chernyshev, A.N., Jonsson, M. & Forsberg, K. (2018): Characterization and degradation of a polyaryl ether based superplasticizer for use in concrete barriers in deep geological repositories. Applied Geochemistry, 95, 172-181. https://doi.org/10.1016/j.apgeochem.2018.05.014

Chitty, W.J., Dillmann, P., L'Hostis, V. & Lombard, C. (2005): Long-term corrosion resistance of metallic reinforcements in concrete – a study of corrosion mechanisms based on archaeological artefacts. Corrosion Science, 47/6, 1555-1581. https://doi.org/10.1016/J.CORSCI.2004.07.032

Churakov, S.V., Labbez, C., Pegado, L. & Sulpizi, M. (2014): Intrinsic Acidity of Surface Sites in Calcium Silicate Hydrates and Its Implication to Their Electrokinetic Properties. The Journal of Physical Chemistry C, 118/22, 11752-11762. https://doi.org/10.1021/jp502514a

Claret, F., Bauer, A., Schäfer, T., Griffault, L. & Lanson, B. (2002): Experimental investigation of the interaction of clays with high-pH solutions: A case study from the Callovo-Oxfordian formation, Meuse-Haute Marne underground laboratory (France). Clays and Clay Minerals 2002, 50:5, 50/5, 633-646. https://doi.org/10.1346/000986002320679369

Claude, A., Naki, A., Susan, I.-O., Fritz, S., Peter, K.W., Andreas, D., Joachim, K., Meinert, R. & Christian, S. (2017): Timing of early Quaternary gravel accumulation in the Swiss Alpine Foreland. Geomorphology, 276, 71-85. https://doi.org/10.1016/j.geomorph.2016.10.016

Cloet, V., Curti, E., Kosakowski, G., Lura, P., Lothenbach, B. & Wieland, E. (2018): Cementitious backfill for a high-level waste repository: impact of repository induced effects. Nagra Arbeitsbericht NAB 18-41.

Cloet, V., Schwyn, B. & Wieland, E. (2014): Geochemische Nahfeld-Daten zu den SMA und ATA für die provisorischen Sicherheitsanalysen in SGT Etappe 2. Nagra Arbeitsbericht NAB 14-52 Rev. 1.

Criado, M., Martínez-Ramirez, S., Fajardo, S., Gõmez, P.P. & Bastidas, J.M. (2013): Corrosion rate and corrosion product characterisation using Raman spectroscopy for steel embedded in chloride polluted fly ash mortar. Materials and Corrosion, 64/5, 372-380. https://doi.org/10.1002/MACO.201206714

Cross, M.M., Manning, D.A.C., Bottrell, S.H. & Worden, R.H. (2004): Thermochemical sulphate reduction (TSR): Experimental determination of reaction kinetics and implications of the observed reaction rates for petroleum reservoirs. In Organic Geochemistry (Vol. 35, pp. 393-404). Pergamon.
https://doi.org/10.1016/j.orggeochem.2004.01.005

Crusset, D., Deydier, V., Necib, S., Gras, J.M., Combrade, P., Féron, D. & Burger, E. (2017): Corrosion of carbon steel components in the French high-level waste programme: evolution of disposal concept and selection of materials. Corrosion Engineering Science and Technology, 52, 17-24. https://doi.org/10.1080/1478422X.2017.1344416

Curti, E., Thoenen, T., Kosakowski, G., Miron, G.D., Baeyens, B., Van Loon, L.R. & Leupin, O.X. (2023): The chemical near-field evolution within the HLW/SF repository (update of NTB 12-01). Nagra Technical Report NTB 23-02.

Damiani, L.H., Kosakowski, G., Vinsot, A. & Churakov, S.V. (2022): Hydrogen gas transfer between a borehole and claystone: experiment and geochemical model. Environmental Geotechnics, 1-14. https://doi.org/10.1680/jenge.21.00061

Dauzeres, A., Achiedo, G., Nied, D., Bernard, E., Alahrache, S. & Lothenbach, B. (2016): Magnesium perturbation in low-pH concretes placed in clayey environment - Solid characterizations and modeling. Cement and Concrete Research, 79, 137-150. https://doi.org/10.1016/j.cemconres.2015.09.002

Dauzeres, A., Le Bescop, P., Sardini, P. & Cau Dit Coumes, C. (2010): Physico-chemical investigation of clayey/cement-based materials interaction in the context of geological waste disposal: Experimental approach and results. Cement and Concrete Research, 40/8, 1327-1340. https://doi.org/10.1016/J.CEMCONRES.2010.03.015

De Windt, L., Marsal, F., Tinseau, E. & Pellegrini, D. (2008): Reactive transport modeling of geochemical interactions at a concrete/argillite interface, Tournemire site (France). Physics and Chemistry of the Earth, Parts A/B/C, 33/1, 295-305.
https://doi.org/10.1016/j.pce.2008.10.035

De Windt, L., Miron, G.D., Fabian, M., Goethals, J. & Wittebroodt, C. (2020): First results on the thermodynamic databases and reactive transport models for steel-cement interfaces at high temperature. Final version as of 18.02.2021 of deliverable D2.8 of the HORIZON 2020 project EURAD. EC Grant agreement no: 847593.

Degueldre, C. (1996): Groundwater Colloid Properties and their Potential Influence on Radionuclide Transport. In W. J. Gray & I. R. Triay (Eds.), MRS Proceedings (Vol. 465, p. 835). Materials Research Society, Warrendale, USA. https://doi.org/10.1557/PROC-465-835

Degueldre, C., Aeberhard, P., Kunze, P. & Bessho, K. (2009): Colloid generation/elimination dynamic processes: Toward a pseudo-equilibrium? Colloids and Surfaces A: Physicochemical and Engineering Aspects, 337/1-3, 117-126. https://doi.org/10.1016/j.colsurfa.2008.12.007

Degueldre, C., Scholtis, A., Laube, A., Turrero, M.J. & Thomas, B. (2003): Study of the pore water chemistry through an argillaceous formation: a paleohydrochemical approach. Applied Geochemistry, 18/1, 55-73. https://doi.org/10.1016/S0883-2927(02)00048-3

Deinert, M.R. & Parlange, J.Y. (2009): Effect of pore structure on capillary condensation in a porous medium. Physical Review E - Statistical, Nonlinear, and Soft Matter Physics, 79/2, 021202. https://doi.org/10.1103/PhysRevE.79.021202

Derjaguin, B. & Landau, L. (1993): Theory of the stability of strongly charged lyophobic sols and of the adhesion of strongly charged particles in solutions of electrolytes. Progress in Surface Science, 43/1-4, 30-59. https://doi.org/10.1016/0079-6816(93)90013-L

Devol-Brown, I., Tinseau, E., Bartier, D., Mifsud, A. & Stammose, D. (2007): Interaction of Tournemire argillite (Aveyron, France) with hyperalkaline fluids: Batch experiments performed with powdered and/or compact materials. Physics and Chemistry of the Earth, Parts A/B/C, 32/1-7, 320-333. https://doi.org/10.1016/J.PCE.2006.02.046

Diana, W., Hartono, E. & Muntohar, A.S. (2019): The Permeability of Portland Cement-Stabilized Clay Shale. IOP Conference Series: Materials Science and Engineering, 650/1, 012027. https://doi.org/10.1088/1757-899X/650/1/012027

DiBlasi, N.A., Tasi, A.G., Gaona, X., Fellhauer, D., Dardenne, K., Rothe, J., Reed, D.T., Hixon, A.E. & Altmaier, M. (2021): Impact of Ca(II) on the aqueous speciation, redox behavior, and environmental mobility of Pu(IV) in the presence of EDTA. Science of The Total Environment, 783, 146993. https://doi.org/10.1016/j.scitotenv.2021.146993

DiBlasi, N.A., Tasi, A.G., Trumm, M., Schnurr, A., Gaona, X., Fellhauer, D., Dardenne, K., Rothe, J., Reed, D. T., Hixon, A. E. & Altmaier, M. (2022): Pu(III) and Cm(III) in the presence of EDTA: aqueous speciation, redox behavior, and the impact of Ca(II). RSC Advances, 12/15, 9478-9493. https://doi.org/10.1039/D1RA09010K

Didier M. (2012a): Etude du transfert réactif de l'hydrogène au sein de l'argilite intacte. Université de Grenoble.

Didier, M., Leone, L., Greneche, J.M., Giffaut, E. & Charlet, L. (2012b): Adsorption of hydrogen gas and redox processes in clays. Environmental Science and Technology, 46/6, 3574-3579. https://doi.org/10.1021/es204583h

Dilnesa, B.Z., Lothenbach, B., Le Saout, G., Renaudin, G., Mesbah, A., Filinchuk, Y., Wichser, A. & Wieland, E. (2011): Iron in carbonate containing AFm phases. Cement and Concrete Research, 41/3, 311-323. https://doi.org/10.1016/j.cemconres.2010.11.017

Dilnesa, B.Z., Lothenbach, B., Renaudin, G., Wichser, A. & Kulik, D. (2014b): Synthesis and characterization of hydrogarnet $Ca_3(Al_xFe_{1-x})_2(SiO_4)_y(OH)_{4(3-y)}$. Cement and Concrete Research, 59, 96-111. https://doi.org/10.1016/j.cemconres.2014.02.001

Dilnesa, B.Z., Lothenbach, B., Renaudin, G., Wichser, A. & Wieland, E. (2012): Stability of monosulfate in the presence of iron. Journal of the American Ceramic Society, 95/10, 3305-3316. https://doi.org/10.1111/j.1551-2916.2012.05335.x

Dilnesa, B.Z., Wieland, E., Lothenbach, B., Dähn, R. & Scrivener, K.L. (2014a): Fe-containing phases in hydrated cements. Cement and Concrete Research, 58, 45-55. https://doi.org/10.1016/j.cemconres.2013.12.012

Diomidis, N. (2014): Scientific Basis for the Production of Gas due to Corrosion in a Deep Geological Repository. Nagra Arbeitsbericht NAB 14-30.

Diomidis, N., Cloet, V., Leupin, O.X., Marschall, P., Poller, A. & Stein, M. (2016): Production, consumption and transport of gases in deep geological repositories according to the Swiss disposal concept. Nagra Technical Report 16-03.

Diomidis, N., Guillemot, T. & King, F. (2023): Definition of reference corrosion rates for performance and safety assessment in the framework of the general licence application. Nagra Arbeitsbericht NAB 23-22.

Dove, P.M. & Elston, S.F. (1992): Dissolution kinetics of quartz in sodium chloride solutions: Analysis of existing data and a rate model for 25 °C. Geochimica et Cosmochimica Acta, 56/12, 4147-4156. https://doi.org/10.1016/0016-7037(92)90257-J

Duro, L., Bruno, J., Grivé, M., Montoya, V., Kienzler, B., Altmaier, M. & Buckau, G. (2014b): Redox processes in the safety case of deep geological repositories of radioactive wastes. Contribution of the European RECOSY Collaborative Project. Applied Geochemistry, 49, 206-217. https://doi.org/10.1016/j.apgeochem.2014.04.013

Duro, L., Domènech, C., Grivé, M., Roman-ross, G., Bruno, J. & Källström, K. (2014a): Applied geochemistry assessment of the evolution of the redox conditions in a low and intermediate level nuclear waste repository (SFR1 , Sweden). Applied Geochemistry, 49, 192-205. https://doi.org/10.1016/j.apgeochem.2014.04.015

Dutzer, V., Dridi, W., Poyet, S., Le Bescop, P. & Bourbon, X. (2019): The link between gas diffusion and carbonation in hardened cement pastes. Cement and Concrete Research, 123, 105795. https://doi.org/10.1016/j.cemconres.2019.105795

Eddaoui, N., Panfilov, M., Ganzer, L. & Hagemann, B. (2021): Impact of Pore Clogging by Bacteria on Underground Hydrogen Storage. Transport in Porous Media, 139/1, 89-108. https://doi.org/10.1007/S11242-021-01647-6/FIGURES/12

Edge, J.S. (2014): Hydorgen adsorption and dynamics in clay minerals. Doctoral thesis. University College London.

Edge, J.S., Skipper, N.T., Fernandez-Alonso, F., Lovell, A., Srinivas, G., Bennington, S.M., Garcia Sakai, V. & Youngs, T.G.A. (2014): Structure and dynamics of molecular hydrogen in the interlayer pores of a swelling 2:1 clay by neutron scattering. Journal of Physical Chemistry C, 118/44, 25740-25747. https://doi.org/10.1021/jp5082356

Elakneswaran, Y., Noguchi, N., Matumoto, K., Morinaga, Y., Chabayashi, T., Kato, H. & Nawa, T. (2019): Characteristics of ferrite-rich portland cement: Comparison with ordinary portland cement. Frontiers in Materials, 6, 97. https://doi.org/10.3389/fmats.2019.00097

Elsener, B. & Rossi, A. (2018): Passivation of Steel and Stainless Steel in Alkaline Media Simulating Concrete. Encyclopedia of Interfacial Chemistry: Surface Science and Electrochemistry, 365-375. https://doi.org/10.1016/B978-0-12-409547-2.13772-2

Enning, D. & Garrelfs, J. (2014): Corrosion of iron by sulfate-reducing bacteria: New views of an old problem. Applied and Environmental Microbiology, 80/4, 1226-1236. https://doi.org/10.1128/AEM.02848-13

ENSI (2020): Geologische Tiefenlager. Richtlinie für die schweizerischen Kernanlagen ENSI-G03/d.

Esnault, L., Jullien, M., Mustin, C., Bildstein, O. & Libert, M. (2011): Metallic corrosion processes reactivation sustained by iron-reducing bacteria: Implication on long-term stability of protective layers. Physics and Chemistry of the Earth, 36/17-18, 1624-1629. https://doi.org/10.1016/j.pce.2011.10.018

Esposito, R. & Hendriks, M.A.N. (2019): Literature review of modelling approaches for ASR in concrete: a new perspective. European Journal of Environmental and Civil Engineering, 23/11, 1311-1331. https://doi.org/10.1080/19648189.2017.1347068

Faucon, P., Le Bescop, P., Adenot, F., Bonville, P., Jacquinot, J.F., Pineau, F. & Felix, B. (1996): Leaching of cement: Study of the surface layer. Cement and Concrete Research, 26/11, 1707-1715. https://doi.org/10.1016/S0008-8846(96)00157-3

Fernandes, I., Noronha, F. & Teles, M. (2004): Microscopic analysis of alkali-aggregate reaction products in a 50-year-old concrete. Materials Characterization, 53/2-4, 295-306. https://doi.org/10.1016/j.matchar.2004.08.005

Filella, M. (2007): Colloidal properties of submicron particles in natural waters. In K. J. Wilkinson & J. R. Lead (Eds.), Environmental colloids and particles: Behaviour, separation and characterisation. John Wiley & Sons, Chichester. https://doi.org/10.1002/9780470024539.ch2

Fischer, C., Kurganskaya, I., Schäfer, T. & Lüttge, A. (2014): Variability of crystal surface reactivity: What do we know? Applied Geochemistry. https://doi.org/10.1016/j.apgeochem.2014.02.002

Frohlich, D.R., Koke, C., Maiwald, M.M., Chomyn, C., Plank, J. & Panak, P.J. (2019): A spectroscopic study of the complexation reaction of trivalent lanthanides with a synthetic acrylate based PCE-superplasticizer. Spectrochimica Acta Part A-Molecular and Biomolecular Spectroscopy, 207, 270-275. https://doi.org/10.1016/j.saa.2018.09.025

Fujita, T., Sugiyama, D., Swanton, S.W. & Myatt, B.J. (2003): Observation and characterization of colloids derived from leached cement hydrates. Journal of Contaminant Hydrology, 61/1-4, 3-16. https://doi.org/10.1016/S0169-7722(02)00109-2

Fukatsu, Y., Van Loon, L.R., Shafizadeh, A., Grolimund, D., Ikeda, Y. & Tsukahara, T. (2017): Effect of Celestite Precipitation in Compacted Illite on the Diffusion of HTO, $^{36}Cl^-$, and $^{22}Na^+$. Energy Procedia 131, pp. 133-139. https://doi.org/10.1016/j.egypro.2017.09.450

Furcas, F.E., Lothenbach, B., Isgor, O.B., Mundra, S., Zhang, Z. & Angst, U.M. (2022): Solubility and speciation of iron in cementitious systems. Cement and Concrete Research, 151, 106620. https://doi.org/10.1016/J.CEMCONRES.2021.106620

Gaboreau, S., Lerouge, C., Dewonck, S., Linard, Y., Bourbon, X., Fialips, C.I., Mazurier, A., Pret, D., Borschneck, D., Montouillout, V., Gaucher, E.C. & Claret, F. (2012): In-situ interaction of cement paste and shotcrete with claystones in a deep disposal context. American Journal of Science, 312/3, 314-356. https://doi.org/10.2475/03.2012.03

Gaboreau, S., Prêt, D., Tinseau, E., Claret, F., Pellegrini, D. & Stammose, D. (2011): 15 years of in situ cement-argillite interaction from Tournemire URL: Characterisation of the multi-scale spatial heterogeneities of pore space evolution. Applied Geochemistry, 26/12, 2159-2171. https://doi.org/10.1016/j.apgeochem.2011.07.013

Gaboreau, S., Rodríguez-Cañas, E., Mäder, U.K., Jenni, A., Turrero, M.J. & Cuevas, J. (2020): Concrete perturbation in a 13-year in situ concrete/bentonite interaction from FEBEX experiments. New insight of 2:1 Mg phyllosilicate precipitation at the interface. Applied Geochemistry, 118/March, 104624. https://doi.org/10.1016/j.apgeochem.2020.104624

Gaona, X., Montoya, V., Colàs, E., Grivé, M. & Duro, L. (2008): Review of the complexation of tetravalent actinides by ISA and gluconate under alkaline to hyperalkaline conditions. Journal of Contaminant Hydrology, 102/3-4, 217-227. https://doi.org/10.1016/j.jconhyd.2008.09.017

Garcia, D., Grive, M., Duro, L., Brassinnes, S. & de Pablo, J. (2018): The potential role of the degradation products of cement superplasticizers on the mobility of radionuclides. Applied Geochemistry, 98, 1-9. https://doi.org/10.1016/j.apgeochem.2018.09.004

Gaucher, E.C. & Blanc, P. (2006): Cement/clay interactions - a review: experiments, natural analogues, and modeling. Waste Management, 26/7, 776-788. https://doi.org/10.1016/j.wasman.2006.01.027

Geckeis, H. (2004): Colloid influence on the radionuclide migration from a nuclear waste repository. Geological Society, London, Special Publications, 236/1, 529-543. https://doi.org/10.1144/GSL.SP.2004.236.01.29

Georget, F., Lothenbach, B., Wilson, W., Zunino, F. & Scrivener, K.L. (2022): Stability of hemicarbonate under cement paste-like conditions. Cement and Concrete Research, 153, 106692. https://doi.org/10.1016/J.CEMCONRES.2021.106692

Gimmi, T. & Churakov, S.V. (2019): Water retention and diffusion in unsaturated clays: Connecting atomistic and pore scale simulations. Applied Clay Science, 175/December 2018, 169-183. https://doi.org/10.1016/j.clay.2019.03.035

Glasser, F.P. (2001): Mineralogical aspects of cement in radioactive waste disposal. Mineralogical Magazine, 65/5, 621-633. https://doi.org/10.1180/002646101317018442

Glasser, F.P. (2013): Cements in Radioactive Waste Disposal. In: International Atomic Energy Agency (2013): The behaviours of cementitious materials in long term storage and disposal of radioactive waste : Results of a coordinated research project. IAEA-TECDOC-1701. IAEA, Vienna.

Glasser, F.P., Marchand, J. & Samson, E. (2008): Durability of concrete – Degradation phenomena involving detrimental chemical reactions. Cement and Concrete Research, 38/2, 226-246. https://doi.org/10.1016/j.cemconres.2007.09.015

Glaus, M.A. & Van Loon, L.R. (2008): Degradation of cellulose under alkaline conditions: New insights from a 12 years degradation study. Environmental Science and Technology, 42/8, 2906-2911. https://doi.org/10.1021/es7025517

Glaus, M.A., Laube, A. & Van Loon, L.R. (2004): A generic procedure for the assessment of the effect of concrete admixtures on the sorption of radionuclides on cement: Concept and selected results. In: V.M. Oversby & L.O. Werme (Eds.), Scientific Basis for Nuclear Waste Management XXVII Vol. 807. Materials Research Society MRS, 365-370.

Gong, L., Rimstidt, J.D., Zhang, Y., Chen, K. & Zhu, C. (2019): Unidirectional kaolinite dissolution rates at near-equilibrium and near-neutral pH conditions. Applied Clay Science, 182, 105284. https://doi.org/10.1016/j.clay.2019.105284

González-Santamaría, D.E., Fernández, R., Ruiz, A.I., Ortega, A. & Cuevas, J. (2020a): Bentonite/CEM-II cement mortar INTERFACE EXPERIMENTS: A proxy to in situ deep geological repository engineered barrier system surface reactivity. Applied Geochemistry, 117/August 2019, 104599. https://doi.org/10.1016/j.apgeochem.2020.104599

González-Santamaría, D.E., Fernández, R., Ruiz, A.I., Ortega, A. & Cuevas, J. (2020b): High-pH/low pH ordinary Portland cement mortars impacts on compacted bentonite surfaces: Application to clay barriers performance. Applied Clay Science, 193. https://doi.org/10.1016/j.clay.2020.105672

Govaerts, J., Jacques, D., Samper, J., Neeft, E. & Montaya, V. (2022): Model abstraction methods for upscaling and integration of process knowledge in reactive transport models for geological disposal of radioactive waste. Deliverable D2.18 of the HORIZON 2020 project EURAD. EC Grant agreement no: 847593.

Grattan-Bellew, P.E. & Katayama, T. (2019): So-Called Alkali-Carbonate Reaction (ACR). In I. Sims & A. Poole (Eds.), Alkali-Aggregate Reaction in Concrete : A World Review. CRC Press. https://doi.org/10.1201/9781315708959-3

Greenfield, B.F., Linklater, C.M.C.M., Moreton, A.D.A.D., Spindler, M.W. & Williams, S.W.J. (1994): The effects of organic degradation products on actinide disposal. Actinide Processing:, 289-302.

Greenfield, B.F., Moreton, A.D., Spindler, M.W., Williams, S.J. & Woodwark, D.R. (1992): The Effects of the Degradation of Organic Materials in the Near Field of a Radioactive Waste Repository. MRS Proceedings, 257, 299-306. https://doi.org/10.1557/PROC-257-299

Gregory, S., Barnett, M., Field, L. & Milodowski, A. (2019): Subsurface Microbial Hydrogen Cycling: Natural Occurrence and Implications for Industry. Microorganisms, 7/2, 53. https://doi.org/103390/microorganisms7020053

Guillemot, T., Wieland, E., Warthmann, R. & Mosberger, L. (2023): Degradation of organic materials in an L/ILW repository. Nagra Arbeitsbericht NAB 23-11.

Hagemann, B., Rasoulzadeh, M., Panfilov, M., Ganzer, L. & Reitenbach, V. (2016): Hydrogenization of underground storage of natural gas: Impact of hydrogen on the hydrodynamic and bio-chemical behavior. Computational Geosciences, 20/3, 595-606. https://doi.org/10.1007/s10596-015-9515-6

Hallbeck, L. (2010): Principal organic materials in a repository for spent nuclear fuel. SKB Technical Report TR-10-19.

Hallet, V., Pedersen, M.T., Lothenbach, B., Winnefeld, F., De Belie, N. & Pontikes, Y. (2022): Hydration of blended cement with high volume iron-rich slag from non-ferrous metallurgy. Cement and Concrete Research, 151, 106624. https://doi.org/10.1016/j.cemconres.2021.106624

Harris, A., Manning, M., Tearle, W. & Tweed, C. (2002): Testing of models of the dissolution of cements – leaching of synthetic CSH gels. Cement and Concrete Research, 32/5, 731-746. https://doi.org/10.1016/S0008-8846(01)00748-7

Harrison, A.L., Dipple, G.M., Song, W., Power, I.M., Mayer, K.U., Beinlich, A. & Sinton, D. (2017): Changes in mineral reactivity driven by pore fluid mobility in partially wetted porous media. Chemical Geology, 463, 1-11. https://doi.org/10.1016/j.chemgeo.2017.05.003

Hassannayebi, N., Azizmohammadi, S., De Lucia, M. & Ott, H. (2019): Underground hydrogen storage: application of geochemical modelling in a case study in the Molasse Basin, Upper Austria. Environmental Earth Sciences, 78/5, 1-14. https://doi.org/10.1007/s12665-019-8184-5

Havlova, V., Kiczka, M., Miranda, M.A., Klajmon, M. & Wersin, P. (2020): Modelling of the steel-clay interface - approaches, first results and model refinements. Deliverable D 2.6 of the HORIZON 2020 project EURAD. EC Grant agreement no: 847593.

Hayek, M., Kosakowski, G., Jakob, A. & Churakov, S.V. (2012): A class of analytical solutions for multidimensional multispecies diffusive transport coupled with precipitation-dissolution reactions and porosity changes. Water Resources Research, 48/3, W03525. https://doi.org/10.1029/2011WR011663

Heep, W. (2010): The Zwilag Plasma Facility: Five Years of Successful Operation. In: ASME 2010 13th International Conference on Environmental Remediation and Radioactive Waste Management, Volume 1 (pp. 141-147). ASMEDC. https://doi.org/10.1115/ICEM2010-40128

Herrera, L.K. & Videla, H.A. (2009): Role of iron-reducing bacteria in corrosion and protection of carbon steel. International Biodeterioration and Biodegradation, 63/7, 891-895. https://doi.org/10.1016/j.ibiod.2009.06.003

Herzog, A. & Mitchell, J.K. (1963): Reactions accompanying stabilization with cement. Highway Research Record 36, 146-171.

Huang, Y., Shao, H., Wieland, E., Kolditz, O. & Kosakowski, G. (2021): Two-phase transport in a cemented waste package considering spatio-temporal evolution of chemical conditions. Npj Materials Degradation, 5/1, 4. https://doi.org/10.1038/s41529-021-00150-z

Hudcová, B., Veselská, V., Filip, J., Číhalová, S. & Komárek, M. (2017): Sorption mechanisms of arsenate on Mg-Fe layered double hydroxides: A combination of adsorption modeling and solid state analysis. Chemosphere, 168, 539-548. https://doi.org/10.1016/J.CHEMOSPHERE.2016.11.031

Hummel, W. & Thoenen, T. (2023): The PSI Chemical Thermodynamic data base 2020. Nagra Technical Report NTB 21-03.

Hummel, W. (2004): The influence of cyanide complexation on the speciation and solubility of radionuclides in a geological repository. Environmental Geology, 45/5, 633-646.

Hummel, W., Kulik, D.A. & Miron, G.D. (2022): Solubility of radionuclides and influence of EDTA for use in the development of the cement sorption database (SDB 2022). Nagra Arbeitsbericht NAB 22-38.

Idiart, A., Laviña, M., Kosakowski, G., Cochepin, B., Meeussen, J.C.L., Samper, J., Mon, A., Montoya, V., Munier, I., Poonoosamy, J., Montenegro, L., Deissmann, G., Rohmen, S., Damiani, L.H., Coene, E. & Naves, A. (2020): Reactive transport modelling of a low-pH concrete / clay interface. Applied Geochemistry, 115, 104562. https://doi.org/10.1016/j.apgeochem.2020.104562

Ione, K.G. & Vostrikova, L.A. (1987): The isomorphism and catalytic properties of silicates with the zeolite structure. Russian Chemical Reviews, 56/3, 231.

Jackson, M.D., Mulcahy, S.R., Chen, H., Li, Y., Li, Q., Cappelletti, P. & Wenk, H.R. (2017): Phillipsite and Al-tobermorite mineral cements produced through low-temperature water-rock reactions in Roman marine concrete. American Mineralogist, 102/7, 1435-1450. https://doi.org/10.2138/am-2017-5993CCBY

Jacobs, F., Mayer, G. & Wittmann, F.H. (1994): Hochpermeabler, zementgebundener Verfüllmörtel für SMA Endlager. Nagra Technischer Bericht NTB 92-11.

Jakobsen, R. & Cold, L. (2007): Geochemistry at the sulfate reduction-methanogenesis transition zone in an anoxic aquifer-A partial equilibrium interpretation using 2D reactive transport modeling. Geochimica et Cosmochimica Acta, 71/8, 1949-1966. https://doi.org/10.1016/j.gca.2007.01.013

Jenni, A. & Mäder, U.K. (2021): Reactive Transport Simulation of Low-pH Cement Interacting with Opalinus Clay Using a Dual Porosity Electrostatic Model. Minerals, 11/7, 664. https://doi.org/10.3390/min11070664

Jenni, A., Gimmi, T., Alt-Epping, P., Mäder, U.K. & Cloet, V. (2017): Interaction of ordinary Portland cement and Opalinus Clay: Dual porosity modelling compared to experimental data. Physics and Chemistry of the Earth, Parts A/B/C, 99, 22-37. https://doi.org/10.1016/j.pce.2017.01.004

Jenni, A., Mäder, U.K., Lerouge, C., Gaboreau, S. & Schwyn, B. (2014): In situ interaction between different concretes and Opalinus Clay. Physics and Chemistry of the Earth, 70-71, 71-83. https://doi.org/10.1016/j.pce.2013.11.004

Jenni, A., Wersin, P., Thoenen, T., Baeyens, B., Ferrari, A., Gimmi, T., Mäder, U.K., Marschall, P., Hummel, W. & Leupin, O.X. (2019): Bentonite backfill performance in a high-level waste repository: a geochemical perspective. Nagra Technical Report NTB 19-03.

Ji, L., Zhang, T., Milliken, K.L., Qu, J. & Zhang, X. (2012): Experimental investigation of main controls to methane adsorption in clay-rich rocks. Applied Geochemistry, 27/12, 2533-2545. https://doi.org/10.1016/j.apgeochem.2012.08.027

Jin, Z. & Firoozabadi, A. (2014): Effect of water on methane and carbon dioxide sorption in clay minerals by Monte Carlo simulations. Fluid Phase Equilibria, 382, 10-20. https://doi.org/10.1016/j.fluid.2014.07.035

Jung, H. & Navarre-Sitchler, A. (2018a): Physical heterogeneity control on effective mineral dissolution rates. Geochimica et Cosmochimica Acta, 227, 246-263. https://doi.org/10.1016/j.gca.2018.02.028

Jung, H. & Navarre-Sitchler, A. (2018b): Scale effect on the time dependence of mineral dissolution rates in physically heterogeneous porous media. Geochimica et Cosmochimica Acta, 234, 70-83. https://doi.org/10.1016/j.gca.2018.05.009

Kalhori, H. & Bagherpour, R. (2017): Application of carbonate precipitating bacteria for improving properties and repairing cracks of shotcrete. Construction and Building Materials, 148, 249-260. https://doi.org/10.1016/j.conbuildmat.2017.05.074

Kangni-Foli, E., Poyet, S., Le Bescop, P., Charpentier, T., Bernachy-Barbé, F., Dauzères, A., L'Hôpital, E. & d'Espinose de Lacaillerie, J.-B. (2021): Carbonation of model cement pastes: The mineralogical origin of microstructural changes and shrinkage. Cement and Concrete Research, 144, 106446. https://doi.org/10.1016/j.cemconres.2021.106446

Kayali, O., Khan, M.S.H. & Sharfuddin Ahmed, M. (2012): The role of hydrotalcite in chloride binding and corrosion protection in concretes with ground granulated blast furnace slag. Cement and Concrete Composites, 34/8, 936-945. https://doi.org/10.1016/j.cemconcomp.2012.04.009

KEG (2003): Kernenergiegesetz (KEG) vom 21. März 2003, Stand am 1. Januar 2021. Systematische Sammlung des Bundesrechts SR 732.1, Schweiz.

Keith-Roach, M.J. (2008): The speciation, stability, solubility and biodegradation of organic co-contaminant radionuclide complexes: A review. Science of The Total Environment, 396/1, 1-11. https://doi.org/10.1016/j.scitotenv.2008.02.030

Kiczka, M., Pekala, M., Maanoja, S., Muuri, E. & Wersin, P. (2021): Modelling of solute transport and microbial activity in diffusion cells simulating a bentonite barrier of a spent nuclear fuel repository. Applied Clay Science, 211, 106193. https://doi.org/10.1016/J.CLAY.2021.106193

Kim, J.I. (1994): Actinide Colloids in Natural Aquifer Systems. MRS Bulletin, 19/12, 47-53. https://doi.org/10.1557/S0883769400048703

King, F., Kolar, M., Stroes-Gascoyne, S., Bellingham, P., James, C.H.U. & Awe, P. v.d. (1999): Modelling the Activity of Sulphate-Reducing Bacteria and the Effects on Container Corrosion in an Underground Nuclear Waste Disposal Vault. MRS Online Proceedings Library (OPL), 556, 1167. https://doi.org/10.1557/PROC-556-1167

Kosakowski, G. & Berner, U. (2013): The evolution of clay rock/cement interfaces in a cementitious repository for low- and intermediate level radioactive waste. Physics and Chemistry of the Earth, Parts A/B/C, 64, 65-86. https://doi.org/10.1016/j.pce.2013.01.003

Kosakowski, G. & Smith, P. (2014): Long-term evolution of the Engineered Gas Transport System. Nagra Arbeitsbericht NAB 14-16.

Kosakowski, G. & Wieland, E. (2022): Assessing the impact of chemical processes on the long-term evolution of waste packages by geochemical modelling. In NUWCEM 2022 - International Symposium on Cement-Based Materials for Nuclear Wastes May 4-6 2022, Avignon, France. CEA.

Kosakowski, G., Berner, U., Wieland, E., Glaus, M.A. & Degueldre, C. (2014): Geochemical evolution of the L/ILW near-field. Naga Technical Report NTB 14-11.

Kosakowski, G., Huang, Y. & Wieland, E. (2020): Influence of material heterogeneities, process couplings and aggregate reactivity on the geochemical evolution of the L/ILW repository. Nagra Arbeitsbericht NAB 20-11.

Kretzschmar, R. & Schafer, T. (2005): Metal Retention and Transport on Colloidal Particles in the Environment. Elements, 1/4, 205-210. https://doi.org/10.2113/gselements.1.4.205

Kulik, D.A. (2011): Improving the structural consistency of C-S-H solid solution thermodynamic models. Cement and Concrete Research, 41/5, 477-495. https://doi.org/10.1016/j.cemconres.2011.01.012

Kulik, D.A., Miron, G.D. & Lothenbach, B. (2022): A structurally-consistent CASH+ sublattice solid solution model for fully hydrated C-S-H phases: Thermodynamic basis, methods, and Ca-Si- H_2O core sub-model. Cement and Concrete Research, 151. https://doi.org/10.1016/j.cemconres.2021.106585

Kündig, R., Mumenthaler, T., Eckardt, P., Keusen, H.R., Schindler, C., Hofmann, F., Vogler, R. & Guntli, P. (1997): Die mineralischen Rohstoffe der Schweiz. Schweizerische Geotechnische Kommission, Zürich, Switzerland.

Kunhi Mohamed, A., Moutzouri, P., Berruyer, P., Walder, B. J., Siramanont, J., Harris, M., Negroni, M., Galmarini, S.C., Parker, S.C., Scrivener, K.L., Emsley, L. & Bowen, P. (2020): The Atomic-Level Structure of Cementitious Calcium Aluminate Silicate Hydrate. Journal of the American Chemical Society, 142/25, 11060-11071. https://doi.org/10.1021/jacs.0c02988

Kurganskaya, I. & Rohlfs, R.D. (2020): Atomistic to meso-scale modeling of mineral dissolution: Methods, challenges and prospects. American Journal of Science, 320/1, 1-26. https://doi.org/10.2475/01.2020.02

L'Hôpital, E., Lothenbach, B., Le Saout, G., Kulik, D.A. & Scrivener, K. (2015): Incorporation of aluminium in calcium-silicate-hydrates. Cement and Concrete Research, 75, 91-103. https://doi.org/10.1016/j.cemconres.2015.04.007

L'Hostis, V., Neff, D., Bellot-Gurlet, L. & Dillmann, P. (2009): Characterization of long-term corrosion of rebars embedded in concretes sampled on French historical buildings aged from 50 to 80 years. Materials and Corrosion, 60/2, 93-98. https://doi.org/10.1002/MACO.200805019

Labhasetwar, N.K., Shrivastava, O.P. & Medikov, Y.Y. (1991): Mössbauer study on iron-exchanged calcium silicate hydrate: $Ca_{5-x}Fe_xSi_6O_{18}$ H_2 · n H_2O. Journal of Solid State Chemistry, 93/1, 82-87. https://doi.org/10.1016/0022-4596(91)90277-O

Ladd, A.J.C. & Szymczak, P. (2021): Reactive Flows in Porous Media: Challenges in Theoretical and Numerical Methods. Annual Review of Chemical and Biomolecular Engineering, 12/1, 543-571. https://doi.org/10.1146/annurev-chembioeng-092920-102703

Lalan, P., Dauzères, A., De Windt, L., Bartier, D., Sammaljärvi, J., Barnichon, J.-D., Techer, I. & Detilleux, V. (2016): Impact of a 70 °C temperature on an ordinary Portland cement paste/claystone interface: An in situ experiment. Cement and Concrete Research, 83, 164-178. https://doi.org/10.1016/j.cemconres.2016.02.001

Landolt, D., Davenport, A., Payer, J. & Shoesmith, D.W. (2009): A review of materials and corrosion issues regarding canisters for disposal of spent fuel and high-level waste in Opalinus Clay. Nagra Technical Report NTB 09-02.

Langton, C. & Kosson, D. (2009): Review of mechanistic understanding and modeling and uncertainty analysis methods for predicting cementitious barrier performance. Report No. CBP-TR-2009-002.

Lanyon, G.W. (2019a): Current understanding of self-sealing of clay-rich rocks for deep geological disposal. Nagra Arbeitsbericht NAB 18-46.

Lanyon, G.W. (2019b): Update of synopsis regarding EDZ development and evolution at the Mont Terri Rock Laboratory. Nagra Arbeitsbericht NAB 18-45.

Lasaga, A.C. (1981a): Chapter 4. Transition State Theory. In A. C. Lasaga & J. Kirkpatrick (Eds.), Kinetics of Geochemical Processes (pp. 135-170). De Gruyter, Berlin, Boston. https://doi.org/10.1515/9781501508233-008

Lasaga, A.C. (1981b): Kinetics of Geochemical Processes. (A.C. Lasaga & J. Kirkpatrick, Eds.), Kinetics of Geochemical Processes, Reviews in Mineralogy Vol. 8. De Gruyter, Berlin, Boston. https://doi.org/10.1515/9781501508233

Lassin, A., Dymitrowska, M. & Azaroual, M. (2011): Hydrogen solubility in pore water of partially saturated argillites: Application to Callovo-Oxfordian clayrock in the context of a nuclear waste geological disposal. Physics and Chemistry of the Earth, 36/17-18, 1721-1728. https://doi.org/10.1016/j.pce.2011.07.092

Lau, M.C.Y., Kieft, T.L., Kuloyo, O., Linage-Alvarez, B., Heerden, E. Van, Lindsay, M.R., Magnabosco, C.,Wang, W., Wiggins, J.B., Guo, L., Perlman, D.H., Kyin, S., Shwe, H.H., Harris, R.L., Oh, Y., Yi, M.J., Purtschert, R., Slater, G.F., Wei, S., Li, L., Sherwood Lollar, B., Onstott, T.C. & Ono, S. (2016): An oligotrophic deep-subsurface community dependent on syntrophy is dominated by sulfur-driven autotrophic denitrifiers. Proceedings of the National Academy of Sciences of the United States of America, 113/49, E7927-E7936. https://doi.org/10.1073/PNAS.1612244113

Le Bescop, P., Lothenbach, B., Samson, E. & Snyder, K.A. (2013): Modeling Degradation of Cementitious Materials in Aggressive Aqueous Environments. In M. Alexander, A. Bertron & N. De Belie (Eds.), Performance of Cement-Based Materials in Aggressive Aqueous Envorionments, pp. 177-218. Springer, Dordrecht. https://doi.org/10.1007/978-94-007-5413-3_7

Lee, L.I.N. (2001): Soil-pile interaction of bored and cast in-situ piles. Doctoral thesis. University of Birmingham.

Leemann, A. & Moro, F. (2017): Carbonation of concrete: the role of CO_2 concentration, relative humidity and CO_2 buffer capacity. Materials and Structures, 50/1, 30. https://doi.org/10.1617/s11527-016-0917-2

Leemann, A., Katayama, T., Fernandes, I. & Broekmans, M.A.T.M. (2016): Types of alkali-aggregate reactions and the products formed. Proceedings of the Institution of Civil Engineers – Construction Materials, 169/3, 128-135. https://doi.org/10.1680/jcoma.15.00059

Leemann, A., Shi, Z. & Lindgård, J. (2020): Characterization of amorphous and crystalline ASR products formed in concrete aggregates. Cement and Concrete Research, 137, 106190. https://doi.org/10.1016/j.cemconres.2020.106190

Lerouge, C., Claret, F., Tournassat, C., Grangeon, S., Gaboreau, S., Boyer, B., Borschnek, D. & Linard, Y. (2014): Constraints from sulfur isotopes on the origin of gypsum at concrete/claystone interfaces. Physics and Chemistry of the Earth, Parts A/B/C, 70-71, 84-95. https://doi.org/10.1016/j.pce.2014.01.003

Lerouge, C., Gaboreau, S., Grangeon, S., Claret, F., Warmont, F., Jenni, A., Cloet, V. & Mäder, U.K. (2017): In situ interactions between Opalinus Clay and Low Alkali Concrete. Physics and Chemistry of the Earth, 99, 3-21. https://doi.org/10.1016/j.pce.2017.01.005

Leupin, O.X., Bernier-Latmani, R., Bagnoud, A., Moors, H., Leys, N., Wouters, K. & Stroes-Gascoyne, S. (2017): Fifteen years of microbiological investigation in Opalinus Clay at the Mont Terri rock laboratory (Switzerland). Swiss Journal of Geosciences, 110/1, 343-354. https://doi.org/10.1007/s00015-016-0255-y

Leupin, O.X., Smith, P., Marschall, P., Johnson, L., Savage, D., Cloet, V., Schneider, J. & Senger, R. (2016b): Low- and intermediate-level waste repository-induced effects. Nagra Technical Report 14-14.

Leupin, O.X., Zeyer, J., Cloet, V., Smith, P., Marschall, P., Papafotiou, A., Schwyn, B., Bernier-Latmani, R., Marschall, P., Papafotiou, A., Schwyn, B. & Stroes-Gascoyne, S. (2016a): An assessment of the possible fate of gas generated on a repository for low- and intermediate-level waste. Nagra Technical Report NTB 16-05.

Li, D., Kaplan, D.I., Roberts, K.A. & Seaman, J.C. (2012): Mobile Colloid Generation Induced by a Cementitious Plume: Mineral Surface-Charge Controls on Mobilization. Environmental Science & Technology, 46/5, 2755-2763. https://doi.org/10.1021/ es2040834

Libert, M., Bildstein, O., Esnault, L., Jullien, M. & Sellier, R. (2011): Molecular hydrogen: An abundant energy source for bacterial activity in nuclear waste repositories. Physics and Chemistry of the Earth, 36/17-18, 1616-1623. https://doi.org/10.1016/j.pce.2011.10.010

Lin, L.H., Wang, P.L., Rumble, D., Lippmann-Pipke, J., Boice, E., Pratt, L.M., Lollar, B.S., Brodie, E.L., Hazen, T.C., Andersen, G.L., DeSantis, T.Z., Moser, D.P., Kershaw, D. & Onstott, T. C. (2006): Long-term sustainability of a high-energy, low-diweniff crystal-biome. Science, 314/5798, 479-482. DOI: 10.1126/science.1127376

Lindgård, J., Andiç-Çakır, Ö., Fernandes, I., Rønning, T.F. & Thomas, M.D.A. (2012): Alkali-silica reactions (ASR): Literature review on parameters influencing laboratory performance testing. Cement and Concrete Research, 42/2, 223-243. https://doi.org/10.1016/j.cemconres.2011.10.004

Liu, D., Yuan, P., Liu, H., Li, T., Tan, D., Yuan, W. & He, H. (2013): High-pressure adsorption of methane on montmorillonite, kaolinite and illite. Applied Clay Science, 85/1, 25-30. https://doi.org/10.1016/j.clay.2013.09.009

Lodge, T.P. & Hiemenz, P.C. (2020): Polymer Chemistry 3rd Edition. CRC Press, Boca Raton. https://doi.org/10.1201/9780429190810

López, W. & González, J.A. (1993): Influence of the degree of pore saturation on the resistivity of concrete and the corrosion rate of steel reinforcement. Cement and Concrete Research, 23/2, 368-376. https://doi.org/10.1016/0008-8846(93)90102-F

Lothenbach, B. & Nonat, A. (2015): Calcium silicate hydrates: Solid and liquid phase composition. Cement and Concrete Research, 78, 57-70. https://doi.org/10.1016/j.cemconres.2015.03.019

Lothenbach, B. & Wieland, E. (2006): A thermodynamic approach to the hydration of sulphate-resisting Portland cement. Waste Management, 26/7, 706-19. https://doi.org/10.1016/j.wasman.2006.01.023

Lothenbach, B., Bernard, E. & Mäder, U.K. (2017): Zeolite formation in the presence of cement hydrates and albite. Physics and Chemistry of the Earth, Parts A/B/C, 99, 77-94. https://doi.org/10.1016/j.pce.2017.02.006

Lothenbach, B., Kulik, D.A., Matschei, T., Balonis, M., Baquerizo, L., Dilnesa, B., Miron, G.D. & Myers, R. J. (2019): Cemdata18: A chemical thermodynamic database for hydrated Portland cements and alkali-activated materials. Cement and Concrete Research, 115, 472-506. https://doi.org/10.1016/j.cemconres.2018.04.018

Lothenbach, B., Le Saout, G., Ben Haha, M., Figi, R. & Wieland, E. (2012): Hydration of a low-alkali CEM III/B-SiO_2 cement (LAC). Cement and Concrete Research, 42/2, 410-423. https://doi.org/10.1016/j.cemconres.2011.11.008

Lothenbach, B., Matschei, T., Möschner, G. & Glasser, F.P. (2008): Thermodynamic modelling of the effect of temperature on the hydration and porosity of Portland cement. Cement and Concrete Research, 38/1, 1-18. https://doi.org/10.1016/j.cemconres.2007.08.017

Lothenbach, B., Rentsch, D. & Wieland, E. (2014): Hydration of a silica fume blended low-alkali shotcrete cement. Physics and Chemistry of the Earth, Parts A/B/C, 70-71, 3-16. https://doi.org/10.1016/j.pce.2013.09.007

Luraschi, P., Gimmi, T., Van Loon, L.R., Shafizadeh, A. & Churakov, S.V. (2020): Evolution of HTO and $^{36}Cl^-$ diffusion through a reacting cement-clay interface (OPC paste-Na montmorillonite) over a time of six years. Applied Geochemistry, 104581. https://doi.org/10.1016/j.apgeochem.2020.104581

Luttge, A., Arvidson, R.S. & Fischer, C. (2013): A Stochastic Treatment of Crystal Dissolution Kinetics. Elements, 9/3, 183-188. https://doi.org/10.2113/gselements.9.3.183

Ma, B. & Lothenbach, B. (2020a): Synthesis, characterization, and thermodynamic study of selected Na-based zeolites. Cement and Concrete Research, 135, 106111. https://doi.org/10.1016/j.cemconres.2020.106111

Ma, B. & Lothenbach, B. (2020b): Thermodynamic study of cement/rock interactions using experimentally generated solubility data of zeolites. Cement and Concrete Research, 135, 106149. https://doi.org/10.1016/j.cemconres.2020.106149

Ma, B., Fernandez-Martinez, A., Madé, B., Findling, N., Markelova, E., Salas-Colera, E., Maffeis, T.G.G., Lewis, A.R., Tisserand, D., Bureau, S. & Charlet, L. (2018): XANES-Based Determination of Redox Potentials Imposed by Steel Corrosion Products in Cement-Based Media. Environmental Science & Technology, 52/20, 11931-11940. https://doi.org/10.1021/acs.est.8b03236

Ma, B., Fernandez-Martinez, A., Mancini, A. & Lothenbach, B. (2021): Spectroscopic investigations on structural incorporation pathways of FeIII into zeolite frameworks in cement-relevant environments. Cement and Concrete Research, 140, 106304. https://doi.org/10.1016/j.cemconres.2020.106304

Maanoja, S., Lakaniemi, A.M., Lehtinen, L., Salminen, L., Auvinen, H., Kokko, M., Palmroth, M., Muuri, E. & Rintala, J. (2020): Compacted bentonite as a source of substrates for sulfate-reducing microorganisms in a simulated excavation-damaged zone of a spent nuclear fuel repository. Applied Clay Science, 196, 105746. https://doi.org/10.1016/J.CLAY.2020.105746

MacQuarrie, K.T.B. & Mayer, K.U. (2005): Reactive transport modeling in fractured rock: A state-of-the-science review. Earth-Science Reviews, 72/3-4, 189-227. https://doi.org/10.1016/j.earscirev.2005.07.003

Mäder, U.K. & Adler, M. (2004): Mass balance estimate of cement - clay stone interaction with application to an HLW repository in Opalinus Clay. Chapter 8.4 of ECOCLAY-II, Final Report, WP-3.

Mäder, U.K. & Wersin, P. (2023): Reference porewaters for SGT Stage 3 of the Opalinus Clay for the siting regions Jura Ost (JO), Nördlich Lägern (NL) and Zürich Nordost (ZNO). Nagra Arbeitsbericht NAB 22-47.

Mäder, U.K. (2009): Reference pore water for the Opalinus Clay and "Brown Dogger" for the provisional safety-analysis in the framework of the sectoral plan - interim results (SGT-ZE). Nagra Arbeitsbericht NAB 09-14.

Mäder, U.K., Jenni, A., Lerouge, C., Gaboreau, S., Miyoshi, S., Kimura, Y., Cloet, V., Fukaya, M., Claret, F., Otake, T., Shibata, M. & Lothenbach, B. (2017): 5-year chemico-physical evolution of concrete-claystone interfaces, Mont Terri rock laboratory (Switzerland). Swiss Journal of Geosciences, 110/1, 307-327. https://doi.org/10.1007/s00015-016-0240-5

Maher, K., DePaolo, D.J. & Lin, J.C.F. (2004): Rates of silicate dissolution in deep-sea sediment: In situ measurement using $^{234}U/^{238}U$ of pore fluids. Geochimica et Cosmochimica Acta, 68/22, 4629-4648. https://doi.org/10.1016/J.GCA.2004.04.024

Malik, M., Bhattacharyya, S.K. & Barai, S.V (2021): Thermal and mechanical properties of concrete and its constituents at elevated temperatures: A review. Construction and Building Materials, 270, 121398. https://doi.org/10.1016/J.CONBUILDMAT.2020.121398

Malinowski, R. (1979): Concretes and mortars in ancient aqueducts. Concrete International, 1/1, 66-76.

Mancini, A., Lothenbach, B., Geng, G., Grolimund, D., Sanchez, D.F., Fakra, S.C., Dähn, R., Wehrli, B. & Wieland, E. (2021b): Iron speciation in blast furnace slag cements. Cement and Concrete Research, 140, 106287. https://doi.org/10.1016/J.CEMCONRES.2020.106287

Mancini, A., Wieland, E., Geng, G., Dähn, R., Skibsted, J., Wehrli, B. & Lothenbach, B. (2020): Fe(III) uptake by calcium silicate hydrates. Applied Geochemistry, 113. https://doi.org/10.1016/j.apgeochem.2019.104460

Mancini, A., Wieland, E., Geng, G., Lothenbach, B., Wehrli, B. & Dähn, R. (2021a): Fe(II) interaction with cement phases: Method development, wet chemical studies and X-ray absorption spectroscopy. Journal of Colloid and Interface Science, 588, 692-704. https://doi.org/10.1016/J.JCIS.2020.11.085

Martin, L., Jacobs, F., Loser, R., Lothenbach, B., Leemann, A. & Winnefeld, F. (*in prep.*): Using calcareous aggregates in backfill mortar M1: A suitability assessment in backfill mortar M1. Nagra Arbeitsbericht NAB 22-44.

Martin, L., Kosakowski, G., Papafotiou, A. & Smith, P.A. (2023): Evolution of the Sealing System Porosity and its Impact on Performance. Nagra Arbeitsbericht NAB 23-21.

Martin, L., Leemann, A., Milodowski, A.E., Mäder, U.K., Münch, B. & Giroud, N. (2016): A natural cement analogue study to understand the long-term behaviour of cements in nuclear waste repositories: Maqarin (Jordan). Applied Geochemistry, 71, 20-34. https://doi.org/10.1016/j.apgeochem.2016.05.009

Marty, N.C.M., Bildstein, O., Blanc, P., Claret, F., Cochepin, B., Gaucher, E.C., Jacques, D., Lartigue, J.-E., Liu, S., Mayer, K.U., Meeussen, J.C.L., Munier, I., Pointeau, I., Su, D. & Steefel, C.I. (2015a): Benchmarks for multicomponent reactive transport across a cement/clay interface. Computational Geosciences, 19/3, 635-653. https://doi.org/10.1007/s10596-014-9463-6

Marty, N.C.M., Claret, F., Lassin, A., Tremosa, J., Blanc, P., Madé, B., Giffaut, E., Cochepin, B. & Tournassat, C. (2015b): A database of dissolution and precipitation rates for clay-rocks minerals. Applied Geochemistry, 55, 108-118. https://doi.org/10.1016/j.apgeochem.2014.10.012

Marty, N.C.M., Munier, I., Gaucher, E.C., Tournassat, C., Gaboreau, S., Vong, C. Q., Giffaut, E., Cochepin, B. & Claret, F. (2014): Simulation of cement/clay interactions: Feedback on the increasing complexity of modelling strategies. Transport in Porous Media, 104/2, 385-405. https://doi.org/10.1007/s11242-014-0340-5

Marty, N.C.M., Tournassat, C., Burnol, A., Giffaut, E. & Gaucher, E.C. (2009): Influence of reaction kinetics and mesh refinement on the numerical modelling of concrete/clay interactions. Journal of Hydrology, 364/1-2, 58-72. https://doi.org/10.1016/j.jhydrol.2008.10.013

Martys, N.S. (1999): Diffusion in partially-saturated porous materials. Materials and Structures, 32/8, 555-562. https://doi.org/10.1007/BF02480489

Matschei, T., Lothenbach, B. & Glasser, F.P. (2007): The role of calcium carbonate in cement hydration. Cement and Concrete Research, 37/4, 551-558. https://doi.org/10.1016/J.CEMCONRES.2006.10.013

Mazurek, M., Aschwanden, L., Camesi, L., Gimmi, T., Jenni, A., Kicka, M., Mäder, U.K., Rufer, D., Waber, H.N., Wanner, P., Wersin, P. & Traber, D. (2021): TBO Bülach-1-1: Data Report, Dossier VIII: Rock Properties, Porewater Characterisation and Natural Tracer Profiles. Nagra Arbeitsbericht NAB 20-08.

McCarthy, J.F. & Degueldre, C. (1993): Sampling and Characterization of colloids in groundwater for studying their role in contaminant transport, Environmental Particles. In J. Buffle & H. van Leeuwen (Eds.), Environmental Particles Vol. 2 (IUPAC Seri, Vol. 2, pp. 247-315). Lewis Publishers, Boca Raton, USA.

McCarthy, J.F. & Zachara, J.M. (1989): Subsurface transport of contaminants. Environmental Science and Technology, 23/5, 496-502. https://doi.org/10.1021/es00063a001

McCollom, T. M. & Seewald, J.S. (2001): A reassessment of the potential for reduction of dissolved CO_2 to hydrocarbons during serpentinization of olivine. Geochimica et Cosmochimica Acta, 65/21, 3769-3778. https://doi.org/10.1016/S0016-7037(01)00655-X

McKinley, I.G. & Grogan, H.A. (1991): Consideration of microbiology in modelling the near field of an L/ILW repository. Experientia 1991, 47/6, 573-577. https://doi.org/10.1007/BF01949879

McKinley, I.G., Hagenlocher, I., Alexander, W.R. & Schwyn, B. (1997): Microbiology in nuclear waste disposal: interfaces and reaction fronts. FEMS Microbiology Reviews, 20/3-4, 545-556. https://doi.org/10.1111/J.1574-6976.1997.TB00337.X

Meldrum, F.C. & O'Shaughnessy, C. (2020, August 1): Crystallization in Confinement. Advanced Materials. Wiley-VCH Verlag. https://doi.org/10.1002/adma.202001068

Mercury, L. & Tardy, Y. (2001): Negative pressure of stretched liquid water. Geochemistry of soil capillaries. Geochimica et Cosmochimica Acta, 65/20, 3391-3408. https://doi.org/10.1016/S0016-7037(01)00646-9

Metcalfe, R. & Walker, C. (2004): Proceedings of the International Workshop on Bentonite-Cement Interaction in Repository Environments, 14-16 April 2004, Tokyo, Japan. Technical Report NUMO-TR-04-05October.

Miron, G.D., Kulik, D.A., Yan, Y., Tits, J. & Lothenbach, B. (2022): Extensions of CASH+ thermodynamic solid solution model for the uptake of alkali metals and alkaline earth metals in C-S-H. Cement and Concrete Research, 152, 106667. https://doi.org/10.1016/J.CEMCONRES.2021.106667

Moir, G.K. & Glasser, F.P. (1992): Mineralisers modifiers and activators in the clinkering process. In 9th International Congress on the Chemistry of Cement, Congress Reports, Volume I (pp. 125-152). National Council for Cement and Building Materials, New Dehli, India.

Molins, S. & Knabner, P. (2019): Multiscale approaches in reactive transport modeling. Reviews in Mineralogy and Geochemistry, 85/1, 27-48. https://doi.org/10.2138/rmg.2019.85.2

Mon, A., Samper, J., Montenegro, L., Naves, A. & Fernández, J. (2017): Long-term non-isothermal reactive transport model of compacted bentonite, concrete and corrosion products in an HLW repository in clay. Journal of Contaminant Hydrology, 197, 1-16. https://doi.org/10.1016/J.JCONHYD.2016.12.006

Mondelli, C., Bardelli, F., Vitillo, J. G., Didier, M., Brendle, J., Cavicchia, D. R., Robinet, J.C. & Charlet, L. (2015): Hydrogen adsorption and diffusion in synthetic Na-montmorillonites at high pressures and temperature. International Journal of Hydrogen Energy, 40/6, 2698-2709. https://doi.org/10.1016/j.ijhydene.2014.12.038

Monnier, J., Bellot-Gurlet, L., Baron, D., Neff, D., Guillot, I. & Dillmann, P. (2011): A methodology for Raman structural quantification imaging and its application to iron indoor atmospheric corrosion products. Journal of Raman Spectroscopy, 42/4, 773-781. https://doi.org/10.1002/JRS.2765

Morandeau, A., Thiéry, M. & Dangla, P. (2014): Investigation of the carbonation mechanism of CH and C-S-H in terms of kinetics, microstructure changes and moisture properties. Cement and Concrete Research, 56, 153-170. https://doi.org/10.1016/j.cemconres.2013.11.015

Moropoulou, A., Bakolas, A. & Anagnostopoulou, S. (2005): Composite materials in ancient structures. Cement and Concrete Composites, 27/2, 295-300. https://doi.org/10.1016/j.cemconcomp.2004.02.018

Möschner, G., Lothenbach, B., Winnefeld, F., Ulrich, A., Figi, R. & Kretzschmar, R. (2009): Solid solution between Al-ettringite and Fe-ettringite ($Ca_6[Al_{1-x}Fe_x(OH)_6]_2(SO_4)_3 \cdot 26H_2O$). Cement and Concrete Research, 39/6, 482-489. https://doi.org/10.1016/j.cemconres.2009.03.001

Muhammed, N.S., Haq, B., al Shehri, D., Al-Ahmed, A., Rahman, M.M. & Zaman, E. (2022): A review on underground hydrogen storage: Insight into geological sites, influencing factors and future outlook. Energy Reports, 8, 461-499. https://doi.org/10.1016/J.EGYR.2021.12.002

Muntean, A., Böhm, M. & Kropp, J. (2011): Moving carbonation fronts in concrete: A moving-sharp-interface approach. Chemical Engineering Science, 66/3, 538-547. https://doi.org/10.1016/j.ces.2010.11.011

Nagra (1994): Bericht zur Langzeitsicherheit des Endlagers SMA am Standort Wellenberg (Gemeinde Wolfenschiessen, NW). Nagra Technischer Bericht NTB 94-06.

Nagra (2002a): Project Opalinus Clay: Safety Report. Nagra Technical Report NTB 02-05.

Nagra (2002b): Projekt Opalinuston: Synthese der geowissenschaftlichen Untersuchungsergebnisse: Entsorgungsnachweis für abgebrannte Brennelemente, verglaste hochaktive sowie langlebige mittelaktive Abfälle. Nagra Technischer Bericht NTB 02-03.

Nagra (2008a): Effects of post-disposal gas generation in a repository for low- and intermediate-level waste sited in the Opalinus Clay of Northern Switzerland. Nagra Technical Report NTB 08-07.

Nagra (2008b): Proposal for geological site selection for L/ILW and HLW repositories. Statement of requirements, procedure and results. Nagra Technical Report NTB 08-03.

Nagra (2014a): Modellhaftes Inventar für radioaktive Materialien MIRAM 14. Nagra Technical Report NTB 14-04.

Nagra (2014b): Provisional Safety Analyses for SGT Stage 2: Models, Codes and General Modelling Approach. Nagra Technical Report NTB 14-09.

Nagra (2021a): Methodik zur Definition des Mindestabstands zwischen den HAA- und SMA-Lagerteilen im Kombilager. Nagra Arbeitsbericht NAB 20-31.

Nagra (2021b): The Nagra Research, Development and Demonstration (RD&D) Plan for the Disposal of Radioactive Waste in Switzerland. Nagra Technical Report 21-02.

Nagra (2021c): Verschlusskonzept für ein geologisches Tiefenlager. Nagra Arbeitsbericht NAB 21-12.

Nagra (2021d): Waste Management Programme 2021 of the Waste Producers. Nagra Technical Report NTB 21-01E.

Nagra (2022): Ableitung Anforderungen an Lagerauslegung aus Sicht Langzeitsicherheit. Nagra Arbeitsbericht NAB 21-02.

Nagra (2023a): Chemical Criteria for Waste Group Classification: A model approach. Nagra Arbeitsbericht NAB 23-28.

Nagra (2023b): Modellhaftes Inventar für radioaktive Materialien MIRAM RBG. Nagra Technischer Bericht NTB 22-05.

Nagra NTB 24-17 (*in prep.*): Geosynthesis. Nagra Technischer Bericht NTB 24-17.

Nagra NTB 24-22 (*in prep.*): Synthesis of the Performance Assessment for a Combined Repository at the Nördlich Lägern Site. Nagra Technical Report NTB 24-22.

Nagra NTB 24-23 (*in prep.*): Production, consumption and transport of gases in a deep geological repository for combined disposal in Switzerland. Nagra Technical Report NTB 24-23.

Nakarai, K., Shibata, M., Sakamoto, H., Owada, H. & Kosakowski, G. (2021b): Calcite Precipitation at Cement-Bentonite Interface. Part 1: Effect of Carbonate Admixture in Bentonite. Journal of Advanced Concrete Technology, 19/5, 433-446. https://doi.org/10.3151/jact.19.433

Nakarai, K., Watanabe, M., Koibuchi, K. & Kosakowski, G. (2021a): Calcite Precipitation at Cement-Bentonite Interface. Part 2: Accelera-tion of Transport by an Electrical Gradient. Journal of Advanced Concrete Technology, 19/5, 447-461. https://doi.org/10.3151/j act.19.447

NEA (2013): Chemical thermodynamics of iron Part 1. OECD Publishing, Paris.

Necib, S., Diomidis, N., Keech, P. & Nakayama, M. (2018): Corrosion of carbon steel in clay environments relevant to radioactive waste geological disposals, Mont Terri rock laboratory (Switzerland). Birkhäuser, Cham, Switzerland. https://doi.org/10.1007/978-3-319-70458-6_17

Neeft, E., Jacques, D. & Deissmann, G. (2022): Initial State of the Art on the assessment of the chemical evolution of ILW and HLW disposal cells. Deliverable D 2.1 of the HORIZON 2020 project EURAD. EC Grant agreement no: 847593.

Neff, D., Dillmann, P., Bellot-Gurlet, L. & Beranger, G. (2005): Corrosion of iron archaeological artefacts in soil: characterisation of the corrosion system. Corrosion Science, 47/2, 515-535. https://doi.org/10.1016/J.CORSCI.2004.05.029

Nishiyama, N. & Yokoyama, T. (2013): Does the reactive surface area of sandstone depend on water saturation?-The role of reactive-transport in water film. Geochimica et Cosmochimica Acta, 122, 153-169. https://doi.org/10.1016/j.gca.2013.08.024

Nishiyama, N. & Yokoyama, T. (2021): Water Film Thickness in Unsaturated Porous Media: Effect of Pore Size, Pore Solution Chemistry, and Mineral Type. Water Resources Research, 57/6, e2020WR029257. https://doi.org/10.1029/2020WR029257

Noiriel, C. & Daval, D. (2017): Pore-Scale Geochemical Reactivity Associated with CO_2 Storage: New Frontiers at the Fluid-Solid Interface. Accounts of Chemical Research 50/4, 759-768. https://doi.org/10.1021/acs.accounts.7b00019

Nyyssönen, M., Hultman, J., Ahonen, L., Kukkonen, I., Paulin, L., Laine, P., Itävaara, M. & Auvinen, P. (2013): Taxonomically and functionally diverse microbial communities in deep crystalline rocks of the Fennoscandian shield. The ISME Journal 2014, 8/1, 126-138. https://doi.org/10.1038/ismej.2013.125

O'Donovan, R., O'Rourke, B.D., Ruane, K.D. & Murphy, J.J. (2013): Anaerobic Corrosion of Reinforcement. Key Engineering Materials, 569-570, 1124-1131. https://doi.org/10.4028/WWW.SCIENTIFIC.NET/KEM.569-570.1124

Ochs, M., Dolder, F. & Tachi, Y. (2022): Decrease of radionuclide sorption in hydrated cement systems by organic ligands: Comparative evaluation using experimental data and thermodynamic calculations for ISA/EDTA-actinide-cement systems. Applied Geochemistry, 136. https://doi.org/10.1016/j.apgeochem.2021.105161

Ochs, M., Mallants, D. & Wang, L. (2016): Cementitious Materials and Their Sorption Properties. In Radionuclide and Metal Sorption on Cement and Concrete (Topics in Safety, Risk, Reliability and Quality) (pp. 5-16). Springer, Cham. https://doi.org/10.1007/978-3-319-23651-3_2

Offeddu, F.G., Cama, J., Soler, J.M., Dávila, G., McDowell, A., Craciunescu, T. & Tiseanu, I. (2015): Processes affecting the efficiency of limestone in passive treatments for AMD: Column experiments. Journal of Environmental Chemical Engineering, 3/1, 304-316. https://doi.org/10.1016/j.jece.2014.10.013

Olsson, N., Lothenbach, B., Baroghel-Bouny, V. & Nilsson, L.-O. (2018): Unsaturated ion diffusion in cementitious materials - The effect of slag and silica fume. Cement and Concrete Research, 108, 31-37. https://doi.org/10.1016/J.CEMCONRES.2018.03.007

Owusu, J.P., Karalis, K., Prasianakis, N.I. & Churakov, S.V. (2022): Mobility of Dissolved Gases in Smectites under Saturated Conditions: Effects of Pore Size, Gas Types, Temperature, and Surface Interaction. The Journal of Physical Chemistry C, 126/40, 17441-17455. https://doi.org/10.1021/acs.jpcc.2c05678

Pagel, M., Ruhlmann, F. & Bruneton, P. (1993): The Cigar Lake uranium deposit, Saskatchewan, Canada. Canadian Journal of Earth Sciences, 30/4, 651-652. https://doi.org/10.1139/e93-053

Palandri, J.L. & Kharaka, Y.K. (2004): A compilation of rate parameters of water-mineral interaction kinetics for application to geochemical modeling. U.S. Geological Survey. Open File Report 2004-1068.

Pallagi, A., Bajnoczi, E.G., Canton, S.E., Bolin, T., Peintler, G., Kutus, B., Kele, Z., Palinko, I. & Sipos, P. (2014): Multinuclear Complex Formation between Ca(II) and Gluconate Ions in Hyperalkaline Solutions. Environmental Science & Technology, 48/12, 6604-6611. https://doi.org/10.1021/es501067w

Pally, D., le Bescop, P., Schlegel, M.L., Miserque, F., Chomat, L., Neff, D. & L'Hostis, V. (2020): Corrosion behavior of iron plates in cementitious solution at 80 °C in anaerobic conditions. Corrosion Science, 170, 108650. https://doi.org/10.1016/j.corsci.2020.108650

Panfilov, M. & Panfilov, M. (2010): Underground Storage of Hydrogen: In Situ Self-Organisation and Methane Generation. Transport in Porous Media 2010, 85/3, 841-865. https://doi.org/10.1007/S11242-010-9595-7

Papafotiou, A. & Senger, R. (2014): Sensitivity analyses of gas release from an L/ILW repository in the Opalinus Clay in the candidate siting regions of Northern Switzerland. Nagra Arbeitsbericht NAB 13-92.

Papafotiou, A. & Senger, R. (2016): Sensitivity analyses of gas releases from an L/ILW repository in the Opalinus Clay including the microbial consumption of hydrogen. Nagra Arbeitsbericht NAB 16-07.

Parnell, J., Boyce, A.J., Hurst, A., Davidheiser-Kroll, B. & Ponicka, J. (2013): Long term geological record of a global deep subsurface microbial habitat in sand injection complexes. Scientific Reports, 3. https://doi.org/10.1038/SREP01828

Parrott, L.J. & Killoh, D.C. (1989): Carbonation in a 36 year old, in-situ concrete. Cement and Concrete Research, 19/4, 649-656. https://doi.org/10.1016/0008-8846(89)90017-3

Pauling, L. (1931): The nature of the chemical bond. II. The one-electron bond and the three-electron bond. Journal of the American Chemical Society, 53/9, 3225-3237.

Pekala, M., Wersin, P., Pastina, B., Lamminmäki, R., Vuorio, M. & Jenni, A. (2021): Potential impact of cementitious leachates on the buffer porewater chemistry in the Finnish repository for spent nuclear fuel - A reactive transport modelling assessment. Applied Geochemistry, 131, 105045. https://doi.org/10.1016/j.apgeochem.2021.105045

Phillips, A.J., Lauchnor, E., Eldring, J., Esposito, R., Mitchell, A. C., Gerlach, R., Cunningham, A.B. & Spangler, L.H. (2013): Potential CO_2 leakage reduction through biofilm-induced calcium carbonate precipitation. Environmental Science and Technology, 47/1, 142-149. https://doi.org/10.1021/es301294q

Pichler, M. (2013): Assessment of hydrogen - rock interaction during geological storage of CH_4 - H_2 mixtures. Master thesis. Montanuniversität Leoben.

Pignatelli, I., Kumar, A., Alizadeh, R., Le Pape, Y., Bauchy, M. & Sant, G. (2016): A dissolution-precipitation mechanism is at the origin of concrete creep in moist environments. The Journal of Chemical Physics, 145/5, 054701. https://doi.org/10.1063/1.4955429

Pini, R., Hejazi, A.S.H. & Rabha, S. (2018): Pore and gas sorption properties of Opalinus Clay. ACT Project Number: 271498 ELEGANCY Deliverable D2.3.2.

Pitty, A.F. & Alexander, W.R. (2014): A natural analogue study of cement buffered, hyperalkaline groundwaters and their interaction with a repository host rock IV : an examination of the Khushaym Matruk (central Jordan) and Maqarin (northern Jordan) sites. Technical Report BG-TR-11-02 (Vol. 2).

Poller, A., Mayer, G., Darcis, M. & Smith, P. (2016): Modelling of Gas Generation in Deep Geological Repositories after Closure. Nagra Technical Report 16-04.

Poonoosamy, J., Klinkenberg, M., Deissmann, G., Brandt, F., Bosbach, D., Mäder, U.K. & Kosakowski, G. (2020): Effects of solution supersaturation on barite precipitation in porous media and consequences on permeability: Experiments and modelling. Geochimica et Cosmochimica Acta, 270, 43-60. https://doi.org/10.1016/j.gca.2019.11.018

Pourbaix, M. (1974): Atlas of Electrochemical Equilibrium in Aqueous Solutions. National Association of Corrosion Engineers, Houston, Texas, USA.

Poursaee, A. (2016): Corrosion of steel in concrete structures. In Corrosion of Steel in Concrete Structures (pp. 19-33). Elsevier Inc. https://doi.org/10.1016/B978-1-78242-381-2.00002-X

Prasianakis, N.I., Curti, E., Kosakowski, G., Poonoosamy, J. & Churakov, S.V (2017): Deciphering pore-level precipitation mechanisms. Scientific Reports, 7/1, 13765. https://doi.org/10.1038/s41598-017-14142-0

Prasianakis, N.I., Kosakowski, G., Gimmi, T., Luraschi, P., Miron, G.D., Pfingsten, W. & Churakov, S.V. (2022): Cement-Clay Synthesis of transport across the cement-clay interface. Nagra Arbeitsbericht NAB 22-34.

Prusinski, J.R. & Bhattacharja, S. (1999): Effectiveness of Portland Cement and Lime in Stabilizing Clay Soils. Transportation Research Record: Journal of the Transportation Research Board, 1652/1, 215-227. https://doi.org/10.3141/1652-28

Ramírez, S., Vieillard, P., Bouchet, A., Cassagnabère, A., Meunier, A. & Jacquot, E. (2005): Alteration of the Callovo-Oxfordian clay from Meuse-Haute Marne underground laboratory (France) by alkaline solution. I. A XRD and CEC study. Applied Geochemistry, 20/1, 89-99. https://doi.org/10.1016/J.APGEOCHEM.2004.03.009

Ramsay, J., Avery, R. & Russell, P. (1988): Physical characteristics and sorption behaviour of colloids generated from cementitious systems. Radiochimica. Acta, 44/45, 119-124. https://doi.org/10.1524/ract.1988.4445.1.119

Read, D., Glasser, F.P., Ayora, C., Guardiola, M.T. & Sneyers, A. (2001): Mineralogical and microstructural changes accompanying the interaction of Boom Clay with ordinary Portland cement. Advances in Cement Research, 13/4, 175-183. https://doi.org/10.1680/adcr.2001.13.4.175

Reijonen, H.M. & Alexander, W.R. (2015): Bentonite analogue research related to geological disposal of radioactive waste: current status and future outlook. Swiss Journal of Geosciences, 108/1, 101-110. https://doi.org/10.1007/S00015-015-0185-0/FIGURES/6

Reitenbach, V., Ganzer, L., Albrecht, D. & Hagemann, B. (2015): Influence of added hydrogen on underground gas storage: a review of key issues. Environmental Earth Sciences, 73/11, 6927-6937. https://doi.org/10.1007/s12665-015-4176-2

Renard, F., Brosse, E. & Gratier, J.P. (2000): The Different Processes Involved in the Mechanism of Pressure Solution in Quartz-Rich Rocks and their Interactions. In R. H. Worden & S. Morad (Eds.), Quartz Cementation in Sandstones (pp. 67-78). Blackwell Publishing Ltd., Oxford, UK. https://doi.org/10.1002/9781444304237.ch5

Revil, A. & Jougnot, D. (2008): Diffusion of ions in unsaturated porous materials. Journal of Colloid and Interface Science, 319/1, 226-35. https://doi.org/10.1016/j.jcis.2007.10.041

Roberge, P.R. (2019): Handbook of Corrosion Engineering. (3rd edition). McGraw-Hill Education, New York.

Robie, R. & Hemingway, B.S. (1995): Thermodynamic properties of minerals and related substances at 298.15 K and 1 bar (10^5 pascals) pressure and at higher temperatures. U.S. Geological Survey Bulletin 2131. U.S. Geological Survey Bulletin. https://doi.org/10.3133/ b2131

Robineau, M., Sabot, R., Jeannin, M., Deydier, V., Crusset, D. & Refait, P. (2021): Mechanisms of localized corrosion of carbon steel associated with magnetite/mackinawite layers in a cement grout. Materials and Corrosion, 72/1-2, 194-210. https://doi.org/10.1002/MACO.202011696

Rout, S.P., Payne, L., Walker, S., Scott, T., Heard, P., Eccles, H., Bond, G., Shah, P., Bills, P., Jackson, B.R., Boxall, S.A., Laws, A.P., Charles, C., Williams, S.J., & Humphreys, P.N. (2018): The Impact of Alkaliphilic Biofilm Formation on the Release and Retention of Carbon Isotopes from Nuclear Reactor Graphite. Scientific Reports, 8/1, 4455. https://doi.org/10.1038/s41598-018-22833-5

Rozov, K.B., Berner, U., Kulik, D.A. & Diamond, L.W. (2011): Solubility and thermodynamic properties of carbonate-bearing hydrotalcite-pyroaurite solid solutions with a 3:1 Mg/(Al+Fe) mole ratio. Clays and Clay Minerals, 59/3, 215-232. https://doi.org/10.1346/CCMN.2011.0590301

Russell, D., Basheer, P.A.M., Rankin, G.I.B. & Long, A.E. (2001): Effect of relative humidity and air permeability on prediction of the rate of carbonation of concrete. Proceedings of the Institution of Civil Engineers - Structures and Buildings, 146/3, 319-326. https://doi.org/10.1680/stbu.2001.146.3.319

Ryan, J.N. & Elimelech, M. (1996): Colloid mobilization and transport in groundwater. Colloids and Surfaces A: Physicochemical and Engineering Aspects, 107, 1-56. https://doi.org/10.1016/0927-7757(95)03384-X

Sagoe-Crentsil, K.K. & Glasser, F.P. (1993): "Green rust", iron solubility and the role of chloride in the corrosion of steel at high pH. Cement and Concrete Research, 23/4, 785-791. https://doi.org/10.1016/0008-8846(93)90032-5

Samper, J., Montenegro, L., De Windt, L., Montoya, V., Garibay-Rodrigez, J., Grigaliuniene, D., Narkuniene, A., Poskas, P. & Cochepin, B. (2022): Conceptual model formulation for a mechanistic based model implementing the initial SOTA knowledge (models and parameters) in existing numerical tools. Deliverable D2.16 of the HORIZON 2020 project EURAD. EC Grant agreement no: 847593.

Saripalli, K.P., Meyer, P.D., Bacon, D.H. & Freedman, V.L. (2001): Changes in Hydrologic Properties of Aquifer Media Due to Chemical Reactions: A Review. Critical Reviews in Environmental Science and Technology, 31/4, 311-349. https://doi.org/10.1080/20016491089244

Savage, D. & Cloet, V. (2018): A review of Cement-Clay Modelling. Nagra Arbeitsbericht NAB 18-24.

Savage, D. (2011): A review of analogues of alkaline alteration with regard to long-term barrier performance. Mineralogical Magazine, 75/4, 2401-2418. https://doi.org/10.1180/minmag.2011.075.4.2401

Savage, D., Bateman, K., Hill, P., Hughes, C., Milodowski, A., Pearce, J., Rae, E. & Rochelle, C. (1992): Rate and mechanism of the reaction of silicates with cement pore fluids. Applied Clay Science, 7/1-3, 33-45. https://doi.org/10.1016/0169-1317(92)90026-J

Savage, D., Walker, C., Arthur, R., Rochelle, C.A., Oda, C. & Takase, H. (2007): Alteration of bentonite by hyperalkaline fluids: A review of the role of secondary minerals. Physics and Chemistry of the Earth, Parts A/B/C, 32/1-7, 287-297. https://doi.org/10.1016/j.pce.2005.08.048

Savage, D., Wilson, J., Benbow, S., Sasamoto, H., Oda, C., Walker, C., Kawama, D. & Tachi, Y. (2020): Using natural systems evidence to test models of transformation of montmorillonite. Applied Clay Science, 195, 105741. https://doi.org/10.1016/j.clay.2020.105741

Šavija, B. & Luković, M. (2016): Carbonation of cement paste: Understanding, challenges, and opportunities. Construction and Building Materials, 117, 285-301. https://doi.org/10.1016/j.conbuildmat.2016.04.138

Savoye, S., Lefevre, S., Fayette, A. & Robinet, J.-C. (2017): Effect of Water Saturation on the Diffusion/Adsorption of Na-22 and Cesium onto the Callovo-Oxfordian Claystones. GEOFLUIDS. https://doi.org/10.1155/2017/1683979

Savoye, S., Macé, N., Lefèvre, S., Spir, G. & Robinet, J.C. (2018a): Mobility of chloride through cement-based materials under partially saturated conditions. Applied Geochemistry, 96, 78-86. https://doi.org/10.1016/j.apgeochem.2018.06.011

Savoye, S., Rajyaguru, A., Macé, N., Lefèvre, S., Spir, G. & Robinet, J.C. (2018b): How mobile is tritiated water through unsaturated cement-based materials? New insights from two complementary approaches. Applied Radiation and Isotopes, 139, 98-106. https://doi.org/10.1016/j.apradiso.2018.04.019

Schäfer, D., Manconi, A., Grandel, S. & Dahmke, A. (2005): Consequences of different kinetic approaches for simulation of microbial degradation on contaminant plume development. In Reactive Transport in Soil and Groundwater: Processes and Models (pp. 127-139). Springer Berlin Heidelberg. https://doi.org/10.1007/3-540-26746-8_9

Schimel, J.P. (2018): Life in Dry Soils: Effects of Drought on Soil Microbial Communities and Processes. Annual Review of Ecology, Evolution, and Systematics, 49/1, 409-432. https://doi.org/10.1146/annurev-ecolsys-110617-062614

Schramm, L.L. (1994): The Language of Colloid and Interface Science. Environmental Science and Technology, 28/13. https://doi.org/10.1021/es00062a732

Schweizer, C. (1999): Calciumsilikathydrat-Mineralien: Lösungskinetik und ihr Einfluss auf das Auswaschverhalten von Substanzen aus einer Ablagerung mit Rückständen aus Müllverbrennungsanlagen. Doctoral Thesis Nr. 13074. Swiss Federal Institute of Technology (ETH), Zürich, Switzerland.

Seigneur, N., Mayer, K.U. & Steefel, C.I. (2019): Reactive Transport in Evolving Porous Media. Reviews in Mineralogy and Geochemistry, 85/1, 197-238. https://doi.org/10.2138/rmg.2019.85.7

Senger, R.K. & Ewing, J. (2009): Gas-L/ILW: Gas pressure buildup and transport in a deep geologic L/ILW repository in Opalinus Clay using large-scale and local-scale models. Nagra Arbeitsbericht NAB 09-17.

Senior, N.A., Martino, T., Gaggiano, R. & Diomidis, N. (2021): The corrosion of mild and stainless steel in alkaline anaerobic conditions representing the Belgian “supercontainer” concept and the Swiss L/ILW repository. Materials and Corrosion, 72/1-2, 67-74. https://doi.org/10.1002/MACO.202011782

Senior, N., Martino, T., Diomidis, N. & Gaggiano, R. (2023): The corrosion behavior of nonferrous metals in deep geological repository environments. Materials and Corrosion. https://doi.org/10.1002/maco.202313772

Shafizadeh, A. (2019): Neutron Imaging Study of Evolution of Structural and Transport Properties of Cement-Clay Interfaces. Doctoral thesis. Universität Bern.

Shafizadeh, A., Gimmi, T., Van Loon, L.R., Kaestner, A.P., Mäder, U.K. & Churakov, S.V. (2020): Time-resolved porosity changes at cement-clay interfaces derived from neutron imaging. Cement and Concrete Research, 127, 105924. https://doi.org/10.1016/j.cemconres.2019.105924

Shafizadeh, A., Gimmi, T., Van Loon, L.R., Kaestner, A., Lehmann, E., Mäder, U.K. & Churakov, S.V. (2015): Quantification of water content across a cement-clay interface using high resolution neutron radiography. Physics Procedia, 69, 516-523. https://doi.org/10.1016/j.phpro.2015.07.073

Shannon, R.D. (1976): Revised effective ionic radii and systematic studies of interatomic distances in halides and chalcogenides. Acta Crystallographica Section A, 32/5, 751-767. https://doi.org/10.1107/S0567739476001551

Shao, H., Kosakowski, G., Berner, U., Kulik, D.A., Mäder, U.K. & Kolditz, O. (2013): Reactive transport modeling of the clogging process at Maqarin natural analogue site. Physics and Chemistry of the Earth, Parts A/B/C, 64, 21-31. https://doi.org/10.1016/j.pce.2013.01.002

Shi, Z., Park, S., Lothenbach, B. & Leemann, A. (2020): Formation of shlykovite and ASR-P1 in concrete under accelerated alkali-silica reaction at 60 and 80 °C. Cement and Concrete Research, 137, 106213. https://doi.org/10.1016/j.cemconres.2020.106213

Shrestha, R., Cerna, K., Spanek, R., Bartak, D., Cernousek, T. & Sevcu, A. (2022): The effect of low-pH concrete on microbial community development in bentonite suspensions as a model for microbial activity prediction in future nuclear waste repository. The Science of the Total Environment, 808. https://doi.org/10.1016/J.SCITOTENV.2021.151861

Silva, D.A., Wenk, H.R. & Monteiro, P.J.M. (2005): Comparative investigation of mortars from Roman Colosseum and cistern. Thermochimica Acta, 438/1-2, 35-40. https://doi.org/10.1016/j.tca.2005.03.003

Sims, I. & Brown, B. (1998): Concrete Aggregates. In Lea's Chemistry of Cement and Concrete, 907-1015. Elsevier. https://doi.org/10.1016/B978-075066256-7/50028-X

Sims, I. & Poole, A.B. (2017): Alkali-aggregate reaction in concrete: A world review. Alkali-Aggregate Reaction in Concrete: A World Review, CRC Press London. https://doi.org/10.1201/9781315708959

Small, J.S. (2019): Final synthesis report for MIND WP1. NNL report 15013 and Deliverable D1.9 of the Microbiology in Nuclear waste Disposal (MIND) project.

Smart, N.R. (2009): Corrosion behavior of carbon steel radioactive waste packages: A summary review of Swedish and U.K. Research. Corrosion, 65/3, 195-212. https://doi.org/10.5006/1.3319128

Smart, N.R., Reddy, B., Rance, A.P., Nixon, D.J. & Diomidis, N. (2017): The anaerobic corrosion of carbon steel in saturated compacted bentonite in the Swiss repository concept. Corrosion Engineering Science and Technology, 52, 113-126. https://doi.org/10.1080/1478422X.2017.1316088

Smellie, J. (1998): Maqarin natural analogue study: Phase III. SKB Technical Report TR-98-04.

Soler, J.M. (2013): Reactive transport modeling of concrete-clay interaction during 15 years at the Tournemire Underground Rock Laboratory. European Journal of Mineralogy, 25/4, 639-654. https://doi.org/10.1127/0935-1221/2013/0025-2324

Soler, J.M. (2016): Two-dimensional reactive transport modeling of the alteration of a fractured limestone by hyperalkaline solutions at Maqarin (Jordan). Applied Geochemistry, 66, 162-173. https://doi.org/10.1016/J.APGEOCHEM.2015.12.012

Steefel, C.I. & Lichtner, P.C. (1998): Multicomponent reactive transport in discrete fractures: II: Infiltration of hyperalkaline groundwater at Maqarin, Jordan, a natural analogue site. Journal of Hydrology, 209/1-4, 200-224. https://doi.org/10.1016/S0022-1694(98)00173-5

Stefanoni, M., Angst, U. & Elsener, B. (2018): Corrosion rate of carbon steel in carbonated concrete – A critical review. Cement and Concrete Research, 103, 35-48. https://doi.org/10.1016/j.cemconres.2017.10.007

Stefanoni, M., Angst, U. & Elsener, B. (2020): The mechanism controlling corrosion of steel in carbonated cementitious materials in wetting and drying exposure. Cement and Concrete Composites, 113, 103717. https://doi.org/10.1016/J.CEMCONCOMP.2020.103717

Steiner, S., Lothenbach, B., Proske, T., Borgschulte, A. & Winnefeld, F. (2020): Effect of relative humidity on the carbonation rate of portlandite, calcium silicate hydrates and ettringite. Cement and Concrete Research, 135/January, 106116. https://doi.org/10.1016/j.cemconres.2020.106116

Stumm, A., Garbev, K., Beuchle, G., Black, L., Stemmermann, P. & Nüesch, R. (2005): Incorporation of zinc into calcium silicate hydrates, Part I: formation of C-S-H(I) with C/S=2/3 and its isochemical counterpart gyrolite. Cement and Concrete Research, 35/9, 1665-1675. https://doi.org/10.1016/j.cemconres.2004.11.007

Suckling P., Avis J., Calder N., Nasir O., Humphreys P., King F., Walsh R. (2015): T2GGM Version 3.2: Gas Generation and Transport Code. NWMO-TR-2015-13. Nuclear Waste Management Organisation NWMO, Toronto.

Suzuki, Y., Konno, U., Fukuda, A., Komatsu, D.D., Hirota, A., Watanabe, K., Togo, Y., Morikawa, N., Hagiware, H., Aosai, D., Iwatsuki, T. Tsunogai, U., Nagao, S., Ito, K. & Mizuno, T. (2014): Biogeochemical Signals from Deep Microbial Life in Terrestrial Crust. PLOS ONE, 9/12, e113063. https://doi.org/10.1371/JOURNAL.PONE.0113063

Swenson, E.G. & Gillott, J.E. (1964): Alkali-carbonate rock reaction. Highway Research Record, 45, 21-40.

Swiss Federal Office of Energy SFOE (2008): Sectoral plan for deep geological repositories: Conceptual part. DETEC Bern.

Taborowski, T., Bengtsson, A., Chukharkina, A., Blom, A. & Pedersen, K. (2019): Bacterial activity in compacted bentonites. MIND Deliverable D2.4, v.2.

Taniguchi, N., Kawasaki, M. & Naito, M. (2010): Corrosion Behavior of Carbon Steel in Compacted Bentonite Saturated with Simulated Groundwater under Anaerobic Condition. Zairyo-to-Kankyo, 59/11, 418-429. https://doi.org/10.3323/jcorr.59.418

Tasi, A., Gaona, X., Fellhauer, D., Böttle, M., Rothe, J., Dardenne, K., Polly, R., Grivé, M., Colàs, E., Bruno, J., Källstrom, K., Altmaier, M. & Geckeis, H. (2018): Thermodynamic description of the plutonium - α-d-isosaccharinic acid system ii: Formation of quaternary Ca(II)-Pu(IV)-OH-ISA complexes. Applied Geochemistry, 98, 351-366. https://doi.org/10.1016/j.apgeochem.2018.06.014

Tasi, A., Gaona, X., Rabung, T., Fellhauer, D., Rothe, J., Dardenne, K., Lutzenkirchen, J., Grive, M., Colas, E., Bruno, J., Kallstrom, K., Altmaier, M. & Geckeis, H. (2021): Plutonium retention in the isosaccharinate - cement system. Applied Geochemistry, 126. https://doi.org/10.1016/j.apgeochem.2020.104862

Taubald, H., Bauer, A., Schäfer, T., Geckeis, H., Satir, M. & Kim, J.I. (2000): Experimental investigation of the effect of high-pH solutions on the Opalinus Shale and the Hammerschmiede Smectite. Clay Minerals, 35/3, 515-524. https://doi.org/10.1180/000985500546981

Taylor, H.F.W. (1997): Cement Chemistry. (2nd. ed). Thomas Telford, London, UK.

Techer, I., Bartier, D., Boulvais, P., Tinseau, E., Suchorski, K., Cabrera, J. & Dauzères, A. (2012): Tracing interactions between natural argillites and hyper-alkaline fluids from engineered cement paste and concrete: Chemical and isotopic monitoring of a 15-years old deep-disposal analogue. Applied Geochemistry, 27/7, 1384-1402. https://doi.org/10.1016/j.apgeochem.2011.08.013

Tecon, R. & Or, D. (2017): Biophysical processes supporting the diversity of microbial life in soil. FEMS Microbiology Reviews, 41/5, 599-623. https://doi.org/10.1093/FEMSRE/FUX039

Thiery, M., Villain, G., Dangla, P. & Platret, G. (2007): Investigation of the carbonation front shape on cementitious materials: Effects of the chemical kinetics. Cement and Concrete Research, 37/7, 1047-1058. https://doi.org/10.1016/j.cemconres.2007.04.002

Thom, J. & Anderson, G.M. (2008): The role of thermochemical sulfate reduction in the origin of Mississippi Valley-type deposits. I. Experimental results. Geofluids, 8/1, 16-26. https://doi.org/10.1111/j.1468-8123.2007.00201.x

Thomas, M.D.A. (2013): Supplementary cementing materials in concrete. Supplementary Cementing Materials in Concrete. CRC Press. https://doi.org/10.1201/b14493

Thomas, M.D.A., Fournier, B. & Folliard, K.J. (2013): Alkali-Aggregate Reactivity (AAR) Facts Book. Report FHWA-HIF-13-019.

Thouvenot, P., Bildstein, O., Munier, I., Cochepin, B., Poyet, S., Bourbon, X. & Treille, E. (2013): Modeling of concrete carbonation in deep geological disposal of intermediate level waste. EPJ Web of Conferences, 05004, 1-8. https://doi.org/10.1051/epjconf/20135605004

Tinseau, E., Bartier, D., Hassouta, L., Devol-Brown, I. & Stammose, D. (2006): Mineralogical characterization of the Tournemire argillite after in situ interaction with concretes. Waste Management, 26/7, 789-800. https://doi.org/10.1016/j.wasman.2006.01.024

Tits, J. & Wieland, E. (2018): Actinide sorption by cementitious materials. Nuclear Energy and Safety Research Department, Laboratory for Waste Management (LES). PSI Report No. 18-02.

Tits, J. & Wieland, E. (2023): Radionuclide Retention in the Cementitious Near Field of a Repository for L/ILW: Development of the Cement Sorption Data Base for Use in the License Application. Nagra Technical Report NTB 23-07.

Tits, J., Fujita, T., Harfouche, M., Dähn, R., Tsukamoto, M. & Wieland, E. (2014): Radionuclide uptake by calcium silicate hydrates: Case studies with Th (IV) and U (VI). Nuclear Energy and Safety Research, Department Laboratory for Waste Management (LES). PSI Report No. 14-03.

Tommaseo, C.E. & Kersten, M. (2002): Aqueous Solubility Diagrams for Cementitious Waste Stabilization Systems. 3. Mechanism of Zinc Immobilizaton by Calcium Silicate Hydrate. Environmental Science & Technology, 36/13, 2919-2925. https://doi.org/10.1021/es0102484

Tournassat, C. & Steefel, C.I. (2019): Reactive Transport Modeling of Coupled Processes in Nanoporous Media. Reviews in Mineralogy and Geochemistry, 85/1, 75-109. https://doi.org/10.2138/RMG.2019.85.4

Traber, D. & Mäder, U.K. (2006): Reactive transport modelling of the diffusive interaction between Opalinus Clay and concrete. Nagra Arbeitsbericht NAB 05-06.

Triantafyllidis, K.S., Peleka, E.N., Komvokis, V.G. & Mavros, P.P. (2010): Iron-modified hydrotalcite-like materials as highly efficient phosphate sorbents. Journal of Colloid and Interface Science, 342/2, 427-436. https://doi.org/10.1016/J.JCIS.2009.10.063

Trotignon, L., Thouvenot, P., Munier, I., Cochepin, B., Piault, E., Treille, E., Bourbon, X. & Mimid, S. (2011): Numerical simulation of atmospheric carbonation of concrete components in a deep geological radwaste disposal site during operating period. Nuclear Technology, 174/3, 424-437.

Truche, L., Berger, G., Albrecht, A. & Domergue, L. (2013a): Abiotic nitrate reduction induced by carbon steel and hydrogen: Implications for environmental processes in waste repositories. Applied Geochemistry, 28, 155-163. https://doi.org/10.1016/j.apgeochem.2012.10.010

Truche, L., Berger, G., Albrecht, A. & Domergue, L. (2013b): Engineered materials as potential geocatalysts in deep geological nuclear waste repositories: A case study of the stainless steel catalytic effect on nitrate reduction by hydrogen. Applied Geochemistry, 35, 279-288. https://doi.org/10.1016/j.apgeochem.2013.05.001

Truche, L., Berger, G., Destrigneville, C., Guillaume, D. & Giffaut, E. (2010): Kinetics of pyrite to pyrrhotite reduction by hydrogen in calcite buffered solutions between 90 and 180 °C: Implications for nuclear waste disposal. Geochimica et Cosmochimica Acta, 74/10, 2894-2914. https://doi.org/10.1016/j.gca.2010.02.027

Truche, L., Berger, G., Destrigneville, C., Pages, A., Guillaume, D., Giffaut, E. & Jacquot, E. (2009): Experimental reduction of aqueous sulphate by hydrogen under hydrothermal conditions: Implication for the nuclear waste storage. Geochimica et Cosmochimica Acta, 73/16, 4824-4835. https://doi.org/10.1016/j.gca.2009.05.043

Truche, L., Jodin-Caumon, M.C., Lerouge, C., Berger, G., Mosser-Ruck, R., Giffaut, E. & Michau, N. (2013c): Sulphide mineral reactions in clay-rich rock induced by high hydrogen pressure. Application to disturbed or natural settings up to 250°C and 30bar. Chemical Geology, 351, 217-228. https://doi.org/10.1016/j.chemgeo.2013.05.025

Truche, L., Joubert, G., Dargent, M., Martz, P., Cathelineau, M., Rigaudier, T. & Quirt, D. (2018): Clay minerals trap hydrogen in the Earth's crust: Evidence from the Cigar Lake uranium deposit, Athabasca. Earth and Planetary Science Letters, 493, 186-197. https://doi.org/10.1016/j.epsl.2018.04.038

Tyagi, M., Gimmi, T. & Churakov, S.V. (2013): Multi-scale micro-structure generation strategy for up-scaling transport in clays. Advances in Water Resources, 59, 181-195. https://doi.org/10.1016/j.advwatres.2013.06.002

van Genuchten, M.T. (1980): A closed-form equation for predicting the hydraulic conductivity of unsaturated soils. Soil Science Society of America Journal, 44/5, 892-898. https://doi.org/10.2136/sssaj1980.03615995004400050002x

Van Loon, L.R. & Glaus, M.A. (1998): Experimental and theoretical studies on alkaline degradation of cellulose and its impact on the sorption of radionuclides. PSI Bericht 98-07.

Van Loon, L.R. & Hummel, W. (1995): The radioanalytic and chemical degradation of organic ion exchange resins under alkaline conditions: Effect on radionuclide speciation. Nagra Technical Report NTB 95-08.

Velbel, M.A. (1990): Influence of Temperature and Mineral Surface Characteristics on Feldspar Weathering Rates in Natural and Artificial Systems: A First Approximation. Water Resources Research, 26/12, 3049-3053. https://doi.org/10.1029/WR026i012p03049

Venhuis, M.A. & Reardon, E.J. (2001): Vacuum Method for Carbonation of Cementitious Wasteforms. Environmental Science & Technology, 35/20, 4120-4125. https://doi.org/10.1021/es0105156

Verwey, E.J.W. (1947): Theory of the Stability of Lyophobic Colloids. The Journal of Physical and Colloid Chemistry, 51/3, 631-636. https://doi.org/10.1021/j150453a001

Vespa, M., Wieland, E., Dähn, R. & Lothenbach, B. (2015): Identification of the Thermodynamically Stable Fe-Containing Phase in Aged Cement Pastes. Journal of the American Ceramic Society, 98/7, 2286-2294. https://doi.org/10.1111/jace.13542

Vinsot, A., Appelo, C.A.J., Lundy, M., Wechner, S., Cailteau-Fischbach, C., de Donato, P., Pironon, J., Lettry, Y., Lerouge, C. & De Cannière, P. (2017): Natural gas extraction and artificial gas injection experiments in Opalinus Clay, Mont Terri rock laboratory (Switzerland). Swiss Journal of Geosciences, 110/1, 375-390. https://doi.org/10.1007/s00015-016-0244-1

Vollpracht, A., Lothenbach, B., Snellings, R. & Haufe, J. (2015): The pore solution of blended cements: a review. Materials and Structures 2015, 49/8, 3341-3367. https://doi.org/10.1617/S11527-015-0724-1

von Greve-Dierfeld, S., Lothenbach, B., Vollpracht, A., Wu, B., Huet, B., Andrade, C., Medina, C., Thiel, C., Gruyaert, E. & Vanoutrive, H. (2020): Understanding the carbonation of concrete with supplementary cementitious materials: a critical review by RILEM TC 281-CCC. Materials and Structures, 53/6, 136. https://doi.org/10.1617/s11527-020-01558-w

Wang, L. (2009): Near-field chemistry of an HLW/SF repository in Boom Clay – scoping calculations relevant to the supercontainer design. Report 09/LWa/P-140.

Wang, L., Jacques, D. & De Cannière, P. (2010): Effects of an alkaline plume on the Boom Clay as a potential host formation for geological disposal of radioactive waste. Report prepared by SCK•CEN in the framework of ONDRAF/NIRAS programme on geological disposal, under contract CCHO 2004-2470/00/00. Report SCK-CEN-ER-28.

Wareing, A., Abrahamsen, L., Banford, A., Metcalfe, M. & von Lensa, W. (2013): Treatment and Disposal of irradiated Graphite and other Carbonaceous Waste. Final Deliverable D-0.3.12 of the CARBOWASTE (Treatment and Disposal of Irradiated Graphite and Other Carbonaceous Waste) Project, FP7-EURATOM Grant Agreement Number FP7-211333.

Warthmann, R., Mosberger, L. & Baier, U. (2013): Langzeit-Degradation von organischen Polymeren unter SMA-Tiefenlagerbedingungen. Nagra Technischer Bericht NTB 13-04.

Watkinson, D. & Lewis, M. (2004): Great Britain iron hull: modelling corrosion to define storage relative humidity. In Proceedings of Metal 2004, National Museum of Australia Canberra ACT,4-8 October 2004 (Vol. 44, pp. 88-102).

Watson, C., Benbow, S. & Savage, D. (2007): Modelling the Interaction of Low pH Cements and Bentonite Issues Affecting the Geochemical Evolution of Repositories for Radioactive Waste. Report SKI-R-07-30.

Watson, C., Wilson, J., Savage, D., Benbow, S. & Norris, S. (2016): Modelling reactions between alkaline fluids and fractured rock: The Maqarin natural analogue. Applied Clay Science, 121-122, 46-56. https://doi.org/10.1016/J.CLAY.2015.12.004

Weltje, G.J. & von Eynatten, H. (2004): Quantitative provenance analysis of sediments: Review and outlook. Sedimentary Geology, 171/1-4, 1-11. https://doi.org/10.1016/ j.sedgeo.2004.05.007

Wersin, P., Johnson, L.H., Schwyn, B., Berner, U. & Curti, E. (2003): Redox conditions in the near field of a repository for SF/HLW and ILW in Opalinus clay. Nagra Technical Report NTB 02-13.

Wersin, P., Mazurek, M. & Gimmi, T. (2022): Porewater chemistry of Opalinus Clay revisited: Findings from 25 years of data collection at the Mont Terri Rock Laboratory. Applied Geochemistry, 138, 105234. https://doi.org/10.1016/J.APGEOCHEM.2022.105234

Wersin, P., Pekala, M., Mazurek, M., Gimmi, T., Mäder, U.K., Jenni, A., Rufer, D. & Aschwanden, L. (2020): Porewater Chemistry of Opalinus Clay Methods, Data, Modelling & Buffering Capacity. Nagra Technical Report NTB 18-01.

White, A.F. & Brantley, S.L. (2003): The effect of time on the weathering of silicate minerals: why do weathering rates differ in the laboratory and field? Chemical Geology, 202/3-4, 479-506. https://doi.org/10.1016/j.chemgeo.2003.03.001

Wieland, E. & Hummel, W. (2015): Formation and stability of ^{14}C-containing organic compounds in alkaline iron-water systems: preliminary assessment based on a literature survey and thermodynamic modelling. Mineralogical Magazine, 79/6, 1275-1286. https://doi.org/10.1180/minmag.2015.079.6.03

Wieland, E. & Kosakowski, G. (2020): Review of the compositions of hydrated cements and cement-type pore water at different stages of the cement degradation. Nagra Arbeitsbericht NAB 20-12.

Wieland, E. & Spieler, P. (2001): Colloids in the mortar backfill of a cementitious repository for radioactive waste. Waste Management, 21/6, 511-523. https://doi.org/10.1016/S0956-053X(00)00090-8

Wieland, E. & Van Loon, L.R. (2003): Cementitious Near-Field Sorption Data Base for Performance Assessment of an ILW Repository in Opalinus Clay. PSI Report No. 03-06.

Wieland, E. (2001): Experimental studies on the inventory of cement-derived colloids in the pore water of a cementitious backfill material. PSI Bericht No. 01-01, also published as Nagra Technical Report NTB 01-02.

Wieland, E. (2014): Sorption data base for the cementitious near field of L/ILW and ILW repositories for provisional safety analyses for SGT-E2. Nagra Technical report NTB 14-08.

Wieland, E., Kosakowski, G., Lothenbach, B. & Kulik, D.A. (2020): Geochemical modelling of the effect of waste degradation processes on the long-term performance of waste forms. Applied Geochemistry, 115, 104539. https://doi.org/10.1016/j.apgeochem.2020.104539

Wieland, E., Kosakowski, G., Lothenbach, B., Kulik, D.A. & Cloet, V. (2018): Preliminary assessment of the temporal evolution of waste packages in the near field of the L/ILW repository. Nagra Arbeitsbericht NAB 18-05.

Wieland, E., Tits, J. & Bradbury, M.H. (2004): The potential effect of cementitious colloids on radionuclide mobilisation in a repository for radioactive waste. Applied Geochemistry, 19/1, 119-135. https://doi.org/10.1016/S0883-2927(03)00114-8

Wiesenburg, D.A. & Guinasso, N.L. (1979): Equilibrium Solubilities of Methane, Carbon Monoxide, and Hydrogen in Water and Sea Water. Journal of Chemical and Engineering Data, 24/4, 356-360. https://doi.org/10.1021/JE60083A006/ASSET/JE60083A006.FP.PNG_V03

Wigger, C., Plöze, M. & Van Loon, L.R. (2018): Pore Geometry as a Limiting Factor for Anion Diffusion in Argillaceous Rocks. Clays and Clay Minerals, 66/4, 329-338. https://doi.org/10.1346/CCMN.2018.064101

Wilson, J., Bateman, K. & Tachi, Y. (2021): The impact of cement on argillaceous rocks in radioactive waste disposal systems: A review focusing on key processes and remaining issues. Applied Geochemistry, 130/January, 104979. https://doi.org/10.1016/j.apgeochem.2021.104979

Winter, N.B. (2009): Understanding Cement: An introduction to cement production, cement hydration and deleterious processes in concrete. WHD Microanalysis Consultants, Woodbridge, UK.

Xie, M., Mayer, K. U., Claret, F., Alt-Epping, P., Jacques, D., Steefel, C., Chiaberge, C. & Simunek, J. (2015): Implementation and evaluation of permeability-porosity and tortuosity-porosity relationships linked to mineral dissolution-precipitation. Computational Geosciences, 19/3, 655-671. https://doi.org/10.1007/s10596-014-9458-3

Xiong, J., Liu, X., Liang, L. & Zeng, Q. (2017): Adsorption Behavior of Methane on Kaolinite. Industrial and Engineering Chemistry Research, 56/21, 6229-6238. https://doi.org/10.1021/acs.iecr.7b00838

Yamaguchi, T., Kataoka, M., Sawaguchi, T., Mukai, M., Hoshino, S., Tanaka, T., Marsal, F. & Pellegrini, D. (2013): Development of a reactive transport code MC-CEMENT ver. 2 and its verification using 15-year in situ concrete/clay interactions at the Tournemire URL. Clay Minerals, 48/2, 185-197. https://doi.org/10.1180/claymin.2013.048.2.03

Yan, N. & Dyson, P.J. (2013): Solvents and Ionic Liquids. In Reference Module in Chemistry, Molecular Sciences and Chemical Engineering. Elsevier. https://doi.org/10.1016/B978-0-12-409547-2.01073-8

Yang, L. & Steefel, C.I. (2008): Kaolinite dissolution and precipitation kinetics at 22 °C and pH 4. Geochimica et Cosmochimica Acta, 72/1, 99-116. https://doi.org/10.1016/J.GCA.2007.10.011

Yang, S.-Y., Yan, Y., Lothenbach, B. & Skibsted, J. (2021): Incorporation of Sodium and Aluminum in Cementitious Calcium-Alumino-Silicate-Hydrate C-(A)-S-H Phases Studied by ^{23}Na, ^{27}Al, and ^{29}Si MAS NMR Spectroscopy. The Journal of Physical Chemistry C, 125/51, 27975-27995. https://doi.org/10.1021/acs.jpcc.1c08419

Yang, T., Zhang, Z., Zhang, F., Gao, Y. & Wu, Q. (2020): Chloride and heavy metal binding capacities of hydrotalcite-like phases formed in greener one-part sodium carbonate-activated slag cements. Journal of Cleaner Production, 253. https://doi.org/10.1016/j.jclepro.2020.120047

Yekta, A.E., Pichavant, M. & Audigane, P. (2018): Evaluation of geochemical reactivity of hydrogen in sandstone: Application to geological storage. Applied Geochemistry, 95, 182-194. https://doi.org/10.1016/j.apgeochem.2018.05.021

Yokoyama, S., Shimbashi, M., Minato, D., Watanabe, Y., Jenni, A. & Mäder, U.K. (2021): Alteration of bentonite reacted with cementitious materials for 5 and 10 years in the Mont Terri Rock Laboratory (CI Experiment). Minerals, 11/3, 1-17. https://doi.org/10.3390/min11030251

Zänker, H. & Hennig, C. (2014): Colloid-borne forms of tetravalent actinides: A brief review. Journal of Contaminant Hydrology, 157, 87-105. https://doi.org/10.1016/j.jconhyd.2013.11.004

Zhang, X., Zhang, M., Li, R., Feng, X., Pang, X., Rao, J., Cong, D., Yin, C. & Zhang, Y. (2021): Active Corrosion Protection of Mg-Al Layered Double Hydroxide for Magnesium Alloys: A Short Review. Coatings 2021, 11/11, 1316. https://doi.org/10.3390/COATINGS11111316

Zhang, Y., Zhang, M. & Ye, G. (2018): Influence of moisture condition on chloride diffusion in partially saturated ordinary Portland cement mortar. Materials and Structures, 51/2, 36. https://doi.org/10.1617/s11527-018-1162-7

Zhao, Y. & Jin, W. (2016): Steel Corrosion in Concrete. In Steel Corrosion-Induced Concrete Cracking, 19-29. Elsevier. https://doi.org/10.1016/b978-0-12-809197-5.00002-5

Zhen-Wu, B.Y., Prentice, D.P., Simonetti, D., Ryan, J.N., Sant, G. & Bauchy, M. (2021): Predicting zeolites' stability during the corrosion of nuclear waste immobilization glasses: Comparison with glass corrosion experiments. Journal of Nuclear Materials, 547, 152813. https://doi.org/10.1016/J.JNUCMAT.2021.152813

Zhu, C. (2005): In situ feldspar dissolution rates in an aquifer. Geochimica et Cosmochimica Acta, 69/6, 1435-1453. https://doi.org/10.1016/j.gca.2004.09.005

Ziegler, F., Gieré, R. & Johnson, C.A. (2001a): Sorption Mechanisms of Zinc to Calcium Silicate Hydrate: Sorption and Microscopic Investigations. Environmental Science & Technology, 35/22, 4556-4561. https://doi.org/10.1021/es001768m

Ziegler, F., Scheidegger, A., Johnson, C., Dähn, R. & Wieland, E. (2001b): Sorption mechanisms of zinc to calcium silicate hydrate: X-ray absorption fine structure (XAFS) investigation. Environmental Science & Technology, 35/7, 1550-1555. https://doi.org/10.1021/ ES001437+

Zivar, D., Kumar, S. & Foroozesh, J. (2020): Underground hydrogen storage: A comprehensive review. International Journal of Hydrogen Energy, 46/45, 23436-23462. https://doi.org/10.1016/j.ijhydene.2020.08.138

App. A Definition of cement porewaters for solubility calculations and cement sorption database

The composition of the cement porewater and cement matrix must be defined for the cement degradation stages of the cementitious systems representative for the near-field of a deep geological repository for L/ILW. These data define the chemical reference conditions for various subsequent modelling studies (e.g. carbon speciation, solubility limits for safety-relevant radionuclides, complexation of radionuclides by e.g. EDTA) and the development of the updated cement sorption database (SDB) for documentation for the general licence application. The properties of the cementitious systems should adequately represent the expected conditions of the near-field over the period of concern for a deep geological repository for L/ILW.

A general description of the stages of cement degradation is given in Section 3.3.1. Nevertheless, the specific conditions in these stages have to be assigned for a given repository system based on predictions made with thermodynamic modelling. For a cement-based repository, the thermodynamic model used to calculate the reference porewaters and the mineral compositions of the hardened cement paste is based on the equilibrium of a cement representative of the cement-based near-field in the stages of cement degradation with an Opalinus Clay porewater. It can be assumed that the initial composition of the OPA PW is strongly altered in equilibrium with cement, which is why the initial OPA PW composition plays only a minor role for the modelling of the reference cement porewater (CPW) and the composition of the cement.

We used the recipe for a container concrete from Kosakowski et al. (2020), which consists of a CEM I, to investigate the sensitivity of the concrete porewater with respect to OPA PW composition, redox conditions and interaction of cement cycles (times) with external OPA PW. Only part of the obtained information is documented in this report.

To ensure compatibility of the material with average near-field properties, we calculated three variants with an adjusted water to cement ratio of the container concrete:

1. container concrete based on the original recipe with about 11% porosity
2. a variant with additional water, such that it represents an averaged material with 20% porosity, and
3. a variant with additional water, such that it represents an averaged material with 30% porosity

For these three variants, we calculated scenarios for chemically reducing states with occurrence of magnetite and (iron-) siliceous hydrogarnet (mag/sh), magnetite and ferrihydrite (mag/fh), or magnetite and pyrite[6] (mag/py). The (strongly) reducing state should represent a system in contact with a hydrogen-dominated gas phase, which is assumed to exist in the repository for very long time periods.

Additionally, for the freshly hydrated original stage we also calculated one oxic state to mimic the initial conditions immediately after closure of the emplacement caverns.

In the following text we associate the cement porewater definitions and associated material definitions for documentation for the general licence application (SGT Stage 3) with “SGT-E3” to separate them from previous cement porewater definitions that were used during SGT Stage 2 (SGT-E2), to avoid a mix-up with concrete degradation stages.

---

[6] Reducing conditions in the calculations were enforced by adding hydrogen (or removing oxygen) to the system and choice of secondary mineral phases. For addition of small amounts of hydrogen, Eh was controlled by the presence of magnetite, or magnetite and iron-siliceous hydrogarnet, or magnetite and ferrihydrite. Eh for strongly reducing conditions was fixed by adding hydrogen until magnetite and pyrite were stable.

Selection of a representative cement and setup of the concrete

The primary cement currently envisaged to be used in an L/ILW repository is a Portland cement with the highest possible clinker content. Therefore, a CEM I according to SN EN 197-1 was used for the modelling. CEM I is provisionally foreseen to be used for the production of in-situ concrete elements, the cavern-filling mortar, the concrete containers and it is also contained in the container-filling mortar. Definition of the representative cementitious system is thus based on the CEM I 52.5 R cement (Jura cement), which is considered to be representative for the container concrete as modelled in NAB 20-11 and further considered in NAB 20-12 (Wieland & Kosakowski 2020). The chemical composition used as GEM-Selektor Compos record "CEM-I-525R:RO:JuraCement_52.5R:" was taken from Tab. 8 in NAB 20-12 (Wieland & Kosakowski 2020), in turn taken from sample C3 from Tab. 3 in Bran Anleu (2018), and enhanced for minor/trace elements Mn, Sr, Ba, Br, Cl, F as shown in Tab. A-1 for compatibility with the elemental compositions of the OPA PWs (Tab. A-2).

Three variants of the concrete with 11%, 20% and 30% porosity were calculated by adjusting the water to cement ratio (w/c) of the recipe. The recipes for container concrete (0.001 m^3 at ambient conditions) for different degradation stages are given in Tab. A-3 to Tab. A-6.

Tab. A-1: Composition of CEM I 52.5 R

From NAB 20-12, Tab. 8, with extensions

Chemical composition		**Elemental composition**	**Compos CEM_I_52.5R**	**Normative phase composition********	
	[g]		[mol/100g]		[g]
SiO_2	20.0	Al	9.61E-02	Alite	64.7
Al_2O_3	4.9	Ba	6.52E-05	Belite	14.5
Fe_2O_3	3.3	Br	1.25E-06	Aluminate	5.9
CaO	63.5	C	2.27E-02	Ferrite	8.5
MgO	1.8	Ca	1.13	Gypsum	3.0
MnO	0.1	Cl	2.54E-04	Hemihydrate	0.6
SrO*	0.059	F	1.58E-03	Anhydrite	0.1
BaO**	0.01	Fe	4.13E-02	Periclase	0.3
K_2O	0.7	H	1.33E-01	Calcite	1.8
Na_2O	0.2	K	1.49E-02	Dolomite	1.7
LOI*** 2.0 g/100g	0	Mg	4.47E-02	Quartz	0.4
CO_2***	1.0	Mn	1.41E-03	CaOfree	0.64
H_2O***	1.1946	Na	6.45E-03		
SO_3	3.2	O	2.29E+00		
Br**	0.0001	S	4.00E-02		
Cl*	0.009	Si	3.33E-01		
F**	0.03	Sr	5.69E-04		
P_2O_5****	0.2				
TiO_2****	0.3				
O_2 (mol)*****	-0.00264				
Total (without LOI, P_2O_5, TiO_2)	97.8				102.14
Total (with SrO, BaO, Br, Cl, F; no P_2O_5,TiO_2)	100.0				

* Average content in clinkers from Moir and Glasser (1992); LOI = loss on ignition assumed to be 1.0 g/100 g CO_2 and 1.0 g/100 g H_2O

** Minimum values for clinkers using data from Bhatty (2006) available from website https://www.cementequipment.org/home/everything-you-need-to-know-about-minor-elements-in-cement-manufacturing (accessed 11 January 2022)

*** Set to ½ of LOI, H_2O content modified to achieve 100.0 g total

**** Ignored

***** O_2 removed to make O_2-rich gas phase unstable, yet remain at oxidising redox conditions

****** Normative cement composition from Caruso et al. (2017).

Tab. A-2: NL-ZNO-22 Opalinus Clay porewater compositions

Mäder & Wersin (2023), Mazurek et al. (2021)

Calc. ID	OPAw_NL-ZNO-22	
Implementor	BU	PSI
log p(CO_2) [bar]	-2.20	-2.20
pH	7.10	7.10
pe	-2.66	-2.83
Eh [V]	-0.157	-0.167
IS [mol/kg_w]	0.313	0.319
	Molality [mol/kg_w]	
Al	8.61E-09	2.09E-08
Ba	1.57E-07	1.57E-07
C	2.12E-03	2.21E-03
Ca	2.02E-02	2.03E-02
Cl	0.240	0.240
F	1.33E-04	1.74E-04
Fe	8.63E-05	2.56E-05
K	2.13E-03	2.13E-03
Mg	1.55E-02	1.45E-02
Mn	5.74E-05	8.24E-05
Na	0.214	0.215
S	2.29E-02	2.29E-02
Si	1.77E-04	1.72E-04
Sr	2.71E-04	3.70E-04

BU: Bern University (PHREEQC) variant; PSI: LES PSI (GEMS) variant

Tab. A-3: GEMS recipes of CPW systems at degradation Stage I

Property	**Compos or species name**	**Units**	**Stage-I-mt/sh (oxic)**	**Recipe variants: Porosity after hydration**	**Stage-I-mt/sh (reducing)**	**Recipe variants: Porosity after hydration**	**Stage-I-mt/py (reducing)**	**Recipe variants: Porosity after hydration**
xa_	Aqua (H_2O)	g	254.047 371.2	~ 11 % ~ 20 %	254.047 371.2 533.6	~ 11 % ~ 20 % ~ 30 %	259.722 379.0 541.4	~ 11 % ~ 20 % ~ 30 %
xa_	CEM-I-52.5R	g	400		400		400	
xa_	$CaCO_3$	g	180		180		180	
xa_	O_2***	mol	-		-0.0017		-0.017	
xa_	SiO_2	g	1,603		1,603		1,603	
bi_	N_atm*	mol	2E-6		2E-6		2E-6	
dll**	SiO_2(cr)	mol	26.6972		26.6972		26.6972	
dul**	SiO_2(cr)	mol	26.6972		26.6972		26.6972	

* Added for recipe compatibility with normative atmospheric air.

** "dll" - lower metastability restriction on mole amount of chemical species; "dul" - upper metastability restriction on mole amount of chemical species. dll and dul were set to the same value to avoid the reaction of siliceous aggregates, which are represented by SiO_2(cr) (quartz).

*** "Removal of O_2 mimics the consumption of oxygen during (anoxic) corrosion of metals and allows the redox state to be set.

"xa_" - addition of Compos object quantity; "bi_" - addition of independent component Equilibration of recipe stage-I-mt-SHG resulted in Compos "CEMIPW-DS1"; equilibration of recipe stage-I-mt-py resulted in Compos "CEMIPW-DS1re".

Tab. A-4: GEMS recipes of CPW systems at degradation Stage II

Property	**Compos or species name**	**Units**	**Stage-II-mt/sh (oxic)**	**Stage-II-mt/sh (reducing)**	**Stage-II-mt/py (reducing)**	**Recipe variants: Porosity after hydration**
xa_	Aqua (H_2O)	g	254.047 371.2	254.047 371.2 533.6	254.047	~ 11 % ~ 20 % ~ 30 %
xa_	CEM-I-52.5R	g	400	400	400	
xa_	CEMIPW-DS1 CEMIPW-DS1-20 CEMIPW-DS1-30	g	-113.889 -231.722	-113.889 -231.722 -394.673	-113.889	~ 11 % ~ 20 % ~ 30 %
xa_	$CaCO_3$	g	180	180	180	
xa_	O_2***	mol		-0.0017	-0.02	
xa_	OPAw_NL-ZNO-22	g	114.185 231.722	114.185 231.722 394.673	114.185	~ 11 % ~ 20 % ~ 30 %
xa_	SiO_2	g	1,603	1,603	1,603	
bi_	N_atm*	mol	2E-6	2E-6	2E-6	
dll**	SiO_2(cr)	mol	26.6972	26.6972	26.6972	
dul**	SiO_2(cr)	mol	26.6972	26.6972	26.6972	

*, **, *** see Tab. A-3.
Equilibration of recipe stage-II-mt resulted in Compos “CEMIPW-DS2Z”

Tab. A-5: GEMS recipes of CPW systems at degradation stage III-pr (pozzolanic reaction only)

Property	Compos or species name	Units	Stage-III--mt/fh (reducing)	Stage-III-mt/py (reducing)	Recipe variant: Porosity after hydration
xa_	Aqua (H_2O)	g	254.047 371.2 533.6	254.047 371.2 533.6	~ 11 % ~ 20 % ~ 30 %
xa_	CEM-I-52.5R	g	400	400	
xa_	CEMIPW-DS1	g	-113.889 -231.722 -394.673	-113.889 -231.722 -394.673	~ 11 % ~ 20 % ~ 30 %
xa_	CEMIPW-DS2Z CEMIPWDS2Z-20 CEMIPWDS2Z-30	g	-114.142 -230.949 -392.741	-114.142 -230.949 -392.741	~ 11 % ~ 20 % ~ 30 %
xa_	$CaCO_3$	g	180	180	
xa_	O_2***	mol	-0.002	-0.02	
xa_	OPAw_NL-ZNO-22	g	272.002 514.371 839.075	272.002 514.371 839.075	~ 11 % ~ 20 % ~ 30 %
xa_	SiO_2	g	1603	1603	
bi_	N_atm*	mol	2E-6	2E-6	
dul**	Low-silica_P-Ca	mol	0	0	
dul**	Thaumasite	mol	0	0	
dul**	Smectite_MX80	mol	0	0	

*, *** see Tab. A-3.
** "dul" - upper metastability restriction on mole amount of chemical species. dul was set to suppress formation of corresponding mineral phases.
Equilibration of recipe stage-III-pr-mt resulted in Compos "CEMIPW-DS23Z"

Tab. A-6: GEMS recipes of CPW systems at degradation Stage III (PW replaced by OPA PW)

Property	Compos or species name	Units	Stage-III-mt/fh (reducing)	Stage-III-mt/py (reducing)	Recipe variant Porosity after hydration
xa_	Aqua (H_2O)	g	254.047 371.2	254.047 371.2	~ 11 % ~ 20 %
xa_	CEM-I-52.5R	g	400	400	
xa_	CEMIPW-DS1	g	-113.889 -231.722	-113.889 -231.722 -394.673	~ 11 % ~ 20 % ~ 30 %
xa_	CEMIPW-DS2Z CEMIPWDS2Z-20 CEMIPWDS2Z-30	g	-114.142 -230.949	-114.142 -230.949 -392.741	~ 11 % ~ 20 % ~ 30 %
xa_	CEMIPW-DS23Z CEMIPWDS23Z20 CEMIPWDS23Z30	g	-105.9 -231.032	-105.9 -231.032 -393.541	~ 11 % ~ 20 % ~ 30 %
xa_	$CaCO_3$	g	180	180	
xa_	O_2***	mol	-0.002	-0.02	
xa_	OPAw_NL-ZNO-22	g	377.184 745.403	377.184 745.403 1232.62	~ 11 % ~ 20 % ~ 30 %
xa_	SiO_2	g	1603	1603	
bi_	N_atm*	mol	2E-6	2E-6	
dul**	Low-silica_P-Ca	mol	0	0	
dul**	Thaumasite	mol	0	0	
dul**	Smectite_MX80	mol	0	0	

*, *** see Tab. A-3.
** "dul" - upper metastability restriction on mole amount of chemical species. dul was set to suppress formation of corresponding mineral phases.
Equilibration of degradation Stage III (PW replaced by OPA PW) is the final PW for Stage III.

Selection of the OPA porewater

For equilibration with concrete at degradation Stages II and III, the chosen reference Opalinus Clay porewater in Tab. A-2 was the in-situ porewater from the NL-ZNO region (Mäder & Wersin 2023). This model porewater has an average salinity among all studied OPA PWs. It is to be noted that OPAw_NL-ZNO-22 in Tab. A-2 is assumed to be representative for the repository at Stadel (NL).

GEMS version, database and model implementation

All calculations were carried out using the updated PSI-Nagra thermodynamic database (TDB) 2020 (Hummel & Thoenen 2023), implemented in the GEM-Selektor version 3.9.3, and the CEMDATA18.1 TDB for cement phases (Lothenbach et al. 2019), adjusted by G.D. Miron for compatibility with the PSI-Nagra TDB 2020 at the level of equilibrium constants at 1 bar, 25 °C. Activity coefficients of aqueous species were calculated based on the Specific Ion-interaction Theory (SIT) for aqueous species using parameters compiled in the PSI-Nagra TDB 2020.

The CSHQ solid solution of C-S-H (Kulik 2011) also present in the Cemdata18.1 TDB, which reproduces the water content of C-S-H including the gel porewater of C-S-H. In this report, the knowledge of the mass (volume) of gel porewater in C-S-H was needed to create a workaround for avoiding an underestimation of the accessible porosity and aqueous phase mass/volume per given mass of the concrete, in turn leading to an overestimation of ionic strength.

Porewater and solid phase compositions (Tab. A-7 - Tab. A-9) were modelled for the three representative cement degradation stages (Stage I, Stage II, Stage III). To model mildly reducing conditions, it was assumed that, in degradation Stages I and II, redox states are buffered by the presence of magnetite (Fe_3O_4(cr)) and Fe/Al siliceous hydrogarnet ($3C_3(AF)S_{0.84}H$) at equilibrium. Magnetite is expected to be present in cementitious systems as it forms as the predominant corrosion product of anoxic steel corrosion. To model the strongly reducing (anoxic) conditions caused by the corrosion of large amounts of metals (steel), it was assumed that the system is equilibrated with both magnetite and pyrite FeS_2(cr) as redox buffers. In Stage III, the cement porewater was found to be always undersaturated with respect to siliceous hydrogarnet, but the system can be in equilibrium with ferrihydrite only (oxidising), magnetite and ferrihydrite (mildly reducing), or magnetite and pyrite (reducing, anoxic) redox buffers. The different redox states can be implemented by removing oxygen from the bulk composition to mimic the influence of iron corrosion, which would form iron oxide (e.g. magnetite). Increasing removal of oxygen moves the redox state from oxidising, via mildly reducing to strongly reducing (cf. the “negative addition” of O_2 in Tab. A-3 to Tab. A-6).

Modelling procedure

It should be noted that the setup of cement degradation stages and equilibration with Opalinus Clay porewater reflects the intended use of the cement porewaters as input for sorption and solubility data required for safety analysis. In the safety assessment for the L/ILW repository, it is assumed that the near-field is approximated by a homogenised, fully saturated cement material from 100 years after repository closure (Nagra 2014b). From the viewpoint of repository saturation (cf. Section 3.2.1), this is a very conservative assumption for the safety assessment. The different cement degradation stages are represented by their associated radionuclide solubility and sorption parameters. Material heterogeneities and temporal and spatial changes in water saturation, as described in Kosakowski et al. (2014), Kosakowski et al. (2020), Martin et al. (2023), and in Chapter 3 of this report are not considered.

The assumed degradation sequence for all three concrete variants was set up as follows:

Stage I (Tab. A-3): Container concrete hydrated with pure H_2O and H_2 added until magnetite is stable (reducing). It was further assumed that siliceous hydrogarnet is the thermodynamically stable Fe-containing cement phase as over longer times, AFm phases are not stable according to Dilnesa et al. (2012).

Stage II (Tab. A-4): In the hydrated concrete from Stage I, all the aqueous solution (including that in C-S-H gel pores) was removed and replaced with the OPA NL-ZNO-22 porewater composition and equilibrated (mildly reducing variants). This mimics ingress of Opalinus Clay formation water causing full liquid saturation of the repository near-field, the conservative conditions assumed by safety assessment to exist 100 years after repository closure (Section 5.3.2 of Nagra 2014b). It was further assumed that portlandite is not completely consumed by internal cement degradation and interaction with waste materials or host rock porewater.

Stage III (Tab. A-6): In the hydrated concrete from Stage II, SiO_2 was assumed to be reactive (i.e. allowing the pozzolanic reaction between cement and filler/aggregates), all the aqueous solution (including C-S-H gel pores) was removed and replaced with OPA NL-ZNO-22 PW composition, and equilibrated also with SiO_2 aggregate, which corresponds to a pozzolanic reaction (Section 3.3.5). This results in an intermediate stage DS-IIIpr (Tab. A-5). Degradation Stage III is reached by completely replacing the intermediate porewater from the DS-IIIpr stage once again with the OPA NL-ZNO-22 PW composition, and equilibrating to DS-III state (Tab. A-6). The porewater exchange mimics the effect of diffusive equilibration of host rock and near-field porewaters for chlorine and alkali metal ions. Note that at the contact between clay host rock and cement materials (tunnel support) with diffusion in the aqueous phase as the dominant transport mechanism, equilibration in terms of alkali and chlorine concentrations can be achieved within timescales of a few thousand years, whereas the progress of cement degradation is very slow (far away from the cement/host rock interface). While the porewater composition (in terms of chlorine and alkali metals ions) is strongly influenced by the contact with host rock water, the majority of cement materials are not strongly degraded by this process after 100,000 years (Kosakowski & Berner 2013).

Comparison of modelling results with porewaters used in the previous phase of the SGT

In the previous phase of the SGT (SGT-E2), the geochemical conditions for the different stages of cement degradation used for the development of the cement SDB in NTB 14-08 (Wieland 2014) were taken from reactive transport calculations using state-of-the-art modelling tools as described in Kosakowski et al. (2014). The three stages of concrete degradation were represented as follows: Stage I was represented by the initial conditions of a freshly hydrated cement paste of the reference concrete. Stage II was represented by geochemical conditions occurring at the OPA/reference concrete interface of an L/ILW near-field as a result of mineral transformations caused by the strong chemical gradients (Kosakowski et al. 2014), while Stage III was represented by geochemical conditions occurring at the bentonite/ESDRED/OPA interface of a high-level waste repository during evolution of the low-pH shotcrete system (Bradbury et al. 2014). We refer to the compilation of the three reference systems given in App. A of NTB 14-11 (Kosakowski et al. 2014).

It should be noted that different cements and concrete recipes were used by Kosakowski et al. (2014) and in this study. In SGT-E2, the concrete used for Stage I and Stage II used an HTS cement[7] and was "tuned" in terms of w/c ratio to represent a concrete with porosity of 20%, the assumed average porosity in the L/ILW disposal caverns. The low-pH shotcrete represents a well-defined cement composition which represents a cement material in Stage III with a porosity of close to 20%. The common basis for the selection of the reference system in SGT-E2 and SGT-E3 are as follows:

- Stage I corresponds to a "fresh" cement system with high concentrations of alkalis in porewater and pH > 13.
- Stage II corresponds to a system that is depleted in alkalis and pH is controlled by portlandite solubility.
- (the "end" of) Stage III corresponds to a system where pH is controlled by the equilibrium between quartz aggregates, C-S-H and other cement phases ("low-pH" stage of hardened cement paste).

The solute concentrations and phase compositions of the cement matrices used in SGT-E2 for the three degradation stages are listed in column 2 of Tab. A-7 - Tab. A-9. They are based on the results reported in App. A of NTB 14-11.

The following columns in Tab. A-7 to Tab. A-9 list the three variations for porosity of the container concrete used in SGT-E3. For Stages II and III, the mildly reducing and strongly reducing redox variants are listed. A comparison with the data from the current modelling allows general trends in the differences in the cation and anion concentrations to be summarised as follows.

Stage I (Tab. A-7): The differences in the solute concentrations and the composition of the hardened cement paste between current and earlier modelling (column 2) are as follows: Alkali ion concentrations (Na, K) are different due to the different cements used. In addition, the recipe for SGT-E2 used the SGT-E2 OPA PW to hydrate the concrete, while for SGT-E3 the concretes are hydrated with pure H_2O. The different waters used for hydration and the different Cl content of the cements explain the difference in Cl^- concentrations. All other cation and anion concentrations obtained from the current modelling in SGT-E3 are within the range of the respective concentrations of CPWs previously modelled within the framework of SGT-E2. The concrete variants for SGT-E3 generally show a reduction of (an)ion concentrations with increasing water content (porosity, w/c ratio). Specifically, dilution of alkali concentrations (K, Na) causes a decrease in pH, which is partly compensated by portlandite dissolution causing an increase in Ca concentration.

C-S-H phases, portlandite, ettringite, hydrotalcite and calcite are the minerals observed in the modelling studies carried out in SGT-E2 and SGT-E3, although their proportions could vary. Siliceous hydrogarnet is thermodynamically stable in the modelling for SGT-E3 at the expense of monocarbonate (AFm phase).

For Stage I we define the variant with magnetite and siliceous hydrogarnet as redox buffering minerals (Stage-I-mt/si (reducing) ~ 20% porosity) as the reference stage. This stage is expected to be the best representation of the initial transition phase from oxidising towards strongly reducing conditions.

[7] Sulphate-resistant ordinary Portland cement (CEM I, HTS = haute teneur en silice)

Stage II (Tab. A-8): For the solute concentrations and the composition of the hardened cement paste, the following differences between the current and previous modelling (column 2) arise: Higher Na concentrations, slightly higher K concentrations along with higher Cl^- concentrations (factor ~ 10) due to equilibration with NL-ZNO OPA PW in the modelling for SGT-E3. All other cation and anion concentrations reported for the modelling in SGT-E3 are within the range of the respective concentrations of CPWs previously modelled within the framework of SGT-E2 (differences are less than a factor of ~ 4). As for Stage I, the types of solids present in hardened cement paste are comparable in all calculations, with C-S-H phases, portlandite, ettringite, and calcite being the main minerals. Furthermore, as for Stage I, siliceous hydrogarnet is formed at the expense of monocarbonate in the modelling for SGT-E3.

As for Stage I, the SGT-E3 concrete variants shows a dilution effect for most (an)ion concentrations with increasing porosity, which also causes a decrease in pH. This is caused by the (de)sorption of K and Na from the C-S-H phase, which is out of equilibrium with the aqueous phase after replacement with NL-ZNO OPA PW. The dilution effect is less pronounced than for Stage I. Cl^- concentrations are close to the concentrations in the host rock porewater. The mildly reducing variant with the highest porosity and the reducing variant for 20% porosity show precipitation of trace amounts of Friedel's salt, which indicates that this phase is close to saturation at this degradation stage.

For this phase we assume that a free hydrogen gas phase exists and that the redox state is best represented by the magnetite-pyrite redox buffer (Stage-II-mt/py (reducing) ~ 20% porosity).

Stage III (Tab. A-9): The following differences in the solute concentrations and the solid composition of the cementitious materials between the current and the previous modelling study are found: The pH is lower, i.e. pH 9.71 - 9.84 instead of pH 11.07, because the end of Stage III was defined in accordance with a C-S-H phase with C/S = 0.7 in the modelling for SGT-E3 instead of C/S = 0.8 in the previous modelling for SGT-E2. This results in a lower equilibrium pH. The Na and K concentrations are similar. However, the Ca concentration is significantly higher (factor ~ 10) in the modelling for SGT-E3. Increased Ca concentrations compensate the high Cl^- concentrations introduced by the equilibration with the OPA PW. The SO_4^{2-}, CO_3^{2-} and Si concentrations are comparable (difference less than a factor of ~ 2). The Fe and Al concentrations are significantly lower due to the different sets of thermodynamic data used. The current modelling reveals C-S-H (C/S = 0.7), calcite and zeolites as the main minerals present in Stage III. C-S-H phases and calcite were already observed in the modelling of Stage III for SGT-E2. Ettringite is not thermodynamically stable according to the modelling for SGT-E3, while its presence was predicted in the earlier modelling carried out for SGT-E2, likely due to the lower pH in the current modelling and the new thermodynamic data implemented for zeolites. Therefore, gypsum is the SO_4^{2-}-containing phase in Stage III, while Al is bound by zeolites rather than ettringite. Furthermore, hydrotalcite is not thermodynamically stable in the modelling for SGT-E3, which leads to the formation of M-S-H as the Mg-containing cement phase. Ferrihydrite and magnetite are the Fe-containing phases present in small amounts in Stage III for the mildly reducing state, while magnetite and pyrite are formed under strongly anoxic conditions. The latter case is assumed to be representative for anoxic conditions with a free hydrogen gas phase present for long times in the repository (Stage-III-mt/py (reducing) ~ 20% porosity).

In summary, the modelling studies carried out for SGT-E2 (Kosakowski et al. 2014) and SGT-E3 (Section 3.5) disclose some differences in the solute concentrations and phase compositions of the cement materials in Stage II and Stage III, while differences are small in Stage I. A notable difference in Stage I and Stage II arises due to the formation of siliceous hydrogarnet at the expense of monocarbonate (AFm phase) and the absence of ettringite and hydrotalcite in Stage III. Otherwise, the same main minerals are present, in particular C-S-H, portlandite, ettringite and calcite in Stage I and Stage II as well as C-S-H and calcite in Stage III.

Tab. A-7: Geochemical conditions (solids, porewater composition) in Stage I reported by Kosakowski et al. (2014) and used in NTB 14-08 (Wieland 2014) (second column) and calculated in this study

The selected reference case is marked grey.

Parameters	**Concrete SGT-E2**	**Stage-I-mt/si (oxic) ~ 11% porosity**	**Stage-I-mt/si (reducing) ~ 11% porosity**	**Stage-I-mt/py (reducing) ~ 11% porosity**	**Stage-I-mt/si (oxic) ~ 20% porosity**	**Stage-I-mt/si (reducing) ~ 20% porosity**	**Stage-I-mt/si (reducing) ~ 30% porosity**
Porosity [%]	20.00	10.99	11.28	10.28	20.14	20.60	30.71
pH	13.10	13.23	13.23	13.20	13.11	13.11	13.00
pe	-8.98	7.50	-6.76	-10.67	7.54	-6.66	-6.56
Eh [mV]	-529.9	443.0	-399.3	-635.0	445.0	-393.2	-387.1
Ionic strength [m]	0.168	0.248	0.248	0.235	0.182	0.182	0.137
Solutes [mol/L]							
Na	$9.68 \cdot 10^{-2}$	$4.16 \cdot 10^{-2}$	$4.16 \cdot 10^{-2}$	$3.73 \cdot 10^{-2}$	$3.64 \cdot 10^{-2}$	$3.64 \cdot 10^{-2}$	$3.00 \cdot 10^{-2}$
K	$7.27 \cdot 10^{-2}$	$2.10 \cdot 10^{-1}$	$2.10 \cdot 10^{-1}$	$2.10 \cdot 10^{-1}$	$1.44 \cdot 10^{-1}$	$1.44 \cdot 10^{-1}$	$1.02 \cdot 10^{-1}$
Ca	$2.43 \cdot 10^{-3}$	$2.04 \cdot 10^{-3}$	$2.04 \cdot 10^{-3}$	$2.17 \cdot 10^{-3}$	$2.76 \cdot 10^{-3}$	$2.76 \cdot 10^{-3}$	$3.76 \cdot 10^{-3}$
S (sulphate)	$6.24 \cdot 10^{-4}$	$1.85 \cdot 10^{-3}$	$1.85 \cdot 10^{-3}$	$3.75 \cdot 10^{-3}$	$9.04 \cdot 10^{-4}$	$9.02 \cdot 10^{-4}$	$4.64 \cdot 10^{-4}$
Cl*	$2.46 \cdot 10^{-4}$	$9.02 \cdot 10^{-3}$	$9.02 \cdot 10^{-3}$	$9.59 \cdot 10^{-3}$	$4.41 \cdot 10^{-3}$	$4.41 \cdot 10^{-3}$	$2.58 \cdot 10^{-3}$
C_{inorg}	$4.46 \cdot 10^{-5}$	$1.10 \cdot 10^{-4}$	$1.10 \cdot 10^{-4}$	$9.60 \cdot 10^{-4}$	$5.74 \cdot 10^{-5}$	$5.74 \cdot 10^{-5}$	$3.23 \cdot 10^{-5}$
Si	$4.34 \cdot 10^{-5}$	$4.37 \cdot 10^{-5}$	$4.37 \cdot 10^{-5}$	$4.17 \cdot 10^{-5}$	$3.60 \cdot 10^{-5}$	$3.60 \cdot 10^{-5}$	$3.19 \cdot 10^{-5}$
Al	$2.61 \cdot 10^{-5}$	$3.56 \cdot 10^{-5}$	$3.56 \cdot 10^{-5}$	$5.20 \cdot 10^{-5}$	$2.63 \cdot 10^{-5}$	$2.64 \cdot 10^{-5}$	$1.98 \cdot 10^{-5}$
Fe	$2.11 \cdot 10^{-7}$	$4.34 \cdot 10^{-8}$	$4.34 \cdot 10^{-8}$	$2.78 \cdot 10^{-8}$	$3.23 \cdot 10^{-8}$	$3.22 \cdot 10^{-8}$	$2.42 \cdot 10^{-8}$
Mg	n.d.	$1.47 \cdot 10^{-9}$	$1.47 \cdot 10^{-9}$	$1.24 \cdot 10^{-9}$	$1.89 \cdot 10^{-9}$	$1.88 \cdot 10^{-9}$	$2.41 \cdot 10^{-9}$
Major solids of hardened/degraded cement paste [wt.-%]							
C-S-H - C/S ratio	Present -	32.7 1.58	33.3 1.58	36.7 1.58	33.3 1.58	33.3 1.58	33.3 1.58
Portlandite	Present	17.4	17.6	17.5	17.6	17.6	17.5
Ettringite	Present	9.7	9.9	9.9	9.9	9.9	9.9
Siliceous hydrogarnet	-	10.0	10.2	0	10.25	10.17	10.2
OH^- hydrotalcite	Present	2.7	2.75	2.7	2.75	2.75	2.75
Calcite	Present	25.6	26.1	23.7	26.1	26.1	26.1
Mono-carbonate	Present	0	0	6.9	0	0	0
Magnetite	-	0	0.025	1.18	0.0	0.025	0.025
Ferrihydrite	-	0	0	0	0	0	0
Pyrite	-	0	0	0.005	0	0	0

* See comment in Wieland & Kosakowski (2020); n.d.: not determined.

Tab. A-8: Geochemical conditions (solids, porewater composition) in Stage II reported by Kosakowski et al. (2014) and used in NTB 14-08 (Wieland 2014), and in this study

The selected reference case is marked grey.

Parameters	**Concrete SGT-E2**	**Stage-II-mt/si (reducing) ~ 11% porosity**	**Stage-II-mt/si (reducing) ~ 20% porosity**	**Stage-II-mt/py (reducing) ~ 20% porosity**	**Stage-II-mt/si (reducing) ~ 30% porosity**
Porosity [%]	20.00	11.22	20.40	19.73	30.37
pH	12.54	12.82	12.62	12.68	12.53
pe	-8.44	-6.36	-6.17	-10.24	-6.08
Eh [mV]	-498.1	-375.5	-364.2	-604.4	-358.8
Ionic strength [m]	0.098	0.340	0.313	0.288	0.306
Solutes [mol/L]					
Na	$4.21 \cdot 10^{-2}$	0.169	0.194	0.187	0.199
K	$3.30 \cdot 10^{-3}$	0.153	$7.21 \cdot 10^{-2}$	$6.68 \cdot 10^{-2}$	$3.57 \cdot 10^{-2}$
Ca	$1.80 \cdot 10^{-2}$	$8.07 \cdot 10^{-3}$	$1.77 \cdot 10^{-2}$	$1.37 \cdot 10^{-2}$	$2.53 \cdot 10^{-2}$
S (sulphate)	$4.70 \cdot 10^{-5}$	$3.55 \cdot 10^{-4}$	$1.39 \cdot 10^{-4}$	$8.91 \cdot 10^{-4}$	$9.36 \cdot 10^{-5}$
Cl	$3.74 \cdot 10^{-2}$	0.240	0.240	0.209	0.237
C_{inorg}	$8.04 \cdot 10^{-6}$	$2.21 \cdot 10^{-5}$	$1.37 \cdot 10^{-5}$	$1.58 \cdot 10^{-5}$	$1.10 \cdot 10^{-5}$
Si	$3.42 \cdot 10^{-5}$	$2.77 \cdot 10^{-5}$	$2.68 \cdot 10^{-5}$	$8.91 \cdot 10^{-4}$	$2.64 \cdot 10^{-5}$
Al	$6.89 \cdot 10^{-6}$	$1.20 \cdot 10^{-5}$	$8.87 \cdot 10^{-6}$	$1.62 \cdot 10^{-4}$	$7.14 \cdot 10^{-6}$
Fe	$5.58 \cdot 10^{-8}$	$1.47 \cdot 10^{-8}$	$1.09 \cdot 10^{-8}$	$2.60 \cdot 10^{-8}$	$8.87 \cdot 10^{-9}$
Mg	n.d.	$3.19 \cdot 10^{-9}$	$7.26 \cdot 10^{-9}$	$4.78 \cdot 10^{-9}$	$9.45 \cdot 10^{-9}$
Major solids of hardened/degraded cement paste [wt.-%]					
C-S-H C/S ratio	Present -	33.3 1.59	33.3 1.59	36.67 1.59	33.3 1.59
Portlandite	Present	17.56	17.43	17.33	17.27
Ettringite	Present	10.0	10.2	10.12	10.4
Siliceous hydrogarnet	-	10.1	10.0	0	9.9
OH^-hydrotalcite	Present	2.77	2.80	2.75	2.83
Calcite	Present	26.1	26.1	24.46	26.1
Monocarbonate	Present	0	0	6.39	0
Friedel's salt	-	0.0	0	0.37	0.05
Magnetite	-	0.025	0.025	1.73	0.025
Ferrihydrite	-	0	0	0	0
Pyrite	-	0	0	0.02	0

Tab. A-9: Geochemical conditions (solids, porewater composition) in Stage III reported by Kosakowski et al. (2014) and used in NTB 14-08 (Wieland 2014), and in this study

The selected reference case is marked grey.

Parameters	**Concrete SGT-E2 CEM I 42.5 N + SF***	**Stage-III-mt/fh (reducing) ~ 11% porosity**	**Stage-III-mt/py (reducing) ~ 11% porosity**	**Stage-III-mt/fh (reducing) ~ 20% porosity**	**Stage-III-mt/py (reducing) ~ 20% porosity**	**Stage-III-mt/py (reducing) ~ 30% porosity**
Porosity [%]	18.00	10.37	10.67	20.27	20.51	30.45
pH	11.07	9.91	9.91	9.89	9.89	9.88
pe	-3.06	-0.06	-6.44	-0.04	-6.42	-6.42
Eh [mV]	-180.7	-3.6	-380.4	-2.4	-379.0	-378.8
Ionic strength [m]	0.150	0.325	0.318	0.329	0.327	0.329
Solutes [mol/L]						
Na	0.104	0.109	0.107	0.114	0.113	0.115
K	$2.55 \cdot 10^{-2}$	0.029	0.028	0.009	0.0089	0.0043
Ca	$5.35 \cdot 10^{-3}$	0.065	0.063	0.071	0.071	0.073
S (sulphate)	$7.81 \cdot 10^{-3}$	0.0144	0.0145	0.013	0.0134	0.0132
Cl	0.123	0.239	0.233	0.239	0.238	0.239
C_{inorg}	$1.67 \cdot 10^{-5}$	$8.36 \cdot 10^{-6}$	$8.60 \cdot 10^{-6}$	$8.20 \cdot 10^{-6}$	$8.41 \cdot 10^{-6}$	$8.37 \cdot 10^{-6}$
Si	$3.45 \cdot 10^{-4}$	$5.98 \cdot 10^{-4}$	$6.00 \cdot 10^{-4}$	$5.88 \cdot 10^{-4}$	$5.88 \cdot 10^{-4}$	$5.86 \cdot 10^{-4}$
Al	$1.15 \cdot 10^{-4}$	$8.04 \cdot 10^{-7}$	$8.10 \cdot 10^{-7}$	$7.68 \cdot 10^{-7}$	$7.70 \cdot 10^{-7}$	$7.60 \cdot 10^{-7}$
Fe	$3.86 \cdot 10^{-8}$	$3.4E \cdot 10^{-10}$	$1.50 \cdot 10^{-9}$	$3.30 \cdot 10^{-10}$	$1.50 \cdot 10^{-9}$	$1.50 \cdot 10^{-9}$
Mg	n.d.	$8.33 \cdot 10^{-6}$	$8.12 \cdot 10^{-6}$	$9.12 \cdot 10^{-6}$	$9.06 \cdot 10^{-6}$	$9.26 \cdot 10^{-6}$
Major solids of hardened/degraded cement paste [wt.-%]						
C-S-H C/S ratio	Present 0.82**	67.6 0.70	67.71 0.70	67.4 0.70	67.53 0.70	67.29 0.70
Portlandite	-	0	0	0	0	0
Ettringite	Present	0	0	0	0	0
Silic. hydrogarnet	-	0	0	0	0	0
OH^-hydrotalcite	Present	0	0	0	0	0
Calcite	Present	17.14	17.17	17.2	17.19	17.21
AFm phases	-	0	0	0	0	0
Gypsum	-	2.54	2.51	2.63	2.60	2.72
Ferrihydrite		1.19	0	1.19	0	0
Magnetite		0.12	1.15	0.12	1.15	1.15
Pyrite	-	0	0.01	0	0.01	0.01
M-S-H	-	2.48	2.49	2.56	2.56	2.66
Chabazites	-	8.83	8.84	8.85	8.86	8.87

* SF: silica fume used to make the "low-pH" ESDRED concrete (Kosakowski et al. 2014)
** The C/S ratio of 0.82 is the lowest possible value for the C-S-H model used in the calculations for SGT-E2.
n.d.: not determined.

Comparison with data used in Wieland & Kosakowski (2020) and in Section 3.5.4

Wieland & Kosakowski (2020) reviewed existing information on the compositions of cement pastes and their equilibrium porewaters for cements and concrete that might be relevant in SGT-E3 compared to those previously used in SGT-E2 (Wieland & Kosakowski 2020). The data reported for SGT-E3 and used by Wieland & Kosakowski (2020) for the comparison are based on the study reported by Kosakowski et al. (2020) which considers cement degradation by carbonation and reaction with silica of three possible cementitious materials (container concrete, mortar M1 and container-filling cement) that could be present in the cementitious near-field of an L/ILW repository. Wieland & Kosakowski (2020) summarised the respective information on the compositions of the cement materials and the corresponding porewaters for the three main stages of the cement degradation, thus providing an appraisal of the uncertainty ranges of cement paste and porewater compositions.

The modelling setup used for the study by Kosakowski et al. (2020) and the modelling setup used in this report show some notable differences in terms of input data and scenarios considered:

Different thermodynamic databases were used for modelling the cementitious systems, i.e. the Cemdata 14.01 TDB of Kosakowski et al. (2020) and the Cemdata 18.1 TDB (Lothenbach et al. 2019) in this study. The further development of the Cemdata TDB has led to significant changes in the thermodynamic data. For example, the Cemdata 18.1 TDB is based on a recent review of the thermodynamic data for iron (Hummel & Thoenen 2023) and new data for Fe-containing siliceous hydrogarnet and zeolites (Lothenbach et al. 2019).

Kosakowski et al. (2020) modelled the uptake of alkalis by C-S-H phases in terms of an ideal solution model between jennite and tobermorite using the thermodynamic properties of the end-members as reported by Wieland et al. (2018). The Cemdata 18 TDB is based on the CSHQ solid solution model of C-S-H phases by Kulik (2011).

The current and previous modelling by Kosakowski et al. (2020) use slightly different compositions for CEM I 52.5R due to different assumptions that have been made regarding the loss on ignition (LOI) and inclusion of trace metals in the current modelling.

The two modelling studies also differ in terms of the scenarios considered. Kosakowski et al. (2020) did not consider an exchange of the cement porewater by OPA PW, which accounts for an additional degradation process of cementitious materials in addition to carbonation and the dissolution of silicate aggregates (“pozzolanic reaction”).

A comparison of the degradation of “container concrete” modelled by Kosakowski et al. (2020) and the corresponding degradation stages in this study show consistent results, despite the differences in model setup and degradation mechanisms.

Regarding Stage I of cement degradation, the differences in solute concentrations and phase compositions of the cement materials are small. This is to be expected as, in both studies, the container concrete was equilibrated with pure water.

For Stage II, the differences in solute concentration and phase composition of the cement material can largely be attributed to equilibration with OPA PW, particularly due to the high concentrations of alkalis and chloride of the OPA PW. It should be noted that Kosakowski et al. (2020) modelled the effect of carbonation and the dissolution of silicate aggregates on concrete degradation in the absence of OPA PW. For example, the high total concentration of alkalis raises the pH to ~ 12.8 from ~ 12.5 typically observed in cement porewaters, as OH^- in addition to Cl^- contributes to charge balance in the solution. Increasing pH leads to a lower Ca concentration buffered by portlandite solubility in this stage of cement degradation, which conversely leads to lower Si concentrations controlled by C-S-H solubility.

As in Stage II, the main differences in solute concentration and phase composition of the cement material in Stage III are due to equilibration of the container concrete with OPA PW and the different thermodynamic data used.